POLSKIE TOWARZYSTWO MIKROBIOLOGÓW
POLISH SOCIETY OF MICROBIOLOGISTS

Polish Journal of Microbiology

2020

Polish Journal of Microbiology
formerly Acta Microbiologica Polonica
2020, Vol. 69, No 4

CONTENTS

INSTRUCTIONS FOR AUTHORS
Instructions for authors: https://www.exeley.com/journal/polish_journal_of_microbiology

Polish Journal of Microbiology
2020, Vol. 69, No 4, 391–399
https://doi.org/10.33073/pjm-2020-044

MINIREVIEW

Hepatitis B Virus: From Diagnosis to Treatment

MERYEM GUVENIR[1] and AYSE ARIKAN[2, 3]

[1] Near East University, Vocational School of Health Services, Nicosia, Northern Cyprus
[2] Near East University, Faculty of Medicine, Department of Medical Microbiology, Nicosia, Northern Cyprus
[3] Near East University, DESAM Institute, Nicosia, Northern Cyprus

Submitted 21 July 2020, revised 22 September 2020, accepted 24 September 2020

Abstract

Hepatitis B infection is still a global concern progressing as acute-chronic hepatitis, severe liver failure, and death. The infection is most widely transmitted from the infected mother to a child, with infected blood and body fluids. Pregnant women, adolescents, and all adults at high risk of chronic infection are recommended to be screened for hepatitis B infection. The initial analysis includes serological tests that allow differentiation of acute and chronic hepatitis. Molecular assays performed provide detection and quantification of viral DNA, genotyping, drug resistance, and precore/core mutation analysis to confirm infection and monitor disease progression in chronic hepatitis B patients. All patients with chronic hepatitis B should be treated with antiviral medications and regularly monitored for efficient treatment. The current treatment is based on nucleos(t)ide analogs and pegylated interferons that save lives by decreasing liver cancer death, liver transplant, slow or reverse the progression of liver disease as well as the virus infectivity.

K e y w o r d s: hepatitis B virus (HBV), serology, nucleic acid testing, antiviral treatment

Introduction

Although there are effective vaccines and treatment strategies against hepatitis B (HB), it is still a significant health concern worldwide that can present in acute, permanent, severe liver failure and cancer forms resulting in high morbidity and death. Globally, 2 billion people have been infected with HB. There is an estimated more than 292 million people living with chronic hepatitis B (CHB) infection worldwide. The global HB surface antigen (HBsAg) positivity was estimated to be 3.9% in 2016 (HBF 2018a; Razavi-Shearer et al. 2018). Annually, 887,000 deaths occur each year due to HB and related illnesses, which were mainly related to advanced liver fibrosis and cirrhosis (WHO 2019a). The risk and progression of chronic infection are age-dependent and occur mainly in immunocompromised individuals. It is known that the younger an infected person is, the higher the risk of developing CHB infection. Although acute infection is generally cleared in immunocompetent, chronic infection develops in approximately 90% of infants, 30–50% of children aged five years, and 5–10% adults (Jefferies et al. 2018; Terrault et al. 2018; Hyun Kim and Ray Kim 2018; CDC 2020a). CHB infection is classified in five different clinical stages according to the HBsAg positivity (i) hepatitis B e antigen (HBe Ag) positive infection; ii) HBe Ag-positive hepatitis; iii) HBe Ag-negative infection; iv) HBe Ag-negative hepatitis, and v) HBsAg-negative stages that reflect the interaction between HBV replication and the immune system. Occult hepatitis B infection (OBI) is another sub-category that is characterized by a detectable HBV DNA with undetectable HBs antigen or serological markers of the previous viral exposure in the plasma (Malagnino et al. 2018). OBI is associated with severe liver damage and hepatocellular carcinoma (HCC), and poses a risk for individuals, especially in blood transfusional infection, HBV reactivation, chronic liver disease, and HCC (Roman 2018; Wang et al. 2020).

HBV spreads from mother to child, after exposure to infected blood or body fluids or sexual contact. In addition, HBV can survive and remain infective for several weeks on moist surfaces at room temperature (de Almeida et al. 2015; Terrault et al. 2018; Than

* Corresponding author: A. Arikan, Near East University, Faculty of Medicine, Department of Medical Microbiology and Clinical Microbiology, Nicosia, Turkish Republic of Northern Cyprus; **e-mail: aysearikancy@yahoo.com, ayse.arikansarioglu@neu.edu.tr**

et al. 2019). Despite being transmitted vertically from infected mother to a child, having sex with an infected partner, contacting the infected needle sticks or sharp object injuries, HBV is not transmitted through breastfeeding, hugging, kissing, coughing, and sneezing, or sharing food and drink (CDC 2020b).

HBV vaccination is the main and the safest precaution from being exposed to the virus (WHO 2019a). HBV vaccine has been administered since 1982 and leads to a dramatic decline in HBV infections globally (Van Damme 2016; WHO 2017a). The vaccine against HBV is available and can be administered from birth to older ages. ENGERIX-B®, RECOMBIVAX HB®, HEPLISAV-™ are three single-antigen vaccines while PEDIARIX®, TWINRIX® are two combination vaccines that are licensed for use in the United States (CDC 2020c). The recommended schedules for HBV vaccine are as follows: three-dose vaccination at 0, 1–2, and 6–18 months of a monovalent HepB (Heplisav-B) vaccine for infants; three-dose vaccination at 0, 1–2, and 6 months for the unvaccinated person, and alternative two doses of Recombivax HB at 11–15 years; two dose vaccinations of HepB at 18 years, and three-dose vaccination with Twinrix. Twinrix is a combination of HepA and HepB vaccine to be administered at 18 years and older (Dynavax 2018; CDC 2020c).

To reduce the spread of infection, the World Health Organization (WHO) European Region recommends the Universal Hepatitis B vaccination programs for infants born from HBsAg-positive mothers, all infants within the first 24 hours after birth, children up to 18 years old, and adults from the groups of high risk for HBV infection, i.e., people with infected sexual partners, homosexual men, hemodialysis patients, injecting drug users, and healthcare workers (WHO 2019b). In May 2016, the WHO addressed the first Global Health Sector Strategy on viral hepatitis 2016–2021 to end new CHB infections by 90% and reduce the mortality rate by 65% by 2030 (WHO 2016).

One of the most severe forms of hepatitis infections is hepatitis delta, also known as hepatitis D. The infection can develop in people infected with HBV (Gilman et al. 2019). Globally, an estimated of 5% of HBV are also infected with the hepatitis D virus (HDV) (WHO 2020). Individuals with HBsAg positive, the elevated alanine aminotransferase (ALT) level with undetectable HBV DNA should be screened for HDV antibodies and HDV RNA (Gilman et al. 2019). HBV-HDV co-infection is severe, and the risk of liver disease progression, liver cancer, early decompensated cirrhosis, and liver failure is higher (WHO 2020). Although there is no effective vaccine against HDV, vaccination against HBV also plays a significant role in protecting delta infection.

HBV, is a partially double-stranded DNA virus of 3.2 kilobases, and it transforms from pregenomic ribonucleic acid (RNA) to DNA by reverse transcription during its life cycle. The genome consists of an outer lipid envelope and inner nucleocapsid core encoded by four overlapping open reading frames, named C, X, P, and S (McNaughton et al. 2019; Wang et al. 2019). Although it is known as a virus with high replication ability, due to the absence of the proofreading reverse transcriptase enzyme, the naturally occurring mutations may arise in different genome regions. These regions may encode for polymerase, surface antigen, core/precore promoter, and comprise the X genes that significantly influence HBsAg expression and progression of HCC (Shaha et al. 2018; Arikan et al. 2019). Additionally, due to the complete overlapping of *pol* and *S* genes, drug resistance and nucleos(t)ide resistance mutations occurring in the *pol* gene can lead to changes in its product HBsAg (Kırdar et al. 2019).

The mutations in the gene C that encode for precore and core proteins are significantly correlated with liver disease progression in CHB patients (Al-Qahtani et al. 2018). The changes in the amino acid sequences: W28*, G29D, G1896A, G1899A, G1862T in the precore proteins that affect HBeAg, and F24Y, E64D, E77Q, A80I/T/V, L116I, E180A in the core proteins mutations are commonly identified and related to clinical severity (Kim et al. 2016; Wu et al. 2018).

The global genotype distribution of HBV differs in different geographic regions and areas worldwide (Rajoriya et al. 2017). HBV is classified into ten genotypes (A-J), and 40 sub-genotypes till today, according to the phylogenetic analysis (Rajoriya et al. 2017). Genotype A is predominant in Northwest Europe, North America, and Africa; genotypes B and C prevail in East Asia and far East countries, while genotype D is widespread worldwide (Arikan et al. 2016; Kmet Lunacek et al. 2017). Genotype E occurs only in West Africa (Ambachew et al. 2018). Genotype F has been found in Central and South America, and genotype G has been reported in Turkey, France, Canada, Vietnam, Germany, and America. Genotypes H and I have been isolated in Central America, Mexico, Vietnam, and Laos; the recently identified genotype J has only been found in Japan (Mahmood et al. 2016). Fig. 1 illustrates the distribution of HBV genotypes (A-J) worldwide. Additionally, the rate of HBV infection also differs in geographic regions. According to the HBsAg positivity, the prevalence of HBV infection is classified into low (< 2), low-intermediate (2–4.9%), high intermediate (5–7.9%), and high (≥ 8) (Kim et al. 2018). HBsAg is of the main concern, especially for the Western Pacific regions with 6.25 seropositivity. The global prevalence of CHB infection in the Eastern Mediterranean Region, South-East Asia Region, and European Region is estimated at 3.3%, 2.0%, and 1.6% respectively (Fig. 2) (WHO 2019a). HBV genotypes and sub-genotypes have been reported to

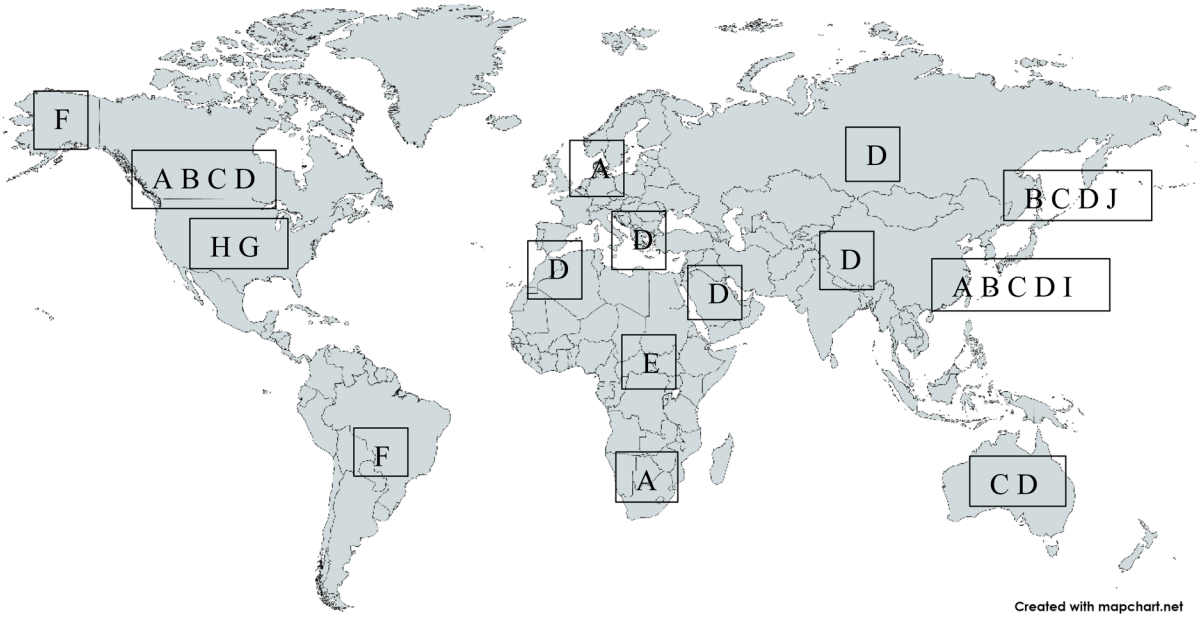

Fig. 1. Hepatitis B virus genotypes (A-J) (Paudel and Suvedi 2019).

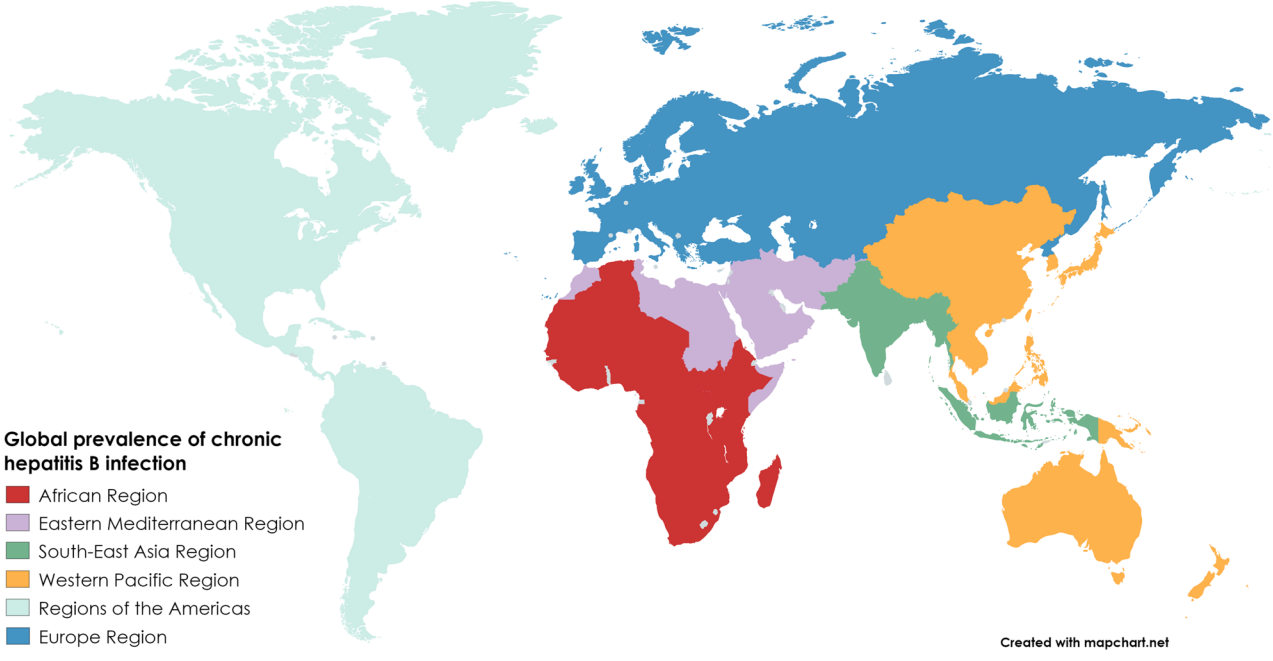

Fig. 2. Global prevalence of chronic hepatitis B infection (WHO 2019a).

effectively affect disease transmission, progression, and treatment outcome (Kmet Lunacek et al. 2017). Therefore, identifying HBV mutations and genotypes is essential for both disease manifestation and identification of individuals at risk of infection progression.

This review describes virological assays, including serological and molecular techniques for diagnosing HB infection and updates on the most effective treatment strategies against the virus for the prevention of liver progression and cirrhosis in chronic HBV carriers.

Laboratory diagnosis of hepatitis B virus

Initial assessment of HBV infection begins with patient history, physical examination, evaluation of liver disease activity, and interpretation of different hepatitis markers and/or their combinations such as HBsAg, HB core antigen (HBcAg), HBeAg, HB surface antibody (anti-HBs/HBsAb), HB core antibody (anti-HBc), anti-HBc IgM, HB e antibody (anti-HBe), and focus on the detection of antigens and antibodies (WHO 2017b). The

Hepatitis B Foundation (HBF) recommends screening all adults for HB with the triple serological marker panel that involves HBsAg, anti-HBs, and anti-HBc total (HBF 2018b). To classify the phases of the infection in HBV infected patients, the followings should be performed: i) the assays for HBsAg, HBeAg/anti-HBe, HBV DNA; ii) liver blood tests including aspartate aminotransferase (AST), alanine transaminase (ALT), and iii) transient elastography (Fibroscan) as a noninvasive test or needle liver biopsy as an invasive method for the presence of cirrhosis (EASL 2017).

HBV serological markers

Various serological assays can detect virus-specific antigens and antibodies which appear during and after HBV infection. These tests are used to determine whether a patient is susceptible to infection or immune due to passed infection or HBV vaccination (CDC 2020d). Currently, various serological diagnostic assays, including rapid diagnostic tests (RDTs) and laboratory-based immunoassays, such as enzyme immunoassays (EIAs), chemiluminescence immunoassays (CLIAs), electrochemiluminescence immunoassays (ECLs) are used (WHO 2017b). These tests can be performed with serum, plasma and/or capillary/venous whole blood and oral fluid specimens to detect the presence of antigens or antibodies against the virus with high analytical sensitivity, specificity, and accuracy (WHO 2017b). Dried blood spot (DBS) specimen may be an alternative type of specimen in settings where blood taking and RDTs laboratory testing are not available and/or accessible or from a person with poor venous access (WHO 2017b). The laboratory reports are given qualitatively or quantitatively as international units (IU) or signal per cutoff (S/Co) values (Terrault et al. 2018).

HBsAg. HBsAg is an envelope protein that is expressed on the surface of the infectious virion called Dane particles. The detection of HBsAg in the serum indicates the current HBV infection. The HBsAg positivity can be considered with a second surface antigen test before further evaluating HBV DNA in the regions with HBsAg prevalence < 0.4 (WHO 2017b). The incubation period for hepatitis is 90 days (60–150 days) after exposure to HBV, and HBsAg appears in the blood for about six weeks (1–10 weeks) after the first exposure to the virus (CDC 2005). During the immunological window period, HBsAg may disappear rapidly without the appearance of HB surface antibodies, and the IgM antibody is the only evidence of the infection during this period (Otero et al. 2018). If HBsAg positivity persists after six months, it implies the progression of a chronic infection. The quantitative immunochemiluminescence analysis is performed to evaluate HBsAg levels of CHB patients and is a useful marker for interferon alfa (IFN-α)-treated CHB patients with HBeAg negative (EASL 2017).

Anti-HBc. Detection of anti-HBc antigens confirms exposure to HBV and indicates acute, chronic, or resolved infection but not vaccine-induced immunity (Terrault et al. 2018). The presence of IgM antibodies, together with HBsAg positivity, generally indicates the acute infection that generally persists positive for not more than six months (Jackson et al. 2018). Individuals who are core-antibody positive and HB surface-antibody negative are chronically infected and show a decreased risk of HBV reactivation. There is also no clinical benefit of vaccination for the group of individuals who are positive only for core antibodies due to exposure to HBV or people who are positive for anti-HBc and anti-HBs due to immune control (Cholongitas et al. 2018; Ganczak et al. 2019).

HBeAg and anti-HBe. The presence of HBeAg correlated with active viral replication is indicative of the contagiousness of the patient. Whereas, the appearance of anti-HBe indicates the low level of viral replication and is strong evidence for infection resolution (CDC 2005). These tests are often used to determine the CHB infection phase (EASL 2017).

Anti-HBs or HBsAb. The presence of anti-HBs indicates the recovery and immunization against HB infection either by HB vaccine or prior infection. People whose first-degree relatives or sex partners are chronic carriers are recommended to be vaccinated if their triple serological screening tests are negative (EASL 2017). The anti-HBs titer should be ≥ 10 mIU/ml in order to be protective (Dini et al. 2017).

Biochemical parameters and fibrosis markers

The severity of liver fibrosis is assessed using biochemical parameters, including AST and ALT, which are enzymes released from the liver in response to damage and disease. The other biochemical parameters are gamma-glutamyl transpeptidase (GGT), alkaline phosphatase (ALP), bilirubin, serum albumin gamma globulin, full blood count, and prothrombin time (PT) (EASL 2017). When biochemical and HBV markers are inconclusive, then invasive and noninvasive methods are used to assess the stage of liver damage (EASL 2017). Since liver biopsy is an invasive, costly, and painful procedure compared to other techniques, various non-invasive methods are preferred to predict the stage of liver fibrosis and the presence of cirrhosis in CHB patients. The WHO recommends AST to platelet ratio index (APRI) calculated according to the formula: APRI = [AST/AST ULN (upper limit of normal) $\times 100$/platelet count (10^9/l] to estimate the stage

of liver fibrosis (WHO 2017b). TE is another noninvasive method; however, due to its limitations such as high cost, inaccurate results with elevated ALT levels, restriction with liver necro-inflammation, and obesity, the WHO recommends the APRI index as a relatively accurate method for predicting advanced liver fibrosis (EASL 2017; WHO 2017b; Huang et al. 2019). It has been recommended that 40 IU/ml as ULN value should be used in the APRI formula (WHO 2017b). ALT levels should also be measured in CHB patients as it correlates with disease severity. According to the WHO guidelines, the ULN ALT level is below 30 U/l and 19 U/l for men and women, respectively (WHO 2017b).

Molecular assays

The molecular diagnostic techniques are used for HBV DNA quantification, genotyping, detection of drug resistance mutations, and precore/core mutation analysis (Villar et al. 2015) Currently, UltraQual HBV PCR Assay, COBAS AmpliScreen HBV Test, Procleix Ultrio Assay, Procleix Ultrio Plus Assay, and COBAS TaqScreen MPX Test are FDA approved nucleic acids amplification tests (NATs) used for diagnosis of HB infection (FDA 2019)

HBV DNA quantification. HBV DNA quantification. HBV DNA by NAT is used to determine the infectivity of individuals and infectivity of HBsAg positive pregnant women to prevent mother to child transmission risk and reach a decision whether to treat diseases. The HBV DNA measurement with molecular technologies enables early detection of people at risk before HBsAg emerges and rules out OBI (Aghasadeghi et al. 2020). The testing of HBV DNA is also used to monitor the treatment response in CHB patients (WHO 2017b). The viral load of HBV is usually measured either in IU/ml or copies/ml by ultraviolet (UV) spectrophotometry, real-time PCR (rt-PCR), digital PCR, loop-mediated isothermal amplification (LAMP), transcription-mediated amplification (TMA), nucleic acid sequence-based amplification (NASBA), rolling circle amplification (RCA) as well as electrochemical, quartz crystal microbalance, microcantilever, and surface plasmon resonance biosensors (Liu and Yao 2015; WHO 2017b; Al-Sadeq et al. 2019; Sayan et al. 2019; Arikan and Sayan 2020). The HBV DNA level represents the disease progression, long-term results of CHB infection, and the treatment's achievement to prevent the progression of HCC. The measurement of the level of HBV DNA is recommended to be performed with a more sensitive rt-PCR assay with 10 IU/ml detection limit (EASL 2017).

HBV DNA genotyping, drug resistance, preC/core mutations. To date, ten genotypes of HBV, A to J, and more than 40 sub-genotypes that differ > 8% and 4–8% nucleotide divergence in the genome, respectively, have been identified (Al-Sadeq et al. 2019). Different genotypes and sub-genotypes show different geographical distribution and are correlated with persistence of viral load, risk of developing cirrhosis, HBsAg seroclearance, antiviral therapy response, and prognosis due to the presence of mutations (Paudel and Suvedi 2019; Wang et al. 2019). It has been known that patients infected with HBV genotype A are more likely to develop CHB infection than patients infected with genotype B, associated with the development of antiviral resistance or genotype C, associated with acute hepatitis (EASL 2017; Wang et al. 2019). HBV genotyping is not required for initial diagnosis; however, genome sequencing for evaluation of HBV genotypes and drug resistance mutations are useful parameters for patients at risk of developing HCC in order to monitor an efficient therapy (EASL 2017).

There are many genotyping systems, including reverse hybridization, restriction fragment polymorphism (RFLP), multiplex nested PCR or real-time PCR, oligonucleotide microarray chips, reverse dot blot, restriction fragment mass polymorphism (RFMP), and invader assay (Fletcher et al. 2019). Molecular identification of HBV genotypes could also be done by sequencing the whole HBV genome, followed by phylogenetic analysis. Phylogenetic analysis is performed by constructing a phylogenetic tree with nucleotide sequences of the entire HBV genome to characterize different HBV genotypes and subgenotypes. A web-based program available through the National Center of Biotechnology Information is used that enables us to make the comparison between the newly obtained HBV sequences with the reference sequences available in GenBank. BLAST or FASTA are tools for searching similar sequences available in the EBI web site (http://www.ebi.ac.uk/Tools/homology.html) (Schreiber 2007).

The whole-genome sequences of different HBV strains are aligned, and the phylogenetic tree is constructed using distance methods including neighboring joining (NJ), un-weighted pair-group using arithmetic averages (UPGMA) or character-based techniques including maximum parsimony (MP) and maximum likelihood (ML) (Rozanov et al. 2004; Schreiber 2007). The similarity method is considered the "gold standard" approach for genotyping and sub-genotyping and can be performed on individual genes on the HBV S gene instead of the complete genome. However, the partial sequencing (HBV S gene) allows determining only the HBV genotype, not the HBV sub-genotype (Pourkarim et al. 2014).

Apart from HBV genotyping, HBV drug resistance mutations are also tested by using sequence-based assays. Several sequence-based assays such as line

probe assay have been developed; however, due to its accuracy, the Sanger sequencing of the PCR amplicon from the HBV reverse transcriptase region is accepted as a "gold standard". Real-time PCR reduces the risk of contamination due to its applicability and speed. Therefore, it is widely used to detect drug resistance mutations (Mou et al. 2016).

Treatment of hepatitis B virus infection

The treatment's primary goal is to save lives by decreasing liver cancer death, liver transplant, slow or reverse liver disease progression, and infectivity (Terrault et al. 2018). Nowadays, there are currently seven approved drugs: two formulations of IFN-standard and pegylated interferon (Peg IFN), and five nucleos(t)ide analogs (NUC): lamivudine (LAM), telbivudine, entecavir (ETV), adefovir (ADV), and tenofovir (TDF) (Lok et al. 2016). Guidelines suggest either standard or Peg IFN-α (IFN-a) immunomodulators such as standard or Peg IFN-α (IFN-a), or NUCs such as LAM adefovirdipivoxil, ETV, TDF, or telbivudine as treatment alternatives for CHB patients (Manzoor et al. 2015).

IFN-α is a host defense against HBV infections by interferon-stimulated genes (ISGs), which have immoral antiviral functions against a variety of viruses (Liang et al. 2015). Some studies have shown that in 76–94% of individuals, the treatment response is extended and is associated with more confirmatory clinical outcomes in terms of liver-related complications and survival (Niederau et al. 1996).

IFN-α-2a/b was the first certified treatment choice for CHB infection, and it replaced the standard IFN-α-2b because of pharmacokinetic properties. The pegylation is used to increase the half-life of interferon (Lok and McMahon 2009). The study reported that the treatment accomplishment percentage of Pegasys is 24% compared to 12% standard interferon (Cooksley et al. 2003). LAM is a cytidine NUC that prevents the reverse transcriptase enzyme of HBV; however, the resistance rates due to mutations in the YMDD locus of HBV polymerase is high (Chan et al. 2007; Manzoor et al. 2015). Hepsera is the tradename for adefovirdipivoxil, and ADV is a NUC. Hepsera has some side effects, including rash, swelling of the throat, lips, tongue, face, difficulty breathing, and proximal kidney tubular dysfunction (Ho et al. 2015). Despite side effects, the resistance rate of ADV is lower compared to LAM (Innaimo et al. 1997). Baraclude or ETV is a potent inhibitor of HBV's DNA polymerase enzyme, and resistance is rarely observed (Lai et al. 2006; Manzoor 2015).

Recommendations for the treatment of HBV/HIV (Human immunodeficiency)-coinfected persons are based on the WHO 2013 combine guidelines, which was updated in 2015, on the use of antiretroviral drugs for treating and preventing HIV infection. Interferon or Peg IFN as antiviral therapy was eliminated from these guidelines because their use is restricted in LMICs due to its high cost and significant adverse effects that need careful monitoring (WHO 2015). In addition, Peg-IFN was found to have only about 20% sustained non-treatment response in terms of viral suppression and low HBsAg loss and seroconversion rates (Lin et al. 2016).

New generation NUCs act by inhibiting HBV DNA replication by normalizing ALT levels. Unfortunately, NUC's use relies on long-term therapy and induces drug-related mutant infection (Tsuge et al. 2013). NUCs rarely eliminate all of the chronic HBV infection and HBV replication (Jeng et al. 2010). In recent years, NUCs or IFN monotherapy or combination therapy in CHB treatment have been investigated to minimize the therapies (Scaglione and Lok 2012). Since the combination of NUCs and IFN can inhibit more than one step of the HBV lifecycle than mainly targeting the reverse transcriptase step by NUCs monotherapy (Wei et al. 2015). Benefits and limitations of antiviral drugs used against for HBV infection are given in Table I (Abdul Basit et al. 2017).

The chemical name of TAF is L-alanine, [(S)[[(1R)-2-(6-amino-9H-purine-9yl)-1 (methylethoxy]methyl] phenoxyphosphinyl]-1-methyl ethyl ester, (2E)-2-butenedioate (Gilead Sciences 2015). TAF pharmacokinetics are linear and dose-dependent. According to the 28-day phase 1b study, which assessed antiviral activity, safety, and pharmacokinetics in CHB patients, TAF was found to be well-tolerated and safe. However, some side-effects, including headache, nausea, fatigue, cough, and constipation, were also reported. The antiviral effect of TAF over the 4 weeks was demonstrated by changes in serum HBV DNA levels of the treated patient groups in the same study (Agarwal et al. 2015).

Conclusions

The review summarized the serological, molecular diagnosis techniques, and current treatment strategies for HBV infection. The initial diagnosis with the serological assays is used to detect HBsAg and other HBV antigens and antibodies. Next, molecular assays are performed to verify the first step of diagnosis, quantify HBV viral load, and identify HBV genotypes and determine drug resistance mutation. Although molecular assays are frequently preferred due to their high sensitivity, high cost, the need for experienced personnel, and numerous equipment for analysis are the main limitations of molecular analysis. In the future, there is a need for new technologies such as biosensors that provide faster time to result with not only high specific-

ity, sensitivity, and low cost but also low false positive/negative ratio that can play a significant role in screening, diagnosis, and management of HBV infection. Additional technologies may also help to develop new treatment targets. A combination of the HBV therapies and small-molecule drugs or biologics will be necessary to control the HBV infection effectively.

Conflict of interest

The authors do not report any financial or personal connections with other persons or organizations, which might negatively affect the contents of this publication and/or claim authorship rights to this publication.

Literature

Abdul Basit S, Dawood A, Ryan J, Gish R. Tenofovir alafenamide for the treatment of chronic hepatitis B virus infection. Expert Rev Clin Pharmacol. 2017 Jul 03;10(7):707–716. https://doi.org/10.1080/17512433.2017.1323633

Agarwal K, Fung SK, Nguyen TT, Cheng W, Sicard E, Ryder SD, Flaherty JF, Lawson E, Zhao S, Subramanian GM, et al. Twenty-eight day safety, antiviral activity, and pharmacokinetics of tenofovir alafenamide for treatment of chronic hepatitis B infection. J Hepatol. 2015 Mar;62(3):533–540. https://doi.org/10.1016/j.jhep.2014.10.035

Aghasadeghi MR, Aghakhani A, Mamishi S, Bidari-Zerehpoosh F, Haghi Ashtiani MT, Sabeti S, Banifazl M, Karami A, Bavand A, Ramezani A. No evidence of occult HBV infection in population born after mass vaccination. Wien Med Wochenschr. 2020 Jun; 170(9–10):218–223. https://doi.org/10.1007/s10354-020-00748-z

Al-Qahtani AA, Al-Anazi MR, Nazir N, Abdo AA, Sanai FM, Al-Hamoudi WK, Alswat KA, Al-Ashgar HI, Khan MQ, Albenmousa A, et al. The correlation between hepatitis B virus Precore/core mutations and the progression of severe liver disease. Front Cell Infect Microbiol. 2018 Oct 22;8:355. https://doi.org/10.3389/fcimb.2018.00355

Al-Sadeq DW, Taleb SA, Zaied RE, Fahad SM, Smatti MK, Rizeq BR, Al Thani AA, Yassine HM, Nasrallah GK. Hepatitis B virus molecular epidemiology, host virus interaction, co infection, and laboratory diagnosis in the MENA Region: an Update. Pathogens. 2019 May 11;8(2):63. https://doi.org/10.3390/pathogens8020063

Ambachew H, Zheng M, Pappoe F, Shen J, Xu Y. Genotyping and sero-virological characterization of hepatitis B virus (HBV) in blood donors, Southern Ethiopia. PLoS One. 2018 Feb 20;13(2):e0193177. https://doi.org/10.1371/journal.pone.0193177

Arikan A, Şanlidağ T, Süer K, Sayan M, Akçali S, Güler E. [Molecular epidemiology of hepatitis B virus in Northern Cyprus] (in Turkish). Mikrobiyol Bul. 2016 Jan 7;50(1):86–93. https://doi.org/10.5578/mb.10292

Arikan A, Sayan M, Sanlidag T, Suer K, Akcali S, Guvenir M. Evaluation of the pol/S gene overlapping mutations in chronic hepatitis B patients in Northern Cyprus. Pol J Microbiol. 2019 Sep; 68(3):317–322. https://doi.org/10.33073/pjm-2019-034

Arikan A, Sayan M. Comparison of Qiagen and Iontek hepatitis B virus DNA polymerase chain reaction quantification kits in chronic hepatitis B patients infected with hepatitis B genotype D. Viral Hepat J. 2020 Apr 28;26(1):9–13. https://doi.org/10.4274/vhd.galenos.2020.2019.0024

CDC. Interpretation of hepatitis B serological test results [Internet]. Atlanta (USA): Centers for Disease Control and Prevention; 2005 [cited 2020]. Available from https://www.cdc.gov/HEPATITIS/HBV/PDFs/SerologicChartv8.pdf

CDC. Morbidity and mortality weekly report recommendations and report. Centers for Disease Control and Prevention. 2018;67(1):1–32.

CDC. Interpretation of hepatitis B serological tests results [Internet]. Atlanta (USA): Centers for Disease Control and Prevention; 2020a [cited 2020 Mar]. Available from https://www.cdc.gov/hepatitis/hbv/index.htm

CDC. Hepatitis B questions and answers for public health professionals [Internet]. Atlanta (USA): Centers for Disease Control and Prevention; 2020b [cited 2020 Mar]. Available from https://www.cdc.gov/hepatitis/hbv/hbvfaq.htm

CDC. Immunization schedules [Internet]. Atlanta (USA): Centers for Disease Control and Prevention; 2020c [cited 2020 Feb]. Available from https://www.cdc.gov/vaccines/schedules/hcp/imz/child-adolescent.html?CDC_AA_refVal=https%3A%2F%2Fwww.cdc.gov%2Fvaccines%2Fschedules%2Fhcp%2Fchild-adolescent.html

CDC. Interpretation of hepatitis B serological Tests results [Internet]. Atlanta (USA): Centers for Disease Control and Prevention; 2020d [cited 2020 Mar]. Available from https://www.cdc.gov/hepatitis/hbv/index.htm

Chan HL, Wang H, Niu J, Chim AM, Sung JJ. Two-year lamivudine treatment for hepatitis B e antigen-negative chronic hepatitis B: a double-blind, placebo-controlled trial. Antivir Ther. 2007;12(3): 345–353.

Cholongitas E, Haidich AB, Apostolidou-Kiouti F, Chalevas P, Papatheodoridis GV. Hepatitis B virus reactivation in HBsAg-negative, anti-HBc-positive patients receiving immunosuppressive therapy: a systematic review. Ann Gastroenterol. 2018;31(4):480–490. https://doi.org/10.20524/aog.2018.0266

Cooksley WGE, Piratvisuth T, Lee SD, Mahachai V, Chao YC, Tanwandee T, Chutaputti A, Chang WY, Zahm FE, Pluck N. Peginterferon alpha-2a (40 kDa): an advance in the treatment of hepatitis B e antigen-positive chronic hepatitis B. J Viral Hepat. 2003 Jul;10(4):298–305. https://doi.org/10.1046/j.1365-2893.2003.00450.x

de Almeida RW, Espírito-Santo MP, Sousa PSF, de Almeida AJ, Lampe E, Lewis-Ximenez LL. Hepatitis B virus DNA stability in plasma samples under short-term storage at 42°C. Braz J Med Biol Res. 2015 Jun;48(6):553–556. https://doi.org/10.1590/1414-431x20144040

Dini G, Toletone A, Barberis I, Debarbieri N, Massa E, Paganino C, Bersi F, Montecucco A, Alicino C, Durando P. Persistence of protective anti-HBs antibody levels and anamnestic response to HBV booster vaccination: A cross-sectional study among healthcare students 20 years following the universal immunization campaign in Italy. Hum Vaccin Immunother. 2017 Feb;13(2):440–444. https://doi.org/10.1080/21645515.2017.1264788

Dynavax. Hepatitis B Recombinant vaccine [Internet]. 2018 [cited 2018 Feb]. Available from https://investors.dynavax.com/static-files/f93ec0ea-c184-4afb-b2d6-98ebd0030a79

EASL. HBV 2017 Clinical practice guidelines on the management of hepatitis B virus infection [Internet]. Geneva (Switzerland): European Association for the Study of the Liver; 2017 [cited 2020 Mar]. Available from https://easl.eu/wp-content/uploads/2018/10/HepB-English-report.pdf

FDA. Hepatitis B [Internet]. Silver Spring (USA): Food and Drug Administration; 2019 [cited 2019 Apr 9]. Available from https://www.fda.gov/vaccines-blood-biologics/blood-donor-screening/hepatitis-b

Fletcher GJ, Eapen CE, Abraham P. Hepatitis B genotyping: the utility for the clinicians. Indian J Gastroenterol. 2019 Oct 15;39(4): 315–320. https://doi.org/10.1007/s12664-019-00995-y

Ganczak M, Topczewska K, Budnik-Szymoniuk M, Korzeń M. Seroprevalence of anti-HBc, risk factors of occupationally acquired HBV infection and HBV vaccination among hospital staff in Poland: a multicenter study. BMC Public Health. 2019 Dec;19(1):298. https://doi.org/10.1186/s12889-019-6628-1

Gilead Sciences. Prescribing information: VEMLIDY® (tenofovir alafenamide) [Internet]. Foster City (USA): Gilead Sciences; 2015 [cited 2020 Sep]. Available from https://www.gilead.com/-/media/files/pdfs/medicines/liver-disease/vemlidy/vemlidy_pi.pdf

Gilman C, Heller T, Koh C. Chronic hepatitis delta: A state-of-the-art review and new therapies. World J Gastroenterol. 2019 Aug 28; 25(32):4580–4597. https://doi.org/10.3748/wjg.v25.i32.4580

HBF. About the Hepatitis B Foundation. Doylestown (USA): Hepatitis B Foundation; 2018a [cited 2020 Sep 3]. Available from https://www.hepb.org/assets/Uploads/About-the-Hepatitis-B-Foundation-Fact-Sheet-final-8-28-18.pdf

HBF. Hepatitis B test [Internet]. Doylestown (USA): Hepatitis B Foundation; 2018b [cited 2020 Sep 3]. Available from https://www.hepb.org/prevention-and-diagnosis/diagnosis/hbv-blood-tests

Ho EY, Yau T, Rousseau F, Heathcote EJ, Lau GKK. Preemptive adefovir versus lamivudine for prevention of hepatitis B reactivation in chronic hepatitis B patients undergoing chemotherapy. Hepatol Int. 2015 Apr;9(2):224–230. https://doi.org/10.1007/s12072-015-9612-6

Huang D, Lin T, Wang S, Cheng L, Xie L, Lu Y, Chen M, Zhu L, Shi J. The liver fibrosis index is superior to the APRI and FIB-4 for predicting liver fibrosis in chronic hepatitis B patients in China. BMC Infect Dis. 2019 Dec;19(1):878. https://doi.org/10.1186/s12879-019-4459-4

Hyun Kim B, Ray Kim W. Epidemiology of hepatitis B virus infection in the United States. Clin Liver Dis (Hoboken). 2018 Jul;12(1): 1–4. https://doi.org/10.1002/cld.732

Innaimo SF, Seifer M, Bisacchi GS, Standring DN, Zahler R, Colonno RJ. Identification of BMS-200475 as a potent and selective inhibitor of hepatitis B virus. Antimicrob Agents Chemother. 1997 Jul;41(7):1444–1448. https://doi.org/10.1128/AAC.41.7.1444

Jackson K, Locarnini S, Gish R. Diagnostics of Hepatitis B virus: standard of care and investigational. Clin Liver Dis (Hoboken). 2018 Jul;12(1):5–11. https://doi.org/10.1002/cld.729

Jefferies M, Rauff B, Rashid H, Lam T, Rafiq S. Update on global epidemiology of viral hepatitis and preventive strategies. World J Clin Cases. 2018 Nov 6;6(13):589–599. https://doi.org/10.12998/wjcc.v6.i13.589

Jeng WJ, Sheen IS, Liaw YF. Hepatitis B virus DNA level predicts hepatic decompensation in patients with acute exacerbation of chronic hepatitis B. Clin Gastroenterol Hepatol. 2010 Jun;8(6):541–545. https://doi.org/10.1016/j.cgh.2010.02.023

Kim H, Lee SA, Do SY, Kim BJ. Precore/core region mutations of hepatitis B virus related to clinical severity. World J Gastroenterol. 2016;22(17):4287–4296. https://doi.org/10.3748/wjg.v22.i17.4287

Kırdar S, Yaşa MH, Sayan M, Aydın N. [HBV pol/S gene mutations in chronic hepatitis B patients receiving nucleoside/nucleotide analogues treatment] (in Turkish). Mikrobiyol Bul. 2019;53(2):144–155. https://doi.org/10.5578/mb.67816

Kmet Lunacek N, Poljak M, Meglic-Volkar J, Rajter M, Prah J, Lesnicar G, Selic Kurincic T, Baklan Z, Remec T, Pal E, et al. Epidemiological, virological and clinical characteristics of hepatitis B virus genotypes in chronically infected persons in Slovenia. Hepat Mon. 2017 Mar 04;17(3):e43838. https://doi.org/10.5812/hepatmon.43838

Lai CL, Shouval D, Lok AS, Chang TT, Cheinquer H, Goodman Z, DeHertogh D, Wilber R, Zink RC, Cross A, et al.; BEHoLD AI463027 Study Group. Entecavir versus lamivudine for patients with HBeAg-negative chronic hepatitis B. N Engl J Med. 2006 Mar 09;354(10):1011–1020. https://doi.org/10.1056/NEJMoa051287

Liang TJ, Block TM, McMahon BJ, Ghany MG, Urban S, Guo JT, Locarnini S, Zoulim F, Chang KM, Lok AS. Present and future therapies of hepatitis B: from discovery to cure. Hepatology. 2015 Dec;62(6):1893–1908. https://doi.org/10.1002/hep.28025

Lin CL, Yang HC, Kao JH. Hepatitis B virus: new therapeutic perspectives. Liver Int. 2016 Jan;36 Suppl 1:85–92. https://doi.org/10.1111/liv.13003

Liu YP, Yao CY. Rapid and quantitative detection of hepatitis B virus. World J Gastroenterol. 2015;21(42):11954–11963. https://doi.org/10.3748/wjg.v21.i42.11954

Lok AS, McMahon BJ, Brown RS Jr, Wong JB, Ahmed AT, Farah W, Almasri J, Alahdab F, Benkhadra K, Mouchli MA, et al. Antiviral therapy for chronic hepatitis B viral infection in adults: A systematic review and meta-analysis. Hepatology. 2016 Jan;63(1):284–306. https://doi.org/10.1002/hep.28280

Lok ASF, McMahon BJ. Chronic hepatitis B: Update 2009. Hepatology. 2009 Sep;50(3):661–662. https://doi.org/10.1002/hep.23190

Mahmood M, Anwar MA, Khanum A, Zaman N, Raza A. Distribution and clinical significance of hepatitis B virus genotypes in Pakistan. BMC Gastroenterol. 2016 Dec;16(1):104. https://doi.org/10.1186/s12876-016-0513-5

Malagnino V, Fofana DB, Lacombe K, Gozlan J. Occult hepatitis B virus infection: An old entity with novel clinical involvements. IDSA. 2018;5(10):ofy227. https://doi.org/10.1093/ofid/ofy227

Manzoor S, Saalim M, Imran M, Resham S, Ashraf J. Hepatitis B virus therapy: what's the future holding for us? World J Gastroenterol. 2015;21(44):12558–12575. https://doi.org/10.3748/wjg.v21.i44.12558

McNaughton AL, D'Arienzo V, Ansari MA, Lumley SF, Littlejohn M, Revill P, McKeating JA, Matthews PC. Insights from deep sequencing of the HBV genome-Inique,tiny, and misunderstood. Gastroenterology. 2019 Jan;156(2):384–399. https://doi.org/10.1053/j.gastro.2018.07.058

Mou Y, Athar MA, Wu Y, Xu Y, Wu J, Xu Z, Hayder Z, Khan S, Idrees M, Nasir MI, et al. Detection of anti-hepatitis B virus drug resistance mutations based o multicolor melting curve analysis. J Clin Microbiol. 2016 Nov;54(11):2661–2668. https://doi.org/10.1128/JCM.00439-16

Niederau C, Heintges T, Lange S, Goldmann G, Niederau CM, Mohr L, Häussinger D. Long-term follow-up of HBeAg-positive patients treated with interferon alfa for chronic hepatitis B. N Engl J Med. 1996 May 30;334(22):1422–1427. https://doi.org/10.1056/NEJM199605303342202

Otero W, Parga J, Gastelbondo J. Serology of hepatitis B virus: multiple scenarios and multiple exams. Rev Col Gastroenterol. 2018; 33(4):404–413. http://doi.org/10.22516/25007440.327

Paudel D, Suvedi S. Hepatitis B genotyping and clinical implications. London (UK): IntechOpen; 2019. http://doi.org/10.5772/intechopen.82492

Pourkarim MR, Amini-Bavil-Olyaee S, Kurbanov F, Van Ranst M, Tacke F. Molecular identification of hepatitis B virus genotypes/subgenotypes: revised classification hurdles and updated resolutions. World J Gastroenterol. 2014;20(23):7152–7168. https://doi.org/10.3748/wjg.v20.i23.7152

Rajoriya N, Combet C, Zoulim F, Janssen HLA. How viral genetic variants and genotypes influence disease and treatment outcome of chronic hepatitis B. Time for an individualised approach? J Hepatol. 2017 Dec;67(6):1281–1297. https://doi.org/10.1016/j.jhep.2017.07.011

Razavi-Shearer D, Gamkrelidze I, Nguyen MH, Chen D-S, Van Damme P, Abbas Z, Abdulla M, Abou Rached A, Adda D, Aho I, et al.; Polaris Observatory Collaborators. Global prevalence, treatment, and prevention of hepatitis B virus infection in 2016: a modelling study. Lancet Gastroenterol Hepatol. 2018 Jun; 3(6):383–403. https://doi.org/10.1016/S2468-1253(18)30056-6

Roman S. Occult hepatitis B and other unexplored risk factors for hepatocellular carcinoma in Latin America. Ann Hepatol. 2018 Jul; 17(4):541–543. https://doi.org/10.5604/01.3001.0012.0914

Rozanov M, Plikat U, Chappey C, Kochergin A, Tatusova T. A web-based genotyping resource for viral sequences. Nucleic Acids Res. 2004 Jul 01;32 Web Server:W654–W659. https://doi.org/10.1093/nar/gkh419

Sayan M, Arikan A, Sanlidag T. Comparison of performance characteristics of DxN VERIS system versus Qiagen PCR for HBV genotype D and HCV genotype 1b quantification. Pol J Microbiol. 2019;68(1):139–143. https://doi.org/10.21307/pjm-2019-008

Scaglione SJ, Lok AS. Effectiveness of hepatitis B treatment in clinical practice. Gastroenterol. 2012;142(6):1360–1368. https://doi.org/10.1053/j.gastro.2012.01.044

Schreiber F. Phylogenetic sequence analysis. Methods course bioinformatics. 2007/08 [cited 2020]. Available from http://gobics.de/fabian/molbio_course/data/handout_phylogeny.pdf

Shaha M, Sarker PK, Hossain MS, Das KC, Jahan M, Dey SK, Tabassum S, Hashem A, Salimullah M. Analysis of the complete genome of hepatitis B virus subgenotype C2 isolate NHB17965 from a HBV infected patient. F1000 Res. 2018;7:1023. https://doi.org/10.12688/f1000research.15090.3

Terrault NA, Lok ASF, McMahon BJ, Chang KM, Hwang JP, Jonas MM, Brown RS Jr, Bzowej NH, Wong JB. Update on prevention, diagnosis, and treatment of chronic hepatitis B: AASLD 2018 hepatitis B guidance. Hepatology. 2018 Apr;67(4):1560–1599. https://doi.org/10.1002/hep.29800

Than TT, Jo E, Todt D, Nguyen PH, Steinmann J, Steinmann E, Windisch MP. High environmental stability of Hepatitis B virus and inactivation requirements for chemical biocides. J Infect Dis. 2019 Mar 15;219(7):1044–1048. https://doi.org/10.1093/infdis/jiy620

Tsuge M, Murakami E, Imamura M, Abe H, Miki D, Hiraga M, Takahashi S, et al. Serum HBV RNA and HBeAg are useful markers for the safe discontinuation of NA treatments in CHB patients. J Gastroenterol. 2013;48:1188–1204. https://doi.org/10.1007/s00535-012-0737-2

Van Damme P. Long-term protection after hepatitis B vaccine. J Infect Dis. 2016 Jul 01;214(1):1–3. https://doi.org/10.1093/infdis/jiv750

Villar LM, Cruz HM, Barbosa JR, Bezerra CS, Portilho MM, Scalioni LP. Update on hepatitis B and C virus diagnosis. World J Virol. 2015;4(4):323–342. https://doi.org/10.5501/wjv.v4.i4.323

Wang J, Zhang P, Zeng J, Du P, Zheng X, Ye X, Zhu W, Fu Y, Candotti D, Allain JP, et al. Occurrence of occult hepatitis B virus infection associated with envelope protein mutations according to anti-HBs carriage in blood donors. Int J Infect Dis. 2020 Mar; 92:38–45. https://doi.org/10.1016/j.ijid.2019.12.026

Wang W, Shu Y, Bao H, Zhao W, Wang W, Wang Q, Lei X, Cui D, Yan Z. Genotypes and hot spot mutations of hepatitis B virus in northwest Chinese population and its correlation with disease progression. BioMed Res Int. 2019 Dec 10;2019:1–9. https://doi.org/10.1155/2019/3890962

Wei W, Wu Q, Zhou J, Kong Y, You H. A better antiviral efficacy found in nucleos(t)ide analog (NA) combinations with interferon therapy than NA monotherapy for HBeAg positive chronic hepatitis B:A meta-analysis. Int J Environ Res Public Health. 2015 Aug 21; 12(8):10039–10055. https://doi.org/10.3390/ijerph120810039

WHO. Guidelines for the prevention, care and treatment of persons with chronic hepatitis B infection [Internet]. Geneva (Switzerland): World Health Organization; 2015 [cited 2020 Mar]. Available from https://www.ncbi.nlm.nih.gov/books/NBK305553/pdf/Bookshelf_NBK305553.pdf

WHO. Global Health Section Strategy on Viral Hepatitis 2016–2021 [Internet]. Geneva (Switzerland): World Health Organization; 2016 [cited 2020 Jun]. Available from https://apps.who.int/iris/bitstream/handle/10665/246177/WHO-HIV-2016.06-eng.pdf;jsessionid=BB8238CF4BF67C1B4A8A93329842962F?sequence=1

WHO. Hepatitis B vaccination has dramatically reduced infection rates among children in Europe, but more is needed to achieve elimination [Internet]. Geneva (Switzerland): World Health Organization; 2017a [cited 2020 Mar]. Available from http://www.euro.who.int/en/health-topics/communicable-diseases/hepatitis/news/news/2017/04/hepatitis-b-vaccination-has-dramatically-reduced-infection-rates-among-children-in-europe,-but-more-is-needed-to-achieve-elimination

WHO. Guidelines on hepatitis B and C testing [Internet]. Geneva (Switzerland): World Health Organization; 2017b [cited 2020 Jun]. Available from https://apps.who.int/iris/bitstream/handle/10665/254621/9789241549981-eng.pdf;jsessionid=A0864CBC8CC4C869B57151EFE7359170?sequence=1

WHO. Hepatitis B Key Facts [Internet]. Geneva (Switzerland): World Health Organization; 2019a [cited 2020 Jul]. Available from https://www.who.int/news-room/fact-sheets/detail/hepatitis-b

WHO. Hepatitis B in the WHO European region [Internet]. Geneva (Switzerland): World Health Organization; 2019b [cited 2020 Jul]. Available from http://www.euro.who.int/__data/assets/pdf_file/0007/377251/Fact-Sheet-Hepatitis-B_2019-ENG.pdf?ua=1

WHO. Hepatitis D [Internet]. Geneva (Switzerland): World Health Organization; 2020 [cited 2020 Jul]. Available from https://www.who.int/news-room/fact-sheets/detail/hepatitis-d

Wu IC, Liu WC, Chang TT. Applications of next generation sequencing analysis for the detection of hepatocellular carcinoma associated hepatitis B virus mutations. J Biomed Sci. 2018;25(51):1–12. https://doi.org/10.1186/s12929-018-0442-4

Polish Journal of Microbiology
2020, Vol. 69, No 4, 401–409
https://doi.org/10.33073/pjm-2020-049

MINIREVIEW

Biofloc Technology: Emerging Microbial Biotechnology for the Improvement of Aquaculture Productivity

MAMDOH T. JAMAL[1], MOHAMMED BROOM[1], BANDAR A. AL-MUR[2], MAMDOUH AL HARBI[1], MOHAMMED GHANDOURAH[3], AHMED AL OTAIBI[4] and MD FAZLUL HAQUE[5]*

[1] Department of Marine Biology, Faculty of Marine Sciences, King Abdulaziz University, Jeddah, Kingdom of Saudi Arabia
[2] Department of Environmental Sciences, Faculty of Meteorology, Environment and Arid Land Agriculture, King Abdulaziz University, Jeddah, Kingdom of Saudi Arabia
[3] Department of Marine Chemistry, Faculty of Marine Sciences, King Abdulaziz University, Jeddah, Kingdom of Saudi Arabia
[4] Department of Chemistry, Faculty of Science, University of Hail, Hail, Kingdom of Saudi Arabia
[5] Department of Zoology, Faculty of Biological Sciences, University of Rajshahi, Rajshahi, Bangladesh

Submitted 17 June 2020, revised 18 October 2020, accepted 19 October 2020

Abstract

With the significant increases in the human population, global aquaculture has undergone a great increase during the last decade. The management of optimum conditions for fish production, which are entirely based on the physicochemical and biological qualities of water, plays a vital role in the prompt aquaculture growth. Therefore, focusing on research that highlights the understanding of water quality and breeding systems' stability is very important. The biofloc technology (BFT) is a system that maximizes aquaculture productivity by using microbial biotechnology to increase the efficacy and utilization of fish feeds, where toxic materials such as nitrogen components are treated and converted to a useful product, like a protein for using as supplementary feeds to the fish and crustaceans. Thus, biofloc is an excellent technology used to develop the aquaculture system under limited or zero water exchange with high fish stocking density, strong aeration, and biota. This review is highlighted on biofloc composition and mechanism of system work, especially the optimization of water quality and treatment of ammonium wastes. In addition, the advantages and disadvantages of the BFT system have been explained. Finally, the importance of contemporary research on biofloc systems as a figure of microbial biotechnology has been emphasized with arguments for developing this system for better production of aquaculture with limited natural resources of water.

Key words: biofloc, BFT, aquaculture, microbes, water quality, wastes

Introduction

The rapid growth of the human population on earth has caused a significant increase in food demand. To meet this demand, the enhancement of animal protein production, which is the main source of nutrition for human consumption, is highly required. Aquaculture is the ideal source of animal proteins, which could be produced at the lowest cost and very fast. Increasing the productivity of aquaculture in vertical and horizontal expansion leads to an excessive increase of pollutants in the surrounding environment (Ahmad et al. 2017). Biofloc technology (BFT) applications are one of the best aquaculture systems and contribute to the achievement of sustainable development and desired objectives for a clean environment (Bossier and Ekasari 2017). Hargreaves (2013) defined the biofloc as "a mixture of algae, bacteria, protozoans and other kinds of particulate organic matter such as feces and uneaten feed in addition to some of zooplankton and nematodes, formed together to be an integrated and interdependent ecosystem". Moreover, biofloc systems can operate with zero or low water exchange (0.5% to 1% per day) under high stocking density of fish or shrimp, assuring it to be an ideal system for saving water exchange (Hargreaves 2013).

However, fish species such as tilapia and carps, and shrimps such as pink, brine, and pacific whiteleg shrimp that are physiologically adapted to digest microbial protein obtained from biofloc consumption are usually

* Corresponding author: MF. Haque, Department of Zoology, Faculty of Biological Sciences, University of Rajshahi, Rajshahi, Bangladesh; **e-mail: drfazlul@ru.ac.bd**

suitable for biofloc systems (Emerenciano et al. 2013; Hargreaves 2013). On the contrary, biofloc systems are not suitable for fish species such as channel catfish and hybrid striped bass as well as for prawns such as giant tiger prawn and giant freshwater prawn. They cannot tolerate low water quality due to the high concentration of solids (Hargreaves 2013; Panigrahi et al. 2019a). Biofloc is generated by adding organic carbon and high aeration, which reduces toxic dissolved nitrogen in the water, where internal waste treatment processes are emphasized and encouraged (Liu et al. 2019). Although it is a potential technology, the data on operational parameters of BFT is still inadequate. Hence, there is an urgent need for more applied research on operational parameters of BFT to optimize the system, such as immunological effects, microbial associated molecular patterns production, and nutrient recycling (Bossier and Ekasari 2017). Hence, this review has been designed to highlight the application of biofloc systems and urge the development of this system to produce more aquaculture products without any pollution to the environment and with limited natural resources of water and land.

Development of biofloc technology as a novel microbial biotechnology

Microbial biotechnology, which deals with applying microorganisms to ensure the security, safety, and usefulness of foods, yielding high-quality products, proper human nutrition, and defense against plant and animal diseases, is still rising with different new technologies for sustainable development in the agricultural field. Nevertheless, uses of microbial biotechnology for sustainable development in aquaculture are critical because of the essential role of microorganisms in the establishment and control of ecosystem facilities, especially nutrient cycling, water quality control, and disease regulation in the culture system (Timmis et al. 2017). Although, several microbial biotechnologies have been applied or are still in the developmental pipeline to increase the productivity in aquaculture by creating the ecofriendly environment to support the growth of other aquatic organisms. These organisms are key agents of pollutant removal and recycling (Bossier and Ekasari 2017; Kabir and Aba 2019; Liu et al. 2019). BFT is one of such novel microbial biotechnologies that has been developed with an excellent ecofriendly technology not only for higher productivity but also for sustainable development (Emerenciano et al. 2017; Abakari et al. 2020a) (Table I). The scientific concepts of BFT grew concomitantly and independently by two groups of researchers. Steve Hopkins led one at the Waddell Mariculture Center, South Carolina, and the other group was led by Avnimelech in Israel (Hopkins et al. 1993; Avnimelech et al. 1994). In both cases, the concepts of active microbial suspension and heterotrophic feed web were used to generate an intensive microbial community for degradation and assimilation of organic residues gathering in the pond in no or limited water exchange condition, which replaced the conventional external biofilter or high water exchange systems in aquaculture (Hopkins et al. 1993; Avnimelech et al. 1994). In BFT, the microbes work for regulation of water quality through the control of nitrogen, resulting in the enhancement of the microbial proteins, which functions as a source of nutrition for aquaculture species. Moreover, the microbes in BFT play a vital role in biosecurity by inhibiting the pathogenic microorganisms' growth (Emerenciano et al. 2017). For example, heterotrophic bacteria such as *Bacillus* spp. that were used as probiotics for bio-augmentation of biofloc enhanced immunity in the Indian white shrimp against pathogenic microorganisms resulting in better growth, survival, and productivity of the shrimp (Panigrahi et al. 2020). Similarly, recent improvements in biofloc-dominated, super-intensive, limited-discharge systems for raising Pacific whitelegs prawn ensure higher biosecurity from viral and bacterial disease outbreaks (Samocha et al. 2012; Prangnell et al. 2020). In a study, the polyphenols isolated from the chestnut (*Castanea sativa*) were supplemented in BFT for the culture of Nile tilapia. It resulted in an enhanced mucosal and serum immunity against pathogenic *Streptococcus agalactiae* (Van Doan et al. 2020). Likewise, Jaggery-based BFT (Jaggery – a potential source of carbon) provided an eco-friendly environment for better bacterial assimilation and nitrification, resulting in improved water quality (Elayaraja et al. 2020). Similarly, a biochar-based BFT caused improvement of water quality through active heterotrophic bacterial assimilation and nitrification, resulting in enhanced levels of NO^{-}_{3} and total nitrogen (Abakari et al. 2020b).

Biofloc composition and work mechanism

Successful fish farming is entirely dependent on the physicochemical and biological qualities of water. Consequently, water quality control is required for optimum ponds management (Sharma et al. 2018). Some studies suggest that the ratio between nitrogen (N) and carbon (C) in the water during the period of aquaculture should be controlled by implementing successful biofloc technology (Avnimelech 2009). Thus, the BFT is an integrated system (Fig. 1), and the quality of this system, which depends on the biotic composition of biofloc and the quantity of suspended solids, is checked with Imhoff cones. For checking the biotic composition of biofloc, water collected from the system is reserved in Imhoff cones for precipitation. After

Table I
Recent use of biofloc technology (BFT) in fish and prawn culture.

Fish/Prawn species cultured	Technology used	Effect on culture water	Effects on fish/prawn	References
Mullet (*Mugil liza*); Shrimp (*Litopenaeus vannamei*)	BFT in integrated cultivation	Modified bacterial nitrification; reduced total suspended solids	Enhanced growth of mullet, but impaired shrimp's growth	(Holanda et al. 2020)
Nile tilapia (*Oreochromis niloticus*)	Jaggery-based BFT	Enhanced bacterial assimilation and nitrification; boosted ammonia immobilization	Improved growth and survival; higher immunity to *A. hydrophila* infection; greater antioxidant capacity	(Elayaraja et al. 2020)
Nile tilapia (*Oreochromis niloticus*)	Biochar-based BFT	Reduced total suspended solids; active heterotrophic bacterial assimilation and nitrification; enhanced levels of NO^-_3 and total nitrogen	No remarkable negative effects of biochar on growth and physiological performance.	(Abakari et al. 2020b)
Genetically improved Nile tilapia (*Oreochromis niloticus*)	FRP tank culture with isolated probiotic bacteria from BFT	Enrichment of probiotic *Bacillus infantis*, *B. subtilis*, *Exiguobacterium profundum* and *B. megaterium*	Enhanced growth and survival; improved immunological parameters	(Menaga et al. 2020)
The Amur minnow (*Rhynchocypris lagowski*)	BFT with differential protein	No significant change in temperature, total ammonia nitrogen, total phosphorus and NO_2-N; reduced pH and dissolved oxygen	Enhanced growth; boosted immune response and digestive enzymes activity; higher expression of antioxidant-related genes	(Yu et al. 2020)
Shrimp (*Litopenaeus vannamei*)	Wheat flour-based zero-water exchange BFT	Effective recovery and sustainable water quality without sodium bicarbonate; higher bacterial diversity	Affected growth performance	(Kim et al. 2020)
Shrimp (*Litopenaeus vannamei*)	Biofloc-based super intensive tank system	Low concentrations of TAN and NO^-_2-N (< 1.0 mg/l) at late stage; higher bacterial diversity including various nitrifying bacteria in biofloc	Better growth performance in outdoor conditions than in indoors	(Xu et al. 2021)
Nile tilapia (*Oreochromis niloticus*)	Chestnut polyphenols-based BFT	No data	Improved growth performance; better survival; enhanced mucosal and serum immunity against pathogenic *Streptococcus agalactiae*	(Van Doan et al. 2020)
Nile tilapia (*Oreochromis niloticus*) juveniles	BFT with prebiotics and probiotics	Reduction of nitrite concentration	Higher rate of the specific growth, weight gain and final weight; better hematological parameters	(Laice et al. 2021)
Indian major carps, e.g., rohu (*Labeo rohita*), catla (*Catla catla*), and mrigal (*Cirrihinus mrigala*)	BFT for polyculture	Maintenance of NH_4-N, NO_2-N and NO_3-N in the acceptable range of water quality	Satisfactory growth performance (higher rate of specific growth)	(Deb et al. 2020)
Juvenile of Cachama blanca (*Piaractus brachypomus*)	BFT	Maintenance of the all parameters of water quality in the acceptable range except NH^-_4 and NO^-_2	Improved growth performance	(Sandoval--Vargas et al. 2020)
Bluegill (*Lepomis macrochirus*) juveniles	Corn starch or sucrose-sugar-based BFT	Lower number of human pathogens; raised ammonia level and reduced dissolved oxygen level	Reduced growth performance and higher mortality rate	(Fischer et al. 2020)

15 minutes of precipitation, we can see the aggregates of heterotrophic bacteria, algae, entangled zooplankton including protozoa, rotifers, diatoms, uneaten feed, other dead organic matter, and the suspended particles, all of which reflect the quality of biofloc (Sharma et al. 2018). Some additives to the water can improve the BFT system; for example, the addition of carbohydrates to reduce toxic ammonia can promote the concentration

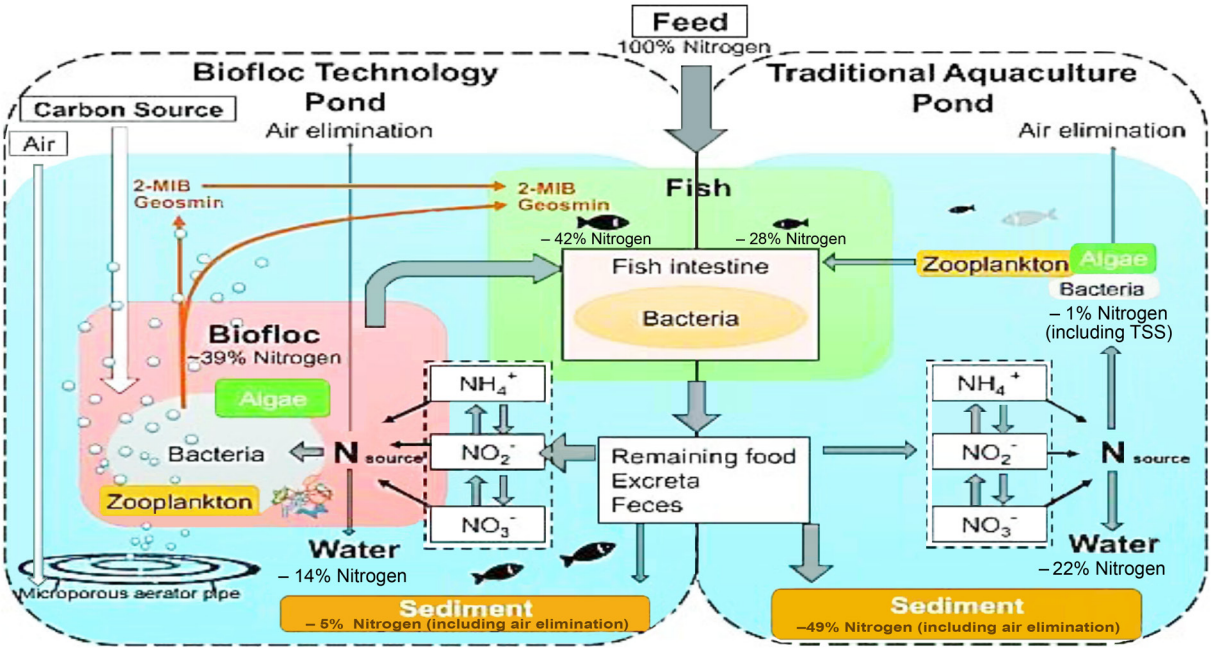

Fig. 1. Role of microbial communities in biofloc technology (BFT) to improved water quality and fish yield in freshwater indoor and outdoor pond aquaculture (Liu et al. 2019).

of microorganisms within the biofloc as well as multiplication of heterotrophic bacteria to enhance the production of proteins and to reduce the growth of pathogenic strains (Panigrahi et al. 2019b).

Biofloc is the best system for water utilization and waste treatment

Fish and shrimp ponds contain a high load of nutrients because of the vast amount of feeds. Almost 50–70% of feeds is in the water or in the sediment, thus resulting in water quality deterioration due to the imbalance of carbon and nitrogen in the culture pond. In such fish and shrimp ponds, biofloc technology can improve water quality by balancing carbon and nitrogen in the aquaculture system by photosynthesis and nitrification processes (Crab et al. 2012). It was reported that the optimum ratio of carbon and nitrogen in biofloc could help to maintain the water quality to raise Pacific white leg shrimp in lower salinity for inland culture. In turn, it decreases the possibility of land pollution by the release of saline wastewater from the shrimp pond (Kumar et al. 2019). Furthermore, the biofloc working on enhancement of the physicochemical parameters of water to the optimum range is essential for the proper growth of fishes and shrimp (Sharma et al. 2018). A study reported that mullet (*Mugil liza*) was able to reduce total suspended solids originating from shrimp (*Litopenaeus vannamei*) culture in a BFT system by consumption of solids, but their culture in the same tank caused the decreased growth of shrimp (Holanda et al. 2020). Moreover, in the combined culture of mullet and shrimp, the nitrifying bacterial community could be modified by applying biofloc inoculum (Holanda et al. 2020). Another study revealed that the bacterial community structure in culture water and digestive tracts of shrimp *L. vannamei* were depended on the environmental factors in the wheat flour-based BFT system. Moreover, the BFT system showed the capacity for adequate recovery and sustainable water quality management without any supplementation of sodium bicarbonate (Kim et al. 2021).

In BFT, heterotrophic bacteria are the most common microbial community members forming the structure of biofloc. Simultaneously, the chemoautotrophic nitrifiers are fewer in number than other types of bacteria, which in turn leads to less efflux of nitrogen to the ecosystem of the pond. Also, actinobacteria stimulate the formation of biofloc and could be necessary for secondary benefits of protecting against fish pathogens. However, they may upsurge the accumulation of off-flavor in the fish flesh and water (Liu et al. 2019). Some additives like glucose, starch, and glycerol are preferred as carbon sources to cultivate the biofloc outdoor, and these carbon sources are not only affecting the microbial community structure and composition but also affect the number of pathogenic bacteria, for example, *Vibrio* spp. (Wei et al. 2020). Many studies have revealed that heterotrophic microbes are often induced to assimilate total ammonia nitrogen, resulting in the accumulation of comparatively higher nitrate levels in a culture system of biofloc technology (Azim et al. 2008; Nootong et al. 2011; Chen et al. 2019).

Table II
The key factors of water quality checked in BFT systems and its optimal and/or normal detected ranges (Emerenciano et al. 2017).

Factors	Normal and/or ideal detected ranges	Remarks
Temperature	28–30° (usually perfect for species in tropical region)	In addition to shrimp and fish, microbial growth might be affected by low temperatures (~ 20°C)
pH	pH 6.8 to 8.0	Optimum pH values in BFT are less than pH 7.0 but these might disturb the process of nitrification
Dissolved oxygen (DO)	Optimum level is above of 4.0 mg/l and as a minimum 60% of saturation	For precise growth and respiration of fish, shrimp and microbiota
TAN	Depend on pH, optimum level is less than 1 mg/l in pH ≤ 7.0	pH could play a vital role on toxicity values
Salinity	Optimum range relied on the cultured fish/shrimp species	It is promising to produce BFT, e.g., from 0 to 50 ppt
Alkalinity	Ideal level is greater than 100 mg/l	Greater values of alkalinity aid in assimilation of nitrogen by heterotrophic bacteria as well as assist in process of nitrification by chemoautotrophic bacteria
Nitrite	Optimum level is less than 1 mg/l	One of the critical factors (hard to regulate). Distinct attention to be required
Orthophosphate	Optimum range from 0.5 mg/l to 20 mg/l	In these ranges, usually nontoxic to the cultured fish and shrimp
Nitrate	Optimum range from 0.5 mg/l to 20 mg/l	The same as orthophosphate
Total suspended solids (TSS)	Ideal level is less than 500 mg/l	As measured in Imhoff cones, the excessive levels of TSS contributes to the DO intake by gill occlusion and heterotrophic community
Settling solids (SS)	Optimum range relied on the cultured fish/shrimp species. 5–20 ml/l for tilapia fingerlings, 5–15 ml/l for shrimp, and 20–50 ml/l for adult and juveniles tilapia	The same as TSS

Moreover, nitrifying bacteria in biofloc, such as ammonia oxidizers, oxidize ammonia to nitrite, and then nitrite oxidizers, oxidize nitrite to nitrate (Chen et al. 2006). Both nitrite and nitrate can damage aquatic animals' gill tissue, resulting in problems with respiration and/or higher mortality (Lin and Chen 2001; Kuhn et al. 2010b). Hence, some factors such as temperature, salinity, alkalinity, pH, dissolved oxygen, settling solids, total suspended solids, and orthophosphate have to be monitored continuously and practically in biofloc technology as shown in Table II (Emerenciano et al. 2017). Better water quality in BFT results from a complex interaction among different water parameters. Hence, the demand for more research in this field is increasing day by day to better understand this complex interaction of parameter of water quality to develop the aquaculture production methods.

Biofloc is a significant food source in the recirculating aquaculture system (RAS)

RAS is a modern aquaculture system that could be applied to nurture fish fingerlings in a biosecurity environment to assist in the production schemes; nevertheless, it is still obscure what kind of RAS could be the best for such activities. A comparative study on the role of RAS and BFT on the growth of *Tinca tinca* fry revealed that the microbial community in RAS and BFT was different and the microbial diversity was relatively higher in the RAS than in the BFT (Vinatea et al. 2018). In another study, the performance of the BFT versus the RAS on Nile tilapia, *Oreochromis niloticus* in monoculture and polyculture with giant freshwater prawn, *Macrobrachium rosenbergii* was evaluated. It was reported that the BFT offers better growth performance for *O. niloticus* in monoculture and in polyculture with *M. rosenbergii* compared to RAS (Hisano et al. 2019).Thus, both RAS and BFT systems play a significant role optimizing the growth performance of aquatic animals resulting in the reduction of their production expenses (Fleckenstein et al. 2018). Nevertheless, fossil fuel-based RAS increases both the operational cost and the bad environmental impact because of its high energy requirements (Badiola et al. 2018). The development of renewable energy-based, more efficient RAS and its integration with other systems could be a favorable choice. Hence, integrating RAS and biofloc systems in aquaculture would be promising to enhance their positive features through combined effects. Moreover, biofloc itself is a protein-rich

live natural feed formed as a result of the conversion of unused feed and excreta in an aquaculture system upon exposure to sunlight. In a biofloc system, the loose matrix of mucus, which is secreted by various microbes, assists in linking each floc together, which is bound by electrostatic attraction or filamentous microbes form a large floc. The large flocs, which are easily consumed by fish can be observed by the bare eyes, but the maximum flocs are minute in size ranging from 45 to 250 microns. Some technical studies reported that some aquaculture animals preferred the consumption of microbial biofloc generated in BFT systems instead of consumption of processed biofloc as a feed component (Kuhn et al. 2009; Kuhn et al. 2010a; Anand et al. 2014; Bossier and Ekasari 2017). Moreover, BFT application in larvae culture may provide an easily accessible food source for the larvae of Nile tilapia (*O. niloticus*) between different feeding times and reduce the possible harmful competition during feeding (Ekasari et al. 2015). Similarly, a marked improvement in the growth of the juveniles of Nile tilapia was observed when they were reared with biofloc and compared with the others in control without biofloc (Durigon et al. 2020). Thus, the better growth performance of the aquaculture animals is resulted from the adequate nutritional value of biofloc, especially for high content of proteins and fat as their dry weight ranges from 25–50% and 0.5–15%, respectively. It is also a good source of vitamins and minerals, particularly phosphorous (Verster 2017). Because of good nutritional quality, the dried biofloc is proposed as an ingredient to replace the fishmeal or soybean partially in the feed for aquaculture; but the availability and diversity of dried biofloc are limited. Moreover, biofloc is also a probiotic source and has a probiotic-like beneficial effect in aquaculture production (Ferreira et al. 2015; Vikaspedia 2019; Jamal et al. 2020). Altogether, in an integrated system of BFT and RAS, excessive feeds which are used for the rapid growth of cultured animals would be converted more efficiently into microbial biomass, which in turn can be consumed as food by the animals resulting in less pollution of water (Choo and Caipang 2015).

Biofloc is a safe, integrated aquaculture system for higher productivity

The high-density fish and shrimp culture usually demand a waste treatment infrastructure, and biofloc is the best waste treatment system. It was revealed that BFT systems could be efficiently applied to upsurge fish production by establishing an encouraging relationship between biofloc and fish density, which showed a higher capacity to recycle nitrogenous waste at high culture densities (4 million fishes per ha) (Park et al. 2017). Moreover, BFT systems are suitable for achieving aquaculture with an intensive aeration, low or no exchange of water, higher stocking densities and organic input, heavy mixing and an additional advantage of the generation of an additional feed source for some species well-suited for these conditions. However, BFT was developed to secure fish rearing ponds from diseases caused by the pathogens available in incoming water (Hargreaves 2013). It was reported that Jaggery-based BFT enhanced the immunity of Nile tilapia against the pathogenic *Aeromonas hydrophila* infection through upregulation of various immune-cells, immune-related genes and enzymes, and antioxidant capacity. Thus, Jaggery-based BFT was capable of increasing the growth performances and the survival rate of Nile tilapia (Elayaraja et al. 2020). Another study revealed that the probiotic bacteria viz. *Bacillus infantis*, *Bacillus subtilis*, *Exiguobacterium profundum* and *Bacillus megaterium* isolated from BFT were able to enhance growth performance and survival rate of genetically improved Nile tilapia while cultured in 500 l FRP tank. However, *B. subtilis* and *B. megaterium* showed better antioxidant and immunological capacity than the remaining two strains (Menaga et al. 2020). Likewise, the intensive cultivation of Nile tilapia can be established by using water discharged from biofloc systems during the growing period without negative effects on fish survival and productive performance (Gallardo-Collí et al. 2019). The discharge water from the BFT system could be a good source of a healthy microbial community. It was reported that the beneficial microorganisms, which were liable for nitrogen conversion, showed the diverse and dense growth in the water column of intensive, minimal-exchange production systems. Moreover, a part of the beneficial microbiota was linked with particles of biofloc, and the density of these particles could be regulated to some degree to increase production (Ray et al. 2011). A study revealed that the aquaculture performance of the shrimp *Marsupenaeus japonicus* in a high-intensive, zero exchange farming system was improved by biofloc technology, and this high performance might be related to the biodiversity of microbial flora (Zhao et al. 2012). Furthermore, biofloc particle size has played a vital role in some aquaculture species' nutritional quality and productivity. It was demonstrated that the combination of BFT with an integrated culture system resulted in lower suspended solids, higher biomass production, enhanced total feed efficiency, and higher nitrogen and phosphorus recovery (Ekasari 2014).

Advantages and strengths of biofloc technology

BFT has many benefits that distinguish it from many other advanced fish farming systems, such as an eco-friendly culture system with zero drain water after cul-

ture. BFT is dominated over other systems because of its higher capacity for reduction of environmental impact, improvement of effective use of land and water, maintenance of the suitable quality of water with minimal water usage and exchange within the rearing ponds, and production of protein-rich biofloc as a supplementary feed for aquatic organisms (Reddy 2019). Likewise, Arias-Moscoso et al. (2018) stated that biofloc could ensure clean water and higher biosecurity by reduction of wastewater pollution as well as lowering the risk of introduction and spread of diseases and pathogens. Moreover, BFT enhances survival rate, growth performance, and feed conversion in fish culture systems, urging its application as a more economical alternative to other culture systems. Because of the generation of biofloc as non-costly and adequate feed, BFT also reduces the need to utilize protein-rich feed resulting in the cost-effective production of cultured animals. Thus, BFT also reduces the burden on capturing fisheries to market cheaper food fish and trash fish for the fishmeal industry (Reddy 2019).

Disadvantages and weaknesses of biofloc technology

There are many weaknesses in the biofloc system, such as the urgent need for high aeration and water movement, which leads to the increased energy requirement for mixing and aeration. Furthermore, several disadvantages are also reported for BFT, such as reduced response time because of consumption of dissolved oxygen in the water and higher respiration rates, potential pollution from nitrate accumulation, and the requirement of start-up period and alkalinity supplementation (Reddy 2019). Moreover, the performance of BFT may be inconsistent and dependent on seasonal variation of the daylight period for sunlight-exposed systems (Reddy 2019). Finally, BFT has sown frequent requirements of maintenance, which sometimes may be too expensive.

Conclusions

Biofloc technology is an innovative and effective microbial biotechnology in which toxic materials such as nitrogen components can be treated and converted to a useful product like proteins, which can be used by the fish and crustaceans as supplementary feeds. It is an excellent technique to develop the aquaculture system under limited or zero water exchange with high fish stocking density, vigorous aeration, and biota formed by biofloc. BFT presented aquaculture as a sustainable tool for the environmental, social, and economic issues that synchronize with its growth. So this technique needs to be developed by more researches to keep up and maintain the aquaculture systems in the future.

Conflict of interest

The authors do not report any financial or personal connections with other persons or organizations, which might negatively affect the contents of this publication and/or claim authorship rights to this publication.

Literature

Abakari G, Luo G, Kombat EO. Dynamics of nitrogenous compounds and their control in biofloc technology (BFT) systems: A review. Aquacult Fish. 2020a;Article in Press. https://doi.org/10.1016/j.aaf.2020.05.005

Abakari G, Luo G, Meng H, Yang Z, Owusu-Afriyie G, Kombat EO, Alhassan EH. The use of biochar in the production of tilapia (*Oreochromis niloticus*) in a biofloc technology system – BFT. Aquacult Eng. 2020b Nov;91:102123. https://doi.org/10.1016/j.aquaeng.2020.102123

Ahmad I, Babitha Rani AM, Verma AK, Maqsood M. Biofloc technology: an emerging avenue in aquatic animal healthcare and nutrition. Aquacult Int. 2017 Jun;25(3):1215–1226. https://doi.org/10.1007/s10499-016-0108-8

Anand PSS, Kohli MPS, Kumar S, Sundaray JK, Roy SD, Venkateshwarlu G, Sinha A, Pailan GH. Effect of dietary supplementation of biofloc on growth performance and digestive enzyme activities in *Penaeus monodon*. Aquaculture. 2014 Jan;418–419:108–115. https://doi.org/10.1016/j.aquaculture.2013.09.051

Arias-Moscoso JL, Espinoza-Barrón LG, Miranda-Baeza A, Rivas-Vega ME, Nieves-Soto M. Effect of commercial probiotics addition in a biofloc shrimp farm during the nursery phase in zero water exchange. Aquacult Rep. 2018 Aug;11:47–52. https://doi.org/10.1016/j.aqrep.2018.06.001

Avnimelech Y, Kochva M, Diab S. Development of controlled intensive aquaculture systems with a limited water exchange and adjusted carbon to nitrogen ratio. Isr J Aquacult Bamidgeh. 1994; 46(3):119–131.

Avnimelech Y. Biofloc technology: a practical guide book. Sorrento (USA): World Aquaculture Society; 2009.

Azim ME, Little DC, Bron JE. Microbial protein production in activated suspension tanks manipulating C:N ratio in feed and the implications for fish culture. Bioresour Technol. 2008 Jun; 99(9): 3590–3599. https://doi.org/10.1016/j.biortech.2007.07.063

Badiola M, Basurko OC, Piedrahita R, Hundley P, Mendiola D. Energy use in recirculating aquaculture systems (RAS): A review. Aquacult Eng. 2018 May;81:57–70. https://doi.org/10.1016/j.aquaeng.2018.03.003

Bossier P, Ekasari J. Biofloc technology application in aquaculture to support sustainable development goals. Microb Biotechnol. 2017 Sep;10(5):1012–1016. https://doi.org/10.1111/1751-7915.12836

Chen S, Ling J, Blancheton JP. Nitrification kinetics of biofilm as affected by water quality factors. Aquacult Eng. 2006 May;34(3): 179–197. https://doi.org/10.1016/j.aquaeng.2005.09.004

Chen X, Luo G, Meng H, Tan H. Effect of the particle size on the ammonia removal rate and the bacterial community composition of bioflocs. Aquacult Eng. 2019 Aug;86:102001. https://doi.org/10.1016/j.aquaeng.2019.102001

Choo HX, Caipang CMA. Biofloc technology (BFT) and its application towards improved production in freshwater tilapia culture. Aquacult Aquarium Conserv Legis. 2015;8(3):362–366.
Crab R, Defoirdt T, Bossier P, Verstraete W. Biofloc technology in aquaculture: beneficial effects and future challenges. Aquaculture. 2012 Aug;356–357:351–356.
https://doi.org/10.1016/j.aquaculture.2012.04.046
Deb S, Noori MT, Rao PS. Application of biofloc technology for Indian major carp culture (polyculture) along with water quality management. Aquacult Eng. 2020 Nov;91:102106.
https://doi.org/10.1016/j.aquaeng.2020.102106
Durigon EG, Lazzari R, Uczay J, Lopes DLA, Jerônimo GT, Sgnaulin T, Emerenciano MGC. Biofloc technology (BFT): adjusting the levels of digestible protein and digestible energy in diets of Nile tilapia juveniles raised in brackish water. Aquacult Fish. 2020 Jan;5(1):42–51. https://doi.org/10.1016/j.aaf.2019.07.001
Ekasari J, Rivandi DR, Firdausi AP, Surawidjaja EH, Zairin M Jr, Bossier P, De Schryver P. Biofloc technology positively affects Nile tilapia (*Oreochromis niloticus*) larvae performance. Aquaculture. 2015 Apr;441:72–77.
https://doi.org/10.1016/j.aquaculture.2015.02.019
Ekasari J. Biofloc technology as an integral approach to enhance production and ecological performance of aquaculture. Ghent (Belgium): Ghent University; 2014.
Elayaraja S, Mabrok M, Algammal A, Sabitha E, Rajeswari MV, Zágoršek K, Ye Z, Zhu S, Rodkhum C. Potential influence of jaggery-based biofloc technology at different C:N ratios on water quality, growth performance, innate immunity, immune-related genes expression profiles, and disease resistance against *Aeromonas hydrophila* in Nile tilapia (*Oreochromis niloticus*). Fish Shellfish Immunol. 2020 Dec;107 Pt A:118–128.
https://doi.org/10.1016/j.fsi.2020.09.023
Emerenciano MGC, Gaxiola G, Cuzon G. Biofloc technology (BFT): a review for aquaculture application and animal food industry. In: Matovic MD, editor. Biomass now-cultivation and utilization. London (UK): IntechOpen; 2013. p. 301–328.
https://doi.org/10.5772/53902
Emerenciano MGC, Martínez-Córdova LR, Martínez-Porchas M, Miranda-Baeza A. Biofloc technology (BFT): a tool for water quality management in aquaculture. In: Tutu H, editor. Water Quality. London (UK): IntechOpen; 2017 Jan 18;5:92–109.
https://doi.org/10.5772/66416
Ferreira GS, Bolívar NC, Pereira SA, Guertler C, Vieira FN, Mouriño JLP, Seiffert WQ. Microbial biofloc as source of probiotic bacteria for the culture of *Litopenaeus vannamei*. Aquaculture. 2015 Nov; 448:273–279. https://doi.org/10.1016/j.aquaculture.2015.06.006
Fischer H, Romano N, Renukdas N, Egnew N, Sinha AK, Ray AJ. The potential of rearing juveniles of bluegill, *Lepomis macrochirus*, in a biofloc system. Aquacult Rep. 2020 Jul;17:100398.
https://doi.org/10.1016/j.aqrep.2020.100398
Fleckenstein LJ, Tierney TW, Ray AJ. Comparing biofloc, clearwater, and hybrid recirculating nursery systems (Part II): Tilapia (*Oreochromis niloticus*) production and water quality dynamics. Aquacult Eng. 2018 Aug;82:80–85.
https://doi.org/10.1016/j.aquaeng.2018.06.006
Gallardo-Collí A, Pérez-Rostro CI, Hernández-Vergara MP. Reuse of water from biofloc technology for intensive culture of Nile tilapia (*Oreochromis niloticus*): effects on productive performance, organosomatic indices and body composition. Int Aquatic Research. 2019 Mar;11(1):43–55.
https://doi.org/10.1007/s40071-019-0218-9
Hargreaves JA. Biofloc production systems for aquaculture. Stoneville (USA): Southern Regional Aquaculture Center; 2013. p. 1–11.
Hisano H, Barbosa PTL, Hayd LA, Mattioli CC. Evaluation of Nile tilapia in monoculture and polyculture with giant freshwater prawn in biofloc technology system and in recirculation aquaculture system. Int Aquatic Research. 2019 Dec;11(4):335–346.
https://doi.org/10.1007/s40071-019-00242-2
Holanda M, Santana G, Furtado P, Rodrigues RV, Cerqueira VR, Sampaio LA, Wasielesky W Jr, Poersch LH. Evidence of total suspended solids control by *Mugil liza* reared in an integrated system with pacific white shrimp *Litopenaeus vannamei* using biofloc technology. Aquacult Rep. 2020 Nov;18:100479.
https://doi.org/10.1016/j.aqrep.2020.100479
Hopkins JS, Hamilton RD, Sandier PA, Browdy CL, Stokes AD. Effect of water exchange rate on production, water quality, effluent characteristics and nitrogen budgets of intensive shrimp ponds. J World Aquacult Soc. 1993 Sep;24(3):304–320.
https://doi.org/10.1111/j.1749-7345.1993.tb00162.x
Jamal MT, Ahmed Sumon MA, Pugazhendi A, Al Harbi M, Hussain MA, Haque MF. Use of probiotics in commercially important finfish aquaculture. Int J Probiotics Prebiotics. 2020 Apr 07;15(1):7–21.
https://doi.org/10.37290/ijpp2641-7197.15:7-21
Kabir A. Aba M. Biofloc an ultimate solution for sustainable aquaculture in Africa [Internet]. 2019 [cited 2020 May]. Available from https://aquacultureinafrica.com/?p=1589
Kim Y-S, Kim S-E, Kim S-J, Jung H-K, Park J, Jeon YJ, Kim D-H, Kang J-H, Kim K-H. Effects of wheat flour and culture period on bacterial community composition in digestive tracts of *Litopenaeus vannamei* and rearing water in biofloc aquaculture system. Aquaculture. 2021;531:735908.
https://doi.org/10.1016/j.aquaculture.2020.735908
Kuhn DD, Boardman GD, Lawrence AL, Marsh L, Flick GJ Jr. Microbial floc meal as a replacement ingredient for fish meal and soybean protein in shrimp feed. Aquaculture. 2009 Nov;296(1–2): 51–57. https://doi.org/10.1016/j.aquaculture.2009.07.025
Kuhn DD, Lawrence AL, Boardman GD, Patnaik S, Marsh L, Flick GJ Jr. Evaluation of two types of bioflocs derived from biological treatment of fish effluent as feed ingredients for Pacific white shrimp, *Litopenaeus vannamei*. Aquaculture. 2010a May;303(1–4): 28–33. https://doi.org/10.1016/j.aquaculture.2010.03.001
Kuhn DD, Smith SA, Boardman GD, Angier MW, Marsh L, Flick GJ Jr. Chronic toxicity of nitrate to Pacific white shrimp, *Litopenaeus vannamei*: impacts on survival, growth, antennae length, and pathology. Aquaculture. 2010b Nov;309(1–4):109–114.
https://doi.org/10.1016/j.aquaculture.2010.09.014
Kumar A, Reddy A, Rani A, Rathore G, Lakra W, Jayant M. Water quality and nutrient dynamics of biofloc with different C/N ratios in inland saline water. J Animal Res. 2019 Oct 15;9(5):783–791.
https://doi.org/10.30954/2277-940X.05.2019.23
Laice LM, Corrêa Filho RAC, Ventura AS, Farias KNN, Silva ALN, Fernandes CE, Silva ACF, Barbosa PTL, de Souza AI, Emerenciano MGC, et al. Use of symbiotics in biofloc (BFT)-based Nile tilapia culture: production performance, intestinal morphometry and hematological parameters. Aquaculture. 2021 Jan;530:735715.
https://doi.org/10.1016/j.aquaculture.2020.735715
Lin YC, Chen JC. Acute toxicity of ammonia on *Litopenaeus vannamei* Boone juveniles at different salinity levels. J Exp Mar Biol Ecol. 2001 Apr;259(1):109–119.
https://doi.org/10.1016/S0022-0981(01)00227-1
Liu H, Li H, Wei H, Zhu X, Han D, Jin J, Yang Y, Xie S. Biofloc formation improves water quality and fish yield in a freshwater pond aquaculture system. Aquaculture. 2019 May;506:256–269.
https://doi.org/10.1016/j.aquaculture.2019.03.031
Menaga M, Felix S, Charulatha M, Gopalakannan A, Mohanasundari C, Boda S. *In vivo* efficiency of *Bacillus* sp. isolated from biofloc system on growth, haematological, immunological and antioxidant status of genetically improved farmed tilapia (GIFT). Indian J Exp Biol. 2020;58(10):714–721.

Nootong K, Pavasant P, Powtongsook S. Effects of organic carbon addition in controlling inorganic nitrogen concentrations in a biofloc system. J World Aquacult Soc. 2011 Jun;42(3):339–346. https://doi.org/10.1111/j.1749-7345.2011.00472.x

Panigrahi A, Das RR, Sivakumar MR, Saravanan A, Saranya C, Sudheer NS, Kumaraguru Vasagam KP, Mahalakshmi P, Kannappan S, Gopikrishna G. Bio-augmentation of heterotrophic bacteria in biofloc system improves growth, survival, and immunity of Indian white shrimp *Penaeus indicus*. Fish Shellfish Immunol. 2020 Mar;98:477–487. https://doi.org/10.1016/j.fsi.2020.01.021

Panigrahi A, Saranya C, Kumaran M, Das R. Biofloc technology: standard operating procedure. In: Vijayan kk, editor. Biofloc Technology for Nursery and Growout Aquaculture. Chennai (India): Central Institute of Brackishwater Aquaculture; 2019a. p. 22–32.

Panigrahi A, Sundaram M, Chakrapani S, Rajasekar S, Syama Dayal J, Chavali G. Effect of carbon and nitrogen ratio (C:N) manipulation on the production performance and immunity of Pacific white shrimp *Litopenaeus vannamei* (Boone, 1931) in a biofloc-based rearing system. Aquacult Res. 2019b Jan;50(1):29–41. https://doi.org/10.1111/are.13857

Park J, Roy LA, Renukdas N, Luna T. Evaluation of a biofloc system for intensive culture of fathead minnows, *Pimephales promelas*. J World Aquacult Soc. 2017 Aug;48(4):592–601. https://doi.org/10.1111/jwas.12387

Prangnell DI, Castro LF, Ali AS, Browdy CL, Samocha TM. The performance of juvenile *Litopenaeus vannamei* fed commercial diets of differing protein content, in a super-intensive biofloc-dominated system. J Appl Aquacult. 2020 May;25:1–22. https://doi.org/10.1080/10454438.2020.1766632

Ray AJ, Dillon KS, Lotz JM. Water quality dynamics and shrimp (*Litopenaeus vannamei*) production in intensive, mesohaline culture systems with two levels of biofloc management. Aquacult Eng. 2011 Nov;45(3):127–136. https://doi.org/10.1016/j.aquaeng.2011.09.001

Reddy J. Biofloc fish farming advantages, Training in India [Internet]. 2019 [cited 2020 May]. Available from https://www.agrifarming.in/biofloc-fish-farming-advantages-training-in-india

Samocha T, Schveitzer R, Krummenauer D, Morris T. Recent advances in super-intensive, zeroexchange shrimp raceway systems. Global Aquacult Advocate. 2012;15(6):70–71.

Sandoval-Vargas LY, Jiménez-Amaya MN, Rodríguez-Pulido J, Guaje-Ramírez DN, Ramírez-Merlano JA, Medina-Robles VM. Applying biofloc technology in the culture of juvenile of *Piaractus brachypomus* (Cuvier, 1818): effects on zootechnical performance and water quality. Aquacult Res. 2020 Sep;51(9):3865–3878. https://doi.org/10.1111/are.14734

Sharma A, Singh R, Bandhana, Sangotra R. Comparison of water quality and composition of bioflocs reared in indoor and outdoor conditions. Int Res J Biol Sci. 2018;7(11):1–9.

Timmis K, de Vos WM, Ramos JL, Vlaeminck SE, Prieto A, Danchin A, Verstraete W, de Lorenzo V, Lee SY, Brüssow H, et al. The contribution of microbial biotechnology to sustainable development goals. Microb Biotechnol. 2017 Sep;10(5):984–987. https://doi.org/10.1111/1751-7915.12818

Van Doan H, Hoseinifar SH, Hung TQ, Lumsangkul C, Jaturasitha S, Ehab El-Haroun, Paolucci M. Dietary inclusion of chestnut (*Castanea sativa*) polyphenols to Nile tilapia reared in biofloc technology: impacts on growth, immunity, and disease resistance against Streptococcus agalactiae. Fish Shellfish Immunol. 2020 Oct;105:319–326. https://doi.org/10.1016/j.fsi.2020.07.010

Verster N. Comparison of growth rates of tilapia species (*Oreochromis mossambicus* and *Oreochromis niloticus*) raised in a biofloc and a standard recirculating. Ghent (Belgium): Ghent University; 2017.

Vikaspedia. Biofloc culture [Internet]. Hyderabad (India): Vikaspedia; 2019 [cited 2020 May]. Available from https://vikaspedia.in/agriculture/fisheries/fish-production/ culture-fisheries/types-of-aquaculture/biofloc

Vinatea L, Malpartida J, Carbó R, Andree KB, Gisbert E, Estévez A. A comparison of recirculation aquaculture systems versus biofloc technology culture system for on-growing of fry of Tinca tinca (Cyprinidae) and fry of grey *Mugil cephalus* (Mugilidae). Aquaculture. 2018 Jan;482:155–161. https://doi.org/10.1016/j.aquaculture.2017.09.041

Wei Y, Wang A, Liao S. Effect of different carbon sources on microbial community structure and composition of ex-situ biofloc formation. Aquaculture. 2020 Jan;515:734492. https://doi.org/10.1016/j.aquaculture.2019.734492

Xu W, Xu Y, Su H, Hu X, Xu Y, Li Z, Wen G, Cao Y. Production performance, inorganic nitrogen control and bacterial community characteristics in a controlled biofloc-based system for indoor and outdoor super-intensive culture of *Litopenaeus vannamei*. Aquaculture. 2021 Jan;531:735749. https://doi.org/10.1016/j.aquaculture.2020.735749

Yu Z, Huang ZQ, Du HL, Li HJ, Wu LF. Influence of differential protein levels of feed on growth, copper-induced immune response and oxidative stress of *Rhynchocypris lagowski* in a biofloc-based system. Aquacult Nutr. 2020 Dec;26(6):2211–2224. https://doi.org/10.1111/anu.13158

Zhao P, Huang J, Wang XH, Song XL, Yang CH, Zhang XG, Wang GC. The application of bioflocs technology in high-intensive, zero exchange farming systems of *Marsupenaeus japonicus*. Aquaculture. 2012 Jul;354–355:97–106. https://doi.org/10.1016/j.aquaculture.2012.03.034

Polish Journal of Microbiology
2020, Vol. 69, No 4, 411–419
https://doi.org/10.33073/pjm-2020-042

ORIGINAL PAPER

Biofilm-Forming Ability and Effect of Sanitation Agents on Biofilm-Control of Thermophile *Geobacillus* sp. D413 and *Geobacillus toebii* E134

TUGBA KİLİC[1, 2*]

[1] Graduate School of Natural and Applied Sciences, Ankara University, Ankara, Turkey
[2] Vocational School of Health Services, Medical Laboratory Techniques Program, Gazi University, Ankara, Turkey

Submitted 11 May 2020, revised 24 August 2020, accepted 2 September 2020

Abstract

Geobacillus sp. D413 and *Geobacillus toebii* E134 are aerobic, non-pathogenic, endospore-forming, obligately thermophilic bacilli. Gram-positive thermophilic bacilli can produce heat-resistant spores. The bacteria are indicator organisms for assessing the manufacturing process's hygiene and are capable of forming biofilms on surfaces used in industrial sectors. The present study aimed to determine the biofilm-forming properties of *Geobacillus* isolates and how to eliminate this formation with sanitation agents. According to the results, extracellular DNA (eDNA) was interestingly not affected by the DNase I, RNase A, and proteinase K. However, the genomic DNA (gDNA) was degraded by only DNase I. It seemed that the eDNA had resistance to DNase I when purified. It is considered that the enzymes could not reach the target eDNA. Moreover, the eDNA resistance may result from the conserved folded structure of eDNA after purification. Another assumption is that the eDNA might be protected by other extracellular polymeric substances (EPS) and/or extracellular membrane vesicles (EVs) structures. On the contrary, DNase I reduced unpurified eDNA (mature biofilms). Biofilm formation on surfaces used in industrial areas was investigated in this work: the D413 and E134 isolates adhered to all surfaces. Various sanitation agents could control biofilms of *Geobacillus* isolates. The best results were provided by nisin for D413 (80%) and α-amylase for E134 (98%). This paper suggests that sanitation agents could be a solution to control biofilm structures of thermophilic bacilli.

Key words: *Geobacillus* sp., abiotic surfaces, biofilm, sanitation agents

Introduction

Bacteria display two modes of growth: free-living planktonic or the sessile and surface-attached within biofilms (Rumbaugh and Sauer 2020). The bacteria colonize by adhering to surfaces, growing, and forming a self-produced polymeric matrix in which microbial species may grow together as a biofilm (González-Rivas et al. 2018). Biofilm growth is observed in many industrial and indigenous areas such as dairy, water systems, maritime, dentistry, food, paper, oil, optics, and healthcare fields (Garrett et al. 2008). One of the most prevalent biofilm-forming microorganisms in dairy manufacturing is the thermophilic bacilli (Burgess et al. 2013). The presence of the bacteria is an indicator of poor plant hygiene (Burgess et al. 2013). *Geobacillus* sp. is among the most widespread contaminants of milk powders. The bacteria survive during industrial pasteurization of milk, and spores adhere to surfaces and germinate to constitute biofilms, thus resulting in spoilage of milk products (Gopal et al. 2015). In addition, *Geobacillus stearothermophilus* strains were isolated from a milk powder manufacturing plant (Burgess et al. 2013). Simultaneously, members of the *Geobacillus* genus were isolated from hot springs, geothermal soil, composts, and water (Mandic-Mulec et al. 2015). *Geobacillus toebii* was first isolated by Sung et al. (2002) from hay compost.

Biofilms have become problematic in a wide range of food industries (González-Rivas et al. 2018). Examples of biofilms' harmful effects are product spoilage, reduced production capacity, corrosion, equipment failure, pipe blockages, and infection (Garrett et al. 2008). Spoilage bacteria are responsible for nearly one-third of losses in the food chain supply (González-Rivas et al. 2018). Biofilm formation of the bacteria in food manufacturing concerns the dairy industry (Lindsay and Flint

* Corresponding author: T. Kilic, Graduate School of Natural and Applied Sciences, Ankara University, Ankara, Turkey; Vocational School of Health Services, Medical Laboratory Techniques Program, Gazi University, Ankara, Turkey; **e-mail: tubakilic84@gmail.com, tugbakilic@gazi.edu.tr**

2009). The reason behind is that thermophilic bacilli are hard to remove due to their broad temperature range of growth; they have a fast growth rate; their spores show high resistance to heat and chemicals; and they can form biofilms (Scott et al. 2007; Burgess et al. 2009; Eijlander et al. 2019). Eijlander et al. (2019) reported that *Geobacillus* spp. was identified after a heat treatment at 100°C for 30 min. Therefore, it is vital to remove the biofilms formed by the bacteria. The efficient cleaning of bacterial biofilms includes a combination of detergents, mechanical action, and sanitation agents. These regimes still appear to be the most effective way of combating *Bacillus* spp. biofilms. Biofilm control of thermophilic spore-forming bacilli can be achieved by temperature manipulation to limit growth, developing cleaning/sanitation, and treating surfaces to prevent attachment (Lindsay and Flint 2009). The cleaning processes involve the clean-in-place (CIP) system. The CIP regimes show variability in eliminating surface adherents. The cleaning chemicals play a significant role in the regime. They are based on firstly to decrease the surface population of bacteria thorough cleaning with detergent formulations, and then to kill the residual population through the application of disinfectants (Bremer et al. 2009). The primary strategy to eliminate biofilm formation is to clean and disinfect surfaces routinely before bacteria attach tightly (Shemesh and Ostrov 2020). Enzymes form an alternative for biofilm control, break up the biofilm matrix components, cause cell lysis, support biofilm degradation, and interrupt the cell-to-cell signaling (Meireles et al. 2016). Enzymatic solutions can be an eco-friendly, greener, and safe alternative for biofilm removal in the food industry (Mazaheri et al. 2020). Enzymes, including proteases, lipases, cellulases, and DNases, are frequently used (Ripolles-Avila et al. 2020). However, bacteria may be resistant to conventional treatments. Therefore, there is a need to enhance the methods and consider new strategies due to bacterial resistance's serious problem (Ripolles-Avila et al. 2019).

In our previous studies, we carried out the preliminary biofilm experiments, including pellicle formation, complex exopolysaccharide production, biofilm morphotypes, and viable biofilm cell counting on stainless steel of *Geobacillus* sp. D413 and *G. toebii* E134. We determined that the isolates were strong biofilm producers by the crystal violet binding assay (Cihan et al. 2017). The purpose of this study was to investigate the biofilm-forming abilities of *Geobacillus* strains on different abiotic surfaces and the effects of sanitation agents on the control of biofilm formation. In addition, it was aimed to screen the removal of the biofilms with DNase I, RNase A, and proteinase K enzymes and to determine the presence of eDNA in the biofilm matrix. There are very few research articles on this topic related to *Geobacillus* strains.

Experimental

Materials and Methods

Bacteria strain and culture conditions. *Geobacillus* sp. D413 was isolated from a soil sample from the hot spring (Dikili, Camur Hot Spring, Izmir, Turkey) and *G. toebii* E134 was isolated from a branch of a tree in the hot spring (Altinsu, Kozakli, Nevsehir, Turkey). The sequences of these isolates' 16S rRNA gene were registered with GenBank Accession Number FJ430040 and EU477771 for D413 and E134, respectively (Cihan et al. 2011). The isolates were primarily cultured in Tryptic Soy Agar (TSA, Merck, Germany) for 18 h at 55°C and then incubated in Tryptic Soy Broth (TSB, Merck, Germany) in a shaking incubator (170 rpm) at 55°C for 18 h and 6 h, respectively. All biofilm assays were carried out with the culture that was 6 h old in the mid-exponential growth phase, and the presence of non-sporulating vegetative cells was confirmed with phase-contrast microscopy. The inoculation process was essential to accelerate thermophilic bacilli's biofilm production capabilities by delaying their transition to the sporulation phase. The process was substantial to biofilm formation by endospore-forming thermophilic bacilli.

Effect of environmental conditions for bacterial growth. This assay was to study the influence of pH, salinity (sodium chloride, Merck, Germany), and temperature on the planktonic growth and biofilm formation. The optimal planktonic and biofilm growth of these isolates was determined at various ranges of pH (4.0 to 11.0), salinity (0 to 5%), and temperature (50 to 65°C) in 96-well polystyrene microtiter plates (LP, Italy). The bacterial growth was monitored spectrophotometrically (OD_{595} nm) at 0, 6, 18, 24, and 48 h in TSB. Furthermore, the biofilm growth was assayed with the crystal violet staining method at the end of the 48-hour incubation period. The optimal biofilm growth values were used in all other experiments. The negative controls contained only TSB.

Investigation of biofilm formation with crystal violet. The biofilm-forming ability of D413 and E134 on 96-well polystyrene microtiter plates was determined using the method of Woodward et al. (2000) and Stepanović et al. (2000) with some modifications. The wells were filled with 10 µl of culture and 90 µl of TSB without salt. The plate wells were cleaned two times with physiological saline at the end of 48 h of incubation to eliminate planktonic cells. The remaining adherent bacteria were fixed with 95% methanol (Merck, Germany) (200 µl) and incubated at room temperature. After that, the plates were emptied and air-dried. The wells were stained using 1% crystal violet (CV, Merck, Germany) for 30 min at 22°C. The plates were rinsed off with running tap water to remove the stain's surplus

and were air-dried. The dye bound to the biofilm cells was dissolved with ethanol: acetone (Merck, Germany). Finally, CV was quantified at an optical density (OD) of 595 nm using a microplate reader (BioTek Elisa reader, μQuant, Biotek Inc., USA). The negative controls contained only TSB.

Determination of the molecular weight of gDNA and eDNA. The bacterial biomass was collected after 18 h of incubation from the TSA. The biomass was dissolved with physiological saline and centrifuged. The pellet was used for gDNA isolation. The supernatant was filtered (0.22 μm membrane filter, Sartorius, France) and used for eDNA isolation. Extracellular DNA isolation was conducted partially by the method described by Wilson (2001), while gDNA isolation was done with a gDNA purification kit (Fermentas K0512, Thermo Fisher Scientific Inc., USA). Thus, gDNA and eDNA were partially purified. Ultimately, gDNA and eDNA values were measured at the absorbance values of 260 nm/280 nm with a Nanodrop spectrophotometer (Thermo Scientific NanoDrop Lite, USA). The samples were subjected to 1.5% agarose gel electrophoresis at 120 V for 45 min. After agarose gel electrophoresis, DNA products were visualized via a Quantum ST4 Gel Documentation System (Vilber Lourmat, France). The molecular weights of DNA samples were determined with the help of the Quantum-Capp software system (Vilber Lourmat, France).

Treatment of partially purified gDNA and eDNA with enzymes. In this assay, 10 μl of partially purified gDNA or eDNA sample was treated with DNase I of different concentrations (1.45, 1.7, 2.5, and 3.0 mg/ml) (Sigma-Aldrich, DN25, USA), RNase A (0.90 mg/ml) (Sigma-Aldrich, R6513, USA), and proteinase K (0.85 mg/ml) (Sigma-Aldrich, P2308, USA) for 1 h at 37°C. Then, agarose gel electrophoresis (1.5%) was applied for 45 min at 120 V, and the products were visualized with the Vilber Lourmat Quantum ST4 Gel Documentation System. The negative controls were contained in the samples not treated by the enzymes.

Treatment of mature biofilms with DNase I. This assay was conducted as defined before by Grande et al. (2010) with a few modifications. First, TSB and bacteria culture was added to a 96-well polystyrene microtiter plate and incubated at 65°C for 40 h. The plates were then depleted and washed two times with physiological saline. The biofilms were treated with 100 μl of DNase I (Sigma-Aldrich, DN25, 100 μg/ml) for 2, 4, 8, and 12 h at 37°C. The wells were cleaned and air-dried. Finally, the CV staining assay was used. The biofilm samples were treated with physiological saline for positive controls.

Determination of biofilm mass on abiotic surfaces. The bead vortexing method was applied with some modifications for the cell viability assay on various material surfaces (Giaouris and Nychas 2006). The materials were stainless steel (grade 316L), polypropylene, polystyrene, polyvinyl chloride, polycarbonate coupons (R: 14 mm), and glass slides (26 mm × 20 mm × 1 mm). For sterilization, first, the materials were treated with isopropanol (Merck, Germany) overnight and agitated with a chlorinated detergent (Johnson & Johnson, Philippines) for 30 min. Then, the materials were washed with deionized water, air-dried, and autoclaved. The sterile materials were placed into 6-well polystyrene microtiter plates containing TSB and bacteria culture, and then the plates were incubated for 48 h. After this period, the materials were removed with sterile forceps and rinsed with 4.5 ml of physiological saline to purge planktonic cells. The material's surfaces were scratched. The materials and biofilm samples were taken to the tubes containing only glass beads and were vortexed for ~ 2 min. The drop plate method was applied to calculate the number of viable cells in MI (medium) agar plates (Herigstad et al. 2001). The results were calculated as colony-forming units per unit area (cfu/cm^2) and were log-transformed (log cfu/cm^2). Negative controls were surfaces in the only TSB.

Prevention of biofilm formation using sanitation agents on polystyrene surface. Fifteen agents were used for this assay. The agents were alkaline protease (AP; Sigma P-4860, USA), protease (Sigma P-3111, USA), subtilisin (Sigma P-5380, USA), trypsin (Sigma T-2600000, USA), sodium dodecyl sulfate (SDS; Sigma L-5750, USA), α-amylase (Sigma A-4551, USA), cellulose (Sigma C-1184, USA), sodium metaperiodate (SM; Sigma 71859, USA), lysozyme (Sigma L-7651, USA), trichloroacetic acid (TCA; Sigma 27242, USA), nisin (Sigma N-5764, USA), potassium monopersulfate (PM; Sigma 228036, USA) and sodium thiosulfate (ST; Sigma 72049, USA) combination, furanone (Sigma 283754, USA), and triclosan (Sigma LRAA-1072, USA). Bacterial culture (5 μl) and TSB (95 μl) were added in 96-well polystyrene microtiter plates. After incubation, the wells were emptied and rinsed with physiological saline. The wells were treated with 15 different sanitation agents (100 μl) under suitable conditions with some modifications (Table I). Again, the wells were emptied and washed. Finally, the CV staining assay was applied to the wells. Wells containing only the suitable solvent without sanitation agents served as the positive control. The results were calculated using the formula of Pitts et al. (2003).

Statistical analysis. All the experiments were conducted in three replicates on three independent days, and the means and the standard deviations were calculated. In the evaluation of the results obtained with the SPSS 17.0 statistical program (SPSS Inc., USA), one-way analysis of variance (ANOVA) was used to assess the difference between the averages of the values, and

Table I
Treatment of biofilms with sanitation agents.

Agent (Concentration)	Temperature – Time	References
AP (0.16 U/g)	37°C – 60 min	Parkar et al. 2004
Protease 0.16 U/g)	37°C – 60 min	Parkar et al. 2004
Subtilisin (1%)	37°C – 30 min	Parkar et al. 2004
Trypsin (3%)	37°C – 3 h	Parkar et al. 2003
SDS (3%)	100°C – 10 min	Parkar et al. 2003
α-Amylase (1%)	37°C – 30 min	Parkar et al. 2004
Cellulase (1.66%)	37°C – 30 min	Parkar et al. 2004
SM (100 mM)	22°C – 60 min	Parkar et al. 2003
Lysozyme (2%)	37°C – 60 min	Parkar et al. 2003
TCA (10%)	100°C – 15 min	Parkar et al. 2003
Nisin (2 mg/ml)	37°C – 24 h	Parkar et al. 2003
PM (2 mg/ml)	22°C – 30 min	Parkar et al. 2003
ST (10 mg/ml)	22°C – 5 min	Parkar et al. 2003
2(5H)-Furanone (1 mg/ml)	22°C – 60 min	Ponnusamy et al. 2010
Triclosan (2 mg/ml)	22°C – 60 min	Tabak et al. 2007

Tukey and Dunnett's tests were applied to compare each group in pairs. Probability levels of $p < 0.05$ were considered statistically significant.

Results

Effect of environmental conditions on the bacterial growth. The optimal planktonic and biofilm growth conditions of the D413 strain were determined at 65°C, pH 7.0, and 0% NaCl. Those of the E134 strain were similar, except that the planktonic and biofilm growth conditions' optimal pH were 8.5 and 9.0, respectively. Both bacteria did not need salt to grow and form a biofilm. Moreover, these isolates achieved optimal growth at 65°C. It was observed that these bacteria had neutral or alkaline environment requirements for their growth.

Determination of the molecular weight of gDNA and eDNA. The presence of eDNA was confirmed for the first time with electrophoresis and spectrophotometric DNA measurements for the D413 and E134 isolates. The molecular weight of gDNA was calculated as 26.1 kb and 29.8 kb for D413 and E134, respectively. Moreover, the molecular weight of eDNA was calculated as 18.2 kb and 21.4 kb for D413 and E134, respectively. It was shown that the molecular weight of the gDNA was larger than the molecular weight of the eDNA in both bacteria. In addition, the molecular weight of gDNA and eDNA of E134 was higher than in the D413 strain. Thus, the presence of eDNA in the biofilm matrix was indicated by electrophoresis and spectrophotometry.

Treatment of partially purified gDNA and eDNA with enzymes. gDNA and eDNA were partially purified in this study. The results indicated that eDNA was interestingly not affected by any of the enzymes. The enzymes could not reach the target eDNA. Furthermore, the eDNA resistance may result from the conserved folded structure of eDNA after purification. Another assumption is that the eDNA might be protected by other EPS and/or EVs structures. However, the gDNA was degraded by only DNase I. It seemed that the eDNA of the D413 and E134 isolates had resistance to DNase I (1.45 mg/ml) when partially purified (Fig. 1A). To confirm

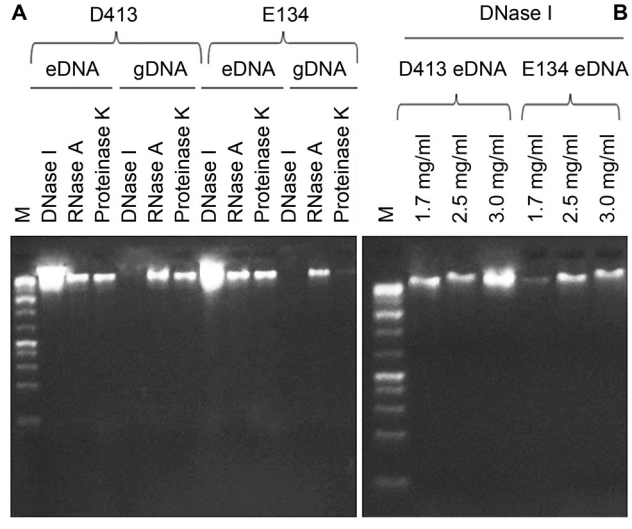

Fig. 1. Agarose gel electrophoresis photographs displaying differences between the gDNA and eDNA of D413 and E134. M, Marker (Fermentas Gene Ruler 1 kb Plus DNA Ladder, 75–20.000 bp) (A) DNase I (1.45 mg/ml), RNase A (0.90 mg/ml) and proteinase K (0.85 mg/ml) treatment of both the gDNA and eDNA; (B) Different DNase I concentrations on eDNA (1.7, 2.5 and 3.0 mg/ml).

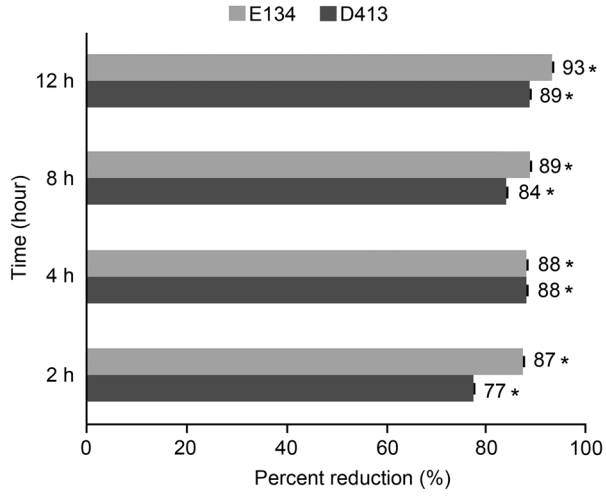

Fig. 2. Treatment of mature biofilms with DNase I. $P < 0.05$* for comparisons of data obtained in the absence and in the presence of DNase I (Dunnett's test).

the resistance, the eDNA was treated with higher concentrations of 1.7, 2.5, and 3.0 mg/ml of DNase I. However, the result remained the same (Fig. 1B).

Treatment of mature biofilms with DNase I. In this assay, partially unpurified eDNA (40 h-old mature biofilms) was treated with DNase I for 2, 4, 8, and 12 h in polystyrene plates. The mature biofilms were scattered for 2 h and 12 h of treatment with biomass removal of 77–89%, and 87–93% for D413 and E134 bacteria, respectively. It was observed that biomass removal increased up to 12 h when eDNA was partially unpurified ($p < 0.05$*) (Fig. 2).

Determination of biofilm mass on abiotic surfaces. For the assay, both scraping and bead vortexing were applied to the adherence substrate. Six abiotic surfaces were compared in terms of viable cell counts with the plate counting method. According to the results, the D413 and E134 cells could attach to all material surfaces. The viable cell numbers ranged from 3.91 to 5.12 log cfu/cm^2 and 2.25 to 4.70 log cfu/cm^2, respectively. Polystyrene (4.70 log cfu/cm^2) and glass (5.12 log cfu/cm^2) were determined to be the most effective materials for biofilm formation by D413 and E134 isolates, respectively. The relationship between each material was statistically significant ($p < 0.05$*) (Fig. 3 and 4).

Prevention of biofilm formation using sanitation agents. Fifteen different sanitation agents were used to test for the control of bacterial biofilm. The best results were provided by nisin for D413 (80%) and α-amylase for E134 (98%). This work showed that nisin, furanone, α-amylase, AP, subtilisin, SDS, TCA, lysozyme, protease, and cellulase provided over 30% biofilm removal in both bacterial species ($p < 0.05$*). Furthermore, the combination of PM and ST did not affect biofilm removal of both bacteria ($p > 0.05$) (Fig. 5).

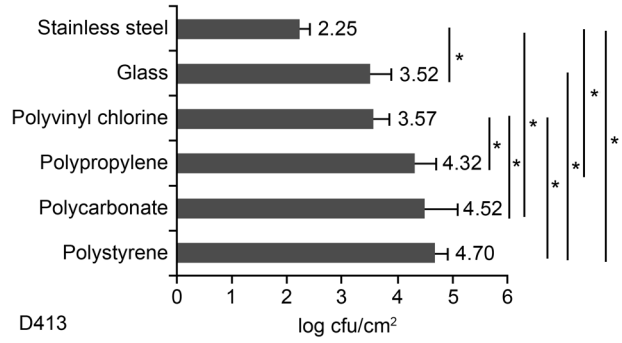

Fig. 3. The viable cell counts of D413 biofilms formed on surfaces (Tukey test; $p < 0.05$*).

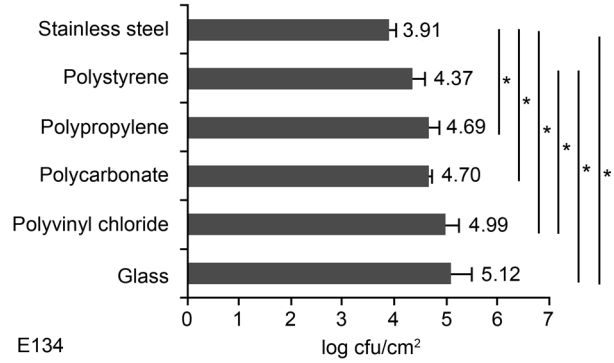

Fig. 4. The viable cell counts of E134 biofilms formed on surfaces (Tukey test; $p < 0.05$*).

Discussion

The temperature range of growth for *Geobacillus* species is 37–75°C, with the optimal temperature being from 55 to 65°C (Wells-Bennik et al. 2019). The optimal temperature for growth of the D413 and E134 isolates was 65°C. Interestingly, the necessary optimal conditions for biofilm growth of these isolates were determined to have similar values. As a result, both bacteria did not need salt to form a biofilm. The increase in the concentration of salt unfavorably affected the formation of biofilm for these isolates. In addition, these bacteria did grow in a neutral or alkaline environment. This could be explained by the intense relationship between the bacterial adherence conditions and the optimal metabolic activity (Elhariry et al. 2012).

Exopolysaccharide, proteinaceous polymers, lipids, and eDNA may be important biofilm matrix components (Allesen-Holm et al. 2006; Soler-Arango et al. 2019). Many microorganisms release eDNA within their biofilm matrix. Moreover, eDNA was reported as a component of the EPS matrix of numerous Gram-negative and Gram-positive bacteria (Ibáñez de Aldecoa et al. 2017; Ramirez et al. 2019). However, as far as it is known, there is no information about the eDNA of *Geobacillus* strain. Using electrophoresis and spectrophotometric methods, the presence of eDNA

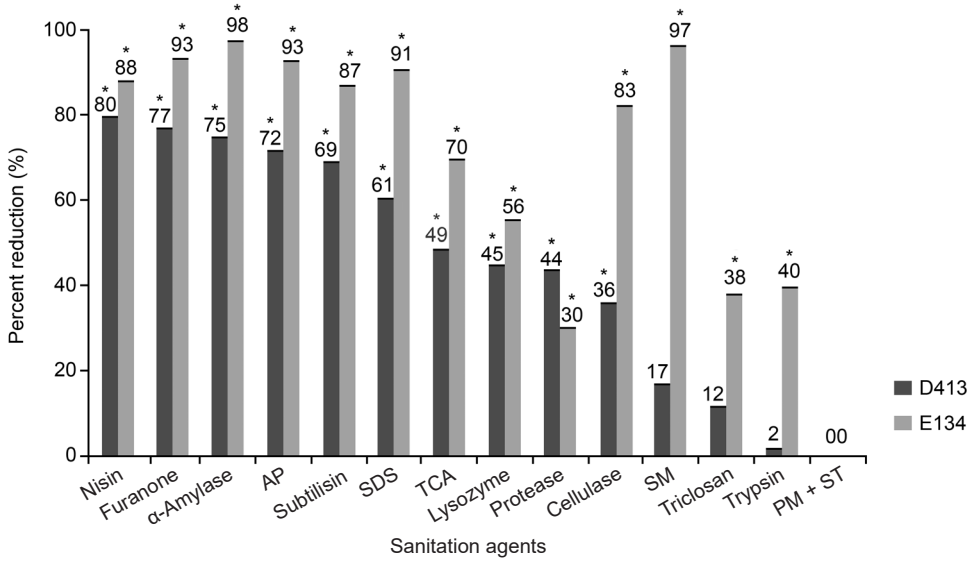

Fig. 5. The effects of sanitation agents on the biofilm of D413 and E134 isolates (Dunnett's test; $p < 0.05$*).

in D413 and E134 isolates was confirmed (Fig. 1). As a result, the gDNA's molecular weights for D413 and E134 were found as 26.1 kb, and 29.8 kb, respectively. The molecular weights of the eDNA for D413 and E134 were found as 18.2 kb, and 21.4 kb, respectively. The molecular weight of the gDNA was larger than the molecular weight of the eDNA for both bacteria.

Potential target sites of Gram-positive bacteria to antimicrobials are the cell wall, the cytoplasmic membrane, functional and structural proteins, DNA, RNA, and other cytosolic components (Bridier et al. 2011). In this study, eDNA in the biofilm matrix was not affected by DNase I, RNase A, and proteinase K enzymes. However, the gDNA was degraded only by DNase I. It seemed that the eDNA of the D413 and E134 had resistance to DNase I when purified (Fig. 1). Böckelmann et al. (2006) reported that agarose gel electrophoresis of purified microfilaments of strain F8 resulted in a distinct band of large size (more than 29 kb) and the band of the eDNA of the strain exactly disappeared after treatment with DNase I but remained stable after treatment with RNase A and proteinase K. Dengler et al. (2015) indicated that *Staphylococcus aureus* biofilm became less sensitive to proteinase K. In contrast, Nguyen and Burrows (2014) determined that proteinase K reduced biofilm formation of *Listeria monocytogenes*.

Qin et al. (2007) showed that DNase I severely decreased the biofilm formation of *Staphylococcus epidermidis*. In another study, Izano et al. (2008) reported that DNase I prevented biofilm formation of *S. aureus* and *S. epidermidis*. DNase I began to dissolve biofilms of *Bacillus subtilis* after 3 h, whereas the biofilms dissolved at the slight degree at the 24 and 48 h (Peng et al. 2020). In addition, Peng et al. (2020) reported that young biofilms were easily disturbed by DNase I, whereas the latter was not effective against aged biofilms. On the contrary, this study determined that aged biofilms of *Geobacillus* isolates were markedly affected by DNase I. As a result, DNase I reduced mature biofilms (40 h) of D413 and E134 by 77–89% and 87–93% (2–12 h), respectively ($p < 0.05$*) (Fig. 2).

Thermophilic bacteria can attach to stainless steel coupons and support biofilms' development (Jindal et al. 2016; Gupta and Anand, 2018). In this paper, six abiotic surfaces were compared in terms of viable cell counts within biofilms. D413 and E134 were observed to adhere to all surfaces. The viable cell numbers ranged from 3.91 to 5.12 log cfu/cm^2 and 2.25 to 4.70 log cfu/cm^2, respectively. Polystyrene surface (4.70 log cfu/cm^2) and glass surface (5.12 log cfu/cm^2) were determined to be the most effective surface for biofilm formation of D413 and E134 isolates, respectively ($p < 0.05$*) (Fig. 3 and 4). Karaca et al. (2019) reported that *Geobacillus vulcanii* DSM 13174^T produced the most abundant biofilm on glass and polystyrene surfaces at 65°C.

Biofilm dispersal can be provided by the disruption of the polysaccharide matrix, proteins, and eDNA. To remove irreversibly attached cells, the implementation of a powerful shear force as scrubbing, scraping or chemical breaking of the adherence forces through the applications of enzymes, sanitizers, and heat is required (Elhariry et al. 2012). It was determined that various sanitation agents could help to reduce the number of D413 and E134 cells on the polystyrene surface (Fig. 5). The best results were provided by nisin for D413 (80%) and α-amylase for E134 (98%) ($p < 0.05$*). Nisin is active upon the cytoplasmic membrane of Gram-positive bacteria, including bacterial spores, and it has been widely used as a food protective for many years

(Delves-Broughton et al. 1992; Boziaris and Adams 1999; Rojo-Bezares et al. 2007). Furthermore, nisin exhibits antimicrobial activity by binding to the pyrophosphate moiety of lipid II. Nisin also inhibited biofilm formation of *S. aureus* (Angelopoulou et al. 2020). In another study, nisin (1 mg/ml) killed 100% of *Bacillus flavothermus* B12-C^{m} biofilm cells (Parkar et al. 2003). Fleming et al. (2017) indicated that treatments of *S. aureus* and *Pseudomonas aeruginosa* biofilms with α-amylase and cellulase resulted in an important decrease in the biofilm biomass. In this study, α-amylase (98%) and SM (97%), which are glycoside hydrolases that break down polysaccharides, affected the E134 strain biofilm. Degradation of quorum sensing (QS) signals could be considered a promising approach in biofilm control (Algburi et al. 2017). The results of this study showed that furanone was very effective for removing biofilms of D413 (77%) and E134 (93%) ($p < 0.05^{*}$) strains. 2(5H)-Furanone acts as a potential quorum-inhibition agent in a biofilm community and could displace the AHL signals from the LuxR protein. Furanones have been commonly used to remove biofilm from medical catheters and diverse other substrates (Ponnusamy et al. 2010). In this study, it was observed that both protein-degrading agents and polysaccharide-degrading agents were effective for the biofilm control of *Geobacillus*. Lequette et al. (2010) found that proteases were more efficient than polysaccharides for the removal of *Bacillus* spp. biofilms while polysaccharide-degrading enzymes were more efficient for control of *Pseudomonas fluorescens* biofilms. However, the combination of PM and ST had no inhibitory effect on biofilm formation of both bacteria ($p > 0.05$) (Fig. 5).

In conclusion, this paper showed that DNase I degraded the eDNA of *Geobacillus* genus bacteria. The importance of eDNA for mature biofilm stability after the DNase I application was demonstrated. Besides, sanitation agents like α-amylase, nisin, and furanone significantly impacted these bacteria's biofilm formation. This work suggests that sanitation agents could be a solution to control biofilm structures of thermophilic bacilli. Biofilm control can be determined by a combination of these sanitation agents in future studies. It seemed that *Geobacillus* strains could form biofilms on stainless steel, glass, and plastic surfaces. In addition, this work suggest that biofilm control could be improved by using new sanitation strategies on these surfaces.

ORCID
Tugba Kilic https://orcid.org/0000-0002-5474-0288

Funding
This research was funded by the Scientific Research Project Office of Ankara University with project number 14B0430003.

Acknowledgments
I would like to thank Prof. Arzu Coleri Cihan and Dr. Basar Karaca (Ankara University, Faculty of Science, Biology Department) for their supports.

Conflict of interest
The authors do not report any financial or personal connections with other persons or organizations, which might negatively affect the contents of this publication and/or claim authorship rights to this publication.

Literature

Algburi A, Comito N, Kashtanov D, Dicks LM, Chikindas ML. Control of biofilm formation: antibiotics and beyond. App Environ Microbiol. 2017 Feb; 83(3):e02508–16. https://doi.org/10.1128/AEM.02508-16

Allesen-Holm M, Barken KB, Yang L, Klausen M, Webb JS, Kjelleberg S, Molin S, Givskov M, Tolker-Nielsen T. A characterization of DNA release in *Pseudomonas aeruginosa* cultures and biofilms. Mol Microbiol. 2006 Nov; 59(4):1114–1128. https://doi.org/10.1111/j.1365-2958.2005.05008.x

Angelopoulou A, Field D, Pérez-Ibarreche M, Warda AK, Hill C, Ross RP. Vancomycin and nisin A are effective against biofilms of multi-drug resistant *Staphylococcus aureus* isolates from human milk. Plos One. 2020 May; 15(5):e0233284. https://doi.org/10.1371/journal.pone.0233284

Boziaris IS, Adams MR. Effect of chelators and nisin produced in situ on inhibition and inactivation of Gram negatives. Int J Food Microbiol. 1999 Jul; 53(2–3):105–113. https://doi.org/10.1016/S0168-1605(99)00139-7

Böckelmann U, Janke A, Kuhn R, Neu TR, Wecke J, Lawrence JR, Szewzyk U. Bacterial extracellular DNA forming a defined network-like structure. FEMS Microbiol Lett. 2006 Sep; 262(1):31–38. https://doi.org/10.1111/j.1574-6968.2006.00361.x

Bremer P, Seale B, Flint S, Palmer J. Biofilms in dairy processing. In: Fratamico PM, Annous BA, Gunther IV NW, editors. Biofilms in the food and beverage industries. Sawston (UK): Woodhead Publishing. 2009; p. 396–431. https://doi.org/10.1533/9781845697167.4.396

Bridier A, Briandet R, Thomas V, Dubois-Brissonnet F. Resistance of bacterial biofilms to disinfectants: a review. Biofouling. 2011 Oct; 27(9):1017–1032. https://doi.org/10.1080/08927014.2011.626899

Burgess SA, Brooks JD, Rakonjac J, Walker KM, Flint SH. The formation of spores in biofilms of *Anoxybacillus flavithermus*. J Appl Microbiol. 2009 Feb; 107(3):1012–1018. https://doi.org/10.1111/j.1365-2672.2009.04282.x

Burgess SA, Flint SH, Lindsay D. Characterization of thermophilic bacilli from a milk powder processing plant. J Appl Microbiol. 2013 Oct; 116(2):350–359. https://doi.org/10.1111/jam.12366

Cihan AC, Ozcan B, Tekin N, Cokmus C. Phylogenetic diversity of isolates belonging to genera *Geobacillus* and *Aeribacillus* isolated from different geothermal regions of Turkey. World J Microb Biot. 2011 Apr;27(11):2683. https://doi.org/10.1007/s11274-011-0742-2

Cihan AC, Karaca B, Ozel BP, Kilic T. Determination of the biofilm production capacities and characteristics of members belonging to Bacillaceae family. World J Microb Biot. 2017 May;33(6):118. https://doi.org/10.1007/s11274-017-2271-0

Delves-Broughton J, Williams GC, Wilkinson S. The use of the bacteriocin, nisin, as a preservative in pasteurized liquid whole egg. Lett Appl Microbiol. 1992 Oct;15(4), 133–136. https://doi.org/10.1111/j.1472-765X.1992.tb00746.x

Dengler V, Foulston L, DeFrancesco AS, Losick R. An electrostatic net model for the role of extracellular DNA in biofilm formation by *Staphylococcus aureus*. J Bacteriol. 2015 Sep;197(24):3779–3787. https://doi.org/10.1128/JB.00726-15

Eijlander RT, van Hekezen R, Bienvenue A, Girard V, Hoornstra E, Johnson NB, Meyer R, Wagendorp A, Walker DC, Wells-Bennik MHJ. Spores in dairy-new insights in detection, enumeration and risk assessment. Int J Dairy Technol. 2019 May;72(2):303–315. https://doi.org/10.1111/1471-0307.12586

Elhariry H, Gherbawy Y, El-Deeb B, Altalhi A. Molecular identification and biofilm-forming ability of culturable aquatic bacteria in microbial biofilms formed in drinking water distribution networks. Geomicrobiol J. 2012 May;29(6):561–569. https://doi.org/10.1080/01490451.2011.596254

Fleming D, Chahin L, Rumbaugh K. Glycoside hydrolases degrade polymicrobial bacterial biofilms in wounds. Antimicrob Agents Ch. 2017 Nov; 61(2):e01998-16. https://doi.org/10.1128/AAC.01998-16

Garrett TR, Bhakoo M, Zhang Z. Bacterial adhesion and biofilms on surfaces. Prog Nat Sci. 2008 Sep;18(9):1049–1056. https://doi.org/10.1016/j.pnsc.2008.04.001

Giaouris ED, Nychas GJE. The adherence of *Salmonella Enteritidis* PT4 to stainless steel: The importance of the air-liquid interface and nutrient availability. Food Microbiol. 2006 Apr;23:747–752. https://doi.org/10.1016/j.fm.2006.02.006

Gopal N, Hill C, Ross PR, Beresford TP, Fenelon MA, Cotter PD. The prevalence and control of *Bacillus* and related spore-forming bacteria in the dairy industry. Front Microbiol. 2015 Dec;6:1418. https://doi.org/10.3389/fmicb.2015.01418

González-Rivas F, Ripolles-Avila C, Fontecha-Umaña F, Ríos-Castillo AG, Rodríguez-Jerez JJ. Biofilms in the spotlight: Detection, quantification, and removal methods. Compr Rev Food Sci Food Saf. 2018 Jun;17(5):1261–1276. https://doi.org/10.1111/1541-4337.12378

Grande R, Di Giulio M, Bessa LJ, Di Campli E, Baffoni M, Guarnieri S, Cellini L. Extracellular DNA in *Helicobacter pylori* biofilm: a backstairs rumour. J Appl Microbiol. 2010 Nov;110:490–498. https://doi.org/10.1111/j.1365-2672.2010.04911.x

Gupta S, Anand S. Induction of pitting corrosion on stainless steel (grades 304 and 316) used in dairy industry by biofilms of common sporeformers. Int J Dairy Technol. 2018 May;71(2):519–531. https://doi.org/10.1111/1471-0307.12444

Herigstad B, Hamilton M, Heersink J. How to optimize the drop plate method for enumerating bacteria. J Microbiol Meth. 2001 Mar;44:121–129. https://doi.org/10.1016/s0167-7012(00)00241-4

Ibáñez de Aldecoa AL, Zafra O, González-Pastor JE. Mechanisms and regulation of extracellular DNA release and its biological roles in microbial communities. Front Microbiol. 2017 Jul;8:1390. https://doi.org/10.3389/fmicb.2017.01390

Izano EA, Amarante MA, Kher WB, Kaplan JB. Differential roles of poly-N acetylglucosamine surface polysaccharide and extracellular DNA in *Staphylococcus aureus* and *Staphylococcus epidermidis* biofilms. Appl Environ Microbiol. 2008 Jan;74(2):470–476. https://doi.org/10.1128/AEM.02073-07

Jindal S, Anand S, Huang K, Goddard J, Metzger L, Amamcharla J. Evaluation of modified stainless steel surfaces targeted to reduce biofilm formation by common milk sporeformers. J Dairy Sci. 2016 Sep;99(12):9502–9513. https://doi.org/10.3168/jds.2016-11395

Karaca B, Buzrul S, Coleri Cihan A. *Anoxybacillus* and *Geobacillus* biofilms in the dairy industry: effects of surface material, incubation temperature and milk type. Biofouling. 2019 Jul;35(5):551–560. https://doi.org/10.1080/08927014.2019.1628221

Lequette Y, Boels G, Clarisse M, Faille C. Using enzymes to remove biofilms of bacterial isolates sampled in the food-industry. Biofouling. 2010 May; 26(4): 421–431. https://doi.org/10.1080/08927011003699535

Lindsay D, Flint S. Biofilm formation by spore-forming bacteria in food processing environments. In: Fratamico PM, Annous BA, Gunther IV NW, editors. Biofilms in the food and beverage industries. Sawston (UK): Woodhead Publishing. 2009; p. 270–299. https://doi.org/10.1533/9781845697167.2.270

Mandic-Mulec I, Stefanic P, van Elsas JD. Ecology of *Bacillaceae*. Microbiol Spect. 2015 Mar;3(2):1–24. https://doi.org/10.1128/microbiolspec.TBS-0017-2013

Mazaheri T, Ripolles-Avila C, Hascoët AS, Rodríguez-Jerez JJ. Effect of an enzymatic treatment on the removal of mature *Listeria monocytogenes* biofilms: A quantitative and qualitative study. Food Control, 2020 Mar;107266. https://doi.org/10.1016/j.foodcont.2020.107266

Meireles A, Borges A, Giaouris E, Simões M. The current knowledge on the application of anti-biofilm enzymes in the food industry. Food Res Int. 2016 Jun; 86:140–146. https://doi.org/10.1016/ j.foodres.2016.06.006

Nguyen UT, Burrows LL. DNase I and proteinase K impair *Listeria monocytogenes* biofilm formation and induce dispersal of pre-existing biofilms. Int J Food Microbiol. 2014 Jul;187:26–32. https://doi.org/10. 1016/j.ijfoodmicro.2014.06.025

Parkar SG, Flint SH, Brooks JD. Physiology of biofilms of thermophilic bacilli – potential consequences for cleaning. J Ind Microbiol Biot. 2003 Aug;30: 553–560. https://doi.org/10.1007/s10295-003-0081-x

Parkar SG, Flint SH., Brooks JD. Evaluation of the effect of cleaning regimes on biofilms of thermophilic bacilli on stainless steel. J Appl Microbiol. 2004 Nov; 96:110–116. https://doi.org/10.1046/j.1365-2672.2003.02136.x

Peng N, Cai P, Mortimer M, Wu Y, Gao C, Huang Q. The exopolysaccharide-eDNA interaction modulates 3D architecture of *Bacillus subtilis* biofilm. BMC Microbiol. 2020 May;20:1–12. https://doi.org/10.1186/s12866-020-01789-5

Pitts B, Hamilton MA, Zelver N, Stewart PS. A microtiter-plate screening method for biofilm disinfection and removal. J Microbiol Meth. 2003 Aug; 54:269–276. https://doi.org/10.1016/S0167-7012(03)00034-4

Ponnusamy K, Paul D, Kim YS, Kweon JH. 2(5H)-Furanone: a prospective strategy for biofouling-control in membrane biofilm bacteria by quorum sensing inhibition. Braz J Microbiol. 2010 Mar;41:227–234. https://doi.org/10.1590/S1517-83822010000100032

Ramirez T, Shrestha A, Kishen A. Inflammatory potential of monospecies biofilm matrix components. In Endod J 2019 Feb;52(7): 1020–1027. https://doi.org/10.1111/iej.13093

Rojo-Bezares B, Sáenz Y, Zarazaga M, Torres C, Ruiz-Larrea F. Antimicrobial activity of nisin against *Oenococcus oeni* and other wine bacteria. Int. J Food Microbiol. 2007 May;116(1):32–36. https://doi.org/10.1016/j.ijfoodmicro.2006.12.020

Rumbaugh KP, Sauer K. Biofilm dispersion. Nat Rev Microbiol. 2020 Jun;18:571–586. https://doi.org/10.1038/s41579-020-0385-0

Qin Z, Ou Y, Yang L, Zhu Y, Tolker-Nielsen T, Molin S, Qu D. Role of autolysin-mediated DNA release in biofilm formation of *Staphylococcus epidermidis*. Microbiology. 2007 Jul;153(7):2083–2092. https://doi.org/10.1099/mic.0.2007/006031-0

Ripolles-Avila C, Ríos-Castillo AG, Fontecha-Umaña F, Rodríguez-Jerez JJ. Removal of *Salmonella enterica* serovar Typhimurium and *Cronobacter sakazakii* biofilms from food contact surfaces through enzymatic catalysis. J Food Safety. 2019 Dec;40(2):e12755. https://doi.org/10.1111/jfs.12755

Ripolles-Avila C, Ramos-Rubio M, Hascoët AS, Castillo M, Rodríguez-Jerez JJ. New approach for the removal of mature biofilms formed by wild strains of *Listeria monocytogenes* isolated from food contact surfaces in an Iberian pig processing plant. Int J Food Microbiol. 2020 Mar;108595. https://doi.org/10.1016/j.ijfoodmicro.2020.108595

Scott SA, Brooks JD, Rakonjac J, Walker KM, Flint SH. The formation of thermophilic spores during the manufacture of whole milk powder. Int J Dairy Technol. 2007 May;60(2):109–117. https://doi.org/10.1111/j.1471-0307.2007.00309.x

Shemesh M, Ostrov I. Role of *Bacillus* species in biofilm persistence and emerging antibiofilm strategies in the dairy industry. J Sci Food Agric. 2020 Jan; 100(6):2327–2336. https://doi.org/10.1002/jsfa.10285

Soler-Arango J, Figoli C, Muraca G, Bosch A, Brelles-Mariño G. The *Pseudomonas aeruginosa* biofilm matrix and cells are drastically impacted by gas discharge plasma treatment: A comprehensive model explaining plasma-mediated biofilm eradication. PloS One. 2019 Jun;14(6):e0216817. https://doi.org/10.1371/journal.pone.0216817

Stepanović S, Vuković D, Dakić I, Savić B, Švabić-Vlahović M. A modified microtiter-plate test for quantification of staphylococcal biofilm formation. J Microbiol Meth. 2000 Apr;40:175–179. https://doi.org/10.1016/ s0167-7012(00)00122-6

Sung MH, Kim H, Bae JW, Rhee SK, Jeon CO, Kim K, Kim JJ, Hong SP, Lee SG, Yoon JH, Park YH, Baek DH. *Geobacillus toebii* sp. nov., a novel thermophilic bacterium isolated from hay compost. Int J Syst Evol Micr. 2002 Jun;52(6):2251–2255. https://doi.org/10.1099/00207713-52-6-2251

Tabak M, Scher K, Hartog E, Romling U, Matthews KR, Chikindas ML, Yaron S. Effect of triclosan on *Salmonella typhimurium* at different growth stages and in biofilms. FEMS Microbiol Lett. 2007 Dec;267:200–206. https://doi.org/10.1111/j.1574-6968.2006.00547.x

Wells-Bennik MH, Janssen PW, Klaus V, Yang C, Zwietering MH, Den Besten HM. Heat resistance of spores of 18 strains of *Geobacillus stearothermophilus* and impact of culturing conditions. Int J Food Microbiol. 2019 Nov;291:161–172. https://doi.org/10.1016/j.ijfoodmicro.2018.11.005

Wilson K. Preparation of genomic DNA from bacteria. Curr Protoc Mol Biol. 2001 Nov;56:2–4. https://doi.org/10.1002/0471142727.mb0204s56

Woodward MJ, Sojka M, Sprigings KA, Humphrey TJ. The role of SEF14 and SEF17 fimbriae in the adherence of *Salmonella enterica* serotype Enteritidis to inanimate surfaces. J Med Microbiol. 2000 May;49:481–487. https://doi.org/10.1099/0022-1317-49-5-48

Polish Journal of Microbiology
2020, Vol. 69, No 4, 421–426
https://doi.org/10.33073/pjm-2020-045

ORIGINAL PAPER

Application of PCR for Specific Diagnosis of Leptospirosis in Humans in Ukraine

OLENA ZUBACH[1*], OKSANA SEMENYSHYN[2], LILYA VASIUYNETS[2], OKSANA VELYCHKO[2] and ALEXANDER ZINCHUK[1]

[1] Danylo Halytsky Lviv National Medical University, Lviv, Ukraine
[2] State Institution Lviv Oblast Laboratory Center of the Ministry of Health of Ukraine, Lviv, Ukraine

Submitted 8 July 2020, revised 28 September 2020, accepted 29 September 2020

Abstract

Leptospirosis remains one of the most widespread zoonotic diseases in the world and Ukraine, in particular. Ukrainian clinicians have been faced with early detection of the disease due to the availability of only a serological method for routine diagnostics in Ukraine, namely the microscopic agglutination test (MAT). This paper demonstrates the first results of the complex application of MAT and polymerase chain reaction (PCR) for routine verification of leptospirosis, which were first applied simultaneously in Lviv Oblast of Ukraine in 2016. We examined the sera of 150 patients clinically suspected of leptospirosis, 31 of whom were treated at the Lviv Oblast Clinical Hospital for Infectious Diseases (LOCHID). The application of PCR during the first seven days of the disease allowed increasing the share of confirmed leptospirosis cases by 16,1% in patients that were treated in LOCHID during 2016–2017.

Key words: Leptospirosis, diagnostics, microagglutination test, polymerase chain reaction

Introduction

Leptospirosis is a zoonotic bacterial infection, which the causative agent is *Leptospira* spp. that may infect both wild and domestic animals and humans. Humans contract leptospirosis from animals through exposure to contaminated water or by direct contact with an infected animal. Person to person spread does not occur (Dupouey et al. 2014). In Ukraine, a relatively high incidence rate of leptospirosis has been reported (0.70 per 100,000 population in 2019; 295 cases were recorded) (Centers for Disease Control (CDC) of Ministry of Health (MH) of Ukraine 2019; Tsarenko et al. 2019). Between 2006 and 2019 (15 years), leptospirosis's average incidence rate in Ukraine was 0,94 per 100,000.

According to the World Health Organization (WHO) recommendations, leptospirosis in humans should be diagnosed based on a combination of epidemiological and clinical data with mandatory laboratory tests to confirm the diagnosis (WHO 2003). Physicians often diagnose leptospirosis based on epidemiological and clinical data, with subsequent confirmation based on laboratory tests.

Serology tests with different sensitivity and specificity are most commonly used for leptospirosis diagnostics (Postic et al. 2000; Panwala et al. 2015). Several techniques are often used either together or sequentially to establish a correct diagnosis reliably.

The microscopic agglutination test (MAT) developed in 1918 by Martin and Pettit is considered the gold standard for serodiagnosis of leptospirosis and is still recognized as the reference method of diagnostics in leptospirosis laboratory (WHO 2003). Antibodies for leptospirosis develop between 3–10 days after symptom onset; thus, any serologic test must be interpreted accordingly. Serological testing should be tested with a series of two samples; the first sample collected after the onset of disease and a second convalescent sample 7–10 days after the first.

The MAT is rather complicated for implementation, interpretation, and control (Lucchesi et al. 2004). The accuracy of the MAT is approximately 75–80%; however, this sensitivity and specificity are typically only attained during the third week of the disease and often only have a retrospective value for clinicians and patients (OiE Terrestrial Manual 2018). Furthermore, antibodies to

* Corresponding author: O. Zubach, Danylo Halytsky Lviv National Medical University, Department of Infectious Diseases, Lviv, Ukraine; **e-mail: zubachlena@gmail.com**

different spirochetes may cross-react with *Leptospira,* which causes the results to be less reliable (Postic et al. 2000). Therefore, it is highly recommended to increase the MAT's sensitivity using local isolates rather than reference strains (OiE Terrestrial Manual 2018).

The MAT allows detecting of two classes of antibodies, IgM and IgG, in a single reaction. Since live cultures are used, factors such as age and density of *Leptospira* cultures (as they may influence the agglutination titer), the method is still not standardized (WHO 2003). The viability of live cultures of all *Leptospira interrogans* serovars needed for use as antigens must be constantly maintained by the laboratory staff, which is a laborious and challenging task. Another disadvantage of the method is the late appearance of antibodies in the body of patients with leptospirosis, which often has only historical value. During the last 15 years (2003–2017), 378 patients were discharged from LOCHID with leptospirosis diagnosis. Among them, 272 (71.9%) patients were diagnosed with MAT, the remaining 106 (28,1%) patients were diagnosed based on clinical manifestations only since the MAT result was negative, and no other methods were used.

Considering the above-mentioned drawbacks of MAT, the laboratory network in Ukraine has improved the specific diagnostics of leptospirosis at the early stages of the disease. Such laboratory practices are focused on the detection of the *Leptospira* spp. genetic material in the biological fluids of infected patients (Vasiunets et al. 2019). Here we describe an evaluation of a PCR for detecting a specific part of pathogenic *Leptospira* DNA in patient samples during the early phase of infection (Postic 2000). The implementation of the PCR is divided into two categories. The first one is based on detecting the genes, which are universal for these bacteria (*gryB*, *rrs* and *secY*). The second one is based on the detection of genes inherent for pathogenic *Leptospira* (for example, *lipL21*, *lipL32*, *lipL41*, *ligA* or *ligB*) (Thaipadungpanit et al. 2011). However, both PCR categories do not allow identifying *Leptospira* serogroup that caused the disease. Identification of the pathogen is possible only for the genotype *L. interrogans.*

PCR primers that are based on the *lipL32* gene are the most commonly used in PCR kits that have been developed and evaluated for human sample testing. The presence of amplification inhibitors in clinical samples may lead to false-negative results, especially in specimens that could be contaminated. The quality control of PCR for *Leptospira* detection requires attention to the laboratory facilities conditions, the equipment, the workflow process, and the mandatory use of appropriate control samples (Dragon et al. 1993; OiE Terrestrial Manual 2018). Additionally, strict compliance with the procedure and conditions for the selection, as well as the treatment of clinical specimens for PCR, plays a crucial role in order to receive reliable results. The main objective of our study was to analyze the effectiveness of using the MAT with *Leptospira* and PCR of urine for specific laboratory diagnostics of leptospirosis.

Experimental

Materials and Methods

Patient population. The study subjects were patients with suspected leptospirosis, treated in different Lviv Oblast hospitals from 2016 to 2017. We conducted a retrospective analysis of medical records and studied registration data of 150 patients with suspected leptospirosis, whose samples were tested at the Laboratory of Especially Dangerous Infections of the State Institution Lviv Oblast Laboratory Center of Ministry of Health of Ukraine (Laboratory of EDI of SI LOLC). In case of symptoms similar to leptospirosis and/or epidemiological anamnesis typical for this disease, the patients' biological materials were sent to the Laboratory of EDI of SI LOLC to confirm or deny leptospirosis. Also, the biological material of patients whose symptoms even partially resembled leptospirosis was sent to the laboratory. Thus, doctors of different specialties carried out a diagnostic search so that the diagnosis of leptospirosis was in the list of those that should be excluded to establish the final correct diagnosis.

The MAT procedure. The diagnostic kit of live *Leptospira* containing 13 serogroups (*L. icterohaemorrhagiae*, *L. javanica*, *L. canicola*, *L. autumnalis*, *L. australis*, *L. pomona*, *L. grippotyphosa*, *L. bataviae*, *L. tarassovi*, *L. hebdomadis*, *L. pyrogenes*, *L. ballum*, *L. cynopteri*) was used to perform the MAT. The Laboratory of EDI provided these strains. The MAT assay was performed according to the WHO recommendation and internal standard operation protocol (WHO 2003).

The result was considered as a positive and the endpoint titre of serum, with agglutination score equal to or greater than 2, and no lysis signs and agglutination in control. If the MAT results were positive for a few Leptospira serogroups, the serogroup's agglutination with the highest serum titres was considered the final positive result.

The PCR procedure. We used AmpliSens® *Leptospira*-FRT PCR kit (Russian Federation) for the qualitative detection of 16S RNA of pathogenic *Leptospira* genospecies in the biological fluids (blood and urine) by real-time PCR.

The test was performed according to the manufacturer's instruction using Rotor-Gene 3000/6000 (Corbett Research, Australia). The samples were considered positive if the determined Ct value was less than 32. If

Table I
The diagnosis of patients with suspected leptospirosis.

Method of investigation	Total number of patients with suspected leptospirosis (n = 150)		Positive results by different methods		Total confirmation	
	Number of the samples examined (absolute)	Number of the samples examined (%)	Number of positive samples (absolute)	Number of positive samples (%)	Number of positive samples (absolute)	Number of positive samples (%)
MAT	148	98.66	20	13.33	33	22
PCR	30	20	5	3.33		
MAT + PCR	28	18.66	8	5.33		

the Ct value in a sample was higher than this boundary-value than the sample was equivocal.

Urine for analysis (volume 100 ml) was taken into a sterile container. The sample was centrifuged at 9,000–10,000 g for 10 min, and then approximately 99 ml of the supernatant was discarded. 1 ml of the supernatant was left over the precipitate in a test tube and resuspended respectfully. The suspension was transferred to a new tube and concentrated via centrifugation at 13,000 g for 10 min. 900 µl of the supernatant was discarded, and the remaining pellet and supernatant were used for DNA/RNA isolation. If there was no chance to test material within 24 h after sampling, urine was transferred to a centrifuge tube or an Eppendorf tube. The tube's content was mixed with glycerol (~10% v/v) and frozen. It could be stored at ≤ –16°C for one week or at ≤ –68°C for an extended period (Guidelines to AmpliSens® Leptospira-FRT PCR 2017).

For the DNA/RNA extraction, the RIBO-prep kit (Federal Budget Institute of Science Central Research Institute for Epidemiology, Russian Federation) was used (Guidelines to AmpliSens® Leptospira-FRT PCR 2017).

Data analysis. The data on all patients have been grouped into a single database in Microsoft Excel. The results were statistically processed using descriptive statistics and comparative data analysis. All calculations were performed using the StatSoft's Statistica 8.0 application package by Windows.

Ethical approval. The protocol was reviewed and approved by the Ethical Review Board of the Danylo Halytsky Lviv National Medical University.

Results

During 2016–2017, the biological samples collected from 150 patients suspected (clinically) to have leptospirosis were tested at the Laboratory of EDI by MAT (blood was collected after the 7th day of the disease onset) and PCR assay (urine was collected between the 1st and seventh day of the disease). The diagnosis of leptospirosis was confirmed for 33 patients (using MAT or PCR, or MAT and PCR simultaneously) that were equal to 22.0% of the total number of patients, including three fatal cases. (Table I). The diagnosis of two patients who died during the first week of the disease was confirmed by PCR and MAT (the *Leptospira* lysis was observed in the titer 1:100–1:200) but the diagnosis of the patient died on the seventh day of the disease was confirmed only by MAT (1:800).

A more detailed analysis of the data mentioned above for patients who have been treated in the department of the Lviv Oblast Clinical Hospital for Infectious Diseases (during the specified period) revealed that the number of the confirmed diagnoses of leptospirosis among the suspicious cases was significantly different. From 2016 to 2017, 31 patients were discharged from the Lviv Oblast Clinical Hospital for Infectious Diseases with a diagnosis of leptospirosis. Twenty-six of them (83.87%) were diagnosed based on clinical signs and laboratory tests such as MAT and PCR. Despite the negative results of MAT and PCR, five patients (16.13%) were discharged from the hospital with clinical leptospirosis diagnosis because of undeniable clinical and epidemiological findings. Each of those patients had severe jaundice with acute renal insufficiency and changes of parameters in clinical and biochemical assays that are typical for leptospirosis. These patients also responded well to the prescribed treatment and recovered.

Discussion

For many decades, in Lviv Oblast, sporadic cases of leptospirosis have been recorded as isolated cases that are unrelated to each other. In 2016, within the territory of Lviv Oblast, the incidence rate was equal to 0.56 per 100,000 population; in 2017 it was equal to 0.72 per 100,000 population ($p > 0.05$) (Centers for Disease Control (CDC) of Ministry of Health (MH) of Ukraine 2019).

It is worthwhile to say that the number of confirmed cases of leptospirosis among the total number of

examined patients within the oblast is characterized by a very low percentage of diagnosis confirmation (21.71%). This could be explained by the fact that both the samples from the patients with clinical leptospirosis-like symptoms and the patients with generic symptoms that could be due to leptospirosis were sent for testing. In such cases, the diagnosis of leptospirosis was included on the list of diseases to be excluded from to establish a correct diagnosis. Blood/urine collected not only from patients of infectious hospitals/departments was sent to the Laboratory of EDI, but also from the patients who were treated in intensive care units, therapeutic and surgical departments of multi-specialty hospitals of the Lviv Oblast.

Among the patients from specialized hospitals such as the Lviv Oblast Clinical Hospital for Infectious Diseases, the percentage of confirmed leptospirosis cases was significantly different from the suspected cases of leptospirosis. A large number of patients with other diagnoses are treated in this health care establishment, and their diagnoses may often resemble a clinical picture similar to leptospirosis (that have a non-infectious nature of the disease: mechanical jaundice, acute kidney damage of various etiologies, mushroom poisoning, etc.); however, such diagnoses are excluded at the pre-hospitalization stage. Those diseases that have a clinical picture similar to leptospirosis include viral hepatitis, malaria, hemorrhagic fevers, however, these are excluded in the Lviv Oblast Clinical Hospital for Infectious Diseases during the diagnostic phase. Therefore, the number of selected patients suspected of leptospirosis compared to patients with the final diagnosis of leptospirosis was significantly higher. The percentage of confirmed diagnoses among the above-stated patients by the specific laboratory diagnostic methods such as MAT or PCR was equal to 83.87%.

In Ukraine, the issue of a final diagnosis establishment for patients with a typical clinical picture of leptospirosis has remained a subject for discussion, especially in cases when the specific laboratory diagnostic methods do not provide positive results. In the Lviv Oblast Hospital for Infectious Diseases, the number of such patients was equal to 5 (16.13%). These patients' symptoms comply with leptospirosis diagnostic criteria in Ukraine for likely cases of leptospirosis (Order of MOH of Ukraine N° 905 2015). According to this regulation, there is not a standard diagnostic protocol to consistently determine leptospirosis infection. Any patient who meets the clinical criteria and has a possible epidemiological risk meets the criteria of a probable case of leptospirosis, and any patient who complies with the clinical and laboratory criteria meets the criteria of a confirmed case. In our opinion, this position seems to be biased. As we may see, there is a particular reason to use the term neglected or lost zoonosis concerning leptospirosis (Allan et al. 2015). According to some authors, up to 70% of patients with leptospirosis do not seek medical assistance because the clinical course of the disease is relatively mild or similar to other diseases like acute respiratory infections or mild disorders of the gastrointestinal tract and therefore, patients often are self-treated (Phraisuwan et al. 1999; Ashford et al. 2000; Levett 2001; Guerrier 2013; Tubiana et al. 2013).

Therefore, the disease is not identified, and information about these patients is lost. Furthermore, such neglect concerning leptospirosis takes place in Ukraine because of a lack of laboratory confirmation. Therefore, cases of leptospirosis are excluded from the annual state statistical reports, and therefore, the official leptospirosis incidence is underestimated. In contrast to Ukraine, European countries include all of the patients with diagnosed leptospirosis in their annual reports, regardless of laboratory confirmation (ECDC 2014). A similar position is observed in leptospirosis hyperendemic regions. Thus, within the studies conducted in India during the outbreak of leptospirosis, which included 169 patients, only 15.9% of them had positive MAT results, and 36.6% had positive IgM ELISA, whereas the rest of the patients were diagnosed with leptospirosis based on clinical signs alone (Bharadwaj et al. 2002). Obviously, that in case of an outbreak of infectious disease, it is not necessary to obtain a specific confirmation of all cases of the disease (Morgan et al. 2002; Guillois et al. 2018).

However, India is an endemic zone for different hemorrhagic fevers that are characterized by leptospirosis-like symptoms. Coinfection of leptospirosis and Crimean-Congo hemorrhagic fever or hemorrhagic fever with renal syndrome (CCHF, GF with renal syndrome) is common among humans (Golubić and Markotić 2003; Seifi et al. 2016). Consequently, the lack of research data that would exclude the presence of these diseases or their coexistence did not prevent the authors of this research from confirming that there were patients with leptospirosis diagnosed based on clinical findings during this outbreak.

Researchers promote a similar approach to data reporting for leptospirosis cases (confirmed case/probable case) from other countries endemic for leptospirosis such as Sri Lanka and Malaysia (Agampodi et al. 2011; Wei Leon Tan 2016).

In Ukraine, which is endemic for hemorrhagic fever (CCHF, GF with renal syndrome), there are no test systems (for general use) to verify this group of diseases. This omission increases the risk of errors while establishing the diagnosis for patients with leptospirosis-like symptoms based on clinical and epidemiological data only. The research we have conducted has the following advantages: the investigation of samples collected from all patients was conducted in the same

laboratory using the same protocol, equipment, and identical test systems.

The main disadvantage of this study is its retrospective nature, as well as the short study period (2 years). However, the use of PCR for the routine verification of leptospirosis has been started in the Lviv Oblast only since 2016; therefore, the analysis of obtained data over a more extended period would not be possible.

The first results of the PCR implementation have shown the potential to improve the specific diagnosis of leptospirosis in humans at the early stages of the disease. It increased the number of confirmed cases of leptospirosis among all suspected patients by 3.29% and 16.13% among all the patients who were ultimately discharged with a final diagnosis of leptospirosis. Simultaneously, the MAT is considered the gold standard for the diagnosis because it detects and confirms the serogroup of the pathogen and, respectively, to suspect (predict) cause-and-effect relationships with possible sources of human infection. In our opinion, currently, the combined use of PCR and the MAT could be considered as the most practical combination of specific methods for detecting leptospirosis in humans. For Ukrainian clinicians and epidemiologists, the issue of final diagnosis establishment based on a typical clinical picture of leptospirosis and epidemiological anamnesis has remained a subject for discussion. However, the use of new techniques for specific confirmation of this disease reduces the percentage of such patients.

ORCID

Olena Zubach https://orcid.org/0000-0001-9110-577X

Acknowledgments

Authors would like to express their gratitude to the Defense Threat Reduction Agency (DTRA) and Ukraine Biological Threat Reduction Program (BTRP) to support the publication of this paper. While DTRA/BTRP did not support the research described in this publication, the Program supported the presentation of this research at an international forum and grantsmanship/science writing training related to this manuscript's development. This publication's contents are the responsibility of the authors and do not necessarily reflect the views of DTRA or the United States Government. The authors are thankful to Dr. Wojciech Iwaniak (Poland) for mentoring this manuscript development. The Authors also are thankful to the Lviv Oblast Hospital for Infectious Diseases and the State Institution Lviv Oblast Laboratory Center of the Ministry of Health of Ukraine for conducting MAT, PCR and archives of these organizations for providing access to official annual reports on human (suspected and confirmed) leptospirosis.

Conflict of interest

The authors do not report any financial or personal connections with other persons or organizations, which might negatively affect the contents of this publication and/or claim authorship rights to this publication.

Literature

Agampodi SB, Thevanesam V, Burns MA, Palihawadana P, Thaipadungpanit J, Perera S, Craig SB, Senaratne T, Kumara A, Nugegoda DB, et al. Leptospirosis outbreak in Sri Lanka in 2008: lessons for assessing the global burden of disease. Am J Trop Med Hyg. 2011 Sep 01;85(3):471–478. https://doi.org/10.4269/ajtmh.2011.11-0276

Allan KJ, Biggs HM, Halliday JEB, Kazwala RR, Maro VP, Cleaveland S, Crump JA. Epidemiology of leptospirosis in Africa: A systematic review of a neglected zoonosis and a paradigm for 'One Health' in Africa. PLoS Negl Trop Dis. 2015 Sep 14;9(9):e0003899. https://doi.org/10.1371/journal.pntd.0003899

Ashford DA, Kaiser RM, Spiegel RA, Perkins BA, Weyant RS, Bragg SL, Plikaytis B, Jarquin C, Reyes J, Amador J. Asymptomatic infection and risk factors for leptospirosis in Nicaragua. Am J Trop Med Hyg. 2000;63(5,6):249–254.

Bharadwaj R, Bal AM, Joshi SA, Kagal A, Pol SS, Garad G, Arjunwadkar V, Katti R. An urban outbreak of leptospirosis in Mumbai, India. Jpn J Infect Dis. 2002 Dec;55(6):194–196.

Centers for Disease Control of Ministry of Health of Ukraine. About leptospirosis morbidity levels and preventive measures in Ukraine in 2018 / Information letter of State Establishment «Centers for Disease Control of Ministry of Health of Ukraine» [Internet]. 2019 [cited 2020 Jul 01]. Available from https://kagarlyk-mrada.gov.ua/news/p2945

Dragon EA, Spadoro JP, Madey R, Persing DH, Smith TF, Tenover FC, White TJ. Quality control of polymerase chain reaction. In: Persing DH, Smith TF, Tenover FC, White TJ. Diagnostic Molecular Microbiology. Principals and Applications. Washington DC (USA): American Society for Microbiology; 1993. p. 160–168.

Dupouey J, Faucher B, Edouard S, Richet H, Kodjo A, Drancourt M, Davoust B. Human leptospirosis: an emerging risk in Europe? Comp Immunol Microbiol Infect Dis. 2014 Mar;37(2):77–83. https://doi.org/10.1016/j.cimid.2013.12.002

ECDC. Annual epidemiological report 2014 – food and waterborne diseases and zoonoses. Stockholm (Sweden): European Centre for Disease Prevention and Control; 2014 [cited 2020 Jul 01]. Available from http://ecdc.europa.eu/en/publications/Publications/food-waterborne-diseases-annual-epidemiological-report-2014.pdf

Golubić D, Markotić A. [Leptospirosis and hemorrhagic fever with renal syndrome in northwestern Croatia] (Croatian). Acta Med Croatica. 2003;57(5):369–372.

Guerrier G, Hie P, Gourinat AC, Huguon E, Polfrit Y, Goarant C, D'Ortenzio E, Missotte I. Association between Age and Severity to Leptospirosis in Children. PLoS Negl Trop Dis. 2013;7(9):e2436. https://doi.org/10.1371/journal.pntd.0002436

Guidelines to AmpliSens® Leptospira-FRT PCR kit for qualitative detection of 16S RNA of pathogenic *Leptospira* genospecies in the clinical material, autopsy material and biological material by the polymerase chain reaction (PCR) with real-time hybridization-fluorescence detection. Moscow (Russia): InterLabService; 2017 [cited 2020 Jul 01]. Available from https://interlabservice.ru/upload/iblock/8ce/Leptospira-FRT(Guidelines)_IvI_310119.pdf

Guillois Y, Bourhy P, Ayral F, Pivette M, Decors A, Aranda Grau JH, Champenois B, Malhère C, Combes B, Richomme C, et al. An outbreak of leptospirosis among kayakers in Brittany, North-West France, 2016. Euro Surveill. 2018 Nov 29;23(48):1700848. https://doi.org/10.2807/1560-7917.ES.2018.23.48.1700848

Levett PN. Leptospirosis. Clin Microbiol Rev. 2001 Apr 01;14(2):296–326. https://doi.org/10.1128/CMR.14.2.296-326.2001

Lucchesi PMA, Arroyo GH, Etcheverría AI, Parma AE, Seijo AC. Recommendations for the detection of *Leptospira* in urine by PCR. Rev Soc Bras Med Trop. 2004 Mar;37(2):131–134. https://doi.org/10.1590/S0037-86822004000200003

Morgan J, Bornstein SL, Karpati AM, Bruce M, Bolin CA, Austin CC, Woods CW, Lingappa J, Langkop C, Davis B, et al.; Leptospirosis Working Group. Outbreak of leptospirosis among triathlon participants and community residents in Springfield, Illinois, 1998. Clin Infect Dis. 2002 Jun 15;34(12):1593–1599. https://doi.org/10.1086/340615

OiE Terrestrial Manual. Chapter 3.1.12. Leptospirosis [Internet]. 2018 [cited 2020 Jul 01]. Available from https://www.oie.int/standard-setting/terrestrial-manual/access-online/

Order of MOH of Ukraine №905 dated 12.28.2015. On approval of the criteria by which cases of infectious and parasitic diseases to be registered are determined [Internet]. 2015 [cited 2020 Jul 01]. Available from https://zakon.rada.gov.ua/laws/show/z0379-16

Panwala T, Rajdev S, Mulla S. To evaluate the different rapid screening tests for diagnosis of leptospirosis. J Clin Diagnostic Res. 2015;9(2):DC21-DC24. https://doi.org/10.7860/JCDR/2015/11188.5587

Phraisuwan P, Whitney EAS, Tharmaphornpilas P, Guharat S, Thongkamsamut S, Aresagig S, Liangphongphanthu J, Junthima K, Sokampang A, Ashford DA. Leptospirosis: skin wounds and control strategies, Thailand, 1999. Emerg Infect Dis. 2002 Dec; 8(12):1455–1459. https://doi.org/10.3201/eid0812.020180

Postic D, Merien F, Perolat P, Baranton G. Diagnostic biologique leptospirose – borréliose de Lyme / Biological diagnosis leptospirosis – Lyme borreliosis, Paris, Collection des Laboratoires de Référence et d'Expertise. Paris (France): Institut Pasteur à Paris; 2000. p. 177–186.

Seifi A, Hajiabdolbaghi M, Mohammadnejad E. Co-infection of leptospirosis and Crimean-Congo hemorrhagic fever. Arch Clin Infect Dis. 2016 Jun 22;11(3):e32380. https://doi.org/10.5812/archcid.32380

Tan WL, Soelar SA, Suan MA, Hussin N, Cheah WK, Verasahib K, Goh PP. Leptospirosis incidence and mortality in Malaysia. Southeast Asian J Trop Med Public Health. 2016 May;47(3):434–440.

Thaipadungpanit J, Chierakul W, Wuthiekanun V, Limmathurotsakul D, Amornchai P, Boonslip S, Smythe LD, Limpaiboon R, Hoffmaster AR, Day NPJ, et al. Diagnostic accuracy of real-time PCR assays targeting 16S rRNA and lipL32 genes for human leptospirosis in Thailand: a case-control study. PLoS One. 2011 Jan 24; 6(1):e16236. https://doi.org/10.1371/journal.pone.0016236

Tsarenko T, Uhovskyi V, Korniienko L, Sakhniuk N, Kassich V, Palii A. Genotyping method (MLVA) of pathogenic leptospires for monitoring their distribution in ecosystems. Ukr J Ecol. 2019; 9(1):81–85.

Tubiana S, Mikulski M, Becam J, Lacassin F, Lefèvre P, Gourinat AC, Goarant C, D'Ortenzio E. Risk factors and predictors of severe leptospirosis in New Caledonia. PLoS Negl Trop Dis. 2013 Jan 10;7(1):e1991. https://doi.org/10.1371/journal.pntd.0001991

Vasiunets L, Semenyshyn O, Velychko O, Hatsiy L, Kulish I. Laboratory based of surveillance for leptospirosis in Lviv Oblast, Ukraine. Online J Public Health Inform. 2019 May 30;11(1):e251. https://doi.org/10.5210/ojphi.v11i1.9760

WHO. Human leptospirosis: guidance for diagnosis, surveillance and control [Internet]. Geneva (Switzerland): World Health Organization; 2003 [cited 2020 Jul 01]. Available from https://apps.who.int/iris/handle/10665/42667

Polish Journal of Microbiology
2020, Vol. 69, No 4, 427–439
https://doi.org/10.33073/pjm-2020-046

ORIGINAL PAPER

Biofilm Production Potential of *Salmonella* Serovars Isolated from Chickens in North West Province, South Africa

STEPHEN ABIOLA AKINOLA[1, 2], MPINDA EDOAURD TSHIMPAMBA[3], MULUNDA MWANZA[3] and COLLINS NJIE ATEBA[1]

[1] Department of Microbiology, Bacteriophage Therapy and Phage Bio-Control Laboratory, Faculty of Natural and Agricultural Sciences, North West University, Mmabatho, South Africa
[2] Phytochemical Food Network Research Group, Department of Crop Sciences, Tshwane University of Technology, Pretoria, South Africa
[3] Center for Animal Health Studies, Food Security and Safety Niche, Faculty of Natural and Agricultural Sciences, North West University, Mmabatho, South Africa

Submitted 10 August 2020, revised 24 September 2020, accepted 24 September 2020

Abstract

Bacterial biofilms have recently gained considerable interest in the food production and medical industries due to their ability to resist destruction by disinfectants and other antimicrobials. Biofilms are extracellular polymer matrices that may enhance the survival of pathogens even when exposed to environmental stress. The effect of incubation temperatures (25°C, 37°C, and 40°C) and *Salmonella* serotype on biofilm-forming potentials was evaluated. Previously typed *Salmonella* serotypes (55) isolated from the gut of chickens were accessed for biofilms formation using a standard assay. *Salmonella* Typhimurium ATCC 14028™ and *Salmonella* Enteritidis ATCC 13076™ (positive controls), *Escherichia coli* (internal control) and un-inoculated Luria Bertani (LB) broth (negative control) were used. The isolates formed no biofilm (11.86–13.56%), weak (11.86–45.76%), moderate (18.64–20.34%), strong biofilms (23.73–54.24%) across the various temperatures investigated. Serotypes, *Salmonella* Heidelberg and *Salmonella* Weltevreden were the strongest biofilm formers at temperatures (25°C, 37°C, and 40°C, respectively). The potential of a large proportion (80%) of *Salmonella* serotypes to form biofilms increased with increasing incubation temperatures but decreased at 40°C. Findings indicate that average temperature favours biofilm formation by *Salmonella* serotypes. However, the influence of incubation temperature on biofilm formation was greater when compared to serotype. A positive correlation exists between *Salmonella* biofilm formed at 25°C, 37°C and 40°C ($p \geq 0.01$). The ability of *Salmonella* species to form biofilms at 25°C and 37°C suggests that these serotypes may present severe challenges to food-processing and hospital facilities.

Key words: *Salmonella*, biofilm, biofilm production potential, crystal violet microtitre

Introduction

Biofilms exist as summative clusters of microorganisms that could be from a single or multiple species. Biofilms are densely populated microbial communities comprising microorganisms of the same or different species that live close to each other and therefore facilitate social interaction (Davey and O'Toole 2000; Li and Tian 2012). The multicellular properties of biofilms assist in the survival of microorganisms when exposed to undesirable environmental and stressful conditions. The attachment of planktonic microorganisms to surfaces is critical for biofilm formation (Arunasri and Mohan 2019). Biofilms can be formed on food contact surfaces, contaminated food materials, natural environments such as water bodies, and on human tissues (Hall-Stoodley et al. 2004). The formation of biofilms is an important virulence factor that enhances the pathogenicity of most microbes that cause infections in humans and animals and therefore alleviate their public health significance (Costerton et al. 1999). The formation of biofilms by bacteria has resulted in increasing rates of antimicrobial resistance emerging from the potential to prevent the penetration of antibacterial agents into cells during treatment (Patel 2005) thus making biofilm control medically important. However, very few data has been reported on a substantial correlation that could exists between *Salmonella* serotypes isolated from chickens, the multiple antibiotic resistance behavior, incubation/storage temperature, and

* Corresponding author: S.A. Akinola, Department of Microbiology, North West University, Mmabatho, South Africa; **e-mail:akinolastephen3@gmail.com**

their ability to form biofilms (Díez-García et al. 2012; Wang et al. 2013; Borges et al. 2018).

Similarly, the strive to achieve food safety through the inactivation of pathogenic microorganisms from food and food products is important and often faced with challenges such as biofilm formation (Sadekuzzaman et al. 2015). Microbial biofilms on food and food processing plants constitute a threat to food safety and health of consumers due to the huge tolerance to exogenous stress that results in ineffective disinfection process during plant sanitation and reduced options of antibiotics treatment, which could lead to food poisoning (Hall-Stoodley and Stoodley 2009; Sofos and Geornaras 2010). The abilities of bacteria to form biofilms have been investigated using the qualitative or the quantitative assays. In recent times, the qualitative biofilm assays have given way to the quantitative assays, which give more precise results than just findings based on observation. The quantitative biofilm assays allow for a numerical evaluation of the ability of bacteria to form biofilms. In this study, the quantitative assays were adopted based on its accuracy, reliability, and potential to enable precise quantification instruments.

Biofilm forming pathogens (*Salmonella* Typhimurium, *Pseudomonas aeruginosa*, *Escherichia coli*, *Staphylococcus aureus*, and *Staphylococcus epidermidis*) have been isolated in food and food processing plants in developed and developing countries (Dourou et al. 2011; Cook et al. 2012; Wang et al. 2013; Li et al. 2017; Papa et al. 2018). Some pathogenic bacteria are capable of growing at low temperatures on food and contact surfaces. Recently, according to Webber et al. (2019) *Salmonella* Enteritidis have been reported to form biofilms on industrial food surfaces at relatively low temperatures (3°C). This provokes concerns for safety in cold store food preservation. Therefore it is important to research into the biofilm formation potentials of *Salmonella* serotypes colonizing chickens reared for food in the North West province, South Africa, which is an agricultural hub of the nation to ensure safety of foods and encourage regional trade.

Food poisoning may ensue from consuming contaminated raw, fresh, and minimally processed food commodities. *Salmonella* borne infection outbreaks have been associated with the ingestion of *Salmonella* infected livestock products such as eggs, poultry meat and pork (Hur et al. 2012; EFSA-ECDC 2018). In the European Union and the United State of America, *Salmonella* spp. has been implicated as the causative agent for food poisoning, which results in ill-health with many cases of the outbreak in recent years. Based on previous epidemiological studies, salmonellosis outbreaks have been traced to the food of animal origin, and research interest has been geared at investigating the occurrence of pathogenic strains of *Salmonella* in animal food products (Dallal et al. 2010). The rate of deaths among humans resulting from non-typhoidal salmonellosis has been increasing, especially in developing countries, and the mortality rate among children and adults in Africa ranges from 22–47% (Gordon et al. 2008). *Salmonella* Typhimurium is known as the main cause of foodborne salmonellosis globally, including South Africa; however, in recent years *Salmonella* Enteritidis have soon become the dominant cause of Salmonellosis in South Africa (Muvhali et al. 2017). From 2003 to 2007, 2013 to 2015, and October 2019 an outbreak of foodborne salmonellosis emanating from national food programme was reported in the rural areas of the Kwazulu Natal province and North West province, South Africa causing severe conditions in humans (Niehaus et al. 2011; Motladiile et al. 2019). Malangu and Ogunbanjo (2009) reported an acute *Salmonella* poisoning in 2005 emanating from South African Hospitals. Biofilm production was reported in drinking water (Mulamattathil et al. 2014), while Isoken (2015) reported the isolation of biofilm-forming *Salmonella* species in cabbage and spinach sold in South Africa. The presence of *Salmonella* species in food and water provides opportunities for cross-contamination along the food chain and accounts for diseases in susceptible individuals (Karkey et al. 2016; Byrd-Bredbenner, 2017). Unfortunately, investigation along the critical control points on the food value chain has not been comprehensive. Most research has focused on the retail stores, processing utensils, and processing environment (Cook et al. 2012) as a source of *Salmonella* contamination while few focus on the livestock rearing environment, which is critical to an effective epidemiological survey. Therefore, this research hypothesized that the incubation temperature and type of *Salmonella* serotypes would affect the biofilm-forming potentials of *Salmonella* pathogens. This will help identify the biofilm formation status of microbial communities colonizing the food environment and possibly give an explanation to the observed cases of antibiotic resistance of *Salmonella* serotypes so as to develop informed strategies to counteract the menace of food poisoning that could emanate from such microbial communities. The study investigated the effect of incubation temperature on biofilm-forming potentials of selected *Salmonella* serotypes isolated from Chickens in North-West Province, South Africa.

Experimental

Materials and Methods

Materials. The following reagents and materials were used in the study; analytical grade absolute ethanol (95%), Luria Bertani broth medium (Merck, South

Africa), phosphate buffer saline tablets (Merck, South Africa), Crystal violet (Merck, South Africa) and sterile 96 well Eppendorf polystyrene flat-bottom microtitre plate (Greiner bio-one, Hamburg, Germany). All the reagents used were of analytical grades. Typed *Salmonella* cultures used were isolated from live Chickens in Mafikeng, North West Province, South Africa, and previously identified (Akinola et al. 2019). *Salmonella* Typhimurium ATCC 14028™ and *Salmonella* Enteritidis ATCC 13076™ were used as positive controls, un-inoculated media broth (negative control), and an environmental strain of *E. coli* was used as an internal control in the experiment.

Methods. Culturing of *Salmonella* isolates. Luria Bertani (LB) broth was prepared following the manufacturer's instruction and was sterilized in an autoclave at 121°C for 15 minutes. Presumptive *Salmonella* strains were isolated using the International Organization for Standardization (2002) ISO 6579:2002 protocols, characterized and serotyped as previously reported by Akinola et al. (2019). Individual *Salmonella* serotypes (55) were inoculated into sterile LB broth and were incubated aerobically at 37°C overnight. Re-activated cultures were then used to investigate the biofilm-forming potentials of the isolates.

Determination of biofilm formation by *Salmonella* isolates. The biofilm production abilities of *Salmonella* isolates was determined using the crystal violet based microtitre plate assay method as described by Silagyi et al. (2009) and Stepanović et al. (2000). A loop full of *Salmonella* cultures were inoculated and grown overnight in LB (Balbontin et al. 2014) broth at 25°C, 37°C, and 40°C. The turbidimetry method was used to determine the concentration of *Salmonella* serotypes in a UV-spectrophotometer through the instrument of absorbance at 600 nm (Moosdeen et al. 1988). Dilution was made till an average of 5×10^6 CFU/ml concentration was reached and confirmed using the pour plating techniques on prepared *Salmonella Shigella* agar plates. One hundred microliters of grown culture was diluted in 10 ml sterile LB broth (1:100). Then, 200 µl of diluted culture was dispensed in 96 wells microtitre plate and was incubated at 25°C, 37°C, and 40°C for 24 hours. *Salmonella* Typhimurium ATCC 14028™, and *Salmonella* Enteritidis ATCC 13076™ (positive control) and the environmental strain of *E. coli* was used as an internal positive control in the experiment. Un-inoculated sterile LB broth was used as a negative control in the experiment. The experiment was done in three replicated wells. After 24 hours of incubation, LB broth was discarded by turning upside down and shaking off the liquid broth prior to washing of the plate in a tub of phosphate buffer saline solution. The washing process was repeated twice to enable the removal of unattached cells. A 200 µl of crystal violet dye (1% w/v) was added to each well and plates were incubated at room temperature for 1 h. After incubation, the dye was discarded, and wells were washed five times in phosphate buffer saline solution. The microtitre plate was blot dry with laboratory paper towels and was allowed to dry at room temperature. After, 200 µl of 95% ethanol was added to each well and was incubated at room temperature for 5 min. The resulting solution was thereafter transferred into a new 96 well microtitre plate. The optical density (OD) of the resulting solution was quantified in terms of absorbance at a wavelength of 630 nm in an automatic Enzyme-Linked Immunosorbent Assay (ELISA) microtitre plate reader (MB-580, Zhengzhou, China). Sterile LB broth was used as blank in the determination, while the optical densities was used to investigate the biofilm formation potential of *Salmonella* isolates using the following conditions as stated by Papa et al. (2018); $OD_S < OD_C$ = No biofilm formation, $OD_C < OD_S < 2OD_C$ = Weak biofilm formation, $2OD_C < OD_S < 4OD_C$ = Moderate biofilm formation, $4OD_C < OD_S$ = Strong biofilm formation; Where: OD_C = OD of negative control, OD_S = OD of sample. Optical densities were obtained in triplicates, and the mean obtained was regarded as optical densities for each *Salmonella* serotype.

Statistical analysis. The statistical analysis was done using percentages and central tendency measures such as mean and frequencies using Statistical Package for Social Sciences. The significance of the effect of incubation temperatures on biofilm formation was evaluated using the one-way analysis of variance (ANOVA). The relationship between incubation temperature and biofilm-forming potentials of *Salmonella* isolates was evaluated using Pearson correlation analysis. The significance of variables was evaluated at a 90% confidence interval using the Statistical Package for Social Sciences (SPSS version 17, Illinois USA).

Results and Discussion

In Table I, the identity of *Salmonella* serotypes used in this study is presented. The isolates were from chickens reared in North West Province, South Africa, as earlier reported by Akinola et al. (2017). The optical densities and degree of biofilm formation by *Salmonella* serotypes isolated from chickens as influenced by incubation temperature is as presented in Table II. The values obtained represent the optical densities obtained from the crystal violet biofilm microtitre plate assay using various *Salmonella* serotypes as inoculum. At incubation temperature of 25°C, the optical density of *Salmonella* serotypes ranged from 0.008 to 1.048 while at 37°C (0.04–1.02) and 40°C (0.023–1.509). At 37°C the OD of CHG16 (*Salmonella enterica* subsp.

Table I
Identities of *Salmonella* isolates used for biofilm assay.

Isolate number	Sources	Accession number	Organism
CHG1	Broiler	MG663456	*Salmonella enterica* subsp. *enterica*
CHG2	Broiler	MG663457	*Salmonella enterica* subsp. *enterica*
CHG3	Broiler	MG663458	*Salmonella enterica* subsp. *enterica*
CHG4	Broiler	MG663459	*Salmonella enterica ser.* Weltevreden
CHG5	Broiler	MG663460	*Salmonella enterica ser.* Chingola
CHG6	Broiler	MG663461	*Salmonella enterica ser.* Arizonae
CHG7	Broiler	MG663462	*Salmonella enterica ser.* Bovismorbificans
CHG8	Layer	MG663463	*Salmonella enterica* subsp. *enterica*
CHG9	Layer	MG663464	*Salmonella enterica* subsp. *enterica*
CHG10	Layer	MG663465	*Salmonella enterica ser.* Typhimurium
CHG11	Layer	MG663466	*Salmonella enterica ser.* Salamae
CHG12	Layer	MG663467	*Salmonella enterica ser.* Houten
CHG13	Layer	MG663468	*Salmonella enterica* subsp. *enterica*
CHG14	Indigenous Venda	MG663469	*Salmonella enterica ser.* Bareilly
CHG15	Indigenous Venda	MG663470	*Salmonella enterica* subsp. *enterica*
CHG16	Indigenous Venda	MG663471	*Salmonella enterica* subsp. *enterica*
CHG17	Indigenous Venda	MG663472	*Salmonella enterica* subsp. *enterica*
CHG18	Indigenous Venda	MG663473	*Salmonella enterica ser.* Heidelberg
CHG19	Indigenous Venda	MG663474	*Salmonella enterica ser.* Arizonae
CHG20	Indigenous Venda	MG663475	*Salmonella enterica* subsp. *enterica*
CHG21	Indigenous Venda	MG663476	*Salmonella enterica ser.* India
CHG22	Indigenous Venda	MG663477	*Salmonella enterica ser.* Crossness
CHG23	Indigenous Venda	MG663478	*Salmonella enterica ser.* Albany
CHG24	Indigenous Venda	MG663479	*Salmonella enterica ser.* Yovokome
CHG25	Indigenous Venda	MG663480	*Salmonella enterica ser.* Pullorum
CHG26	Indigenous Venda	MG663481	*Salmonella enterica ser.* Infantis
CHG27	Broiler	MG663482	*Salmonella enterica ser.* Arizonae
CHG28	Broiler	MG663483	*Salmonella enterica ser.* Heidelberg
CHG29	Broiler	MG663484	*Salmonella enterica* subsp. *enterica*
CHG30	Broiler	MG663485	*Salmonella enterica* subsp. *enterica*
CHG31	Broiler	MG663486	*Salmonella bongori*
CHG32	Broiler	MG663487	*Salmonella bongori*
CHG33	Broiler	MG663488	*Salmonella enterica ser.* Arizonae
CHG34	Layer	MG663489	*Salmonella enterica* subsp. *enterica*
CHG35	Layer	MG663490	*Salmonella enterica ser.* Wandsworth
CHG36	Layer	MG663491	*Salmonella enterica* subsp. *enterica*
CHG37	Layer	MG663492	*Salmonella bongori*
CHG38	Layer	MG663493	*Salmonella enterica ser.* Kentucky
CHG39	Layer	MG663494	*Salmonella bongori*
CHG40	Layer	MG663495	*Salmonella enterica ser.* Blockley
CHG41	Layer	MG663496	*Salmonella enterica ser.* Newport
CHG42	Layer	MG663497	*Salmonella enterica ser.* Typhimurium
CHG43	Indigenous koekoek	MG663498	*Salmonella bongori*
CHG44	Indigenous koekoek	MG663499	*Salmonella enterica ser.* Manchester
CHG45	Indigenous koekoek	MG663500	*Salmonella enterica* subsp. *enterica*
CHG46	Indigenous koekoek	MG663501	*Salmonella enterica* subsp. *enterica*
CHG47	Indigenous koekoek	MG663502	*Salmonella enterica ser.* Typhimurium

Table I. Continued

Isolate number	Sources	Accession number	Organism
CHG48	Indigenous koekoek	MG663503	*Salmonella enterica* subsp. *enterica*
CHG49	Indigenous koekoek	MG663504	*Salmonella enterica ser.* Typhimurium
CHG50	Indigenous koekoek	MG663505	*Salmonella enterica ser.* Typhimurium
CHG51	Indigenous koekoek	MG663506	*Salmonella enterica ser.* Typhimurium
CHG52	Indigenous koekoek	MG663507	*Salmonella enterica ser.* Koessen
CHG53	Indigenous koekoek	MG663508	*Salmonella bongori*
CHG54	Indigenous koekoek	MG663509	*Salmonella enterica ser.* Blegdam
CHG55	Indigenous koekoek	MG663456	*Salmonella enterica* subsp. *enterica*

Akinola et al. (2019)

Table II
Optical densities and degree of biofilms formed by *Salmonella* serotypes as influenced by incubation temperatures.

ID	*Salmonella* isolates	Incubation temperature			Degree of biofilms formed		
		25°C	37°C	40°C	25°C	37°C	40°C
CHG1	*Salmonella enterica* subsp. *enterica*	0.107 ± 0.003	0.312 ± 0.089	0.132 ± 0.020	Moderate	Weak	Moderate
CHG2	*Salmonella enterica* subsp. *enterica*	0.075 ± 0.009	0.969 ± 0.065	0.342 ± 0.106	Moderate	Strong	Strong
CHG3	*Salmonella enterica* subsp. *enterica*	0.023 ± 0.018	0.946 ± 0.123	0.063 ± 0.032	No biofilm	Strong	Weak
CHG8	*Salmonella enterica* subsp. *enterica*	0.247 ± 0.099	0.271 ± 0.030	0.300 ± 0.071	Strong	Weak	Strong
CHG9	*Salmonella enterica* subsp. *enterica*	0.120 ± 0.052	0.291 ± 0.015	0.082 ± 0.041	Moderate	Weak	Weak
CHG13	*Salmonella enterica* subsp. *enterica*	0.095 ± 0.017	0.319 ± 0.058	0.261 ± 0.081	Moderate	Weak	Strong
CHG15	*Salmonella enterica* subsp. *enterica*	0.037 ± 0.013	1.006 ± 0.031	0.167 ± 0.136	Weak	Strong	Moderate
CHG16	*Salmonella enterica* subsp. *enterica*	0.067 ± 0.009	1.022 ± 0.108	0.085 ± 0.033	Moderate	Strong	Weak
CHG17	*Salmonella enterica* subsp. *enterica*	0.405 ± 0.222	1.010 ± 0.045	0.082 ± 0.060	Strong	Strong	Weak
CHG20	*Salmonella enterica* subsp. *enterica*	0.278 ± 0.071	0.885 ± 0.120	0.083 ± 0.027	Strong	Strong	Weak
CHG29	*Salmonella enterica* subsp. *enterica*	0.149 ± 0.061	0.961 ± 0.180	0.077 ± 0.024	Strong	Moderate	Weak
CHG30	*Salmonella enterica* subsp. *enterica*	0.303 ± 0.085	0.591 ± 0.174	0.112 ± 0.006	Strong	Strong	Moderate
CHG34	*Salmonella enterica* subsp. *enterica*	0.039 ± 0.032	1.227 ± 0.273	0.010 ± 0.005	Weak	Weak	No biofilm
CHG36	*Salmonella enterica* subsp. *enterica*	0.026 ± 0.024	0.704 ± 0.220	0.065 ± 0.046	No biofilm	Weak	Weak
CHG45	*Salmonella enterica* subsp. *enterica*	0.800 ± 0.572	0.983 ± 0.177	1.098 ± 0.736	Strong	Weak	Strong
CHG46	*Salmonella enterica* subsp. *enterica*	0.937 ± 0.668	1.017 ± 0.244	1.089 ± 0.803	Strong	Weak	Strong
CHG48	*Salmonella enterica* subsp. *enterica*	0.259 ± 0.308	1.248 ± 0.080	0.407 ± 0.447	Strong	Moderate	Strong
CHG55	*Salmonella enterica* subsp. *enterica*	0.341 ± 0.115	1.605 ± 0.066	0.395 ± 0.098	Strong	Weak	Strong
CHG31	*Salmonella bongori*	0.276 ± 0.037	0.561 ± 0.150	0.034 ± 0.012	Strong	Moderate	No biofilm
CHG32	*Salmonella bongori*	0.012 ± 0.007	0.422 ± 0.191	0.034 ± 0.017	No biofilm	No biofilm	No biofilm
CHG37	*Salmonella bongori*	0.030 ± 0.001	0.700 ± 0.204	0.066 ± 0.013	No biofilm	Weak	Weak
CHG39	*Salmonella bongori*	0.277 ± 0.094	1.075 ± 0.340	0.489 ± 0.192	Strong	Weak	Strong
CHG43	*Salmonella bongori*	0.077 ± 0.003	0.812 ± 0.288	0.129 ± 0.012	Moderate	Weak	Moderate
CHG53	*Salmonella bongori*	0.769 ± 0.205	1.244 ± 0.104	1.020 ± 0.207	Strong	Weak	Strong
Serovars							
CHG4	*Salmonella enterica ser.* Weltevreden	0.138 ± 0.042	0.817 ± 0.273	1.509 ± 0.453	Strong	Strong	Strong
CHG5	*Salmonella enterica ser.* Chingola	0.181 ± 0.107	0.308 ± 0.055	0.446 ± 0.011	Strong	Weak	Strong
CHG6	*Salmonella enterica ser.* Arizonae	0.108 ± 0.090	0.287 ± 0.035	0.198 ± 0.044	Moderate	Weak	Strong
CHG19	*Salmonella enterica ser.* Arizonae	0.151 ± 0.045	0.574 ± 0.145	0.152 ± 0.036	Strong	Moderate	Moderate
CHG27	*Salmonella enterica ser.* Arizonae	0.026 ± 0.011	0.901 ± 0.040	0.472 ± 0.040	No biofilm	Strong	Strong
CHG33	*Salmonella enterica ser.* Arizonae	0.038 ± 0.017	0.848 ± 0.453	0.064 ± 0.031	Weak	Weak	Weak
CHG7	*Salmonella enterica ser.* Bovismorbificans	0.586 ± 0.116	0.220 ± 0.032	0.163 ± 0.147	Strong	No biofilm	Moderate

Table II. Continued

ID	*Salmonella* isolates	Incubation temperature			Degree of biofilms formed		
		25°C	37°C	40°C	25°C	37°C	40°C
CHG10	*Salmonella enterica ser.* Typhimurium	1.028 ± 0.507	0.230 ± 0.059	0.167 ± 0.166	Strong	No biofilm	Moderate
CHG42	*Salmonella enterica ser.* Typhimurium	0.069 ± 0.064	0.089 ± 0.038	0.039 ± 0.018	Moderate	Weak	No biofilm
CHG47	*Salmonella enterica ser.* Typhimurium	0.024 ± 0.011	0.920 ± 0.315	0.053 ± 0.026	No biofilm	Weak	Weak
CHG49	*Salmonella enterica ser.* Typhimurium	0.167 ± 0.107	0.468 ± 0.142	0.163 ± 0.071	Strong	No biofilm	Moderate
CHG50	*Salmonella enterica ser.* Typhimurium	0.116 ± 0.084	0.310 ± 0.098	0.099 ± 0.007	Moderate	No biofilm	Weak
CHG51	*Salmonella enterica ser.* Typhimurium	0.098 ± 0.041	1.132 ± 0.333	0.185 ± 0.051	Moderate	Weak	Strong
CHG11	*Salmonella enterica ser.* Salamae	0.008 ± 0.004	0.284 ± 0.024	0.173 ± 0.019	No biofilm	Weak	Moderate
CHG12	*Salmonella enterica ser.* Houten	0.327 ± 0.059	0.360 ± 0.053	0.248 ± 0.118	Strong	Weak	Strong
CHG14	*Salmonella enterica ser.* Bareilly	0.182 ± 0.061	0.906 ± 0.163	1.009 ± 0.642	Strong	Strong	Strong
CHG18	*Salmonella enterica ser.* Heidelberg	1.048 ± 0.915	0.976 ± 0.104	0.064 ± 0.022	Strong	Strong	Weak
CHG28	*Salmonella enterica ser.* Heidelberg	0.098 ± 0.012	0.695 ± 0.167	0.038 ± 0.019	Weak	Strong	No biofilm
CHG21	*Salmonella enterica ser.* India	0.390 ± 0.091	1.024 ± 0.077	0.238 ± 0.094	Strong	Strong	Strong
CHG22	*Salmonella enterica ser.* Crossness	0.097 ± 0.008	0.640 ± 0.154	0.402 ± 0.366	Moderate	Moderate	Strong
CHG23	*Salmonella enterica ser.* Albany	0.212 ± 0.088	0.700 ± 0.108	0.303 ± 0.108	Strong	Moderate	Strong
CHG24	*Salmonella enterica ser.* Yovokome	0.107 ± 0.011	0.906 ± 0.277	0.041 ± 0.014	Weak	Strong	No biofilm
CHG25	*Salmonella enterica ser.* Pullorum	0.183 ± 0.082	0.733 ± 0.035	0.729 ± 0.082	Strong	Moderate	Strong
CHG26	*Salmonella enterica ser.* Infantis	0.320 ± 0.115	0.754 ± 0.124	0.743 ± 0.137	Strong	Moderate	Strong
CHG35	*Salmonella enterica ser.* Wandsworth	0.056 ± 0.018	0.723 ± 0.240	0.101 ± 0.031	Weak	Weak	Moderate
CHG38	*Salmonella enterica ser.* Kentucky	0.214 ± 0.088	1.012 ± 0.224	0.304 ± 0.255	Strong	Weak	Strong
CHG40	*Salmonella enterica ser.* Blockley	0.057 ± 0.030	0.387 ± 0.077	0.077 ± 0.037	Weak	No biofilm	Weak
CHG41	*Salmonella enterica ser.* Newport	0.245 ± 0.376	0.604 ± 0.310	0.388 ± 0.554	Strong	Weak	Strong
CHG44	*Salmonella enterica ser.* Manchester	0.078 ± 0.012	1.107 ± 0.172	0.128 ± 0.020	Moderate	Weak	Moderate
CHG52	*Salmonella enterica ser.* Koessen	0.206 ± 0.038	1.021 ± 0.169	0.290 ± 0.034	Strong	Weak	Strong
CHG54	*Salmonella enterica ser.* Blegdam	0.155 ± 0.078	0.584 ± 0.194	0.135 ± 0.027	Strong	Weak	Moderate
BLNK	Blank (LB broth)	0.089 ± 0.009	0.278 ± 0.017	0.0385 ± 0.036	–	–	–
CNTRL1	Negative control (un-inoculated broth)	0.025 ± 0.038	0.267 ± 0.002	0.023 ± 0.017	No biofilm	No biofilm	No biofilm
CNTRL2	Positive control *(Salmonella enterica ser.* Typhimurium ATCC 14028™)	0.352 ± 0.106	1.397 ± 0.107	0.493 ± 0.167	Strong	Moderate	Strong
CNTRL3	Positive control (*Salmonella enterica ser.* Enteritidis ATCC 13076™)	0.410 ± 0.017	1.725 ± 0.009	0.602 ± 0.059	Strong	Moderate	Strong
CNTRL4	Internal Control (*E. coli* 0157)	1.031 ± 0.072	1.236 ± 0.030	1.309 ± 0.076	Strong	Moderate	Strong

Values represents means of triplicate determinations.
No biofilm formation (if $OD_S < OD_C$), weak biofilm formation (if $OD_C < OD_S < 2OD_C$), moderate biofilm formation ($2OD_C < OD_S < 4OD_C$) and strong biofilm formation ($4OD_C < OD_S$). Optical density (OD) ± standard deviation at 630 nm.
CNTRL1 – Negative control (un-inoculated nutrient broth), CNTRL2 – Positive control (*Salmonella enterica ser.* Typhimurium), CNTRL3 – Positive control 2 (*Salmonella enterica ser.* Enteritidis), CNTRL4 – Positive Internal Control (*Escherichia coli*), BLNK – Luria Bertani broth.

enterica) was highest while CHG18 (*Salmonella* Heidelberg) at 25°C and CHG4 (*Salmonella* Weltevreden) at 40°C. As expected, the negative control (un-inoculated broth) had low OD (0.267 ± 0.002) hence did not form biofilm, while the positive controls *Salmonella* Typhimurium (1.397 ± 0.107) and *Salmonella* Enteritidis (1.725 ± 0.009), and the internal control *E. coli* (1.236 ± 0.030) were positive to biofilm production at 24 hours of incubation. As obtained in this study, biofilm formation was greatly influenced by the *Salmonella* serotype colonizing the substrates than the temperature of incubation at 24 hours of incubation. The optical density of eighty percent *Salmonella* serotypes increased at increasing incubation temperatures of 25°C to 37°C but decreased at a higher incubation temperature of 40°C. However, the optical densities of samples CHG4, CHG5, CHG14, CHG25, CHG26, CHG45, and CHG46 increased with increasing incubation temperature. The optical density of the *Salmonella* serotype was optimum at incubation temperatures of 37°C except in isolates CHG7, CHG10 and CHG18 that were optimum at 25°C. Similarly, the incubation temperatures had a significant effect on the optical density obtained in the positive and internal controls, while

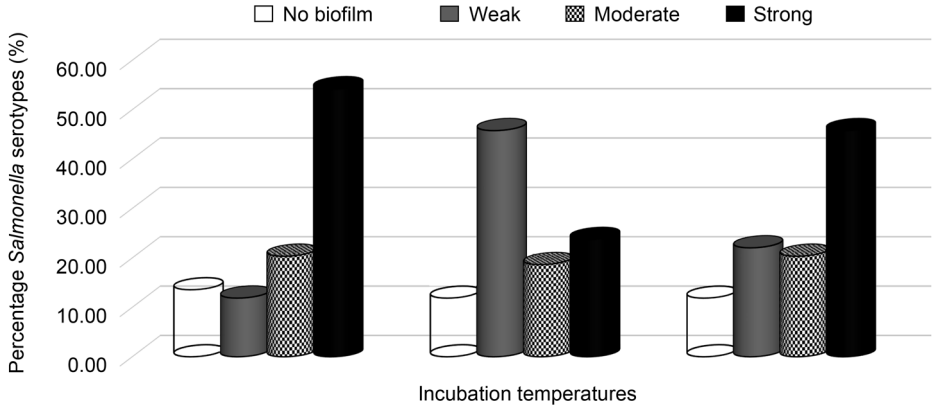

Fig. 1. Effect of incubation temperatures on biofilm-forming potentials of *Salmonella* serotypes.

there was no effect on the negative control. Hence, incubation temperature and type of *Salmonella* serotype influences the biofilm-forming abilities of *Salmonella*. Biofilm formation by *Salmonella* serotypes are well favored at an incubation temperature of 37°C.

The degree of biofilm formed by test *Salmonella* serotypes is as presented in Table II. The degree of biofilms formed by the *Salmonella* serotypes ranged from no biofilm, weak, moderate to strong biofilm. Fig. 1 presents the percent distribution of the degree of biofilm formed by selected pathogens. *Salmonella* serotypes that produced no biofilms ranged from 11.86% to 13.56%. The percent *Salmonella* serotypes that produced weak biofilms at varying temperatures ranged from 11.86% to 45.76%, and this observation was optimum at an incubation temperature of 37°C (45.76%). The percent distribution of moderate *Salmonella* biofilm producers at varied incubation temperatures ranged from 18.64 to 20.34% and was highest at both 25°C and 40°C (20.34%). The percent *Salmonella* serotype that produced strong biofilms ranged from 23.73 to 54.24% and was highest at 25°C incubation temperatures.

This study observed that biofilm production by selected *Salmonella* serotypes was influenced by the incubation temperature and type of *Salmonella* serotypes. A strong *Salmonella* biofilm can be produced at 25°C (room temperature) within 24 hours of incubation. An incubation temperature of 25°C favors *Salmonella* biofilm formation than at much higher temperatures. The ability of *Salmonella* serotypes to form strong biofilms at room temperatures could pose a threat to food safety and hygiene practices especially in food processing facilities. Public health pathogens, including *Salmonella*, has been identified to have the ability to form biofilms on food contact surfaces (Bridier et al. 2014), which supports the findings in this study. The occurrence of this *Salmonella* serotype in food or food contact surfaces could incur extra cost in plant sanitation, thereby increasing the overhead cost of food production, which in turn results in high food prices. Biofilm formation has been identified as one of the mechanisms of bacterial pathogens to evade antimicrobial treatment (Floyd et al. 2017). Bacteria biofilms are able to tolerate harsh conditions and resist antibiotics treatments due to a unique biofilm matrix (Sharma et al. 2019). Microbial cells can sense the extracellular environment and cause the cellular response's triggering in favor of biofilm formation (Koo and Yamada 2016). Biofilm matrices act as both physical and chemical barriers (Khan et al. 2017) that could prevent antimicrobials from reaching their targets in microbes, thus preventing the control of pathogens and increasing resistance among microorganisms implicated in biofilm formation or infections. Besides the barrier to penetration, the depletion of nutrient sources and triggering of stress response and development of biofilm resistant phenotypes in microorganism have been proved as mechanisms that aid antibiotic resistance of pathogens (Mah and O'Toole 2001). Similarly, *Salmonella* pathogens have been reported to contain the alternative sigma factor (RpoS) and flagella architectures that could enable its biofilm formation (Lee et al. 1995; Kroupitski et al. 2009) which supports the biofilm formation in this study. Hence, *Salmonella* biofilms could pose a serious threat to the effective treatment of salmonellosis through antimicrobial.

Fig. 2, 3 and 4 presents the behavioral patterns of *Salmonella* serotypes to biofilm production at 25°C, 37°C, and 40°C, respectively. At 25°C, 50% of the total *Salmonella enterica* subsp. *enterica* produced strong biofilms while at 37°C and 40°C only 38.7% had strong biofilm formation. *Salmonella bongori* (50%) produced strong biofilm at 25°C and 40°C (33.3%) whereas could not produce strong biofilms at 37°C. Only 33.3% of *Salmonella* Typhimurium produced strong biofilms at 25°C, while 16.7% at 40°C. However, none of the isolate produced strong biofilms at 40°C. Furthermore, 27.8% of *Salmonella enterica* subsp. *enterica, Salmonella* Typhimurium (50%) and *Salmonella bongori* (16.7%) produced moderate biofilms. Also, at 37°C, *Salmonella* Arizonae (25%) and *Salmonella bongori* (16.7%) produced

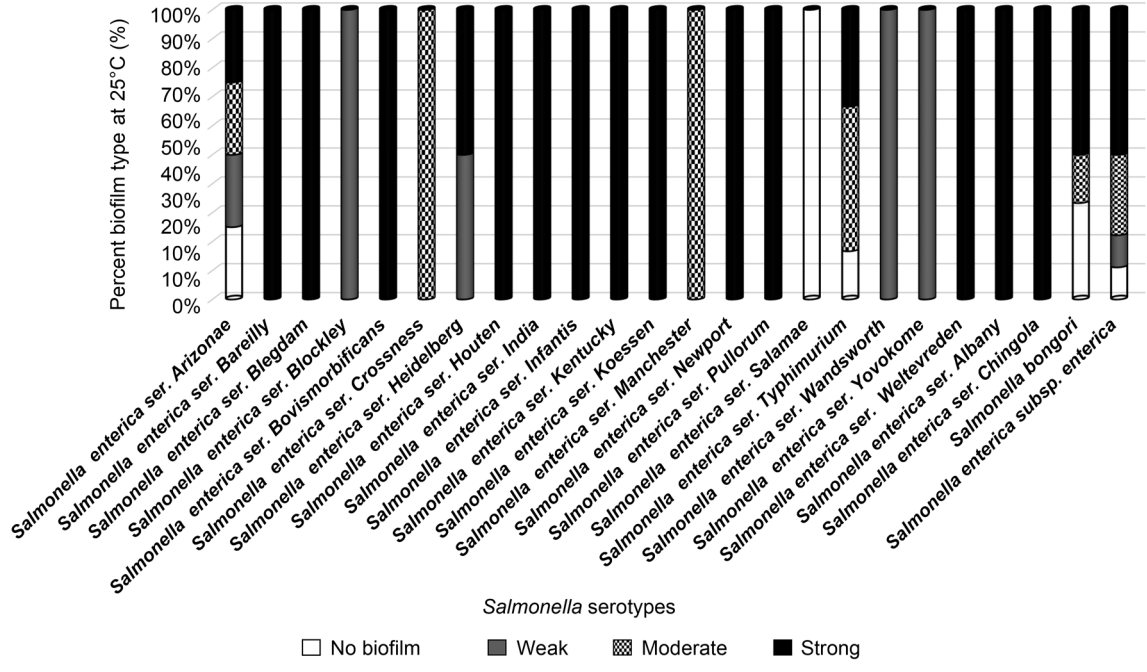

Fig. 2. Behavioral pattern of *Salmonella* serotypes to biofilm production at 25°C incubation temperature.

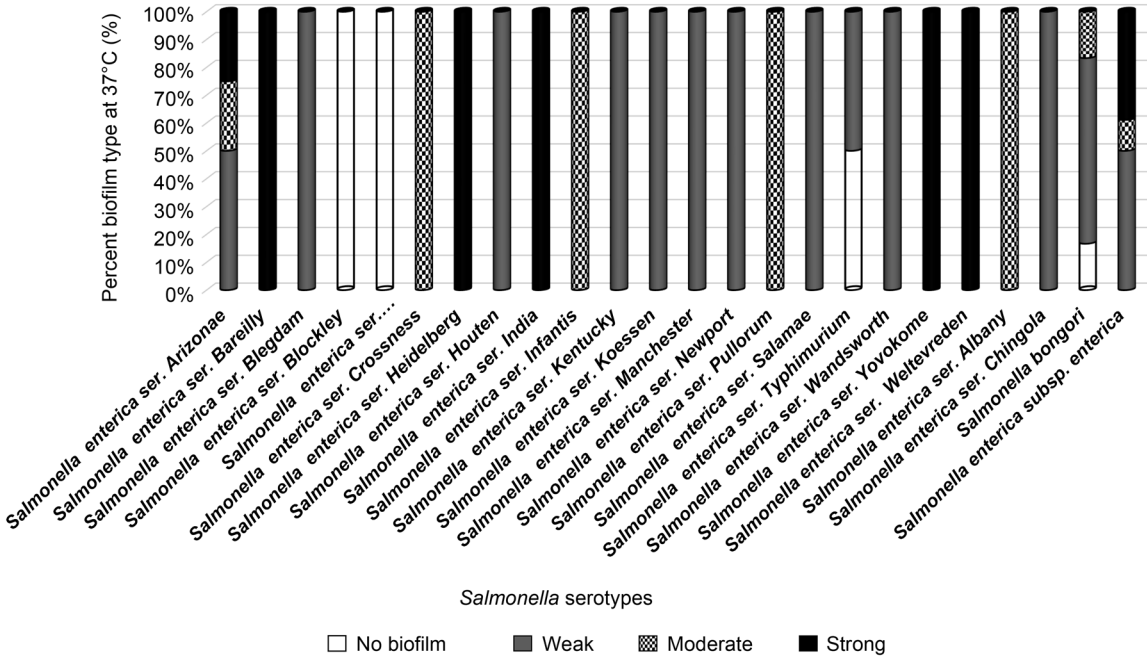

Fig. 3. Behavioral pattern of *Salmonella* serotypes to biofilm production at 37°C incubation temperature.

moderate biofilms. However, *Salmonella* serotypes Crossness and Manchester could only produce moderate biofilms at 25°C and 37°C. *Salmonella* Pullorum, *Salmonella* Albany, and *Salmonella* Infantis could only produce moderate biofilms at 37°C, while *Salmonella* Bovismobifacens, *Salmonella* Kentucky, and *Salmonella Salamae* produced moderate biofilms at 40°C.

Furthermore, fifty percent of total *Salmonella* Heidelberg, *Salmonella* Arizonae, *Salmonella* Typhimurium, and *Salmonella* Arizonae (25%) were weak biofilms producers at 25°C, 37°C, and 40°C, while *Salmonella* Yovokome, *Salmonella* Wandsworth, and *Salmonella* Blockley were all weak biofilm producers at 25°C. Weak biofilm formation by *Salmonella* serotypes is indicative of decreased potentials of adherence to surfaces, auto-aggregation among cells, and increased sensitivity to biocides treatments (Rendueles et al. 2013). Eleven percent of *Salmonella enterica* subsp. *enterica*, *Salmonella*

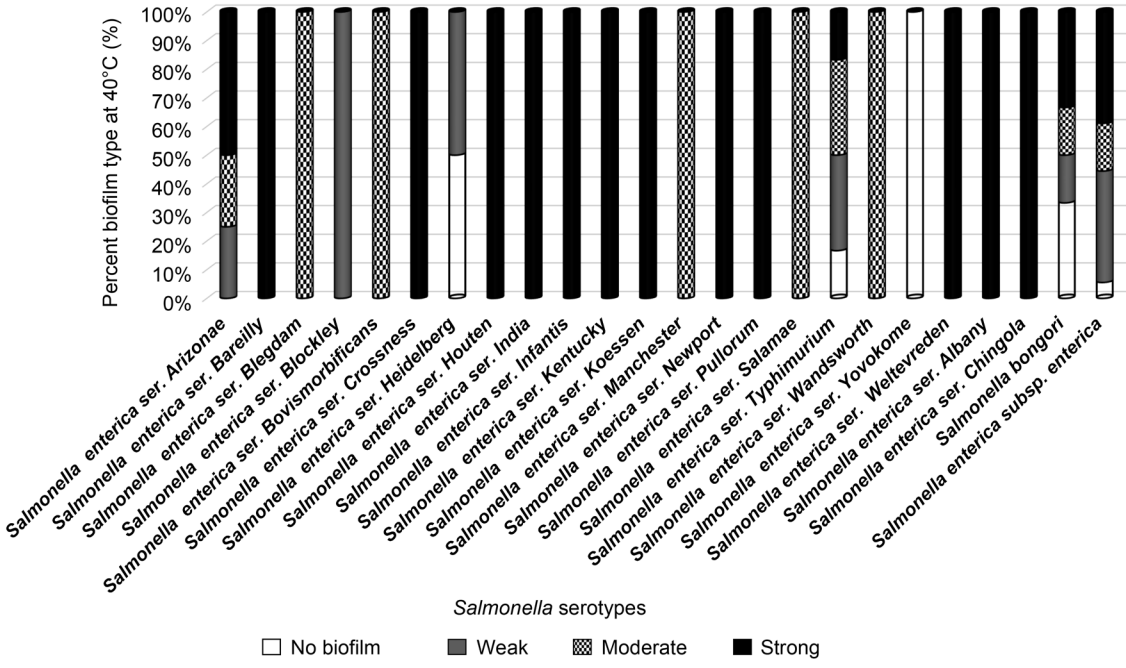

Fig. 4. Behavioral pattern of *Salmonella* serotypes to biofilm production at 40°C incubation temperature.

Typhimurium (16.7%) and *Salmonella bongori* (33.3%) isolates were non-biofilm producers at 25°C and 40°C while at 37°C *Salmonella* Typhimurium (50%) lost their biofilm producing abilities. The potentials of bacteria to form biofilms on food contact surfaces have been related to the type of media or substrate, incubation time, and type of microorganisms (Díez-García et al. 2012). The detection of biofilm-producing *Salmonella* serotypes isolated from chicken in this study corroborates the previous reports of Wang et al. (2013) on the occurrence and isolation of biofilm-forming *Salmonella* isolated from chicken processing surfaces in China. Similarly, biofilm-forming *Salmonella* has been isolated from tomatoes (Iturriaga et al. 2007), cereals (Cui et al. 2015), and almond (Suehr et al. 2015). The dependence of temperature and *Salmonella* type on the quality of biofilm formation agrees with the report of Shi and Zhu (2009) on the dependence of *Salmonella* type and environmental factors on the quality, quantity, and ability of *Salmonella* to form biofilms.

Similar to the observation made in this study, Almaguer-Flores (2013) has reported the influence of nutrient medium and bacterial cell characteristics on biofilm formation. In this study, the quality of biofilm formed by *Salmonella* serotypes was a function of the *Salmonella* serotype involved in biofilm formation. The process of biofilm formation is such a vibrant process whereby bacterium attaches itself to another cell of similar or different strains or onto surfaces, thereby producing an exopolysaccharides matrix through which they achieve survival against antibiotics or detergents (Tanaka et al. 2017). This process is affected by factors such as availability of nutrient/growth medium, pH, temperature, hydrodynamics of cells, and the hydrophobicity of contact surfaces (Irie and Parsek 2008; Dourou et al. 2011). Biofilms are extracellular polymeric substances that facilitate the interaction between bacterial cells and surfaces, which are important for the stability and survival of bacteria colonies (Olaya et al. 2013). Several authors have reported the production of biofilms in bacteria such as *P. aeruginosa*, *S. aureus*, *S. epidermidis*, *E. coli* O157:H7, *Campylobacter* spp. and *Salmonella* Typhimurium, *Salmonella* Enteritidis to mention but a few (Zogaj et al. 2001; Solano et al. 2002; Olaya et al. 2013; Chen et al. 2015; Yang et al. 2016; Li et al. 2017). Some strains of *Salmonella* Typhimurium isolated in this study do not produce biofilms, contrary to the previous report of Solano et al. (2002) on biofilm production in *Salmonella* Typhimurium. This observation may be due to genetic variation within the genetic make-up of *Salmonella* serotypes used in the investigation.

Table III presents the Pearson correlation between biofilm-forming potentials of *Salmonella* serotypes as influenced by incubation temperatures. The Pearson correlation coefficients ranged from 0.17 to 0.50. The correlation coefficient ($r = 0.50$) was highest between the biofilm-forming potentials obtained at 25°C and 40°C, indicating a significant temperature-dependent association. A positive correlation existed between the biofilm-forming potentials of *Salmonella* serotypes incubated at 25°C, 37°C, and 40°C. A significant positive correlation exists between *Salmonella* biofilm production at 25°C and 37°C ($p \leq 0.05$), while a positive and

Table III
Pearson correlations between biofilm production potential of *Salmonella* serotypes incubated at varied temperatures.

Incubation temperatures		25°C	37°C	40°C
25°C	Pearson correlation	1	0.170*	0.501**
	p-value		0.021	0.000
37°C	Pearson correlation	0.170*	1	0.263**
	p-value	0.021		0.000
40°C	Pearson correlation	0.501**	0.263**	1
	p-value	0.000	0.000	

* – correlation is significant at the 0.05 level (2-tailed)
** – correlation is significant at the 0.01 level (2-tailed)

moderate correlation exists between biofilms formed at 25°C and 40°C ($p \leq 0.01$). Similarly, a positive correlation exists between biofilm formed at 37°C and 40°C at $p \leq 0.01$ with a Pearson correlation coefficient of 0.263. The closer the correlation coefficient to unity the higher the relationship that exists between variables (Benesty et al. 2009; Mukaka 2012). However, a positive correlation, as observed in this study between *Salmonella* biofilm formed at different incubation temperatures, is implicative of a temperature-dependent association; hence, biofilm formation in *Salmonella* serotypes are temperature dependent.

Microbial biofilms are composed of exopolysaccharide matrices that aid the survival and breeding of new bacteria when exposed to harsh environments (Ikuma et al. 2013). Biofilm formation is an adaptation strategy to evade antibiotics or disinfectant treatment in biofilm, producing virulent strains (Patel 2005). Biofilm formation by microorganisms could enhance pathogenicity and provoke food safety issues. Bacterial biofilms make stronger the defense systems of bacterial pathogens to antibiotic treatments (Stewart and Costerton 2001; Patel 2005). Antibiotic resistance could threaten good health, increase economic burden and poverty on both processors and consumers of food products, especially in the developing countries. The presence of selected *Salmonella* serotypes in foods could cause the development of biofilms, which could resist antimicrobial treatment and, thereby, cause ill-health. The control of biofilm through the use of processing plant cleaning and sanitation operations in the poultry industries has become a difficult task due to the associative resistance of *Salmonella* to disinfectants and antimicrobials (Merino et al. 2019). Also, the inaccessibility of antimicrobials to equipment crevices and parts has limited plant sanitation; hence, the use of well-designed and cleaning efficient equipment is important to effectively control biofilm formation (Chmielewski and Frank 2004; Merino et al. 2019). The prevention of biofilm formation still remains the best strategy to control *Salmonella* biofilms (Merino et al. 2019). The combined use of antimicrobials and disinfectant having a broad spectrum has been recommended for *Salmonella* biofilm control in the poultry plants, which resulted in the use of triclosan, nanomaterials, halogenated furanones, antibiotics, disinfectants, and quaternary ammonium salts (Bridier et al. 2011; Steenackers et al. 2012). However, *Salmonella* biofilms formation on food contact surfaces and food processing equipment could increase the cost of cleaning operations in plants. The increased cost of production could lead to an increased cost of food products, which affects consumers' purchasing power, thereby casting a burden on the low- and middle-class income earners. Thus the inactivation of biofilm producers is important to ensure food safety and public health.

Conclusions

Salmonella serotypes isolated from chickens do have the potential to produce biofilms ranging from strong to no biofilm. *Salmonella* Heidelberg, *Salmonella enterica* subsp. *enterica* and *Salmonella* Weltevreden were the highest producers of strong biofilms at 25°C, 37°C and 45°C. A significant positive correlation exists between *Salmonella* biofilm production at 25°C, 37°C, and 40°C. The biofilm production potentials of *Salmonella* are both serotypes and temperature dependent. Ambient temperature (25°C) favors *Salmonella* biofilm formation than at a much higher temperature. This poses a concern to food quality and safety in homes, small and medium scale food enterprises where there is a limit to the power supply, especially in developing countries. The findings from this study are quite important for global tracking on the state of *Salmonella* serotypes biofilms formation and develop effective control strategies as some similar serotypes isolated from this study have been reported in other countries. The detection of strong *Salmonella* biofilm formers in chickens found within the North West province, South Africa, also calls for concern as biofilms forming pathogens are capable of evading antimicrobial treatment. However, a broader screening will be important to further provide information on this subject in other provinces within South Africa. Similarly, the investigation on the relationship between pathogenicity, multiple antibiotic resistance behaviors of *Salmonella* serotypes, and biofilm formation might be necessary to further knowledge in this field.

ORCID
Stephen Abiola Akinola https://orcid.org/0000-0001-9361-7680
Mpinda Edoaurd Tshimpamba
https://orcid.org/0000-0003-4469-3200
Mulunda Mwanza https://orcid.org/0000-0002-9311-6517
Collins Njie Ateba https://orcid.org/0000-0003-1230-5138

Acknowledgments

Authors acknowledge the support of North West University, South Africa and Department of Science and Technology-The World Academy of Science – National Research Foundation South Africa for funds that was provided for this study (UID: 110854).

Authors' contributions

Conceptualization: Stephen Abiola Akinola; Methodology: Stephen Abiola Akinola, Collins Njie Ateba, Mulunda Mwanza; Formal analysis and investigation: Stephen Abiola Akinola; Writing – original draft preparation: Stephen Abiola Akinola, Mpinda Edoaurd Tsimpamba, Collins Njie Ateba, Mulunda Mwanza under Original draft preparation.

Conflict of interest

The authors do not report any financial or personal connections with other persons or organizations, which might negatively affect the contents of this publication and/or claim authorship rights to this publication.

Literature

Akinola SA, Mwanza M, Ateba CN. Occurrence, genetic diversities and antibiotic resistance profiles of *Salmonella* serovars isolated from chickens. Infect Drug Resist. 2019;12:3327–3342. https://doi.org/10.2147/idr.s217421

Almaguer-Flores A. Biofilms in the oral environment. In: Yan Y, editor. Bio-tribocorrosion in biomaterials and medical implants. Duxford (UK): Woodhead Publishing. 2013 Jan 1; p. 169–186. https://doi.org/10.1533/9780857098603.2.169

Anderson TC, Nguyen TA, Adams JK, Garrett NM, Bopp CA, Baker JB, McNeil C, Torres P, Ettestad PJ, Erdman MM, Brinson DL. Multistate outbreak of human *Salmonella* Typhimurium infections linked to live poultry from agricultural feed stores and mail-order hatcheries, United States 2013. One Health. 2016 Dec 1;2: 144–149. https://doi.org/10.1016/j.onehlt.2016.08.002

Arunasri K, Mohan SV. Biofilms: microbial life on the electrode surface. In: Mohan SV, Pandey A, Varjani S, editors. Microbial electrochemical technology sustainable platform for fuels, chemicals and remediation, biomass, biofuels and biochemicals. Amsterdam (Netherlands): Elsevier. 2019 Jan 1; p. 295–313. https://doi.org/10.1016/b978-0-444-64052-9.00011-x

Balbontín R, Vlamakis H, Kolter R. Mutualistic interaction between *Salmonella enterica* and *Aspergillus niger* and its effects on *Zea mays* colonization. Microb Biotechnol. 2014 Nov;7(6):589–600. https://doi.org/10.1111/1751-7915.12182

Benesty J, Chen J, Huang Y, Cohen I. Pearson correlation coefficient. In: Noise reduction in speech processing. Springer Topics in Signal Processing, vol 2. Berlin, Heidelberg (Germany): Springer. 2009; p. 1–4. https://doi.org/10.1007/978-3-642-00296-0_5

Borges KA, Furian TQ, Souza SN, Menezes R, Tondo EC, Salle CT, Moraes HL, Nascimento VP. Biofilm formation capacity of *Salmonella* serotypes at different temperature conditions. Pesqui Vet Brasil. 2018 Jan;38(1):71–76. https://doi.org/10.1590/1678-5150-pvb-4928

Bridier A, Briandet R, Bouchez T, Jabot F. A model-based approach to detect interspecific interactions during biofilm development. Biofouling. 2014 Aug 9;30(7):761–771. https://doi.org/10.1080/08927014.2014.923409

Bridier A, Briandet R, Thomas V, Dubois-Brissonnet F. Resistance of bacterial biofilms to disinfectants: a review. Biofouling. 2011 Oct 15;27(9):1017–1032. https://doi.org/10.1080/08927014.2011.626899

Byrd-Bredbenner C. Food Safety. In: Rippe J, editor. Nutrition in Lifestyle Medicine. Nutrition and Health. Humana Press, Cham. 2017; p. 413–422. https://doi.org/10.1007/978-3-319-43027-0_23

Chen D, Zhao T, Doyle MP. Single-and mixed-species biofilm formation by *Escherichia coli* O157:H7 and *Salmonella*, and their sensitivity to levulinic acid plus sodium dodecyl sulfate. Food Control. 2015 Nov 1;57:48–53. https://doi.org/10.1016/j.foodcont.2015.04.006

Chmielewski RA, Frank JF. A predictive model for heat inactivation of *Listeria monocytogenes* biofilm on buna-N rubber. LWT-Food Sci Technol. 2006 Jan 1;39(1):11–19. https://doi.org/10.4315/0362-028x-67.12.2712

Cook A, Odumeru J, Lee S, Pollari F. *Campylobacter*, *Salmonella*, *Listeria monocytogenes*, verotoxigenic *Escherichia coli*, and *Escherichia coli* prevalence, enumeration, and subtypes on retail chicken breasts with and without skin. J Food Protect. 2012 Jan;75(1):34–40. https://doi.org/10.4315/0362-028x.jfp-11-206

Costerton JW, Stewart PS, Greenberg EP. Bacterial biofilms: a common cause of persistent infections. Science. 1999 May 21;284(5418): 1318–1322. https://doi.org/10.1126/science.284.5418.1318

Cui Y, Walcott R, Chen J. Attachment of various serovars of *Salmonella enterica* to vegetable seeds with different surface characteristics. Presented at: International Association for Food Protection (IAFP) Annual Meeting. IAFP 2015; Portland, OR.

Dallal MM, Doyle MP, Rezadehbashi M, Dabiri H, Sanaei M, Modarresi S, Bakhtiari R, Sharifiy K, Taremi M, Zali MR, Sharifi-Yazdi MK. Prevalence and antimicrobial resistance profiles of *Salmonella* serotypes, *Campylobacter* and *Yersinia* spp. isolated from retail chicken and beef, Tehran, Iran. Food Control. 2010 Apr 1;21(4):388–392. https://doi.org/10.1016/j.foodcont.2009.06.001

Davey ME, O'toole GA. Microbial biofilms: from ecology to molecular genetics. Microbiol Mol Biol R. 2000 Dec 1;64(4):847–867. https://doi.org/10.1128/mmbr.64.4.847-867.2000

Díez-García M, Capita R, Alonso-Calleja C. Influence of serotype on the growth kinetics and the ability to form biofilms of *Salmonella* isolates from poultry. Food Microbiol. 2012 Sep 1;31(2):173–180. https://doi.org/10.1016/j.fm.2012.03.012

Dourou D, Beauchamp CS, Yoon Y, Geornaras I, Belk KE, Smith GC, Nychas GJ, Sofos JN. Attachment and biofilm formation by *Escherichia coli* O157:H7 at different temperatures, on various food-contact surfaces encountered in beef processing. Int J Food Microbiol. 2011 Oct 3;149(3):262–268. https://doi.org/10.1016/j.ijfoodmicro.2011.07.004

European Food Safety Authority and European Centre for Disease Prevention and Control (EFSA and ECDC). The European Union summary report on trends and sources of zoonoses, zoonotic agents and food-borne outbreaks in 2017. EFSA J. 2018 Dec;16(12):e05500. https://doi.org/10.2903/j.efsa.2011.2090

Floyd KA, Eberly AR, Hadjifrangiskou M. Adhesion of bacteria to surfaces and biofilm formation on medical devices. In: Deng Y, Lv W, editors. Biofilms and implantable medical devices. Duxford (UK): Woodhead Publishing. 2017; p. 47–95. https://doi.org/10.1016/b978-0-08-100382-4.00003-4

Giaouris E, Chorianopoulos N, Skandamis P, Nychas GJ. Attachment and biofilm formation by *Salmonella* in food processing environments. In: Mahmoud BSM, editor. *Salmonella*: A dangerous foodborne pathogen. InTech. 2012; p. 157–180. https://doi.org/10.5772/28107

Gordon MA, Graham SM, Walsh AL, Wilson L, Phiri A, Molyneux E, Zijlstra EE, Heyderman RS, Hart CA, Molyneux ME. Epidemics of invasive *Salmonella enterica* serovar Enteritidis and *S. enterica* Serovar Typhimurium infection associated with multidrug resistance among adults and children in Malawi. Clin Infect Dis. 2008 Apr 1;46(7):963–969. https://doi.org/10.1086/529146

Hall-Stoodley L, Costerton JW, Stoodley P. Bacterial biofilms: from the natural environment to infectious diseases. Nat Rev Microbiol. 2004 Feb;2(2):95–108. https://doi.org/10.1038/nrmicro821

Hall-Stoodley L, Stoodley P. Evolving concepts in biofilm infections. Cell Microbiol. 2009 Jul;11(7):1034–1043. https://doi.org/10.1111/j.1462-5822.2009.01323.x

Hur J, Jawale C, Lee JH. Antimicrobial resistance of *Salmonella* isolated from food animals: A review. Food Res Int. 2012 Mar 1;45(2): 819–830. https://doi.org/10.1016/j.foodres.2011.05.014

Ikuma K, Decho AW, Lau BL. The extracellular bastions of bacteria – a biofilm way of life. Nature Education Knowledge. 2013;4(2):2–19.

International Organization for Standardization. Microbiology of food and animal feeding stuffs: horizontal method for the detection of *Salmonella* spp. Detection of *Salmonella* spp. in animal faeces and in environmental samples from the primary production stage. Amendment 1, Annex D. Geneva (Switzerland): ISO. 2007.

Irie Y, Parsek MR. Quorum sensing and microbial biofilms. In: Romeo T, editor. Bacterial Biofilms. Current Topics in Microbiology and Immunology, vol 322. Berlin, Heidelberg (Germany): Springer. 2008; p. 67–84. https://doi.org/10.1007/978-3-540-75418-3_4

Isoken HI. Biofilm formation of *Salmonella* species isolated from fresh cabbage and spinach. JAppl Sci Environ Manage. 2015;19(1): 45–50. https://doi.org/10.4314/jasem.v19i1.6

Iturriaga MH, Tamplin ML, Escartin EF. Colonization of tomatoes by Salmonella Montevideo is affected by relative humidity and storage temperature. J Food Protect. 2007 Jan;70(1):30–34. https://doi.org/10.4315/0362-028x-70.1.30

Karkey A, Jombart T, Walker AW, Thompson CN, Torres A, Dongol S, Tran Vu Thieu N, Pham Thanh D, Tran Thi Ngoc D, Voong Vinh P, Singer AC. The ecological dynamics of fecal contamination and *Salmonella* Typhi and *Salmonella* Paratyphi A in municipal Kathmandu drinking water. PLoS Neglect Trop D. 2016 Jan 6;10(1):e0004346. https://doi.org/10.1371/journal.pntd.0004346

Khan MS, Altaf MM, Ahmad I. Chemical nature of biofilm matrix and its significance. In: Ahmad I, Husain FM, editors. Biofilms in Plant and Soil Health. Hoboken (USA): John Wiley & Sons Ltd. 2017. https://doi.org/10.1002/9781119246329.ch9

Koo H, Yamada KM. Dynamic cell-matrix interactions modulate microbial biofilm and tissue 3D microenvironments. Curr Opin Cell Biol. 2016 Oct 1;42:102–112. https://doi.org/10.1016/j.ceb.2016.05.005

Kroupitski Y, Golberg D, Belausov E, Pinto R, Swartzberg D, Granot D, Sela S. Internalization of *Salmonella enterica* in leaves is induced by light and involves chemotaxis and penetration through open stomata. Appl Environ Microb. 2009 Oct 1;75(19):6076–6086. https://doi.org/10.1128/aem.01084-09

Li J, Feng J, Ma L, de la Fuente Núñez C, Gölz G, Lu X. Effects of meat juice on biofilm formation of *Campylobacter* and *Salmonella*. Int J Food Microbiol. 2017 Jul 17;253:20–28. https://doi.org/10.1016/j.ijfoodmicro.2017.04.013

Li YH, Tian X. Quorum sensing and bacterial social interactions in biofilms. Sensors. 2012 Mar;12(3):2519–2538. https://doi.org/10.3390/s120302519

Mah TF, O'Toole GA. Mechanisms of biofilm resistance to antimicrobial agents. Trends Microbiol. 2001 Jan 1;9 (1):34–39. https://doi.org/10.1016/s0966-842x(00)01913-2

Malangu N, Ogunbanjo GA. A profile of acute poisoning at selected hospitals in South Africa. South Afr J Epidemiol Infect. 2009 Jan 1;24(2):14–16.

Merino L, Procura F, Trejo FM, Bueno DJ, Golowczyc MA. Biofilm formation by *Salmonella* sp. in the poultry industry: Detection, control and eradication strategies. Food Res Int. 2019 May 1;119:530–540. https://doi.org/10.1016/j.foodres.2017.11.024

Moosdeen F, Williams JD, Secker A. Standardization of inoculum size for disc susceptibility testing: a preliminary report of a spectrophotometric method. J Antimicrob Chemoth. 1988 Apr 1;21(4): 439–443. https://doi.org/10.1093/jac/21.4.439

Motladiile TW. *Salmonella* food-poisoning outbreak linked to the National School Nutrition Programme, North West province, South Africa. South Afr J Infect Dis. 2019;34(1):1–6. https://doi.org/10.4102/sajid.v34i1.124

Mukaka MM. A guide to appropriate use of correlation coefficient in medical research. Malawi Med J. 2012;24(3):69–71.

Mulamattathil SG, Bezuidenhout C, Mbewe M. Biofilm formation in surface and drinking water distribution systems in Mafikeng, South Africa. S Afr J Sci. 2014 Dec;110(11–12):01–09. https://doi.org/10.1590/sajs.2014/20130306

Muvhali M, Smith AM, Rakgantso AM, Keddy KH. Investigation of *Salmonella* Enteritidis outbreaks in South Africa using multilocus variable-number tandem-repeats analysis, 2013–2015. BMC Infect Dis. 2017 Dec 1;17(1):661. https://doi.org/10.1186/s12879-017-2751-8

Niehaus AJ, Apalata T, Coovadia YM, Smith AM, Moodley P. An outbreak of foodborne salmonellosis in rural KwaZulu-Natal, South Africa. Foodborne Pathog Dis. 2011 Jun 1;8(6):693–697. https://doi.org/10.1089/fpd.2010.0749

Papa R, Bado I, Iribarnegaray V, Gonzalez MJ, Zunino P, Scavone P, Vignoli R. Biofilm formation in carbapenemase-producing *Pseudomonas* spp. and *Acinetobacter baumannii* clinical isolates. Int J Infect Dis. 2018 Aug 1;73:119–120. https://doi.org/10.1016/j.ijid.2018.04.3688

Patel R. Biofilms and antimicrobial resistance. Clin Orthop Relat R. 2005 Aug 1;437:41–47. https://doi.org/10.1097/01.blo.0000175714.68624.74

Rendueles O, Kaplan JB, Ghigo JM. Antibiofilm polysaccharides. Environ Microbiol. 2013 Feb;15(2):334–346. https://doi.org/10.1111/j.1462-2920.2012.02810.x

Römling U, Sierralta WD, Eriksson K, Normark S. Multicellular and aggregative behaviour of *Salmonella typhimurium* strains is controlled by mutations in the agfD promoter. Mol Microbiol. 1998 Apr;28(2):249–264. https://doi.org/10.1046/j.1365-2958.1998.00791.x

Sadekuzzaman M, Yang S, Mizan MF, Ha SD. Current and recent advanced strategies for combating biofilms. Compr Rev Food Sci F. 2015 Jul;14(4):491–509. https://doi.org/10.1111/1541-4337.12144

Sharma D, Misba L, Khan AU. Antibiotics versus biofilm: an emerging battleground in microbial communities. Antimicrob Resist In. 2019 Dec;8(76):1–10. https://doi.org/10.1186/s13756-019-0533-3

Shi X, Zhu X. Biofilm formation and food safety in food industries. Trends Food Sci Tech. 2009 Sep 1;20(9):407–413. https://doi.org/10.1016/j.tifs.2009.01.054

Silagyi K, Kim SH, Lo YM, Wei CI. Production of biofilm and quorum sensing by *Escherichia coli* O157:H7 and its transfer from contact surfaces to meat, poultry, ready-to-eat deli, and produce products. Food Microbiol. 2009 Aug 1;26(5):514–519. https://doi.org/10.1016/j.fm.2009.03.004

Sofos JN, Geornaras I. Overview of current meat hygiene and safety risks and summary of recent studies on biofilms, and control of *Escherichia coli* O157:H7 in nonintact, and *Listeria monocytogenes* in ready-to-eat, meat products. Meat Sci. 2010 Sep 1;86(1):2–14. https://doi.org/10.1016/j.meatsci.2010.04.015

Solano C, García B, Valle J, Berasain C, Ghigo JM, Gamazo C, Lasa I. Genetic analysis of *Salmonella enteritidis* biofilm formation: critical role of cellulose. Mol Microbiol. 2002 Feb;43(3):793–808. https://doi.org/10.1046/j.1365-2958.2002.02802.x

Soo Lee I, Lin J, Hall HK, Bearson B, Foster JW. The stationary-phase sigma factor σS (RpoS) is required for a sustained acid tolerance response in virulent *Salmonella* Typhimurium. Mol Microbiol. 1995 Jul;17(1):155–167. https://doi.org/10.1111/j.1365-2958.1995.mmi_17010155.x

Steenackers H, Hermans K, Vanderleyden J, De Keersmaecker SC. *Salmonella* biofilms: an overview on occurrence, structure, regulation and eradication. Food Res Int. 2012 Mar 1;45(2):502–531. https://doi.org/10.1016/j.foodres.2011.01.038

Stepanović S, Ćirković I, Ranin L, Svabić-Vlahović M. Biofilm formation by *Salmonella* spp. and *Listeria monocytogenes* on plastic surface. Lett Appl Microbiol. 2004 May;38(5):428–432. https://doi.org/10.1111/j.1472-765x.2004.01513.x

Stepanović S, Vuković D, Dakić I, Savić B, Švabić-Vlahović M. A modified microtiter-plate test for quantification of staphylococcal biofilm formation. J Microbiol Meth. 2000 Apr 1;40(2):175–179. https://doi.org/10.1016/s0167-7012(00)00122-6

Stewart PS, Costerton JW. Antibiotic resistance of bacteria in biofilms. Lancet. 2001 Jul 14;358(9276):135–138. https://doi.org/10.1016/s0140-6736(01)05321-1

Suehr Q, Jeong S, Marks BP. Modeling of cross-contamination of *Salmonella* during almond processing. Presented at: International Association for Food Protection (IAFP) Annual Meeting; IAFP 2015; Portland, OR.

Tanaka MH, Lima GM, Ito CK. Biology of the oral environment and its impact on the stability of dental and craniofacial reconstructions. In: Spencer P, Misra A, editors. Material-tissue interfacial phenomena. Duxford (UK): Woodhead Publishing. 2017; p. 181–202. https://doi.org/10.1016/b978-0-08-100330-5.00007-8

Wang H, Ye K, Wei X, Cao J, Xu X, Zhou G. Occurrence, antimicrobial resistance and biofilm formation of *Salmonella* isolates from a chicken slaughter plant in China. Food Control. 2013 Oct 1;33(2):378–384. https://doi.org/10.1016/j.foodcont.2013.03.030

Webber B, Oliveira AP, Pottker ES, Daroit L, Levandowski R, Santos LR, Nascimento VP, Rodrigues LB. *Salmonella* Enteritidis forms biofilm under low temperatures on different food industry surfaces. Ciênc Rural. 2019;49(7):e20181022. https://doi.org/10.1590/0103-8478cr20181022

Yang Y, Mikš-Krajnik M, Zheng Q, Lee SB, Lee SC, Yuk HG. Biofilm formation of *Salmonella* Enteritidis under food-related environmental stress conditions and its subsequent resistance to chlorine treatment. Food Microbiol. 2016 Apr 1;54:98–105. https://doi.org/10.1016/j.fm.2015.10.010

Zogaj X, Nimtz M, Rohde M, Bokranz W, Römling U. The multicellular morphotypes of *Salmonella typhimurium* and *Escherichia coli* produce cellulose as the second component of the extracellular matrix. Mol Microbiol. 2001 Mar;39(6):1452–1463. https://doi.org/10.1046/j.1365-2958.2001.02337.x

Polish Journal of Microbiology
2020, Vol. 69, No 4, 441–451
https://doi.org/10.33073/pjm-2020-047

ORIGINAL PAPER

The Effect of *Lactobacillus salivarius* SGL03 on Clinical and Microbiological Parameters in Periodontal Patients

MAŁGORZATA NĘDZI-GÓRA[1]*, MARTA WRÓBLEWSKA[2, 3] and RENATA GÓRSKA[4]

[1] Department of Oral Hygiene, Medical University of Warsaw, Warsaw, Poland
[2] Department of Dental Microbiology, Medical University of Warsaw, Warsaw, Poland
[3] Department of Microbiology, Central Clinical Hospital, University Clinical Centre, Medical University of Warsaw, Warsaw, Poland
[4] Department of Periodontology and Oral Mucosa Diseases, Medical University of Warsaw, Warsaw, Poland

Submitted 17 June 2020, revised 29 September 2020, accepted 2 October 2020

Abstract

The destruction of periodontal tissues during periodontitis is the result of the immune-inflammatory reactions to the bacteria of dental biofilm. Probiotics may reduce dysbiosis by the modification of the dental microbiome, which can influence the immune-inflammatory mechanisms. The aim of this study was to estimate the clinical and microbiological parameters, before and after 30 days of application of the dietary supplement containing *Lactobacillus salivarius* SGL03 or placebo. The study was conducted in 51 patients with stage I or II periodontitis during the maintenance phase of treatment. The clinical parameters and the number of colony forming units (CFU) of bacteria in supragingival plaque were assessed before and after 30 days of the oral once daily administration of the dietary supplement in the form of suspension containing *L. salivarius* SGL03 or placebo. There were no changes in the PI scores between and within the groups. The value of BOP decreased in both groups. In the study group the significant reduction of the mean pocket depth was revealed (from 2.5 to 2.42, $p = 0{,}027$) but without the difference between the groups. There were no significant changes in the number of bacteria within the groups. In the control, but not the study group, positive correlations were observed between the clinical parameters (variables) and the number of bacteria. The use of the dietary supplement containing *L. salivarius* SGL03 may reduce pocket depth despite the lack of changes in other clinical parameters and the number of bacteria in supragingival plaque.

Key words: probiotics, periodontal treatment, *Lactobacillus salivarius*

Introduction

Gingivitis and periodontitis comprise a large group of diseases of a complex etiology (Hasan and Palmer 2014; Dahlen et al. 2019). Among them, plaque-induced gingivitis and periodontitis constitute diseases in which the primary etiological factors are bacteria in dental plaque and other types of biofilms present in the oral cavity (Bartold and Van Dyke 2019; Geisinger et al. 2019). Epidemiological studies show that these diseases pose a serious problem to public health, they may lead to systemic diseases such as diabetes and cardiovascular diseases (Caton et al. 2018; Dahlen et al. 2019). Therefore, prevention and treatment of periodontitis are crucial not only for the maintenance of teeth and oral health but also for the whole human.

Periodontal tissue destruction in the course of inflammation occurs due to both direct bacterial action and activation of indirect immune-inflammatory mechanisms in host tissues (Dahlen et al. 2019). The constant presence of pathogenic bacteria in the oral cavity, through a number of factors such as pro-inflammatory cytokines or proteolytic enzymes, supports mechanisms of chronic destruction of connective and bone tissue, which causes disease progression and hinders its treatment. For years research studies were mainly concentrated on the composition of dental biofilm microbiota and attempt to determine a specific bacterium eliminating of which would allow effective treatment of the disease (Hasan and Palmer 2014; Dahlen et al. 2019; Proctor 2000). Initially, subgingival biofilm with a range of anaerobic bacteria was considered pathogenic, then

* Corresponding author: M. Nędzi-Góra, Department of Oral Hygiene, Medical University of Warsaw, Warsaw, Poland; **e-mail: mnedzi@wum.edu.pl**

species such as *Aggregatibacter* (previously *Actinobacillus*) *actinomycetemcomitans* or *Porphyromonas gingivalis* were identified as particularly pathogenic. In turn, studies by Socransky et al. (1998) proved the pathogenic role of not individual bacterial species, but rather bacterial complexes such as the red complex: *P. gingivalis*, *Tannerella forsythia*, and *Treponema denticola*. So far, however, no specific species have been identified that would be responsible for developing of the disease (Bartold and Van Dyke 2019). At present, nonspecific bacterial plaque is considered pathogenic in gingivitis, while in periodontitis, the role of additional risk factors, such as genetic and epigenetic factors, nicotinism, diabetes, as well as lifestyle and other environmental factors is emphasized (Hasan and Palmer 2014; Meyle and Chapple 2015; Bartold and Van Dyke 2019; Dahlen et al. 2019). The contemporary model of periodontal disease pathogenesis emphasizes the importance of dysbiosis and inflammation as the factors that directly lead to the destruction of periodontal tissues (Van Dyke et al. 2020). Simultaneously, concepts of so-called health-promoting biofilm appear, which are based on the theory of symbiosis between bacterial species and the specific response of the host to a given type of biofilm. According to these hypotheses, the development of periodontitis results from pathogenic bacteria, lack of beneficial bacteria, and host risk factors (e.g., genetic susceptibility (Haukioja 2010; Devine et al. 2015; Meyle and Chapple 2015; Dahlen et al. 2019)).

Bacterial biofilm reduction is still the basis of treating gingivitis and periodontitis. For many years, new therapeutic methods have been sought to increase biofilm reduction effectiveness, such as scaling and root planning (Geisinger et al. 2019). Supportive treatment includes local and systemic antibiotic therapy, local use of antiseptics, laser therapy, or photodynamic therapy. However, these methods are expensive, may cause undesirable general and local effects, and there is a lack of certain studies confirming their beneficial effects. Therefore, the use of probiotics (or pro- and prebiotics) seems to be particularly beneficial in this respect, which – by influencing the composition of the bacterial biofilm – may simultaneously contribute to the regulation of the immune-inflammatory response in the periodontium (Haukioja 2010; Gruner et al. 2016).

Probiotics are defined by World Health Organization (WHO) and Food and Agriculture Organization (FAO) as non-pathogenic live microorganisms, which – when administered inappropriately, e.g., as dietary supplements – improve the host's health (Teughels et al. 2008; Zarco et al. 2012; Laleman and Teughels 2015). The term a biotherapeutic agent is used in the literature to describe microorganisms that accelerate the treatment or prevent complications of the disease, and their effectiveness has been scientifically proven, involving large groups of patients, randomized trials, placebo tests, and double-blind studies (Elmer et al. 1996; Mcfarland 2000). Attempts to use probiotics in dentistry date back to the 1990s and concern primarily prevention and treatment of caries and periodontal disease. The most popular probiotics belong to the genera *Lactobacillus* and *Bifidobacterium* (Gruner et al. 2016). However, the majority of studies in this area are based on *in vitro* experiments or small groups of subjects, while clinical trials involving large groups of patients are mainly retrospective. With the development of microbiological research, the effect of probiotics on oral microbiota as well as on clinical and immunological parameters in periodontal tissues is being studied increasingly.

The aim of the study was to assess the clinical (plaque index – PI; bleeding on probing – BOP; mean pocket depth – PD; maximal pocket depth – PD max) and microbiological parameters (colony-forming unit – FU, from supragingival plaque) in patients before and after 30 days of use of the dietary supplement containing *Lactobacillus salivarius* SGL03 in the form of an oral suspension, compared to the subjects receiving placebo.

Experimental

Materials and Methods

Study group. The study involved 51 patients (35 women and 16 men, mean age 54.3 years) treated at the Department of Periodontology and Oral Mucosa Diseases, Medical University of Warsaw. The study was conducted from July to December 2019 after obtaining the approval of the Bioethics Committee No. KB/79/2019. The characteristics of the study and control groups in terms of sex and age are presented in Tables I and II, respectively.

Table I
Number and percentage of patients divided according to sex; (A) *Lactobacillus salivarius* SGL03 study group, (B) placebo group.

Sex	Group A	Group B
F (females)	19 (73.1%)	16 (64.0%)
M (males)	7 (26.9%)	9 (36.0%)
Total	26 (100%)	25 (100%)

Table II
Characteristics of *Lactobacillus salivarius* SGL03; (A) study group and placebo (B) group in terms of age.

	Group A		Group B		*p*-value
	Mean	SD	Mean	SD	
Age (years)	55.35	12.42	53.28	14.38	0.585

SD – the standard deviation

The study comprised of patients diagnosed with periodontitis stage I and II (Tonetti 2018). The diagnosis was made based on clinical and radiological examination in accordance with the current classification of periodontal diseases (Caton et al. 2018). All patients were in the maintenance phase of periodontitis treatment and had completed the causal treatment phase at least three weeks earlier. No periodontal procedures were planned for any of the subjects during three months from the start of the study.

The following inclusion criteria were used: 1) age 25–65 years, 2) PD ≤ 5 mm; 3) interproximal clinical attachment level (CAL) ≤ 4 mm, 4) no lost teeth due to periodontal disease, 5) presence of minimum ten teeth and 6) minimum three weeks after scaling. Exclusion criteria were: 1) hypersensitivity to components of the preparation (lemon oil, rosemary oil), 2) nicotinism, 3) pregnancy or lactation, 4) antibiotic or other antibacterial therapy during the past 30 days, 5) the use of antibacterial rinses containing chlorhexidine for the last two weeks. The study was a randomized intervention study; a parallel-group assessment was carried out with the random selection of patients for the study and control group and researchers (double-blind trial). Patients were randomly divided into two groups A and B. The sample size for groups A and B was determined based on the expected values of PD max at the end of the study, i.e., 4.4 for group A and 5.0 for group B. The expected value of a standard deviation for both groups was set at 0.75. The confidence level was set at 95%, and the power of the *t*-test was set at 80%. Such assumptions gave the required sample size of 25 patients for each of the groups. After completing of the examination and statistical analysis of the results, decoding was performed, and group A was nominated as a study group (receiving preparation containing *L. salivarius* SGL03 – Salistat SGL03), whereas group B as control (placebo). Products for both groups were identically factory-packed (prepared and delivered by the manufacturer). The composition of probiotic SGL03 and placebo are shown in Table III. It was recommended to use the product for 30 days, at least 30 minutes after evening toothbrushing. Study participants were instructed to prepare the suspension just before use, to hold it in the mouth for 30 seconds while spreading it over the surface of teeth and gums. After using the preparation, it was recommended to refrain from drinking water for 30 minutes, while from drinks other than water and eating meals – until the next morning.

Clinical examination. Each patient during the first visit (T0) and after 30 days of using *L. salivarius* SGL03 (± 5 days) (T1) underwent a periodontological examination with the collection of material for microbiological testing. The periodontological examination was carried out by two trained for this study investigators using one type of 1 mm graduated probe (UNC probe 15 mm; Hu-Friedy, Chicago, USA) and it included the assessment of 1) dichotomous (yes/no) FMPI (full-mouth plaque index) according to O'Leary et al. (1972) on four tooth surfaces (i.e. distal, buccal, mesial, and lingual). The index was determined by dividing the number of surfaces with a plaque by the number of all tested surfaces; 2) dichotomous (yes/no) BOP index according to Ainamo and Bay (Ainamo and Bay 1975). Bleeding

Table III
Composition of medical product and placebo (active ingredients are shown in bold).

	Medical product (Salistat SGL03)	Placebo
Vial content	Osmotic water	Osmotic water
	Gluco-oligosaccharides; prebiotic	X
	Citric acid	Citric acid
	Potassium sorbate	Potassium sorbate
	Sodium lactate	Sodium lactate
	Vanilla flavor	Vanilla flavor
	Sucralose	Sucralose
	Lemone.o.	X
	Rosemary e.o.	X
Vial cap	Modified tapioca starch	Modified tapioca starch
	Lactoferrin	X
	Live probiotic bacteria (*L. salivarius* SGL03)	X
	Maltodextrin	Maltodextrin
	Magnesium salts of fatty acids	Magnesium salts of fatty acids
	Silicon dioxide	Silicon dioxide
	cholecalciferol/colecalciferol	X

X – the lack of the ingredient in placebo

was assessed at six points of each tooth (i.e., distal-buccal, buccal, mesial-buccal, mesial-lingual, lingual, and distal-lingual). The index was determined by dividing the number of bleeding points by the number of all assessed points; 3) pocket depth (PD) was assessed at six points on each tooth as the distance in millimeters from the gingival margin to the bottom of the pocket. The mean value was calculated by dividing the sum of the measurements obtained by the number of measurement points. Two operators trained and calibrated until their results did not differ from standard. Only one examiner performed all (two) examinations of every patient.

The PI was evaluated on the day plaque was taken for microbiological testing. The supragingival plaque was collected, which is why patients were asked not to perform morning hygiene procedures. Patients were not advised to change their habits, and no hygienization or curative procedures were performed on them during the study.

Microbiological examination. For microbiological examination, a sample of the supragingival plaque was collected from each patient from contiguous surfaces of lower premolars (35/45) with a flat plastic instrument, approximately 1 mm^3 in volume. All visits took place between 8.00 and 10.00 in the morning. Patients were advised not to perform hygienization procedures (including toothbrushing) prior to the visit. Each sample was placed in a sterile test tube containing 1 ml of thioglycolate buffer. The tubes were immediately transported to the laboratory, where they were mixed for 1 minute using a vortex mixer, with glass beads (5 beads/tube) to break down bacterial complexes. Each tube was then subjected to serial dilutions – from 1 : 1 to 1 : 1,000,000 – in phosphate-buffered saline (PBS). Successive dilutions, marked in an identifiable manner, were inoculated on a culture medium (Columbia agar with 5% sheep blood), and then incubated at 37°C for five days under anaerobic conditions (GenBag Anaer, bioMerieux). Thereafter, colonies were counted (CFU), and CFU/ml was determined. The microbiological examination was carried out at the Department of Dental Microbiology of the Medical University of Warsaw.

Questionnaire. Besides, after the study's termination, patients completed an anonymous questionnaire regarding the taste of the preparation, ease of use, subjective assessment of the effect on the state of gingiva and mucosa, and adverse effects (no subject contacted researchers to report any adverse effects while using the preparation).

Statistical analysis. Statistical analysis was performed with Statistica v. 13 (TIBCO Software Inc., Palo Alto, USA). Data were presented as mean ± standard deviation (SD) and 95% confidence intervals. The student's *t*-test was used for comparison of two independent groups for continuous variables. Relationships between clinical and microbiological parameters were assessed using the Spearman rank correlation coefficient (R). *P* values of less than 0.05 ($p < 0.05$) were regarded as statistically significant.

Results

All patients finished the study. The authors excluded one of them because of their doubts about whether he understood the instruction for use well. Finally, in group A there were 26 and in group B 25 patients. Demographic parameters (sex and age) of patients enrolled in study (A), and control (B) groups are shown in Tables I and II, respectively. In the study group, there were 19 females (73.1%) and seven males (26.9%), while in the placebo group – 16 females (64.0%) and nine males (36.0%). The study group's mean age was 55.35 years, and in the placebo group – 53.28 years ($p = 0.585$).

The study (A) and control (B) groups did not differ at baseline in terms of plaque index, bleeding index, mean pocket depth, and maximum pocket depth (Table IV). The mean plaque index in the *L. salivarius* SGL03 group decreased from 55.38% to 51.61%, while in the placebo group – from 56.81% to 52.92%. The differences were not statistically significant (Table V). Similarly, the mean bleeding index decreased in both the *L. salivarius* SGL03 group (from 20.39% to 18.11%), and the placebo group (from 20.3% to 17.57%), but the differences were not statistically significant. However, the reduction of bleeding index in the whole group participating in the study (A + B) turned out to be statistically significant (from 20.34% to 17.84%, $p = 0.011$) (Table V). The average maximum pocket depth in the *L. salivarius* SGL03 group decreased from 4.88 to 4.58, while in the placebo group from 4.96 to 4.84. The differences were not statistically significant (Table V). In turn, the mean pocket depth in the *L. salivarius* SGL03 group underwent a statistically significant reduction

Table IV
Initial mean values of clinical variables (parameters) (PI, BOP, PD max, mean PD) in *Lactobacillus salivarius* SGL03 (A) and placebo (B) group.

	Group A		Group B		*p*-value
	Mean	SD	Mean	SD	
PI	55.38	20.50	56.81	16.14	0.783
BOP	20.39	11.44	20.30	11.74	0.978
PD max	4.88	1.34	4.96	1.06	0.825
Mean PD	2.50	0.48	2.46	0.46	0.757

SD – the standard deviation

Table V
Mean values of clinical variables (parameters) (PI, BOP, PD max, mean PD) in *Lactobacillus salivarius* SGL03 (A) and placebo (B) group and in the whole group (A+B).

Group	PI T0	PI T1	*p*-value	*p*-value A vs. B
A	55.38	51.61	0.186	0.978
B	56.81	52.92	0.309	
A + B	56.08	52.25	0.101	
Group	BOP T0	BOP T1		
A	20.39	18.11	0.071	0.813
B	20.30	17.57	0.077	
A + B	20.34	17.84	**0.011***	
Group	PD max T0	PD max T1		
A	4.88	4.58	0.161	0.484
B	4.96	4.84	0.450	
A + B	4.92	4.71	0.109	
Group	Mean PD T0	Mean PD T1		
A	2.50	2.42	**0.027***	0.291
B	2.46	2.44	0.740	
A + B	2.48	2.43	0.107	

T0 – before treatment; T1 – after treatment;
* – the value statistically significant

from 2.50 to 2.42 ($p = 0.027$) (Table V). This parameter also decreased in the placebo group from 4.96 to 4.84, but the difference was not statistically significant. There was also no significant difference in this parameter between the *L. salivarius* SGL03 and placebo groups (Table V).

The average number of bacterial colonies cultured from samples of supragingival plaque, collected from patients in the L. salivarius SGL03 group, was 5.32×10^7 before the study and 8.77×10^7 after the study (Table VI). The difference was not statistically significant. In the placebo group, the average number of colonies was 1.18×10^8 before the study, and 1.09×10^8 after the study – the difference was also not statistically significant.

Correlations of clinical indices with microbiological parameters are shown in Table VII. In the study (A) group, a negative correlation was found between the maximum depth of periodontal pockets before and after treatment (PD max T0, PD max T1) and the number of bacteria before treatment (CFU T0). A positive correlation was recorded between plaque index before treatment (PI T0) and the number of bacteria after treatment (CFU T1) in the study group (A). In the placebo (B) group, in turn, a positive correlation was observed between the following parameters: the pre- and post-treatment bleeding on probing (BOP T0, BOP T1) indices and the number of bacteria after treatment (CFU T1); the mean pocket depth both before and after treatment (Mean PD T0, Mean PD T1) and the number of bacteria after treatment (CFU T1); the mean pocket depth before treatment (Mean PD T0) and the change in the number of bacteria (ΔCFU); the maximum pocket depth before and after treatment (PD max T0, PD max T1) and the change in the number of bacteria (ΔCFU); the plaque index before treatment (PI T0) and the number of bacteria before treatment (CFU T0) as well as between the plaque index after treatment (PI T1) and the number of bacteria after treatment (CFU T1). Similarly, a positive correlation was found between the change in the plaque index (ΔPI) and the number of bacteria after treatment (CFU T1) and the change of the number of bacteria in the samples (ΔCFU).

Table VIII presents the survey results regarding the subjective evaluation of the taste of the preparation, convenience of use, effect on the state of gingiva and mucosa, and the adverse effects of the dietary supplement in the *L. salivarius* SGL03 and placebo groups. Among the respondents, 61.5% rated the taste of *L. salivarius* SGL03 as good, 26.9% as neutral, and for 11.5%, it was unpalatable. Similarly, 61.5% of patients thought that the preparation was convenient to use, 26.9% – neutral, and 11.5% – uncomfortable. Among patients using *L. salivarius* SGL03 46.2% said that their gums had improved (vs. 60.0% placebo) and 53.8% that they had remained unchanged (vs. 40.0% placebo). No patient reported any deterioration of gingiva. Regarding oral mucosa condition assessment, 57.7% of patients reported that the condition had improved (vs. 52.0%

Table VI
Mean values of colony-forming units (CFU) in *Lactobacillus salivarius* SGL03 (A) and placebo (B) group.

	Group A		Ggroup B		*p*-value (A vs. B)
	mean	SD	mean	SD	
CFU T0	5.32×10^7	7.01×10^7	1.18×10^8	1.65×10^8	0.074
CFU T1	8.77×10^7	1.21×10^8	1.09×10^8	1.15×10^8	0.528
CFU (T1 – T0)	3.45×10^7	1.40×10^8	-8.88×10^6	2.03×10^8	0.377
p-value (T0 vs T1)	0.221		0.829		

T0 – before treatment; T1 – after treatment

Table VII
Spearman's rank correlation indices between microbiological and clinical parameters in *Lactobacillus salivarius* SGL03 (A) and placebo (B) group.

	CFU T1	CFU T0	ΔCFU (T1 – T0)
Group A			
PI T0	0.321	**0.565***	0.279
PI T1	0.299	0.312	0.049
ΔPI (T1 – T0)	0.019	–0.166	–0.172
BOP T0	0.008	0.237	0.025
BOP T1	–0.134	0.360	0.253
ΔBOP (T1 – T0)	–0.035	0.189	0.243
PD max T0	**–0.431***	–0.088	0.106
PD max T1	**–0.423***	0.097	0.227
ΔPD max (T1 – T0)	0.053	0.194	0.098
Mean PD T0	–0.089	0.033	0.057
Mean PD T1	0.017	0.046	0.005
Δmean PD (T1 – T0)	0.082	–0.150	–0.164
Group B			
PI T0	**0.503***	0.136	–0.138
PI T1	0.395	**0.619***	0.323
ΔPI (T1 – T0)	0.211	**0.720***	**0.476***
BOP T0	0.279	**0.441***	0.264
BOP T1	0.271	**0.424***	0.357
ΔBOP (T1 – T0)	–0.028	–0.002	0.119
PD max T0	–0.069	0.309	**0.428***
PD max T1	–0,077	0.379	**0.495***
ΔPD max (T1 – T0)	–0.021	0.166	0.182
Mean PD T0	0.074	**0.578***	**0.456***
Mean PD T1	0.135	**0.496***	0.381
Δmean PD (T1 – T0)	–0.071	–0.183	0.008

T0 – before treatment; T1 – after treatment

Table VIII
The results of a questionnaire regarding subjective assessment of taste, convenience of use, effect on the state of gums and mucosa as well as potential adverse effects of *Lactobacillus salivarius* SGL03 (A) or placebo (B).

	Group A – *Lactobacillus salivarius* SGL03		Group B – Placebo	
	Number of patients	%	Number of patients	%
Taste				
1 – good	16	61.5%	20	80.0%
2 – neutral	7	26.9%	4	16.0%
3 – unpalatable	3	11.5%	1	4.0%
Convenience of use				
1 – convenient	16	61.5%	19	76.0%
2 – neutral	7	26.9%	4	16.0%
3 – uncomfortable	3	11.5%	2	8.0%
Effect on the state of gums				
1 – improved	12	46.2%	15	60.0%
2 – unchanged	14	53.8%	10	40.0%
Effect on the oral mucosa condition				
1 – improved	15	57.7%	13	52.0%
2 – unchanged	11	42.3%	12	48.0%
Adverse reactions				
0 – no	23	88.5%	24	96.0%
1 – yes	3	11.5%	1	4.0%

placebo) and 42.3% (vs. 48.0% placebo) that it had not changed. No patient reported deterioration of mucosa. Three patients (11.5%) from the study group and one patient (4.0%) from the control group reported adverse reactions, and they were related to gastrointestinal disorders.

Discussion

The mechanism of probiotics in the oral cavity is not fully understood (Haukioja 2010; Umar et al. 2015; Laleman and Teughels 2015; Gruner et al. 2016; Seminario-Amez et al. 2017). In caries, probiotics are associated with reducing the number of colony-forming units (CFUs) of cariogenic bacteria (primarily *Streptococcus mutans*). Simultaneously, in periodontal disease, inhibition of periopathogens and so-called biofilm modification is observed (Iniesta et al. 2012; Montero et al. 2017; Barboza et al. 2020).

An interesting issue is the impact of probiotics on oral microbiota. Lactic acid probiotic bacteria produce antibacterial substances such as hydrogen peroxide, bacteriocins, and lactic acid, which provide a probiotic effect (Laleman et al. 2015; Takahashi 2015; Morales et al. 2016, Barzegari et al. 2020). In addition, by reducing levels of proinflammatory cytokines, elastase and prostaglandin E2 (PG E2), they inhibit an inflammatory response – humoral and cellular – in periodontal tissues (Haukioja 2010; Devine et al. 2015). It is also believed that probiotic bacteria compete with pathogens for adhesion surfaces and nutrients. L. salivarius, like other lactobacilli, is a species detected much more often in individuals with healthy periodontium compared to patients with periodontitis (Kõll-Klais et al. 2005). This species has strong antibacterial properties against pathogenic bacteria in the periodontium. The mechanism of its action is not entirely clear. Nissen et al. (2014) showed that *L. salivarius* inhibits the expression of toxins secreted by *A. actinomycetemcomitans*, including leukotoxin A, thus inhibiting its virulence.

Research on the use of probiotics in periodontology can be divided into several groups. Laboratory

tests involve assessing probiotic bacteria's effect on growth or functions (such as adhesion, coaggregation, secretion of antibacterial substances) of other bacterial strains in culture. Clinical studies concern assessing the effect of probiotics on clinical, microbiological, and immunological parameters in experimentally induced gingivitis or patients with disease – gingivitis or periodontitis. In these studies, probiotics are used as the only treatment or as an addition to conventional treatment (scaling and root planning). It is worth emphasizing that there is a lack of recommendations in the literature in which disease entities and phases of treatment probiotics should be used in periodontology. In this study, it was decided to use a probiotic in the maintenance phase of periodontal disease treatment to strengthen or maintain the effects achieved in the causal phase by modifying the microbiota's composition and its impact on inflammatory, immunological and microbiological parameters in the periodontium.

According to literature, the most frequently evaluated clinical parameters comprise the plaque index (PI), bleeding on probing index (BOP), gingival index (GI), and pocket depth (PD), less frequently also the effect of probiotics on gingival crevicular fluid (GCF) volume. Many researchers – using various probiotic bacteria (e.g., *Lactobacillus reuteri*, *L. salivarius*, *Streptococcus oralis*, *Streptococcus uberis*, *Streptococcus ratti*) – reported an improvement in these clinical parameters used in periodontology; however, these differences often were not statistically significant in comparison to the control groups (Krasse et al. 2006; Shimauchi et al. 2008; Laleman et al. 2015).

In our study, no effect of probiotic on the plaque index (PI) was observed. In both groups, it oscillated around 50% before the test, and it slightly decreased after using the probiotic but remained within 50%. The differences between the initial and final visits and between the groups were not statistically significant. As the study group consisted of patients in the maintenance phase of treatment, it is not surprising, i.e., individuals with established hygiene habits. It was assumed that the probiotic administration is only intended to help maintain microbial balance within the bacterial biofilm, partially achieved after the causal phase of treatment, and to sustain this treatment's effects. The relatively high average plaque index values (about 50%) probably resulted only from the lack of hygiene procedures on the day of the examination because they did not correspond to average bleeding indices. The bleeding index decreased in the study group (20.39% vs. 18.11%) and the control group (20.3% vs. 17.57%). Still, the differences were not significant in either of the groups. However, BOP reduction was significant in the whole group (study + control) of patients participating in the study (20.34 vs. 17.84). The lack of plaque index changes and the reduction of the bleeding index in the study and placebo groups indicated that it was not only the result of dental plaque.

It is worth mentioning that in literature, reductions in plaque index and bleeding index were found mainly in those studies where a probiotic was used as an adjunct to conventional therapy, i.e., during active treatment of gingivitis (natural or experimentally induced) and periodontitis (Vivekananda et al. 2010; Teughels et al. 2013; Morales et al. 2016). A statistically significant reduction in the mean pocket depth (PD) was observed in the study group in our study. However, there was no significant difference between the study and control groups. Penala et al. (2016) obtained similar results.

As mentioned in this paper, the study group consisted of patients in the maintenance phase of treatment. From the clinical point of view, reduction of pocket depth is an expected and beneficial therapeutic effect. For patients in the maintenance phase of periodontitis treatment, the most crucial goal is to maintain a low bleeding index, a symptom of active inflammation in the periodontium, and maintenance or progress of reduction of pocket depths obtained during the active treatment phase. In the causal phase of treatment, reduction of pocket depth mainly results from a reduction in the number of bacteria, thus reducing active inflammation in the periodontium. As a result, tissue hyperemia and swelling are reduced. In turn, further reduction of pocket depths in the maintenance phase of treatment may result from the regulation of additional destructive mechanisms in periodontal tissues. Maintaining favorable composition of bacterial biofilm, obtained from the elimination of bacteria in the causal phase, means that the inflammation does not recur, bleeding does not intensify, and inflammatory-immunological mechanisms are gradually modulated. In periodontium, healing processes begin to prevail over destruction processes.

As mentioned earlier, in our study, both plaque and bleeding indices were not significantly reduced, which could mean that the pocket reduction process included additional mechanisms. It may be indirectly confirmed by the results of a clinical parameter correlation analysis (Table VII). In the placebo group, positive correlations were observed between plaque and bleeding indices as well as the mean and maximum pocket depths vs. reduction in the number of bacteria; therefore, changes in the number of bacteria affected clinical parameters. Such correlations were not found in the study group, which may mean that the significant reduction in pocket depth observed in this group was not due to a change in clinical parameters and the number of bacteria but rather a change in biofilm composition and its effect on inflammatory and immunological parameters. In the study group, only a negative correlation

between the maximum depth of periodontal pockets and the number of bacteria before treatment was noted. It means that the greater the maximum depth of periodontal pockets before treatment, the smaller the number of bacteria were detected in tested samples. It may indicate that patients with the most advanced disease were very well motivated to maintain proper oral hygiene. This correlation disappeared after treatment, which may be associated with biofilm composition changes after using *L. alivarius* SGL03.

Microbiological testing of the oral cavity microbiota comprises several approaches, including qualitative or quantitative culture methods for detecting particular species (with the use of selective culture media) or groups of bacteria. PCR techniques are particularly useful as they enable detecting specific species of bacteria, including non-viable or non-cultivable microorganisms. Both probiotic and pathogenic periodontal species (e.g., *P. gingivalis* or *A. actinomycetemcomitans*) may be detected with this method. Metagenomic methods are increasingly used in dentistry, and they make it possible to detect the composition of microorganisms that make up the biofilm, as well as the percentage of individual types of bacteria (Xu and Gunsolley 2014; Dabdoub et al. 2016). These techniques also allow the discovery of new periopathogens, including bacteria that cannot be isolated using classical culture methods (Hiranmayi et al. 2017; Torres et al. 2019). A better understanding of oral microbiota composition and mutual interactions of microorganisms present in the course of the disease will allow for the use of more effective therapeutic procedures, including patients with periodontitis (Proctor et al. 2020).

Several types of samples are used in microbiological studies of the oral cavity; however, in periodontology, they mainly comprise specimens of supragingival and/or subgingival plaque.

According to the authors of the analysis concerning periodontal disease, the use of probiotics improves clinical parameters such as BOP, PD, GI, but not the number of colony-forming units (CFU) of bacterial periopathogens (Seminario-Amez et al. 2017). However, it should be remembered that the microbiology of periodontal pockets is very complex and comprises both periopathogens as well as aerobic, pioneering, and seemingly nonpathogenic bacteria.

A meta-analysis by Gruner et al. (2016), in which three papers on the effectiveness of therapy with probiotics containing Lactobacillus bacteria were evaluated, did not show their effect on the examined periopathogens: *A. actinomycetemcomitans*, *P. gingivalis*, and Prevotella intermedia. However, despite a reduction in gingival inflammation indices (GI and BOP), no impact of probiotics on the plaque index was observed in the analyzed studies. Therefore, the authors of the analysis conclude that its effect results from the influence on host response, not on bacteria themselves.

Several bacteriological studies revealed the effect of probiotic strains of Lactobacillus spp. on the reduction of *A. actinomycetemcomitans*, *P. gingivalis*, *P. intermedia*, and *T. forsythia* in the subgingival plaque of patients with periodontitis, with no significant effect on clinical indices in these patients (Mayanagi et al. 2009; Vivekananda et al. 2010; Iniesta et al. 2012; Montero et al. 2017). On the other hand, in the paper mentioned above by Hallström et al. (2013), the use of *L. reuteri* lozenges did not affect biofilm composition in experimental gingivitis. Similarly, in our research, no influence of the probiotic on the number of bacteria in supragingival plaque samples was observed, with a slight statistically not significant reduction in the number of bacteria in the placebo group and an increase (not statistically significant) in the number of bacteria in the study group. This rise may be related to different bacterial species composition in samples before and after applying the probiotic. Given the statistically significant reduction of pocket depths in the study group, it can be assumed that probiotic use could have a beneficial effect on changing the composition of dental plaque microbiota to microbiota with lower pathogenic potential. However, further studies are needed to evaluate the biofilm composition concerning specific bacterial species.

Long-term use of a probiotic may positively affect the composition of oral microbiota and interactions between individual types of bacteria and inhibit proinflammatory effects of periopathogens; however, it cannot replace daily hygiene procedures (Laleman et al. 2015). The authors of a systematic review of the literature regarding the effect of probiotics on experimentally induced gingivitis in humans concluded that probiotics may be an alternative to rinses containing chlorhexidine (CHX), which could have undesirable adverse effects (Barboza et al. 2020).

Although some studies do not show an improvement in clinical parameters (e.g., plaque and bleeding indices) after the use of probiotic, they indicate the possibility of its action by modulating inflammatory response, e.g., by reducing the level or activity of PGE2, proinflammatory cytokines or proteolytic enzymes (elastase, MMP-3 metalloproteinase) in gingival crevicular fluid (GCF) or saliva (Staab et al. 2009; Lee et al. 2015; Kuru et al. 2017).

Attention should be paid to the form of the supplement used in the study – Salistat SGL03 is a rinse solution, while the majority of supplements on the market are oral tablets or lozenges. This probiotic supplement (and the placebo) in the form of a solution enables the accurate distribution of the suspension on tooth and gum surfaces as well as the mucosa of the entire oral cavity. In addition, as recommended by

the manufacturer, bacteria constituting the contents of the package are kept in the mouth for about 30 seconds before being swallowed. It seems to be a much better and more effective form of probiotic application than tablets or lozenges. It also requires slightly increased patient involvement in the evening application procedure after thorough toothbrushing, which could have contributed to the improvement of clinical parameters in the placebo group.

The effects of probiotics reported in the literature on clinical parameters and inflammatory markers are variable, ranging from no effect to statistically significant decrease in PI, GI, and BOP indices and in GCF volume (Slawik et al. 2011; Iniesta et al. 2012; Hallström et al. 2013; Kuru et al. 2017). Interestingly, Kuru et al. (2017) reported that beneficial effects were also observed after cessation of toothbrushing for five days, which may indicate a beneficial effect of the probiotic in patients with temporarily reduced performance of hygiene procedures, e.g., for health reasons. Further studies are needed to clarify this issue.

It should be noted that in this study, only one probiotic preparation has been evaluated (containing *L. salivarius* SGL03), so our findings cannot rule out other effects of the use of other probiotics.

In this study, the authors also analyzed a questionnaire on subjective assessment of the probiotic preparation containing *L. salivarius* SGL03 (its taste perception, the convenience of use, the effect on the state of gums and mucosa as well as potential adverse effects of dietary supplement), in comparison to the preparation administered to the patients in the placebo group. Over 61% of patients in the study group were satisfied with both the taste of this dietary supplement as well as convenience of its use (in comparison to 80.0% and 76% in the placebo group, respectively). It is important to emphasize that the addition of probiotic strains of microorganisms may alter the taste and aroma of the final food product or dietary supplement due to the production of different metabolites (e.g., organic acids) during fermentation, and extended storage (Terpou et al. 2019). It may determine the patient's adherence to therapy, particularly during long-term treatment for several weeks or months. In this study, 46.2% and 57.7% of patients in the study group reported the improved effect on the gums and oral mucosa compared to 60.0% and 52.0% in the placebo group. As reported in the literature, probiotic dietary supplements increasingly used in dentistry – apart from their direct effects (e.g., inhibition of oral pathogenic microbiota) – may also contribute indirectly to the regulation of mucosal permeability and local immunity in the oral cavity as well as decreased gum bleeding and reduced gingivitis (Krasse et al. 2006; Anusha et al. 2015). There were adverse reactions reported in the questionnaire by three patients in the study group and one individual in the placebo group; however, it should be noted that no patient had reported these adverse effects during therapy or ceased the use of the preparation (probiotic or placebo) because of them.

Conclusions

The use of the probiotic-containing *L. salivarius* SGL03 in the form of an oral suspension in patients in the maintenance phase of periodontitis treatment could have contributed to a reduction in the periodontal depths pockets, with no change in other clinical parameters and the number of bacteria in supragingival plaque. The use of probiotics seems to be justified in the maintenance phase of treatment to sustain the microbiological balance obtained during its causal phase. They can then be an alternative to additional therapies with antiseptics. Further research is needed on individual bacterial species' clinical and microbiological parameters to confirm the long-term effect of the preparation.

ORCID
Małgorzata Nędzi-Góra https://orcid.org/0000-0003-4041-2678
Marta Wróblewska https://orcid.org/0000-0002-9126-7442
Renata Górska https://orcid.org/0000-0002-2769-7587

Acknowledgements
The authors declare that they do not have a conflict of interest. The study was partially supported by the Nutropharma. The authors would particularly like to thank for preparing the placebo. The company read and approved the manuscript before submission without making any suggestions to change content or emphasis. The company was not involved in patients' selection, data collection, analysis, or interpretation.

Conflict of interest
The authors do not report any financial or personal connections with other persons or organizations, which might negatively affect the contents of this publication and/or claim authorship rights to this publication.

Literature

Ainamo J, Bay I. Problems and proposals for recording gingivitis and plaque. Int Dent J. 1975 Dec;25(4):229–235.
Barboza EP, Arriaga PC, Luz DP, Montez C, Vianna KC. Systematic review of the effect of probiotics on experimental gingivitis in humans. Braz Oral Res. 2020;34:e031. https://doi.org/10.1590/1807-3107bor-2020.vol34.0031
Bartold PM, Van Dyke TE. An appraisal of the role of specific bacteria in the initial pathogenesis of periodontitis. J Clin Periodontol. 2019 Jan;46(1):6–11. https://doi.org/10.1111/jcpe.13046
Barzegari A, Kheyrolahzadeh K, Hosseiniyan Khatibi SM, Sharifi S, Memar MY, Zununi Vahed S. The battle of probiotics and their derivatives against biofilms. Infect Drug Resist. 2020 Feb;13:659–672. https://doi.org/10.2147/IDR.S232982

Caton JG, Armitage G, Berglundh T, Chapple ILC, Jepsen S, Kornman KS, Mealey BL, Papapanou PN, Sanz M, Tonetti MS. A new classification scheme for periodontal and peri-implant diseases and conditions – Introduction and key changes from the 1999 classification. J Periodontol. 2018 Jun;89 Suppl 1:S1–S8. https://doi.org/10.1002/JPER.18-0157

Dabdoub SM, Ganesan SM, Kumar PS. Comparative metagenomics reveals taxonomically idiosyncratic yet functionally congruent communities in periodontitis. Sci Rep. 2016 Dec;6(1):38993. https://doi.org/10.1038/srep38993

Dahlen G, Basic A, Bylund J. Importance of virulence factors for the persistence of oral bacteria in the inflamed gingival crevice and in the pathogenesis of periodontal disease. J Clin Med. 2019 Aug 29;8(9):1339. https://doi.org/10.3390/jcm8091339

Devine DA, Marsh PD, Meade J. Modulation of host responses by oral commensal bacteria. J Oral Microbiol. 2015 Jan;7(1):26941. https://doi.org/10.3402/jom.v7.26941

Elmer GW, Surawicz CM, McFarland LV. Biotherapeutic Agents. JAMA. 1996 Mar 20;275(11):870–876. https://doi.org/10.1001/jama.1996.03530350052034

Geisinger ML, Kaur M, Basma H. Nonsurgical periodontal therapy: a review of current standards of care and innovations to improve gingival and periodontal health. Curr Oral Health Rep. 2019 Sep; 6(3):177–187. https://doi.org/10.1007/s40496-019-00224-7

Gruner D, Paris S, Schwendicke F. Probiotics for managing caries and periodontitis: systematic review and meta-analysis. J Dent. 2016 May;48:16–25. https://doi.org/10.1016/j.jdent.2016.03.002

Hallström H, Lindgren S, Yucel-Lindberg T, Dahlén G, Renvert S, Twetman S. Effect of probiotic lozenges on inflammatory reactions and oral biofilm during experimental gingivitis. Acta Odontol Scand. 2013 Jan;71(3–4):828–833. https://doi.org/10.3109/00016357.2012.734406

Hasan A, Palmer RM. A clinical guide to periodontology: pathology of periodontal disease. Br Dent J. 2014 Apr;216(8):457–461. https://doi.org/10.1038/sj.bdj.2014.299

Haukioja A. Probiotics and oral health. Eur J Dent. 2010 Jul;04(03): 348–355. https://doi.org/10.1055/s-0039-1697851

Hiranmayi KV, Sirisha K, Ramoji Rao MV, Sudhakar P. Novel pathogens in periodontal microbiology. J Pharm Bioallied Sci. 2017; 9(3):155–163. https://doi.org/10.4103/jpbs.JPBS_288_16

Iniesta M, Herrera D, Montero E, Zurbriggen M, Matos AR, Marín MJ, Sánchez-Beltrán MC, Llama-Palacio A, Sanz M. Probiotic effects of orally administered *Lactobacillus reuteri*-containing tablets on the subgingival and salivary microbiota in patients with gingivitis. A randomized clinical trial. J Clin Periodontol. 2012 Aug; 39(8):736–744. https://doi.org/10.1111/j.1600-051X.2012.01914.x

Kõll-Klais P, Mändar R, Leibur E, Marcotte H, Hammarström L, Mikelsaar M. Oral lactobacilli in chronic periodontitis and periodontal health: species composition and antimicrobial activity. Oral Microbiol Immunol. 2005 Dec;20(6):354–361. https://doi.org/10.1111/j.1399-302X.2005.00239.x

Krasse P, Carlsson B, Dahl C, Paulsson A, Nilsson A, Sinkiewicz G. Decreased gum bleeding and reduced gingivitis by the probiotic Lactobacillus reuteri. Swed Dent J. 2006;30(2):55–60.

Kuru BE, Laleman I, Yalnızoğlu T, Kuru L, Teughels W. The influence of a Bifidobacterium animalis probiotic on gingival health: A randomized controlled clinical trial. J Periodontol. 2017 Nov; 88(11):1115–1123. https://doi.org/10.1902/jop.2017.170213

Laleman I, Teughels W. Probiotics in the dental practice: a review. Quintessence Int. 2015 Mar;46(3):255–264.

Laleman I, Yilmaz E, Ozcelik O, Haytac C, Pauwels M, Herrero ER, Slomka V, Quirynen M, Alkaya B, Teughels W. The effect of a streptococci containing probiotic in periodontal therapy: a randomized controlled trial. J Clin Periodontol. 2015 Nov;42(11): 1032–1041. https://doi.org/10.1111/jcpe.12464

Lee J-K, Kim S-J, Ko S-H, Ouwehand AC, Ma DS. Modulation of the host response by probiotic *Lactobacillus brevis* CD2 in experimental gingivitis. Oral Dis. 2015 Sep;21(6):705–712. https://doi.org/10.1111/odi.12332

Mayanagi G, Kimura M, Nakaya S, Hirata H, Sakamoto M, Benno Y, Shimauchi H. Probiotic effects of orally administered *Lactobacillus salivarius* WB21-containing tablets on periodontopathic bacteria: a double-blinded, placebo-controlled, randomized clinical trial. J Clin Periodontol. 2009 Jun;36(6):506–513. https://doi.org/10.1111/j.1600-051X.2009.01392.x

Mcfarland LV. A review of the evidence of health claims for biotherapeutic agents. Microb Ecol Health Dis. 2000;12(2):65–76.

Meyle J, Chapple I. Molecular aspects of the pathogenesis of periodontitis. Periodontol 2000. 2015 Oct;69(1):7–17. https://doi.org/10.1111/prd.12104

Montero E, Iniesta M, Rodrigo M, Marín MJ, Figuero E, Herrera D, Sanz M. Clinical and microbiological effects of the adjunctive use of probiotics in the treatment of gingivitis: A randomized controlled clinical trial. J Clin Periodontol. 2017 Jul;44(7):708–716. https://doi.org/10.1111/jcpe.12752

Morales A, Carvajal P, Silva N, Hernandez M, Godoy C, Rodriguez G, Cabello R, Garcia-Sesnich J, Hoare A, Diaz PI, et al. Clinical effects of *Lactobacillus rhamnosus* in non-surgical treatment of chronic periodontitis: a randomized placebo-controlled trial with 1-year follow-up. J Periodontol. 2016 Aug;87(8):944–952. https://doi.org/10.1902/jop.2016.150665

Nissen L, Sgorbati B, Biavati B, Belibasakis GN. *Lactobacillus salivarius* and *L. gasseri* down-regulate *Aggregatibacter actinomycetemcomitans* exotoxins expression. Ann Microbiol. 2014 Jun;64(2):611–617. https://doi.org/10.1007/s13213-013-0694-x

O'Leary TJ, Drake RB, Naylor JE. The plaque control record. J Periodontol. 1972 Jan;43(1):38–46. https://doi.org/10.1902/jop.1972.43.1.38

Penala S, Kalakonda B, Pathakota K, Jayakumar A, Koppolu P, Lakshmi B, Pandey R, Mishra A. Efficacy of local use of probiotics as an adjunct to scaling and root planing in chronic periodontitis and halitosis: A randomized controlled trial. J Res Pharm Pract. 2016;5(2):86–93. https://doi.org/10.4103/2279-042X.179568

Piwat S, Sophatha B, Teanpaisan R. An assessment of adhesion, aggregation and surface charges of *Lactobacillus* strains derived from the human oral cavity. Lett Appl Microbiol. 2015 Jul;61(1):98–105. https://doi.org/10.1111/lam.12434

Proctor DM, Shelef KM, Gonzalez A, Davis CL, Dethlefsen L, Burns AR, Loomer PM, Armitage GC, Ryder MI, Millman ME, et al. Microbial biogeography and ecology of the mouth and implications for periodontal diseases. Periodontol 2000. 2020 Feb;82(1): 26–41. https://doi.org/10.1111/prd.12268

Seminario-Amez M, López-López J, Estrugo-Devesa A, Ayuso-Montero R, Jané-Salas E. Probiotics and oral health: A systematic review. Med Oral Patol Oral Cir Bucal. 2017 May 1;22(3):e282–e288. https://doi.org/10.4317/medoral.21494

Shimauchi H, Mayanagi G, Nakaya S, Minamibuchi M, Ito Y, Yamaki K, Hirata H. Improvement of periodontal condition by probiotics with *Lactobacillus salivarius* WB21: a randomized, double-blind, placebo-controlled study. J Clin Periodontol. 2008 Oct;35(10): 897–905. https://doi.org/10.1111/j.1600-051X.2008.01306.x

Slawik S, Staufenbiel I, Schilke R, Nicksch S, Weinspach K, Stiesch M, Eberhard J. Probiotics affect the clinical inflammatory parameters of experimental gingivitis in humans. Eur J Clin Nutr. 2011 Jul;65(7):857–863. https://doi.org/10.1038/ejcn.2011.45

Socransky SS, Haffajee AD, Cugini MA, Smith C, Kent RL Jr. Microbial complexes in subgingival plaque. J Clin Periodontol. 1998 Feb;25(2):134–144. https://doi.org/10.1111/j.1600-051X.1998.tb02419.x

Staab B, Eick S, Knöfler G, Jentsch H. The influence of a probiotic milk drink on the development of gingivitis: a pilot study. J Clin Periodontol. 2009 Oct;36(10):850–856. https://doi.org/10.1111/j.1600-051X.2009.01459.x

Takahashi N. Oral microbiome metabolism: from "Who are they?" to "What are they doing?". J Dent Res. 2015 Dec;94(12):1628–1637. https://doi.org/10.1177/0022034515606045

Terpou A, Papadaki A, Lappa I, Kachrimanidou V, Bosnea L, Kopsahelis N. Probiotics in food systems: significance and emerging strategies towards improved viability and delivery of enhanced beneficial value. Nutrients. 2019 Jul 13;11(7):1591. https://doi.org/10.3390/nu11071591

Teughels W, Durukan A, Ozcelik O, Pauwels M, Quirynen M, Haytac MC. Clinical and microbiological effects of *Lactobacillus reuteri* probiotics in the treatment of chronic periodontitis: a randomized placebo-controlled study. J Clin Periodontol. 2013 Nov; 40(11):1025–1035. https://doi.org/10.1111/jcpe.12155

Teughels W, Van Essche M, Sliepen I, Quirynen M. Probiotics and oral healthcare. Periodontol 2000. 2008 Oct;48(1):111–147. https://doi.org/10.1111/j.1600-0757.2008.00254.x

Tonetti MS, Greenwell H, Kornman KS. Staging and grading of periodontitis: framework and proposal of a new classification and case definition. J Clin Periodontol. 2018 Jun;45 Suppl 20:S149–S161. https://doi.org/10.1111/jcpe.12945

Torres PJ, Thompson J, McLean JS, Kelley ST, Edlund A. Discovery of a novel periodontal disease-associated bacterium. Microb Ecol. 2019 Jan;77(1):267–276. https://doi.org/10.1007/s00248-018-1200-6

Umar D, Basheer B, Baroudi K, Anusha RL. The magic of magic bugs in oral cavity: probiotics. J Adv Pharm Technol Res. 2015;6(2): 43–47. https://doi.org/10.4103/2231-4040.154526

Van Dyke TE, Bartold PM, Reynolds EC. The nexus between periodontal inflammation and dysbiosis. Front Immunol. 2020 Mar 31;11:511. https://doi.org/10.3389/fimmu.2020.00511

Vivekananda MR, Vandana KL, Bhat KG. Effect of the probiotic *Lactobacilli reuteri* (Prodentis) in the management of periodontal disease: a preliminary randomized clinical trial. J Oral Microbiol. 2010 Jan;2(1):5344. https://doi.org/10.3402/jom.v2i0.5344

Xu P, Gunsolley J. Application of metagenomics in understanding oral health and disease. Virulence. 2014 Apr;5(3):424–432. https://doi.org/10.4161/viru.28532

Zarco MF, Vess TJ, Ginsburg GS. The oral microbiome in health and disease and the potential impact on personalized dental medicine. Oral Dis. 2012 Mar;18(2):109–120. https://doi.org/10.1111/j.1601-0825.2011.01851.x

Polish Journal of Microbiology
2020, Vol. 69, No 4, 453–462
https://doi.org/10.33073/pjm-2020-048

ORIGINAL PAPER

Benefits of Soleris® over the Conventional Method for Enumeration of Microbial Load in *Salacia* Herbal Extract

SADANAND YEWALE[1], ZEBA FARASH[2], SANMAN KOLHE[1], SASIDHARAN SAKKAN[3], SHRINIVAS BHOPE[2], PRADNYA AMBEKAR[4] and SRIRAM PADMANABHAN[1]*

[1] Herbal Division, Sava Healthcare Limited, Research Center, Chinchwad, Pune, India
[2] Analytical Development Laboratory, Sava Healthcare Limited, Research Center, Chinchwad, Pune, India
[3] QC, Microbiology Division, Sava Healthcare Limited, KIADB Industrial Area, Malur, India
[4] Neogen Food and Animal Security (India) Pvt. Ltd., Kochi, India

Submitted 18 July 2020, revised 2 October 2020, accepted 8 October 2020

Abstract

Stems and roots of *Salacia* genus plants have been used as a specific remedy for early-stage diabetes, and one of the four sulphonium sulphates, salacinol is the compound responsible for the anti-diabetic activity. *Salacia* is prone to microbial contamination and insect infestation; hence, methods to estimate the microbial load in such plants will enhance its nutritional value. This paper highlights the novel use of Soleris® to quantify microbes of all types, namely bacteria, yeasts, molds, and coliforms in herbal extracts. The microbial analysis results obtained with Soleris® test vial have been compared with the conventional method, and the results indicate that Soleris® is equally efficient as the conventional method and in fact displays several advantages over the traditional method. The Soleris® method is a real time monitoring system that is highly sensitive, user-friendly, and environmentally friendly since it generates very little biomedical waste and saves a large amount of time. The data presented here demonstrate that for highly contaminated samples, results are available within 24 h. For yeasts and molds, the Soleris® method produces results in 48 h, thus offering considerable time savings compared to other commonly used methods.

Key words: *Salacia*, salacinol, microbial load, bacteria, yeasts, herbals

Introduction

Salacia, a genus is one of the medicinal plants group broadly used to treat many ailments viz. hypoglycemia, hypolipidemia, inflammation, and diabetic patients. *Salacia* is represented by 21 species in India, of which 15 species occur in Peninsular India with *S. reticulata* and *S. oblonga* as predominant species (Bagnazari et al. 2017). The root of *Salacia* spp. (*S. chinensis*, *S. reticulata*, *S. oblonga*) is one of the preferred drug sources for treating diabetes in the indigenous systems of medicine. *Salacia* species contain two active compounds salacinol and kotalanol, which are reported to exhibit α-glucosidase inhibitory activity (Akaki et al. 2014). Apart from its anti-diabetic potential, Homma and coworkers (2019) have attributed skin whitening capabilities to salacinol with low cytotoxicity.

A wide range of diseases affecting humans has been treated since ancient times with medicinal plants, as extracts, individually or as polyherbal preparations. A survey by the World Health Organization (WHO) has indicated that in the developing countries, nearly 70–80% of the population prefers to use non-conventional herbal medicines for their primary health care (Abba et al. 2009). The herbal medicines are safe, natural, relatively accessible, and cheaper than the synthetic drugs.

Factors that influence the contamination of medicinal herbs are several. These include certain environmental factors, mainly humidity, rainfall, storage conditions of crude and processed medicinal-plant materials, and handling and hygiene of people handling the herbs. Also, microorganisms derived from soil, air and water may contaminate the herbal raw materials leading to pathogenic effects to humans (Alonzo et al. 1994; de Freitas Araújo and Bauab 2012). The presence of such pathogens limits the use of medicinal plants and also exerts an important impact on the overall therapeutic

* Corresponding author: S. Padmanabhan, Herbal Division, Sava Healthcare Limited, Research Center, Chinchwad, Pune, India; **e-mail: sriram.p@savaglobal.com**

quality of herbal drugs and preparations. Also, since the presence of such pathogenic microorganisms constitutes a potential hazard to human health, reducing their concentration from their source is critical.

Escherichia coli and *Pseudomonas* spp. are the typical pathogens seen in herbal extract powders. Fungal species such as *Rhizhopus, Penicillium*, *Aspergillus* are also reported (Hitokito et al. 1978; Kneifel et al. 2002). Although bacterial endospores and fungal spores are considered as the two dominating groups of contaminants seen on medicinal plants, the presence of pathogenic bacteria like *B. cereus*, *Aeromonas hydrophila*, *Shigella* spp., *Enterobacter agglomerans*, *E. cloacae*, *Vibrio fluvialis*, *Pasteurella multocida*, *S. epidermidis*, *Acinetobacter iwoffii*, *Klebsiell*a spp., and *B. subtilis* have been reported in plant samples analyzed recently (Idu et al. 2011).

Assessment of medicinal plants' microbial load such as *Matricaria chamomilla*, *Achillea millefolium*, *Ocimum basilicum*, *Calendula officinalis*, and *Tilia cordata*, *Hypericum perforatum*, and *Salacia* has been reported (Kumar et al. 2015; Oprea et al. 2015).

The most widely used technique for a total count of microorganisms in plant materials is a technique recommended by the WHO. In this methodology, 10 g of sample is recommended to be suspended in 90 ml of buffer sodium chloride-peptone of pH to 7.0. Suitable dilutions of the sample is plated on casein-soybean digest agar and incubated at 30–35°C. The total aerobic count is measured after 48 h. For yeast and molds, the technique employed is the sowing depth in Sabouraud dextrose plus a solution of 10% tartaric acid to obtain pH 3.0 to 3.5 and incubated at 20–25°C for five days (WHO 1998). The specification of the WHO for total aerobic microorganisms is not more than 10^7 CFU/g, while the specification of the WHO for yeasts and molds is at most 10^4 CFU/g. Both the Brazilian Pharmacopeia (ANVISA 2010) and the United States Pharmacopeia (USP 2005) have recommended specifications for oral use: 104 aerobic bacteria/g or ml and 102 fungi/g. The European Pharmacopoeia (EDQM 2007) also gives guidance on acceptance criteria (5.1.8 for herbal medicinal products for oral use and 5.1.4 for other herbal medicinal products). The limits of microbial contamination given in European Pharmacopoeia for herbal medicinal products to which boiling water is added before use are total aerobic bacteria (10^7 CFU/g), fungi (10^5 CFU/g) as against 10^5 CFU/g), fungi (10^3 CFU) when water is not added before use.

In Ghana, around 65% of the population depends on herbal medicine and hence estimation of the accurate microbial load becomes essential in such cases to avoid health issues to herbal users (Agyeman-Duah et al. 2017). Herbal medicines in liquid form also have also been shown to have microbial contamination, and hence determination of quantitation of microbial load becomes critical (de Sousa Lima et al. 2020). In this paper, we describe the ease of detecting microbial load in *Salacia* extract powder using Soleris® instrument and strongly believe the applicability of this method to all herbal extracts.

Experimental

Materials and Methods

Reagents and chemicals. All HPLC grade solvents (acetonitrile, methanol, water, and o-phosphoric acid) were purchased from Rankem (Bangalore, India). Standard salacinol was procured from Clear Synth, Mumbai, India.

Collection of samples. Stem and roots of *S. reticulata* were collected from different regions of India. The identity was confirmed and documented by Dr. P. Santhan, a taxonomist at Durva Herbal Centre, Chennai, Tamilnadu, India. The freshly collected samples of stem and roots were stored at room temperature, protected from light and humidity before analysis. Commercial samples of *S. reticulata* raw material were collected from the production unit, SAVA Healthcare, Malur, Karnataka, India.

Preparation of aqueous extract of *Salacia* roots. 100 g *S. reticulata* roots were pulverized and extracted with four volumes of demineralized water three times (each extraction for 3 h) at 80°C. All the three extractable liquids were later pooled and concentrated on a BUCHI rotary evaporator at 55–60°C to obtain a dry powder.

Microbial analysis by the conventional method. Microbiology testing of total viable count (TVC), coliform count, yeast, and mold count were carried out using standard reported methods (IS 5401-1 2012; USP 2014).

Sterilization of *Salacia* extract. Aqueous *Salacia* extract, as prepared above, were processed at Microtrol Sterilization Services Pvt. Ltd., Bangalore, India, for sterilization by three different methods. For steam sterilization, the *Salacia* extract was exposed to 121°C for 20 min, and the sample obtained was collected and designated as RDP/SR/070/SS01 for further analysis. For ETO treatment, the sample was exposed to a mixture of ethylene oxide and air compatible with the chamber design and introduced into the chamber at a concentration of ethylene oxide not to exceed 750 g/m^3, with a dwell time of 6 h. This sample was labeled as RDP/SR/070/ES02. For gamma irradiation of the *Salacia* extract, the powder was subjected to gamma radiation to a target dose of 8 kGy in paper bags for 20 min, and the labeled sample RDP/SR/070/GR03 was used for further analysis.

All the above three samples were examined for microbial analysis using Neogen's Soleris® instrument and conventional method for total viable count, yeasts and molds, and total coliforms. The untreated extract was designated as SR011903.

Preparation of *Salacia* extract after treatment with an anti-fungal agent. The *Salacia* extract was treated with 50 µg of an SAVA's proprietary antifungal agent (Padmanabhan and Jadhav 2020), and the treated sample was designated as RDP/SR/068 and tested for analysis of total viable count (TVC), yeasts and molds, and total coliforms.

Preparation of *Salacia* extract after treatment with an anti-bacterial agent. Suitable amounts of *Salacia* extract (SR011903) was taken and treated with 50 µg of an antibacterial agent (SAVA proprietary, patent pending) in a ratio of 1 : 20 volumes of water at room temperature for 16 h. Next day, the material was heated to 80°C and treated with 2% activated charcoal and filtered through Hyflo supercel bed (Manju Chemtech, Bangalore, India), dried using a rotary evaporator under vacuum at 50–55°C. The dried material was used for further analysis. The treated sample was designated as RDP/SR/134 and analyzed for residual microbial counts both by conventional method and Soleris® method.

Commercially available *Salacia* extract. A commercial sample of *Salacia* extract was purchased from Kisalaya Herbals Limited, Indore, India, and this sample (RDP/SR/136) was examined for total viable count, yeasts and molds, and total coliforms.

Preparation of samples for Soleris®. 10 g of the powder extract of *Salacia* was taken in a sterile container, and 90 ml of sterile peptone water was added. The solution was mixed by vigorous vortexing for 2 min, and further dilutions up to 10^{-5} were prepared by adding 1 ml of the diluted solution to 9 ml of sterile peptone water. For all the analysis, 1 ml of 10^{-1}, 10^{-3} and 10^{-5} dilutions added to the respective vials, and incubated in the machine at required temperatures as recommended by the Soleris® manufacturer.

LC-MS/MS for determination of salacinol. Standard salacinol solution. 2 mg of salacinol reference standard was placed in a 100 ml volumetric flask and 40 ml of diluent was added. The solution was sonicated in an ultrasonicate water bath, cooled and volume made up with the diluent and mixed by inversion. Suitable dilutions of this solution were used for LC-MS studies.

***Salacia* extract sample solution preparation.** 500 mg of *S. reticulata* was extracted and transferred into a 100 ml volumetric flask. About 70 ml of diluent was added, and sonicated for 30 min, then, cooled and made up to the mark with diluent and mixed well. Further, 2 ml of this sample solution was diluted to 200 ml with diluent, mixed well and filtered through 0.2 µm filter by discarding the first few ml of filtrate and then used.

Raw material sample solution preparation. 1 g of powdered dried roots of *Salacia* was taken in a round bottom flask. Nearly 100 ml of diluent (methanol) was added, and the contents were refluxed at 50–60°C for 60 min. The liquid was decanted in a clean rotary flask. The sample's refluxing was repeated by adding another 100 ml of diluent, and the collected liquids were passed through the Whatman No. 1 filter paper. The residue was washed two times with 50 ml quantity of the diluent, concentrated to ~ 50 ml by using a rotary evaporator. This concentrated liquid was diluted to 100 ml with diluent and mixed well. Further 2 ml of this solution was pipetted out in a volumetric flask and volume made up with the diluent. The solution was filtered through a 0.2 µm syringe filter for further use.

LC-MS/MS analytical method and instrumentations. The LC-MS method described by Akaki et al. (2014) was employed with a few modifications for better peak resolutions and separation. The LC-MS analyses were performed using a two-component system composed of mobile phase A (10% ACN/0.1% FA in water) and mobile phase B (0.1% FA in 100% ACN) at a flow rate of 0.4 ml/min. The LC-MS 8045 system (Shimadzu Co., Ltd.) was composed of an autosampler (SIL-30AC), a solvent delivery pump (LC-30AD), and a column oven (CTO-30A) with an API5000 triple-quadrupole instrument (Applied Biosystems, Foster City, CA). The Asahipak NH2P50 2D column (Shodex, Japan) with a dimension of 2 mm ID × 150 mm was used. The optimized interface parameters for the MS were with the nebulizing gas flow: 3 ml/min; heating gas flow: 10 l/min; Dl temperature of 250°C; interface temperature: 300°C and drying gas flow: 10 l/min. The mass spectrometer was operated in a multiple reaction monitoring (MRM) mode that selected one precursor ion and one suitable product ion for each target compound. The flow rate was kept at 0.3 ml/min, and the column temperature was 40°C. 5 µl of sample and standard was injected into the system, and run time was kept as 10 min. The parameters of the *m*/*z* and collision energy of parent ions and quantitative product ions are shown as below:

- precursor ion: 333.4, 333.4, 333.4
- product ion: 97.0, 183.15, 231.05
- Q1 pre bias voltage: 17.0, 17.0, 17.0
- collision energy (V): 35.0, 21.0, 23.0
- Q3 pre bias voltage: 16.0, 18.0, 22.0.

Results and Discussion

The Soleris® system consists of an incubator, ready-to-use vials, and system software that are 21 CFR complaints. The system's flexibility is appreciable since 1 to 512 samples can be tested simultaneously, and up

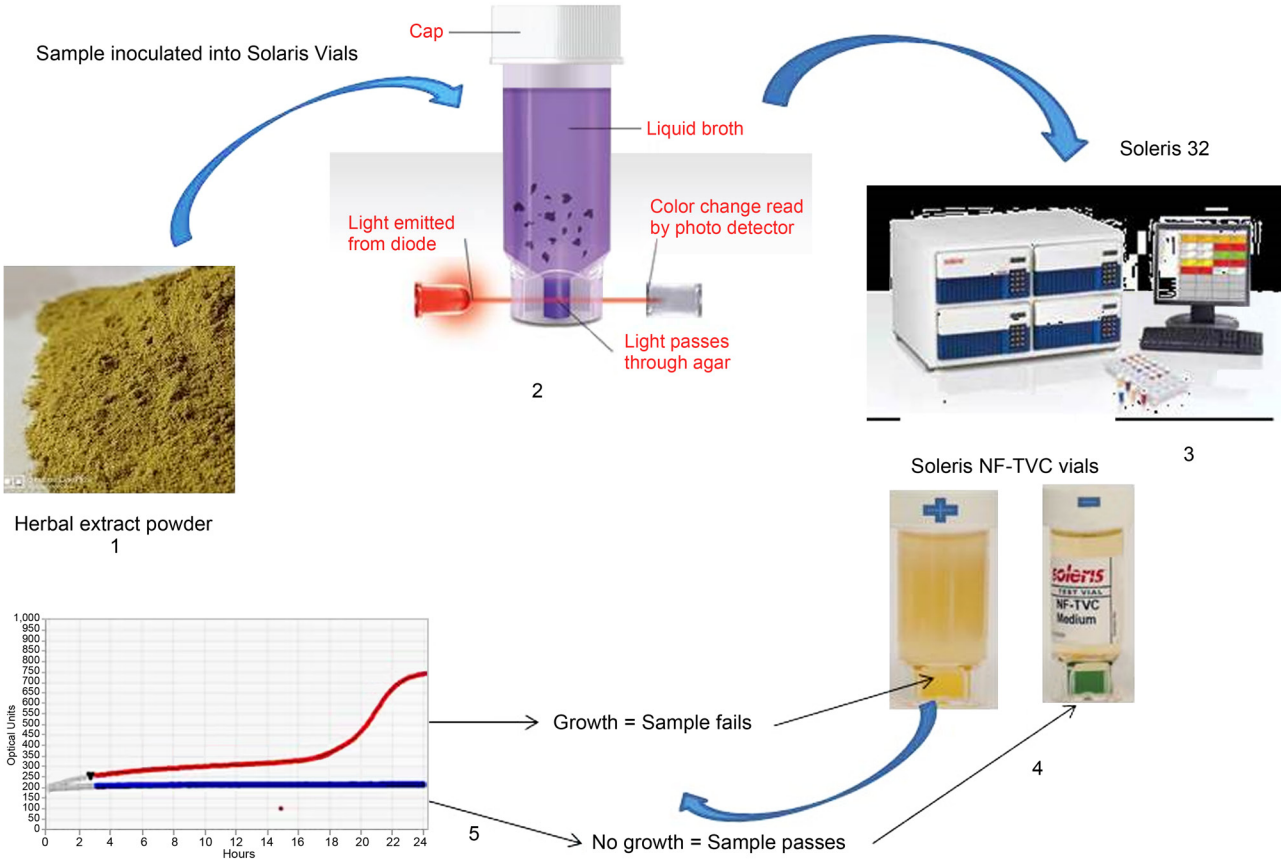

Fig. 1. Schematic representation of the Soleris® system. In Step 1, an aliquot (10 g) of the herbal extract powder is weighed in a sterile container and re-suspended in 90 ml of sterile peptone water. The solution was mixed by vigorous vortexing for 2 min and further dilutions up to 10^{-3} were prepared by adding 1 ml of the diluted solution to 9 ml of sterile peptone and 1 ml of the dilutions were placed in the Soleris® vials in a laminar biosafety hood under sterile conditions (Step 2). In Step 3, the inoculated vials are placed in the selected drawer location in Soleris® instrument and the vials incubated at an appropriate temperature based on type of assay chosen (TVC, yeast and molds or coliforms). As organisms grow in the broth medium, the carbon dioxide (CO_2) produced diffuses through a membrane layer into a soft agar plug containing a dye indicator and the change in the color of the dye is read by the Soleris® instrument (Step 4). A detection curve is generated in real time (Step 5) and the Soleris® software indicates a positive test result in less than 24 h for a sample with microbial contamination and samples producing no detection curve within 24 h are considered negative at the test threshold selected.

to four instruments can be connected to a single PC, allowing any combination of 32 and 128 sample units. The Soleris® instrument with a temperature-controlled incubator is equipped with a photodiode-based optical detection system that allows the growth of microorganisms when inoculated in incubation vials containing selective growth media, supplements, and substrates specific to the microbial species to be detected. The carbon dioxide produced metabolically by the growing microbes results in a color change as metabolic processes happen and it causes a change in pH and denotes a positive detection time (DT). The samples with a higher level of microbial contamination would show a faster DT, and hence this instrument gives a correlation between microbes present and DTs reliably.

The inoculated Soleris® vials are placed into the selected drawer location and experiments are initiated. The Soleris® software indicated positive test results in less than 24 hrs. Determinations producing no detection within 24 h were considered negative. In the case of positive results, the growth curves were evaluated, and the visual validation of medium color change was also carried out Fig. 1. In the case of positive results, confirmation was done using conventional methods. For yeast and mold, the completed system results are available after 72 h, although positive samples were indicated after three rises in CO_2 levels at the preset threshold, usually within 48 h, whereas the yeast and mold detection plates required an incubation of four days and five or more days respectively.

The sensor in the Soleris® Non-Fermenting-Total Viable Count (NF-TVC) vial system utilizes detection of carbon dioxide, a universal bacterial metabolite, rather than detection of acid production, expanding the inclusivity of the vial to include non-fermenting organisms with a sensitivity of 1 CFU (Alles et al. 2009; Mozola et al. 2013). Optical readings from Soleris® test vials are graphed with time (h) in X-axis vs. optical units in the Y-axis. Table I gives the values of total viable count achieved through Soleris® and its compari-

Table I
Soleris® results for total aerobic microbial count.

S.N.	Sample ID	Dilutions inoculated	Growth/ No growth	Detection time (h)
1	SR011903	10^3 10^5	Growth Growth	2.7 4.8
2	RDP/SR/070/SS01	10^2 10^3	Growth No growth	11.4 ND
3	RDP/SR/070/ES02	10^2 10^3	Growth Growth	12.2 11.9
4	RDP/SR/070/GR03	10^2 10^3	Growth Growth	15.1 19.9
5	RDP/SR/068	10^2 10^3	Growth Growth	10.6 12.3
6	RDP/SR/134	10^3 10^5	No growth No growth	No detection No detection
7	RDP/SR/136	10^2 10^3	Growth No growth	13.1 No detection

SR011903 is the *Salacia* extract batch that served as a control. RDP/SR/070/SS01, RDP/SR/070/ES02, and RDP/SR/070/GR03 refer to SR11903 treated after sterilization using steam, ETO, and Gamma irradiation respectively. RDP/SR/068 refers to batch of *Salacia reticulata* is the material treated with the anti-fungal agent that did not show any effect on the bacterial content. RDP/SR/134 and RDP/SR/136 denotes the batch taken after treatment with an anti-bacterial agent and a commercial extract of *S. reticulata* procured from a local Indian vendor.

Table II
Comparison of a total aerobic count between Soleris® (NF-TVC) and the conventional method (Salacinol content).

S.N.	Sample ID	Total aerobic count by Soleris® (CFU/g)*	Total aerobic count by plating in Soleris® medium (CFU/g)**	Conventional plating method***	RLOD#	Salacinol content (%)
1	SR011903 (Control)	> 100,000	109,000	$> 10^5$	1.09	0.52
2	RDP/SR/070/SS01 (Steam sterilized SR011903)	< 1,000	490	350	1.40	ND
3	RDP/SR/070/ES02 (ETO treated SR011903)	> 1,000	1,100	2,700	0.41	ND
4	RDP/SR/070/GR03 (Gamma irradiated SR011903)	< 1,000	280	890	0.31	ND
5	RDP/SR/068 (anti-fungal agent treated SR011903)	> 1,000	1,600	1,500	1.06	0.506
6	RDP/SR/134 (anti-bacterial agent treated SR011903)	> 10	10	20	0.50	0.48
7	RDP/SR/136 (commercial *Salacia* extract)	> 1,000	1,500	2,300	0.65	0.059

ND – not done
* – time of detection < 24 h
** – counts by plating the contents used for the Soleris® vials, and counts obtained after 48 h incubation
*** – time of detection ~ 48 h
\# – relative limit of detection

son with the bacterial CFU enumerated by conventional method plating.

Fig. 2a shows the presence of bacteria for all dilutions. It is inferred through the observation of the bacterial growth curve above the baseline with the count of ~ 1×10^3 CFU/g, a value that corresponds well with the reports of Kumar et al. (2015). The dilution which does not detect any microbes shows a curve touching the baseline while a blue curve indicates the dilutions where bacteria is detected. On the other hand, the red curve indicates the highest amount of organisms present in that particular or lowest dilution. The conventional method for the SR011903 sample yielded 1.09×105 CFU/g, as evident from Table II. The conventional method for the SR011903 sample yielded 1.09×10^5 CFU/g as evident from Table II. The microbial count of the *Salacia* extract after steam sterilization (SS), ETO sterilization (ET), and sterilization by gamma irradiation (GR) showed 50%, 0%, and 75% reduction respectively in comparison to the untreated control, and the values matched well when estimated by the conventional method (Table II). The CFU ranges

indicated in Table II were estimated using the Soleris® system and from the traditional plate counts done in parallel. To compare the sensitivity of the Soleris® method over the conventional method, we opted for calculation of the relative level of detection (RLOD) between the two methods as described (Mărgăritescu and Wilrich 2013). If the RLOD value was below 1, it indicated that the Soleris® method was more sensitive than the conventional plating method while the value was between 1 and 1.5, indicated both the methods to have a similar sensitivity. The RLOD value of above 1.5 indicated that the plating method was more sensitive. It is clear from Table II that the RLOD values of Soleris® in almost all the cases were sensitive over the traditional method of estimation by plating. The growth curve of sample after SS, ET and GR is represented as Figs. 2b, 2c, and 2d, respectively.

The *Salacia*'s microbial load is known to increase upon storage (Kumar et al. 2015), and gamma irradiation has been reported to reduce the microbial load by almost 2 logs. Similar results have been shown by Gupta et al. (2011) for plants such as *Terminalia chebula, Curcuma longa, Syzygium aromaticum,* and *Mentha piperita*.

Our results shown in Table II do indicate differences in efficiencies of microbial killing for the *Salacia* extract with different agents. While gamma irradiation and steam sterilization showed promising microbial load reduction, the ETO treatment did not show any reduction in the microbial load. This could be attributed to the type of microorganism present in *Salacia* extract and the insufficient ETO dose required to efficiently kill resident microbes. Interestingly, differences in efficiency of killing of microorganisms contaminating the herbal extracts has been shown to depend on the types of contaminating organisms, their chemical and physical structure, antiseptic properties of different plants, and their ability to recover from the radiation injury (Gupta et al. 2011), hence, the dose required for efficient microbial killing could be different for different plants.

It is evident from the current observations that none of the traditional methods are efficient enough to reduce the microbial load in *Salacia,* and hence, our observations of reductions in microbial counts in sample RDP/SR/134 by almost 2 logs through the use of an antibacterial agent (proprietary, patent-pending)

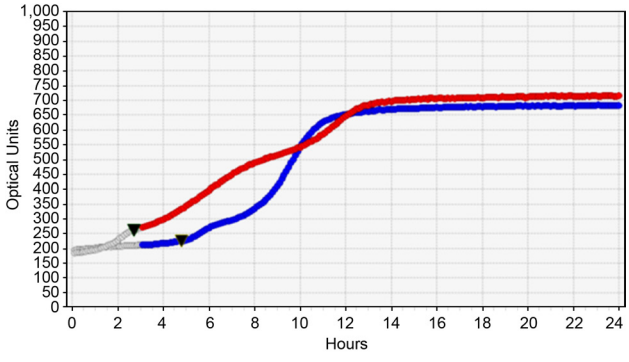

Fig. 2. a) Microbial growth curve in Soleris® NF-TVC vials of various dilutions. Red curve denotes growth with sample SR011903 of 10^{-3} dilution while blue curve denotes 10^{-5} dilution of the sample. Microbial detection was seen in both the dilutions.

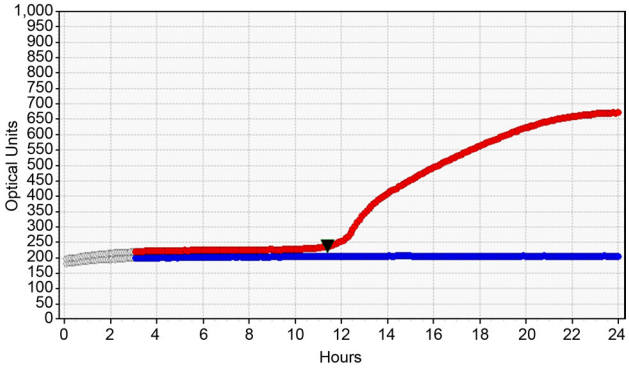

Fig. 2. b) Sample RDP/SR/070/SS01 showed positive results for NF-TVC in Soleris® at 10^{-2} dilution (red curve) while the blue curve denotes 10^{-3} dilution.

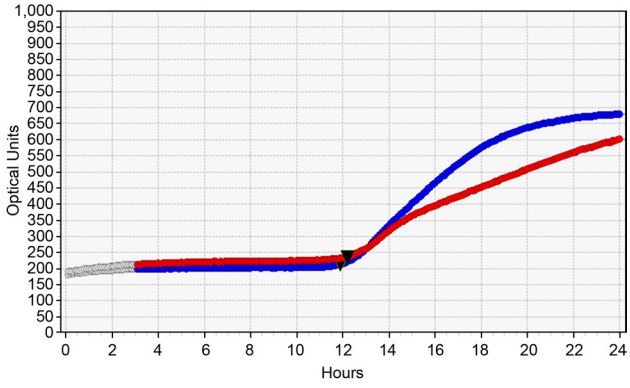

Fig. 2. c) Sample RDP/SR/070/ES02 showed detection of microbes in all the dilutions in Soleris® NF-TVC vials. Blue curve denotes 10^{-3} dilution while the 10^{-2} dilution is represented by the red curve.

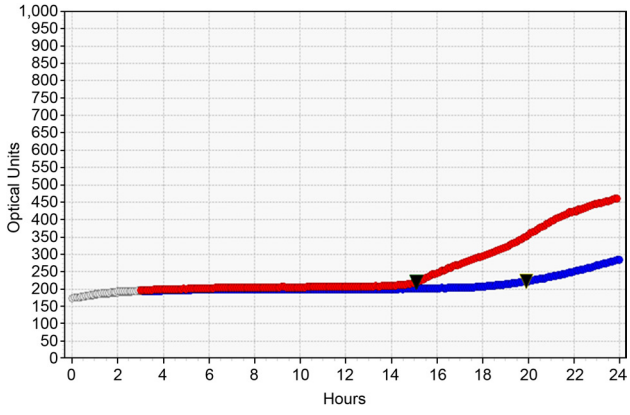

Fig. 2. d) Sample RDP/SR/070/GR03 showed detection in all the dilutions in Soleris® NF TVC vials. Blue curve denotes 10^{-3} dilution while the red curve denotes 10^{-2} dilution.

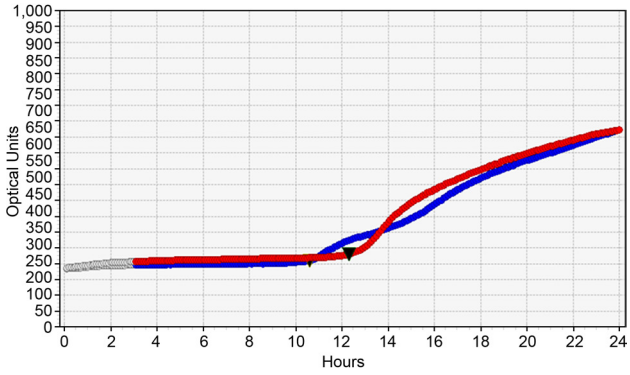

Fig. 2. e) Sample RDP/SR/068 showed detection in all the dilutions in Soleris® NF-TVC vials. Red curve denotes 10^{-3} dilution while the blue curve shows growth with 10^{-2} dilution of the sample.

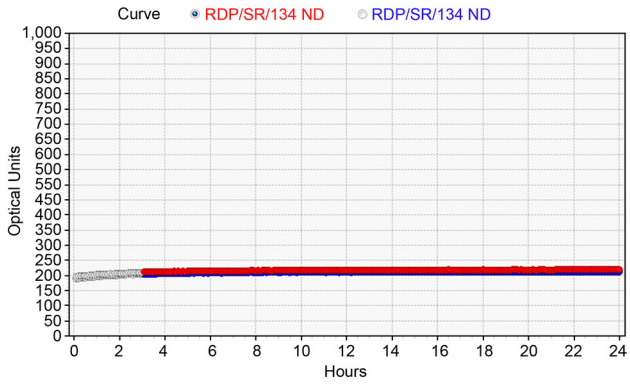

Fig. 2. f) RDP/SR/134 sample showed no bacterial growth in any of the dilutions (10^{-3} and 10^{-5}) tested. This is represented by blue and black flat lines respectively.

appear promising and can be taken up for trials in manufacturing scales.

The sterilization methods using radiations are not readily adaptable for manufacturing plant processes since it requires special equipment and methods. The other methods, such as ethylene oxide, are banned in European Union countries due to the generation of carcinogenic substances such as ethylene glycol, 2-chloroethanol. Also, steam sterilization is not often used for herbal materials since the treated materials become clumped after steam treatment (Brodowska et al. 2014). A new alternative Electron-beam (E-beam) technology, is being used in the food industry to decontaminate food materials (Silindir and Özer 2009). Since installations of such specialized equipment would require investments, alternative methods that are cost-effective to sterilize materials, such as what we describe here, appear to be an attractive proposition.

It is also clear from Table II that the commercially available *Salacia* extract (sample ID RDP/SR/136) showed a TVC of > 1,000 CFU/g. The growth curve seen for TVC for samples RDP/SR/068, RDP/SR/134, and RDP/SR/136 is shown in Figs. 2e, 2f and 2g, respectively. Sample RDP/SR/068 showed microbial detection

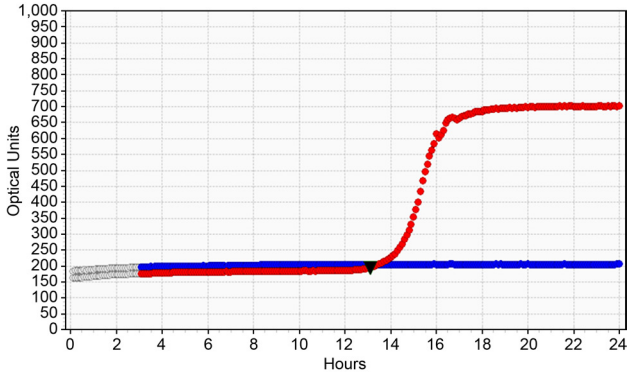

Fig. 2. g) RDP/SR/136 sample showed microbial detection only in 10^{-3} dilution in NF-TVC Soleris® vials denoted by the red curve. The blue flat line denotes no growth seen with 10^{-5} dilution of this sample.

in all the dilutions (10^{-3} and 10^{-2}) which accounts for ~ 1,600 CFU/g obtained by plating one of the dilutions while sample RDP/SR/134 showed no bacterial growth in any of the dilutions (10^{-3} and 10^{-5}) tested, and showed merely 20 CFU/g from 10^{-1} dilution reflecting the efficacy of the antibacterial agent in lysing the microbes contaminating the Salacia extract. RDP/SR/136 sample showed nearly 1,500 CFU/g as seen with the 10^{-2} dilution in NF-TVC Soleris® vials denoted by the red curve (Fig. 2g).

It is evident from Table III that the Soleris® can detect yeast and molds when present within 24 h while it takes more than 5 days when tested by conventional methods. It is also clear that when the extract was pre-treated with the proprietary antifungal agent, the material (RDP/SR/068) showed > 99% reduction in the count of yeasts and molds (Table IV). The Soleris® Direct Yeast and Mold (DYM 109-C) method offers huge time savings for labs engaged in microbial identification in herbal powders. While the yeast and mold results are accessible within 48 h by Soleris®, the conventional methods take up to 5 days. None of the samples tested here showed a growth curve for yeast and molds with the least dilutions except for SR011903 and RDP/SR/136, represented by Figs. 3a and 3b, respectively. Supplementary figures represent the growth curve of other samples, namely SR/011903, RDP/SR/070/SS01, RDP/SR/070/ES02, RDP/SR/070/GR03, RDP/SR/068 and RDP/SR/134, Figs. S1a, S1b, S1c, S1d, S1e, and S1f, respectively. It is interesting to emphasize here that the total yeast and mold counts of the *Salacia* extract enumerated using Soleris® and conventional method of ~ 290 to 380 CFU/g matches well with the reported values of yeast and molds in *Salacia* by other workers (Kumar et al. 2015) demonstrating the sensitivity and accuracy of the Soleris® method of microbial enumeration in the herbal extract of *Salacia* as tested here.

As far as the total coliforms counts were concerned, we found similar results of Solaris® against the

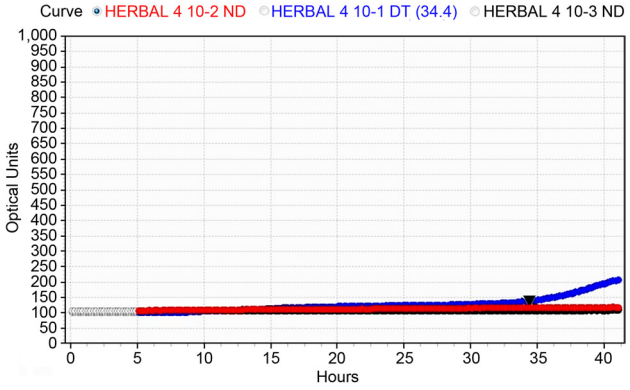

Fig. 3. a) Sample SR011903 showed microbial detection in 10^{-1} dilution in Soleris® DYM 109-C vials represented by blue curve. Black curve denotes 10^{-3} dilution while the red curve denotes 10^{-2} dilution, both of which did not show any growth.

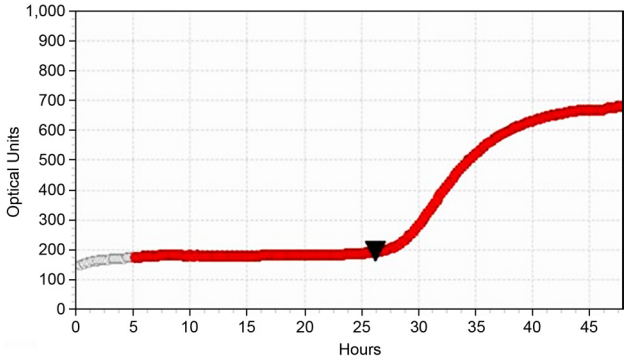

Fig. 3. b) Sample RDP/SR/136 showed microbial detection in 10^{-1} dilution for DYM 109-C Soleris® vials represented by the red curve.

conventional method, indicating the specificity of the tests employed. None of the samples showed any count for total coliforms both by conventional method and by Soleris® test as evident from Table SIa and SIb (supplementary tables). The growth curve pattern on Soleris® also did not show any growth-related optical unit readings (data not shown).

Health surveys conducted in several countries have demonstrated the use of herbal medicines as a mainstream practice among the elderly population, and hence the risk of microbial contamination in herbal drugs might have an adverse effect on the health of such population (de Medeiros et al. 2013; Famewo et al. 2016). Several pathogenic bacteria have been detected in some of the herbal medicines, which is also a severe concern for such medicines' quality issues (Abba et al. 2009; de Medeiros et al. 2013). Hence, it becomes imperative to estimate microbial load in such medicinal herbs and extracts so that such material consumption is safe without any side effects.

Table III
Soleris® results for the total yeast and mold counts.

S.N.	Sample ID	Dilutions inoculated	Growth/ No growth	Detection time (h)
1	SR011903	10^1	Growth	34.4
		10^2	No Growth	–
		10^3	No Growth	–
2	RDP/SR/070/SS01 (Steam sterilized SR011903)	10^1	No Growth	–
		10^2	No Growth	–
		10^3	No Growth	–
3	RDP/SR/070/ES02 (ETO treated SR011903)	10^1	No Growth	–
		10^2	No Growth	–
		10^3	No Growth	–
4	RDP/SR/070/GR03 (Gamma irradiated SR011903)	10^1	No Growth	–
		10^2	No Growth	–
		10^3	No Growth	–
5	RDP/SR/068 (anti-fungal agent treated SR011903)	10^1	No Growth	–
		10^2	No Growth	–
		10^3	No Growth	–
6	RDP/SR/134 (anti-bacterial agent treated SR011903)	10^1	No Growth	–
		10^2	No Growth	–
		10^3	No Growth	–
7	RDP/SR/136 (commercial *Salacia* extract)	10^1	Growth	26.2
		10^2	No growth	–
		10^3	No growth	–

Table IV
Comparison between Soleris® (DYM-109) and the conventional method for the total yeasts and molds.

S.N.	Sample ID	Soleris® (CFU/g)	Conventional method (CFU/g)	Acceptable/Not acceptable
1	SR011903	> 10	380	Not acceptable
2	RDP/SR/070/SS01	< 10	< 10	Acceptable
3	RDP/SR/070/ES02	< 10	< 10	Acceptable
4	RDP/SR/070/GR03	< 10	< 10	Acceptable
5	RDP/SR/068	< 10	< 10	Acceptable
6	RDP/SR/134	< 10	< 10	Acceptable
7	RDP/SR/136	> 10	290	Not acceptable

SR011903 is the *Salacia* extract batch that served as a control. RDP/SR/070/SS01, RDP/SR/070/ES02 and RDP/SR/070/GR03 refer to SR11903 treated after sterilization using steam, ETO and gamma irradiation respectively. RDP/SR/068 refers to batch of *Salacia reticulata* is the material treated with the anti-fungal agent which did not show any effect on the bacterial content, RDP/SR/134 and RDP/SR/136 denote the batch taken after treatment with an antibacterial agent and a commercial batch of *S. reticulata* procured from a local market.

The killing of microorganisms contaminating the herbal extracts is dictated by the dose rate of the antimicrobial agent employed and also by the physical state of the growth of the microbial cells, and other external factors, such as oxygen, water, other chemical agents, and temperature (Halls 1992). Hence, our current data on achieving a microbial reduction of > 99% in *Salacia* is attractive, and obtaining such data from a sensitive instrument like Soleris® assumes critical importance. The Non-Fermenting Total Viable Count (NF-TVC) and the Direct Yeast and Mold (DYM) test methods have been used for various food matrixes, and these have been validated as alternatives to conventional plating techniques (Limberg et al. 2016). The advantages of these growth-based automatic measurements in contrast to conventional plate-counting methods include precision, accuracy, reproducibility, speed, and cost (Blivet 2014; Curda and Svir'akov'a 2014).

Conclusions

Microbial contamination in herbal extracts is one of the issues addressed by the new FDA regulations, and faster and more streamlined microbiological tests are therefore required by the herbal industry to meet the new challenges. Soleris® TVC method has been successfully used for rapid and accurate detection of microorganisms in a variety of food commodities, and its technology is based on monitoring pH change or CO_2 production as a means of microbial growth activity in media vials. The performance of the Soleris® TVC method in detecting microbes in herbal extracts is the first report to date. The sensitivity of the Soleris® method was found to be comparable to that of the reference procedures for the detection of microorganisms. The Soleris® test from Neogen is approved from the AOAC Research Institute as a Performance Tested Method certification 071203 for detecting microorganisms in as little as 4 h, and only takes 24 h to a negative result. The Soleris® vial is substituted for the agar plate. The sensitivity of the equipment is 1 CFU/g. The significant reduction in the generation of biomedical lab waste concerning Solaris® compared to the conventional methods is really attractive. Since Solaris® system reads the vials photometrically by looking into the color change relative to the starting color, it would be the choice of method for all researchers in academics and industries alike who are engaged in determining the microbial contamination in food and other natural products.

Acknowledgments

We thank Dr. P. Santhan for providing plant samples of *Salacia* and Vimta Labs, Pune, India for providing facilities for LC-MS/MS analysis for estimation of salacinol in the *Salacia* samples. Thanks are also due to Mr. Vinod Ramachandra Jadhav, Chairman SAVA Healthcare Limited and Mr. Avinaash Mandale, CEO, SAVA Healthcare Limited for their constant support and encouragement.

Conflict of interest

The authors do not report any financial or personal connections with other persons or organizations, which might negatively affect the contents of this publication and/or claim authorship rights to this publication.

Literature

Abba D, Inabo HI, Yakubu SE, Olonitola OS. Contamination of herbal medicinal products marketed in Kaduna metropolis with selected pathogenic bacteria. Afr J Trad Complement Altern Med. 2009;6(1):70–77. https://doi.org/10.4314/ajtcam.v6i1.57076

Agyeman-Duah E, Quaidoo EY, Mills-Robertson FC. Microbial quality of herbal powders in Ghana. Edorium J Microbiol. 2017; 3:10–17. https://doi.org/10.5348/m08-2017-7-oa-2

Akaki J, Morikawa T, Miyake S, Ninomiya K, Okada M, Tanabe G, Pongpiriyadacha Y, Yoshikawa M, Muraoka O. Evaluation of *Salacia* species as anti-diabetic natural resources based on quantitative analysis of eight sulphonium constituents: A new class of α-glucosidase inhibitors. Phytochem Anal. 2014;25(6):544–550. https://doi.org/10.1002/pca.2525

Alles S, Shrestha N, Ellsworth A, Rider A, Foti D, Knickerbocker J, Mozola M. Validation of the Soleris® yeast and mold test for semi-quantitative determination of yeast and mold in selected foods. Performance tested methods 040901. J AOAC Int. 2009;92(5):1396–1415. https://doi.org/10.1093/jaoac/92.5.1396

Alonzo V, Monforte MT, Tumino G, Ragusa S, Bisignano G. A note on the microbial contamination of medicinal plants. Pharmeuropa. 1994; 6(1):47–55.

ANVISA. Farmacopeia Brasileira, 5th ed., vol. 1. São Paulo (Brazil): Agência Nacional de Vigilância Sanitária; 2010. p. 546.

Bagnazari M, Mehdi S, Chandregowda MM, Prakash SH, Nagaraja G. Phyto-constituents, pharmacological properties and biotechnological approaches for conservation of the anti-diabetic functional food medicinal plant *Salacia:* A review note. Appl Food Biotechnol. 2017;4(1):1–10. https://doi.org/10.22037/afb.v4i1.14499

Blivet D. Electrical techniques. In: Batt CA, Tortorello ML, editors. Encyclopedia of Food Microbiology. Amsterdam (The Netherlands): Academic Press; 2014.

Brodowska A, Śmigielski K, Nowak A. Comparison of methods of herbs and spices decontamination. Chemik 2014;68(2):97–102.

Curda L, Svir'akov'a E. Food spoilage flora and total viable count. In: Batt CA, Tortorello ML, editors. Encyclopedia of Food Microbiology. Amsterdam (The Netherlands): Academic Press; 2014.

de Freitas Araújo MG, Bauab TM. Microbial quality of medicinal plant materials. In: Akyar I, editor. Latest research into quality control. London (UK): IntechOpen; 2012. p. 67–81. https://doi.org/10.5772/51072

de Medeiros PM, Ladio AH, Albuquerque UP. Patterns of medicinal plant use by inhabitants of Brazilian urban and rural areas: a macroscale investigation based on available literature. J Ethnopharmacol. 2013;150(2):729–746. https://doi.org/10.1016/j.jep.2013.09.026

de Sousa Lima CM, Fujishima MAT, de Paula Lima B, Mastroianni PC, Oliveira de Sousa FF, Oliveira da Silva J. Microbial contamination in herbal medicines: a serious health hazard to elderly consumers. BMC Complement Med Ther. 2020;20(1):17. https://doi.org/10.1186/s12906-019-2723-1

EDQM. European Pharmacopoeia 6.0. 5.1.4. Microbiological quality of pharmaceutical preparations. Strasbourg (France): European Directorate for the Quality of Medicines & HealthCare; 2007.

Famewo EB, Clarke AM, Afolayan AJ. Identification of bacterial contaminants in polyherbal medicines used for the treatment of tuberculosis in Amatole District of the Eastern Cape Province, South Africa, using rapid 16S rRNA technique. J Health Popul Nutr. 2016; 35:27. https://doi.org/10.1186/s41043-016-0064-y

Gupta PC, Garg N, Joshi P. Effect of gamma irradiation on the extraction yield and microbial contamination of medicinal plants. Internet J Food Saf. 2011;13:351–354.

Halls N. The microbiology of irradiation sterilization. Med Device Tech. 1992;3(6):37–45.

Hitokito H, Morozumi S, Wauke T, Sakai S, Kurata H. Fungal contamination and mycotoxin detection of powdered herbal drugs. Appl Environ Microbiol. 1978;36(2):252–256.

Homma T, Kageyama S, Nishikawa A, Nagata K. Anti-melanogenic activity of salacinol by inhibition of tyrosinase oligosaccharide processing. J Biochem. 2020;167(5):503–511. https://doi.org/10.1093/jb/mvz115

Idu M, Erhabor JO, Idele SO. Microbial load of some medicinal plants sold in local markets of Benin City, Nigeria. Int J Med Arom Plants. 2011;1(3):272–277.

IS 5401-1 (2012). Microbiology of food and animal feeding stuffs – horizontal method for the detection and enumeration of coliforms, Part 1: Colony count technique. New Delhi (India): Bureau of Indian Standards; 2012.

Kneifel W, Czech E, Kopp B. Microbial contamination of medicinal plants – A review. Planta Medica 2002;68(1):5–15. https://doi.org/10.1055/s-2002-20060

Kumar V, Chatterjee S, Variyar PS. Effect of gamma irradiation on the antioxidant activity of *Salacia reticulata*. Int J Trad Nat Med. 2015;5(1):15–22.

Limberg BJ, Johnstone K, Filloon T, Catrenich C. Performance equivalence and validation of the Soleris® automated system for quantitative microbial content testing using pure suspension cultures. J AOAC Int. 2016;99(5):1331–1337. https://doi.org/10.5740/jaoacint.16-0142

Mărgăritescu I, Wilrich P-Th. Determination of the relative level of detection of a qualitative microbiological measurement method with respect to a reference measurement method. J AOAC Int 2013; 96(5):1086–1091. https://doi.org/10.5740/jaoacint.12-377

Mozola M, Gray RL, Feldpausch J, Alles S, McDougal S, Montei C, Sarver R, Steiner B, Cooper C, Rice J. Validation of the Soleris® NF-TVC method for determination of total viable count in a variety of foods. J AOAC Int. 2013;96(2): 399–403. https://doi.org/10.5740/jaoacint.12-342

Oprea E, Tuchiluș C, Aprotosoaie AC, Cioancă O, Trifan A, Grădinariu V, Miron A, Hăncianu M. Assessment of the microbial load of some medicinal plants commonly used in Romania. Revista medico-chirurgicala a Societatii de Medici si Naturalisti din Iasi. 2015;119(1):267–272.

Padmanabhan S, Jadhav VR. Chemical decontamination process for herbal materials. Reference application Number: 202021035116. Patent Application Number TEMP/E-1/39097/2020-MUM.

Silindir M, Özer AY. Sterilization methods and the comparison of E-beam sterilization with Gamma radiation sterilization. FABAD J. Pharm. Sci. 2009;34(1):43–53.

USP. The United States Pharmacopeia. Rockville (USA): United States Pharmacopeial Convention; 2005.

USP. USP37-NF32 2014: U.S. Pharmacopeia National Formulary. Rockville (USA): United States Pharmacopeial Convention; 2014.

WHO. Quality control methods for medicinal plant materials. Geneva (Switzerland): World Health Organization; 1998.

Supplementary materials are available on the journal's website.

Polish Journal of Microbiology
2020, Vol. 69, No 4, 463–469
https://doi.org/10.33073/pjm-2020-050

ORIGINAL PAPER

The Incidence of Scabies and Head Lice and Their Associated Risk Factors among Displaced People in Cham Mishko Camp, Zakho City, Duhok Province, Iraq

MOHAMMAD I. ALBERFKANI[1]* and WIJDAN M.S. MERO[2]

[1] Zakho Technical Institute, Duhok Polytechnic, Zakho, Duhok, Iraq
[2] Department of Biology, Faculty of Science University of Zakho, Zakho, Duhok, Iraq

Submitted 7 September 2020, revised 4 November, accepted 4 November 2020

Abstract

This study was conducted to estimate the incidence and the effects of associated risk factors of scabies and head lice on displaced people in Cham Mishko camp, Zakho city, Duhok Province, Iraq. The study included 1300 internally displaced people (IDPs) who visited the dermatology clinic and health care center in Cham Mishko camp from January 2018 to December 2019. Participants' bio-information was collected on special questionnaire form after receiving permission from the camp's health authorities and verbal consent from the participants. Monthly weather data were collected from Duhok Directorate of Meteorology and Seismology. The total rate of ectoparasites was 81.2% (45% for scabies and 36.2% for head lice). Ages from 1–10, 21–30, and 31–40 years showed the highest rates with scabies (48.1%, 46.7% and 46.1%, respectively), while the highest rates of head pediculosis were at ages from 1–10 and 11–20 years (40% and 36.6%, respectively). Scabies rate was slightly higher in males than females (46.6% vs. 43.4%), while the rate of head pediculosis was significantly higher in females than males (58.2% vs. 13.9%). Families with more than ten people showed the highest rates of scabies and head pediculosis (49.5% and 74.5%). Scabies was more common in cold months than in summer while head pediculosis was more common in hot months. The number of scabies and head pediculosis cases increased by 123 and 85 cases, respectively, in 2019. It is inferred that the effects of scabies and head pediculosis in IDPs will be considerable, with a higher carriage rate than other studies in Iraq.

Key words: scabies, pediculosis, infestation, displacement, climate, Iraq

Introduction

Ectoparasites are the most prevalent parasites among displaced people and refugees. The most commonest parasites found on human skin are lice, and scabies mite, which can severely affect health in addition to annoyance, irritation, skin infection, and anemia (Yadav et al. 2017; Ali and Hama 2018; Bartosik et al. 2020). The rate of infection with these parasites is due to their direct transmission, as they can be transmitted by direct skin-to-skin contact for scabies, head-to-head contact for pediculosis, physical contact, or through contact with other objects such as combs, brushes, hair accessories, and other headgear (Albonico et al. 1999; Burkhart and Burkhart 2007). The family income, number of family members, or mother's education and occupation have a role in the prevalence of scabies and head pediculosis (Hay et al. 2013; Gharsan et al. 2016; Moradiasl et al. 2018). Both head pediculosis and Scabies are diseases of overcrowding and poverty rather than poor hygiene (Zayyid et al. 2010; Bhat et al. 2017; Alsamarai et al. 2017).

Scabies is considered as one of the most prevalent neglected ectoparasites caused by *Sarcoptes scabiei* var *hominis*, causing skin infestation with asymptomatic or present symptoms, progressing to secondary skin infections. Although scabies is not a notifiable disease, there are over 300 million scabies cases worldwide (Micali et al. 2016; Anderson and Strowd 2017). Scabies is highly contagious and can affect people of any age, sex, race, or cleanliness level. However, it is more common among those living or working in crowded conditions; even if a person had a scabies infestation before, a person could be reinfested when exposed to mites (Walker and Johnstone 2002). There are three clinical forms of scabies: persistent nodules, papulovesicular lesions, and crusted scabies. Individuals infested with scabies may be asymptomatic for up to 4–6 weeks, then

* Corresponding author: M.I. Alberfkani, Zakho Technical Institute, Duhok Polytechnic, Zakho, Duhok, Iraq,
e-mail: mohammad.said@dpu.edu.krd

symptoms of scabies may develop and include intense itching (pruritus), predominantly at night, as sensitization develops to the presence of mites, eggs, or their products such as feces (Chosidow 2000; Chouela et al. 2002). The formation of burrows in the skin surface of the fingers, wrist, penis, and feet is the most apparent sign of scabies. Burrows can appear linear, curved, or S-shaped, 15 mm long, and 2 mm wide (Burgess 2002; Gunning et al. 2012). Extreme scratching of the infested skin may make the body vulnerable to secondary bacterial infection such as impetigo caused by *Streptococcus pyogenes* or *Staphylococcus aureus* (Zayyid et al. 2010; WHO 2015; Bhat et al. 2017). Scabies is more prevalent in urban areas, among women and children, and is more common in winter than summer (Farhana et al. 2018).

Head lice infestation is caused by sucking lice known as *Pediculus humanus capitis*, which infest people of any race, gender, or socioeconomic status. Children ages 5–12 years were most vulnerable for head lice infestation, including refugees, migrants, and internally displaced children and considered as public health problems worldwide (Nazari et al. 2006). Head lice infestation may lead to annoyance, pruritus, sleeplessness, and (in extreme cases) anemia (Frankowski et al. 2002). Head lice can live for around one month on their host. The life cycle of head lice is short (17–18 days). Female louse consumes the blood and lays 6–10 eggs per day, which attach to hair close to the skin's surface and behind the neck and ears. They require an optimal temperature of 28–30°C and humidity of 70–90% for survival. Scalp pruritus is the chief complaint in patients with head lice. Itchy papules may develop as a result of hypersensitivity reaction against the injected saliva of lice during blood-feeding (Miller 2002). A tickling feeling and irritability are other common symptoms of head lice infestation; also, secondary bacterial infection may develop due to the scratching of sores on the scalp (Roberts 2002).

Experimental

Materials and Methods

Study area and sample collection. This study was conducted in a dermatology clinic and health care center at Cham Mishko camp started from January 2018 to December 2019. The distribution of internally displaced people (IDPs) in the Kurdistan region of Iraq was around 1.2 million in 38 camps. Cham Mishko camp is one of the biggest United Nations High Commissioner for Refugees (UNHCR) camps in Zakho city, Duhok province, Kurdistan region, Iraq. This camp was established in 2014 for displaced people during the conflict against the so-called Islamic State of Iraq and Syria (ISIS) and inhabited by 26,478 individuals of internally displaced people (IDPs) comprising more than 5,000 families living in 4,993 shelters (tents), the average number of family members is six persons. The camp located 10 kilometers north of the Zakho city is provided with two nursery schools, three primary and two secondary schools, which were established especially for IDPs residences. Hence, students cannot get access to schools outside camps, while adult IDPs can freely access the institutes and the city's university.

A total of 1,300 individuals were included in the study that complaining of skin problems and head pediculosis who attended the dermatology clinic and health care center at Cham Mishko camp for investigation and treatment. During the interviews, each participant was inspected for head lice and scabies infestation by direct visual examination and microscopic examination. Head lice infestation was checked by careful visual examination of the entire head (neck, ears, and hair), and positive infestion was classified with the presence of at least one development stage (egg, nymph, and adult) of *Pediculus humanus capitis,* including nits' residues, which can be seen by necked eye. To check scabies infestation, skin scraping specimens were taken from individuals with clinically suspicious lesions, and all specimens were examined microscopically, mixed with two drops of 10% potassium hydroxide to digest the cornified skin and were examined at low magnification to observe mites and eggs (Alasaad et al. 2009). Demographic data was collected from the enrolled persons using a questionnaire that included several potential risk factors, including age, gender, and family size.

Statistical analysis. SPSS version 25 software was used to analyze the collected data, represented as numbers and percentages, calculated with a confidence interval of 95%. *Chi*-squared (X^2) test was used. *P*-value ≤ 0.05 was considered significant, and more than that was considered non-significant.

Ethical approval. Ethical approval for this study was obtained from the Board of Relief and Humanitarian Affairs (BRHA).

Results

Out of 1,300 individuals complaining of dermatological problems that visited the health care and dermatological center in Cham Mishko camp over two years, 81.2% (1,056/1,300) of them were infested with ectoparasites, 45% (585/1,300) patients were infested with scabies, including 284 females and 301 males; but this difference was statistically non-significant ($p = 0.251$) difference between both genders. On the other hand, 36.2% (471/1,300) patients were infested with head lice, of which 90 were males, and 381 were

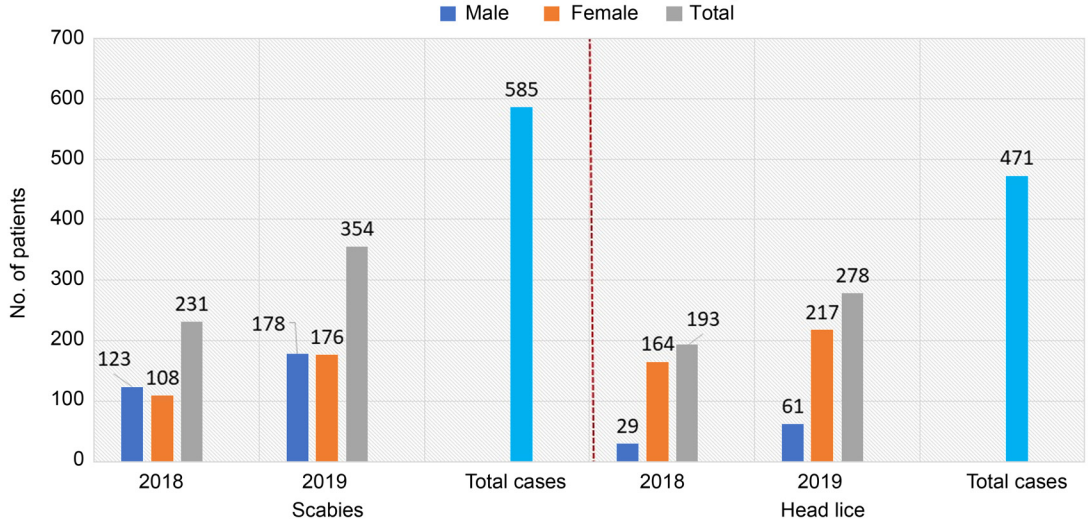

Fig. 1. Number of scabies and head lice cases related to gender in Cham Mishko camp during 2018 and 2019.

females, with a statistically significant ($p < 0.05$) difference between both genders as shown in Fig. 1. Furthermore, the number of scabies and head lice cases increased from 231 and 193 in 2018 to 354 and 278 in 2019, respectively (Fig. 1.)

Table I shows the incidence rate of scabies among participants (IDPs in the UNHCR Cham Mishko camp). Among infested, children aged 1–10 years displayed the highest rate (48.1%), followed by the 21–30 age group (46.7%). Males (46.6%) had a slightly higher rate than females (43.4%). The rates were compared between different age groups, and there was a significantly higher rate of scabies in the age groups (1–10 years) ($p = 0.018$). Similarly, rates were also compared according to a number of family members, and there was a significantly higher rate of scabies in families with more than ten people ($p = 0.023$).

Table II shows the number and percentage of head lice among both genders and different ages. The incidence of head lice among females was higher four times (58.2%) than in males (13.9%). Children aged 1–10 years had the highest infestation rate (40%), and it was more common among girls, followed by the age group 11–20 years (36.6%). The age group, 1–10 years, showed a significantly ($p = 0.033$) higher infestation rate with head lice than other ages. Similarly, when rates were compared with the number of family members, families with more than ten people had a significantly higher head lice rate ($p < 0.05$). Fig. 2 shows the seasonal variation of scabies and pediculosis during 2018

Table I
Prevalence of scabies infestation among 1300 IDPs.

Variables		Scabies infestation		
		Number of infestation/ totals	%	*p*-value
Gender	Male	301/646	46.6	0.251
	Female	284/654	43.4	
Age (years)	1–10	325/675	48.1	0.018
	11– 20	41/101	40.6	
	21–30	35/75	46.7	
	31–40	60/130	46.1	
	41–50	80/180	44.4	
	50^{+}	44/139	31.6	
Family members	1–5	216/533	40.5	0.023
	6–10	260/547	47.5	
	10^{+}	109/220	49.5	
Total		585/1300	45	

Table II
Prevalence of head pediculosis in 1300 IDPs.

Variables		Head pediculosis infestation		
		Number of infestation/ totals	%	*p*-value
Gender	Male	90/646	13.9	0.000
	Female	381/654	58.2	
Age (years)	1–10	270/675	40	0.033
	11–20	37/101	36.6	
	21–30	24/75	32	
	31–40	34/130	26.1	
	41–50	57/180	31.6	
	50^{+}	49/139	35.2	
Family members	1–5	109/533	20.4	0.000
	6–10	198/547	36.1	
	10^{+}	164/220	74.5	
Total		471/1300	36.2	

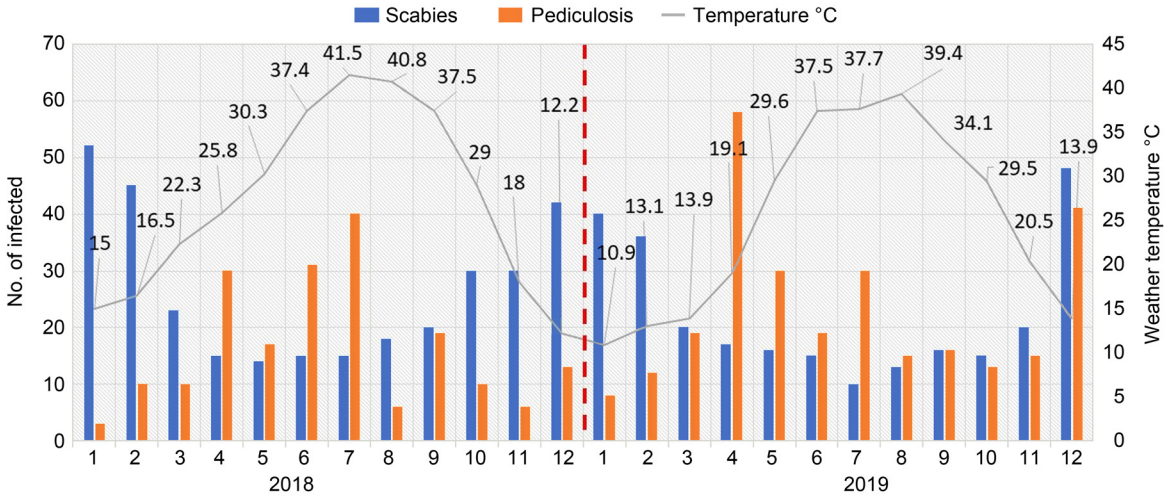

Fig. 2. Seasonal variation of scabies and pediculosis among IDP in Cham Mishko camp in 2018 and 2019 in relation to weather conditions.

and 2019. The results showed a much higher number of scabies cases in winter than in summer. Regarding head pediculosis, when the mean monthly temperature increased, especially in summer, the number of cases increased dramatically, while a low number of cases were recorded in winter.

Discussion

This study showed that the incidence of scabies was higher among children and males, as shown in Table I, due to the closer physical contact among children, particularly within large family units, which facilitates the transmission and explains different rates relative to age and sex indirectly for the spread of scabies. Besides spreading scabies through close direct skin-to-skin contact, infested persons can transmit scabies indirectly by sharing contaminated items with mites such as clothing, bedding, bed linens, furniture, shared hats, and head coverings (Liu et al. 2016; Korycińska et al. 2020). High rate of scabies recorded in males may be due to their intensive social lifestyle in the community as they work outside their households for long period which increased the chance for exposure to potential mite sources (Otero et al. 2004; Hengge et al. 2006; Ursani and Baloch 2009).

In Iraq, many refugees and displaced camps settings are in remote areas in places that are off the way or considerably secluded from cities and Cham Mishko camp is one of these camps located outside Zakho city. Hence, students of IDPs often cannot get access to schools outside camps for reasons of security, lack of documentation, and other restrictions. Therefore, they are obliged to attend two preschools, three primary and two secondary schools located in the camp; hence they become more crowded, leading to an increase in the chances of transmitting infestation between them. Furthermore, household crowding conditions and poor personal hygiene make IDPs more prone to infestion with scabies, including continuously sharing infested items such as clothes and bed linen.

The prevalence of ectoparasites among people living in displaced camps has been investigated on a limited scale in the Kurdistan region in general and Zakho city in particular. Few studies have been conducted in Duhok city on the prevalence of ectoparasites among internal displacement people living in Camps. Barwari (2016) reported a rate of 4.5% of scabies among people living in 35 camps, while the much higher rate was reported by Hassan and Mero (2020), a rate of 10% (395/3,925) for scabies and 7% (277/3,925) for pediculosis among internally displaced people living in five camps around the city of Duhok, Kurdistan, Iraq. The overall rate of scabies was 45%, which was higher than the rates reported in previous studies among various populations (Mahmood 2011; Ibrahim et al. 2012; Mero and Hassan 2014; Barwari 2016).

Regarding head pediculosis, the general rate of head lice (36.2%) was similar to that reported in previous studies (Banaz 2015; Khidhir et al. 2017; Ali and Hama 2018). A prevalence rate of 1.2% was reported in the Sulaimani Governorate, Kurdistan Region, Iraq, among refugees and displaced people (Ali and Hama 2018). On the other hand, a very high rate (42.7%) was reported among displaced secondary school girls in Kirkuk city, Iraq (Kadir et al. 2017). Girls, mothers, and children often have closer physical contact, facilitating transmission, and explaining why these groups have a higher incidence relative to males. Other head lice studies have illustrated an association with female sex, overcrowding, and other infested family members (Kokturk et al.

2003; Bauer et al. 2009; Magalhães et al. 2011). There is only one study in Zakho about the prevalence of scabies among displaced people living in the Bersifi1, Bersifi2, and Cham Mishko camps, in which a rate of 6.1% was reported (Choli 2017). It was much lower than the rate recorded in the present study because during 2018, there was less supporting and funding from the UN Refugee Agency (UNHCR) to IDPs camps, hence less organization of public-awareness campaigns among IDPs, and limited quantities of drugs were provided against such neglected parasitic diseases.

Lice infestation was more common in children due to direct contact, environmental conditions, poor personal hygiene, and the continuous sharing of hair combs and other hair items. Girls have the highest rate of infestation, because they have longer and thicker hair, which provides an optimal environment for the growth and occurrence of head lice; furthermore, girls more likely spend their time in close play areas, and engaging during play in more head-to-head contact. Head lice also flourish indoors, while boys tend to spend more time engaged in active informal sporting activities outdoors (Zayyid et al. 2010). The large population of IDPs in Cham Mishko camp facilitates more close contact among family members, increasing the chance of infestation Mother-to-child head lice transmission is expected due to close body contact, facilitating the spread of lice and reflecting why these groups have a higher occurrence than males. Other survey studies have demonstrated the relation of head lice with sex, overcrowding, and many family members (Mumcuoglu et al. 2001; Frankowski et al. 2002; Ko and Elston 2004; Takano et al. 2005).

Lower rates of scabies infestation were recorded in hot months (May, June, and July), while cold weather in November, December, and January was associated with a higher incidence of scabies. It may enhance overcrowding, which is conducive to scabies mite transmission, in addition to wearing heavy clothes in winter may maintain mite survival and transmission, also changes in host behavior may facilitate transmission, due to people gathering indoors, increasing overcrowding in cold weather (Chosidow 2000; Heukelbach and Hermann 2006). This explains the higher incidence of infection during cold weather, coupled with inadequate and poorly designed ventilation in crowded public places, and people have a tendency to share small spaces which promotes personal contacts beside that during the winter season may also be influenced by greater sexual activity (Savin 2005; Korycińska et al. 2020). In summer, the incidence of scabies in children was lower due to less physical contact and overcrowding during the summer. The difference in the incidence of scabies in this study compared to other similar studies carried out in the middle and southern parts of Iraq may be due to differences in the weather temperature; since the north is relatively cooler, resulting in prolonged mite survival, in addition to the significant number of IDPs in the north of Iraq (Alsamarai 2009; Ibrahim et al. 2012; Mohy et al. 2018). Cham Mishko camp is located in the north of Zakho city, where the ratio of relative humidity is higher in the spring season (65%), which indicated that humid environments might result in higher rates of scabies infestations. The essential element in transmitting scabies is the mite's ability to survive and keep infectivity in the external environment. Therefore, a high humidity ratio associated with low-temperature results in a longer survival time of scabies outside the host body (Liu et al. 2016; Korycińska et al. 2020)

Regarding the effect of seasonal variation of weather temperature on head lice, although lice infestation exists throughout all months of the year at different rates, it increases in hot months. There is a significant association between seasonal variation and head lice infestation among IDPs. April 2019 was the highest month for infestations (58 patients), and January 2018 was the lowest (3 patients only). In hot months (April, May, June, and July), most head lice infestation cases were recorded. Children tend to play together more in the warm weather, creating a greater chance for the transmission of head lice from head-to-head. Lice can lay more eggs and reproduce more rapidly in warm weather, too, so head lice cases are more common at this time of the year compared to the winter months (Liu et al. 2016; Korycińska et al. 2020). During the summer months, especially in the summer holidays (June, July, and August), children have more frequent head-to-head contact than at other periods of the year. In addition, children and their families may travel outside Cham Mishko camp and visit their relatives in other refugee campuses outside Zakho city, who may be infested with head lice. All of these factors led to increased exposure to other people, building up a reservoir of lice infestation, and when schools open after the summer holidays (which in Iraq happens between September and October), head lice are transferred from an enlarged reservoir to classmates, playmates, and siblings. Therefore, when schools are open, there is increased awareness, rapid diagnosis, and appropriate treatment; hence the transmission of head lice will decrease to low levels during late Autumn and remain at a low level for the remaining period of the year.

Concerning head lice, no previous studies are dealing with this parasite's prevalence; this reason encouraged us to adopt this study to explore the distribution of these parasites among displaced people living in Cham Mishko camp and correlate the subsequent data with specific demographic factors. The incidence of scabies and head lice in the IDP camps in Iraq is still high.

Hence, screening and treatment for scabies and head lice among displaced people need to be carried out frequently to reduce infestation rates. The older adults and children should well know the health education concerning the modes of transmission of head lice and scabies and their prevention. It is essential to organize public-awareness campaigns to raise the campus's awareness and strongly emphasize the IDPs to avoid sharing personal belongings such as hair combs to prevent head lice infestation and stop sharing infested clothes and linens to prevent scabies transmission.

Conclusions

Scabies and head lice are still considered the most critical public health problems in developing countries, especially among displaced communities with social and psychological impact. The incidence of scabies infestation is high in males while head lice are higher in children and young women. Scabies is prevalent in cold months while pediculosis in hot months. Therefore, it is still a significant health problem in Iraq as a neglected disease, and it can be reduced by improving social health education and hygienic conditions and promoting more efficient health services.

Conflict of interest

The authors do not report any financial or personal connections with other persons or organizations, which might negatively affect the contents of this publication and/or claim authorship rights to this publication.

Literature

Alasaad S, Rossi L, Soriguer RC, Rambozzi L, Soglia D, Pérez JM, Zhu XQ. Sarcoptes mite from collection to DNA extraction: the lost realm of the neglected parasite. Parasitol Res. 2009;104:723–732. https://doi.org/10.1007/s00436-009-1333-0

Albonico M, Stoltzfus RJ, SavioliL, Chwaya HM, D'Harcourt E, Tielsch JM. A controlled evaluation of two school based anthelminthic chemotherapy regimens on intensity of intestinal helminth infections. Int J Epidemiol.1999;28(3):591–596. https://doi.org/10.1093/ije/28.3.591

Ali FM, Hama AA. Prevalence of head pediculosis among refugees in Sulaimani Governorate/Kurdistan-Iraq. Iraqi J Sci. 2018; 59(2C): 1012–1018. https://doi.org/10.24996/ijs.2018.59.2c.4

Alsamarai AM, Alobaidi AHA. Scabies in displaced families: Health care problem that need urgent action. Our Dermatol Online. 2017; 8(3):250–254. https://doi.org/10.7241/ourd.20173.73

Alsamarai AM. Frequency of scabies in Iraq: survey in a dermatology clinic. J Infect Dev Ctries. 2009;3(10):789-793. https://doi.org/10.3855/jidc.144

Anderson KL, Strowd LC. Epidemiology, diagnosis, and treatment of scabies in a dermatology office. J Am Board Fam Med. 2017;30(1): 78–84. https://doi.org/10.3122/jabfm.2017.01.160190

Banaz SA. Morphological study and prevalence of head lice (*Pediculus humanus capitis*) (Anoplura: Pediculidae) infestation among some primary school students in Erbil City, Kurdistan region. Zanco J Pure Appl Sci. 2015;27(5):29–36.

Bartosik K, Tytuła A, Zając Z, Buczek W, Jasztal-Kniażuk A, Błaszkiewicz PS, Borzęcki A. Scabies and Pediculosis in Penitentiary Institutions in Poland – A study of ectoparasites in confinement conditions. Int J Environ Res Public Health. 2020;17(17):6086. https://doi.org/10.3390/ijerph17176086

Barwari WJO. Prevalence of scabies among refugees in camps of Duhok Province, Kurdistan region, Iraq. Duhok Med J. 2016;10(2): 109–116.

Bauer E, Jahnke C, Feldmeier H. Seasonal fluctuations of head lice infestation in Germany. Parasitol Res. 2009;104:677–681. https://doi.org/10.1007/s00436-008-1245-4

Bhat SA, Mounsey KE, Liu X, Walton SF. Host immune responses to the itch mite, *Sarcoptes scabiei*, in humans. Parasites Vectors. 2017; 10(1):385. https://doi.org/10.1186/s13071-017-2320-4

Burgess I. The life of a head louse. Nurs Times. 2002;98(46):54.

Burkhart CN, Burkhart CG. Fomite transmission in head lice. J Am Acad Dermatol. 2007;56(6):1044–1047. https://doi.org/10.1016/j.jaad.2006.10.979

Choli RR. The Prevalence of human scabies and its correlation with some factors in Zakho District/Duhok Province/Kurdistan Region/ Iraq [dissertation]. Zakho (Iraq): University of Zakho; 2017.

Chosidow O. Scabies and pediculosis. Lancet. 2000;355:819–826. https://doi.org/10.1016/S0140-6736(99)09458-1

Chouela E, Abeldaño A, Pellerano G, Hernández MI. Diagnosis and treatment of scabies: a practical guide. Am J Clin Dermatol. 2002;3(1):9–18. https://doi.org/10.2165/00128071-200203010-00002

Farhana RC, Khalid H, Shumaila N, Dilwar AM, Paolotizzani, Abbas R, Luca R. Scabies prevalence and risk factors in Pakistan: A hospital based survey. Biomed J Sci Tech Res. 2018;2(2): 2498–2502. https://doi.org/10.26717/bjstr.2018.02.000726

Frankowski BL, Weiner LB, Committee on School Health and Committee on Infectious Diseases. Head lice. Pediatrics. 2002; 110(3):638–643.

Gharsan FN, Abdelhamed NF, Elhassan SAM, Gubara NGA. The prevalence of infection with head lice *Pediculus humanus capitis* among elementary girl students in Albaha region – Kingdom of Saudi Arabia. Int J Res Dermatol. 2016;2:12–17. https://doi.org/10.18203/issn.2455-4529.IntJResDermatol20161426

Gunning K, Pippitt K, Kiraly B, Sayler M. Pediculosis and scabies: treatment update. Am Fam Physician. 2012;86(6):535–541.

Hassan AO, Mero WMS. The Prevalence of ectoparasites among displaced people living in displacement camps: Duhok Province Iraqi Kurdistan. Int J Psychosoc Rehabilitation. 2020;24(4):7897–7905. https://doi.org/10.37200/ijpr/v24i4/pr2020739

Hay RJ, Steer AC, Chosidow O, Currie BJ. Scabies: A suitable case for a global control initiative. Current Opinion in Infectious Diseases.2013;26(2):107–109. https://doi.org/10.1097/QCO.0b013e32835e085b

Hengge UR, Currie BJ, Jäger G, Lupi O, Schwartz RA. Scabies: a ubiquitous neglected skin disease. Lancet Infect Dis. 2006 Dec; 6(12):769–779. https://doi.org/10.1016/S1473-3099(06)70654-5

Heukelbach J, Hermann F. Scabies. Lancet. 2006 May 27;367(9524): 1767–1774. https://doi.org/10.1016/S0140-6736(06)68772-2

Ibrahim KK, Ali AI, Mohammad B. Clinical usefulness of IgE as a serological marker for diagnosis of nodular scabies in Diyala Province. Diyala J Med. 2012;2:60–65.

Kadir MA-A, Taher HM, Ali IS. Head lice infestation among local and displaced secondary school girls and its effect on some haematological parameters in Kirkuk city. Kirkuk Univ J Sci Stud. 2017;12(2):286–296.

Khidhir KN, Mahmood CK, Ali WK. Prevalence of infestation with head lice *Pediculus humanus capitis* (De Geer) in primary schoolchildren in the centre of Erbil city, Kurdistan region, Iraq Pak Ent. 2017;39(2):1–4.

Ko CJ, Elston D M, Pediculosis. J Am Acad Dermatol. 2004;50(1): 1–12.

Kokturk A, Baz K, Bugdayci R, Sasmaz T, Tursen U, Kaya TI, Ikizoglu G. The prevalence of pediculosis capitis in schoolchildren in Mersin, Turkey. Int J Dermatol. 2003;42:694–698.

Korycińska J, Dzika E, Kloch M. Epidemiology of scabies in relation to socio-economic and selected climatic factors in north-east Poland. Ann Agric Environ Med. 2020;27(3):374–378. https://doi.org/10.26444/aaem/109319

Liu JM, Wang HW, Chang FW, Liu YP, Chiu FH, Lin YC, Cheng KC, Hsu RJ. The effects of climate factors on scabies. A 14-year population-based study in Taiwan. Parasite. 2016;23:54. https://doi.org/10.1051/parasite/2016065

Magalhães P, Figueiredo EV, Capingana DP. Head Lice Among Primary School Children in Viana, Angola: Prevalence and Relevant Teachers' Knowledge. Hum Parasitic Dis. 2011;3:11–18. https://doi.org/10.4137/hpd.s6970

Mahmood SS. Epidemiology profile of Scabies in Duhok [dissertation]. Iraq (Duhok): College University of Duhok; 2011.

Mero WMS, Hassan HK. Incidence of Human Scabies in Duhok Province, Kurdistan Region/ Iraq. J Univ Zakho. 2014;2(2);285–292.

Micali G, Lacarrubba F, Verzì AE, Chosidow O, Schwartz RA. Scabies: Advances in Noninvasive Diagnosis. PLoS Negl Trop Dis. 2016;10(6):e0004691. https://doi.org/10.1371/journal.pntd.0004691

Miller PF. Parasitic infections. In: Repchinsky C, editor. Patient self-care (PSC): Helping patients make therapeutic choices. 1st ed. Ottawa (Canada): Canadian Pharmacists Association; 2002. p. 592–621.

Mohy AA, Al-Hadraawy SK, Aljanaby AAJ, Epidemiological study of patients infected with scabies caused by *Sarcoptes scabiei* in Al-Najaf Governorate, Iraq. Biomed Res. 2018;29(12):2650–2654. https://doi.org/10.4066/biomedicalresearch.29-18-652

Moradiasl E, Habibzadeh S, Rafinejad J, Abazari M, Ahari SS, Saghafipour A, Edalatkhah H. Risk factors associated with head lice (pediculosis) infestation among elementary school students in Meshkinshahr County, North West of Iran. Int J Pediatr. 2018; 6(3): 7383–7392. https://doi.org/10.22038/IJP.2018.27961.2420

Mumcuoglu KY, Friger M, Ioffe-Uspensky I, Ben-Ishai F, Miller J. Louse comb versus direct visual examination for the diagnosis of head louse infestations. Pediatr Dermatol. 2001;18(1):9–12. https://doi.org/10.1046/j.1525-1470.2001.018001009.x

Nazari M, Fakoorziba MR, Shobeiri F. *Pediculus capitis* infestation according to sex and social factors in Hamedan, Iran. Southeast Asian J Trop Med Public Health. 2006;37(3):95–98.

Otero L, Varela JA, Espinosa E. *Sarcoptes scabiei* in a sexually transmitted infections unit: a 15-year study. Sex Transm Infect. 2004; 31:761–765.

Roberts RJ. Head lice. N Engl J Med. 2002;346:1645–1650.

Savin JA. Scabies in Edinburgh from 1815 to 2000. J R Soc Med. 2005;98(3):124–129.

Takano-Lee M, Edman JD, Mullens BA, Clark JM. Transmission potential of the human head louse, *Pediculus capitis* (Anoplura: Pediculidae). Int J Dermatol. 2005;44(10):811–816. https://doi.org/10.1111/j.1365-4632.2005.02418.x

Ursani NM, Baloch GH. Scabies epidemic at Tando Muhammad Khan, Sindh. J. Pakistan Assoc. Dermatologists. 2009;19:86–89.

Walker G, Johnstone P. Scabies. Clin Evid. 2002;7:1543–1548.

WHO. Investing to overcome the global impact of neglected tropical diseases: third WHO report on neglected tropical diseases. Geneva (Switzerland): World Health Organization; 2015.

Yadav PK, Rafiqi SI, Panigrahi PN, Kumar D, Kumar R, Kumar S. Recent trends in control of ectoparasites: A review. J Entomol Zool Stud. 2017;5:808–813.

Zayyid MM, Saadah SR, Adil AR, Rohela M, Jamaiah I. Prevalence of scabies and head lice among children in a welfare home in Pulau Pinang, Malaysia. Trop Biomed. 2010;27(3):442–446.

Polish Journal of Microbiology
2020, Vol. 69, No 4, 471–478
https://doi.org/10.33073/pjm-2020-051

ORIGINAL PAPER

Identification and Characterization of a Novel Recombinant Porcine Astrovirus from Pigs in Anhui, China

XU CHEN[1], YUMIN HE[1], WEINA LI[2], ULLAH KALIM[1], YUQING XIAO[1], JIE YANG[1], XIAOCHUN WANG[1], SHIXING YANG[1]* and WEN ZHANG[1]*

[1] Department of Microbiology, School of Medicine, Jiangsu University, Zhenjiang, China
[2] Pharmacy Department, People's Hospital of Rizhao, Rizhao, China

Submitted 13 September 2020, revised 17 October 2020, accepted 9 November 2020

Abstract

Porcine astroviruses (PAstVs) have wide distribution in swine herds worldwide. At present, five porcine astrovirus genotypes have been identified. In this study, using viral metagenomics, a novel PAstV strain (designated as Ahast) was identified in fecal samples from pigs in Anhui of China, and the complete genomic sequence of Ahast was obtained by assembling and PCR amplification. Genomic structural analysis indicated that Ahast had a typical ribosomal frameshifting signal, and some conserve amino acid motifs were also found in virally encoded proteins. Phylogenetic analysis and sequence comparison indicated that this virus belonged to porcine astrovirus genotype 4 (PAstV4), which formed a clade clustered with other PAstV4. Multiple recombinant events were confirmed by recombination analysis and indicated that Ahast was a potential recombinant. Epidemiological investigation indicated that PAstV4 has a 10.7% prevalence in this pig farm. The new recombinant identified in this study will be beneficial to comprehend the origin, genetic diversity, and evolution of porcine astroviruses in Anhui of China.

Key words: porcine astroviruses, viral metagenomics, genome recombination

Introduction

Astroviruses belong to the family *Astroviridae*. The virions are small, about 28–30 nm in diameter, non-enveloped, and contain a +ssRNA genome about 6.4–7.7 kb in length (Rivera et al. 2010). The family *Astroviridae* is divided into two genera, *Mamastrovirus* (19 species) and *Avastrovirus* (3 species) (De Benedictis et al. 2011). Members of the genus *Mamastrovirus* infect mammals, including human (Vu et al. 2017), bovine (Bouzalas et al. 2014), feline (Yi et al. 2018), porcine (Arruda et al. 2017), mink (Blomstrom et al. 2010), but members of the genus *Avastrovirus* mainly infect birds such as chicken, turkey, and duck (Bidin et al. 2012a; Bidin et al. 2012b; Sajewicz-Krukowska and Domanska-Blicharz 2016). Infection with Avastroviruses often involves intestinal or extra-intestinal manifestations, while gastroenteritis is the predominant feature of infecting Mamastroviruses.

Porcine astroviruses (PAstVs) belong to the *Mamastrovirus* genus. PAstV was first identified from the feces sample of diarrheal pigs in 1980 using electron microscopy (Bridger 1980). At present, five genotypes of PAstVs were identified (Brnic et al. 2014). The genome of PAstV encodes for three open reading frames (ORF) including ORF1a, ORF1b, and ORF2 (Bosch et al. 2011). The non-structural proteins and an RNA-dependent RNA polymerase (RdRp) were encoded by ORF1a and ORF1b separately, while ORF2 encodes for the viral capsid structural proteins (De Benedictis et al. 2011). PAstVs have been detected in the intestines and faeces of pigs and are responsible for gastrointestinal disorders, mainly in young individuals. However, some porcine astroviruses infections have been described in sick pigs with extra-intestinal manifestations, including respiratory and neurological signs (Padmanabhan and Hause 2016). Additionally, porcine astroviruses still have been detected in clinically healthy pigs

* Corresponding authors: W. Zhang, Department of Microbiology, School of Medicine, Jiangsu University, Zhenjiang, China; **e-mail: z0216wen@yahoo.com**
S. Yang, Department of Microbiology, School of Medicine, Jiangsu University, Zhenjiang, China; **e-mail: 1000004113@ujs.edu.cn**

(Lv et al. 2019). The exact relationship between PAstV and diseases is unclear.

In the present study, using the viral metagenomics method, we obtained one novel PAstV4 from pig feces samples collected in Anhui province, China. Further, the complete genome was obtained and analysed for genetic evolution and recombination. The epidemiological investigation indicated that a comparable lower prevalence (10.7%) of PAstV4 in this pig farm of Anhui province.

Experimental

Materials and Methods

Sample collection. In 2018, 215 pig feces samples were collected from a pig farm in Anhui province of China, using disposable 1.5 ml Eppendorf (EP) tubes and shipped on dry ice. Each sample was resuspended in 1 ml of phosphate-buffered saline (PBS), then violently vortex for 10 min. After centrifugation at 12,000 × g for 10 min, the supernatants were collected and were stored at −80°C for the following research.

Viral metagenomic analysis. Twenty feces supernatants were randomly chosen to generate one pool. Aspirating 25 μl supernatants per sample and the total 500 μl mixed supernatant was firstly filtered via a 0.45 μm filter (Millipore) to remove bacteria and eukaryotes. Then, the viral particle enrichment filtrate was treated with DNase and RNase to digest free non-viral nucleic acid at 37°C for 60 min and mix once halfway (Zhang et al. 2016). According to the manufacturer's protocol, the total nucleic acid was extracted using QiaAmp Mini Viral RNA kit (Qiagen). cDNA of viral RNA was synthesized by reverse transcription with six random base primers, then the Klenow enzyme was used to generate the complementary chain of cDNA. Construction of cDNA libraries was done using Nextera XT DNA Sample Preparation Kit (Illumina), and 250 bases paired ends were sequenced using the MiSeq Illumina platform (Ling et al. 2019). The sequenced reads were debarcoded using vendor software (Illumina). Using Phred quality score ten as the threshold, low sequencing quality tails were trimmed. Adaptors and primer sequences were trimmed using VecScreen software (Altschul et al. 1997). The cleaned reads were then de novo assembled by a combination of software including SOAPdenovo2, ABySS, meta-Velvet, and CAP3. The assembled contigs and singlet sequences were compared to the viral proteome database by BLASTx with an E-value cutoff of $< 10^{-5}$ (Deng et al. 2015).

Genomic acquisition and PCR screening. Using Geneious 11.1.2 software, the partial complete porcine astrovirus genome was assembled. Further, PCR primers were designed to amplify 5' terminal and 3' terminal sequences. The primer sequences used for amplification are shown in Table I. The amplification reactions were performed under the following conditions: 95°C for 5 min, 32 cycles of 95°C for 40 sec, 50°C (for the first round) or 55°C (for the second round) for 30 sec and 72°C for 1 min, a final extension at 72°C for 5 min (Zhao et al. 2019). Putative ORFs were analyzed using Geneious 11.1.2 software and ORF finder in NCBI. To investigate the prevalence of PAstV in pigs, a set of primers was designed based on the nucleotide sequences of Ahast ORF2 to perform PCR screening. Primers astWF and astWR were located at 4313–4333 nt and 4818–4799 nt respectively for the first round of PCR, while astNF and astNR were located at 4421–4440 nt and 4725–4706 nt respectively for the second round. The expected length of the amplified fragment is 305 bp.

Table I
Primers sequences used for screening and amplification for the complete genome of porcine astrovirus.

Primer ID	Application	Primer sequences (5'-3')
astWF astWR	First round	ATCACAGCAACCCTAGGCAC AGGTGCAGGTCATTTCAGCA
astNF astNR	Second round	TGCCTATGGTCCTCTCCAGA ATCCTGCAGTGCACATCTGT
5AstWF 5AstWR	First round	TGGTGGCTATGGCCCGTAGG TGCTGCCTCAAGTATGCACA
5AstNF 5AstNR	Second round	TGGTGGCTATGGCCCGTAGG TGGGCACAAATGGTTTGCTG
3AstWF 3AstWR	First round	GCCCCGATAATGCAGGATGA Oligo(dT)18
3AstNF 3AstNR	Second round	TATTGAAGCCTGGGATGCGG TTTTGCTCAAATTTTTAAATGC

Phylogenetic analysis. The ORF1b and ORF2 amino acid sequences of Ahast and the representative sequences obtained from GenBank were selected for phylogenetic analysis to classify this virus. All sequences were aligned using CLUSTAL X (version 2.1) with the default settings. The aligned result was saved as a Nexus form file for constructing the phylogenetic tree using Bayes' theorem in the Mrbayes 3.2.7 program (Liu et al. 2020). The Markov chain was run for a maximum of 1 million generations, in which every 50 generations were sampled, and the first 25% of Markov chain Monte Carlo (mcmc) samples were discarded as burn-in. Phylogenetic tree for recombination analysis were constructed using the Maximum Likelihood method in MEGA 5.0. Bootstrap values (based on 500 replicates) for each node were given.

Recombination analysis. To test whether this virus is a recombinant, the complete genome sequence of all 24 PAstV4 available in the GenBank database were downloaded, then aligned using the MUSCLE algo-

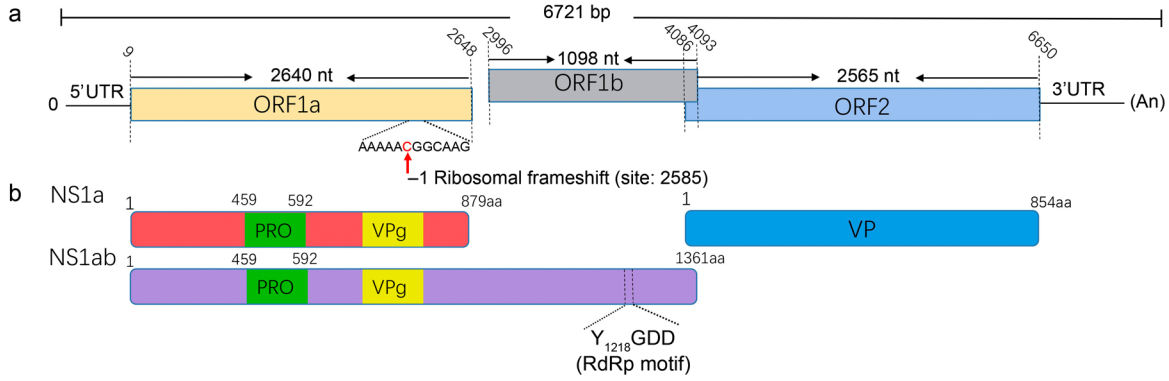

Fig. 1. Genomic structure and conserve amino acid motif of Ahast. (a) Genomic organization of Ahast. The three ORFs (ORF1a, ORF1b, and ORF2) are shown. The conserve ribosomal frameshift site is marked. (b) The conserve amino acid motif of Ahast. The viral encode polyproteins are marked with different colours, the conserve motif of protease (PRO), RNA-dependent RNA polymerse (RdRp), and genome-linked viral protein (VPg) are shown.

rithm in the MEGA-X program, together with this virus. The alignment results were manually check using Geneious 11.1.2 software. Using Recombination Detection Program 5.0 (RDP 5.0), the potential parental sequences and possible recombination sites were identified through eight different test methods, including RDP, Chimaera, MaxChi, SiSCan, GENECONV, BootScan, LARD, and 3Seq.

GenBank accession number. The two nearly complete genomic sequences of Ahast and Ahast-2 were submitted to the GenBank database under accession number MT470220 and MW082586. The raw sequence reads from the metagenomic library were deposited in the Sequence Read Archive of GenBank database under accession number: SRX9247601.

Results

The libraries from pig fecal samples that were sequenced on the MiSeq platform generated 2,476,530 unique sequence reads. Among them, 173,248 sequence reads were viral sequences. Putative mammalian viruses belong to the families *Picornaviridae* (60,763 reads), *Astroviridae* (34,279 reads), *Caliciviridae* (22,628 reads), *Picobirnaviridae* (17,569 reads), *Parvoviridae* (4,434 reads), *Coronaviridae* (2,273 reads), and *Circoviridae* (1,301 reads), etc. This study mainly focus on astrovirus.

Genomic structure. By assembling the 34,279 reads of astrovirus, two nearly complete genomes of PAstVs were obtained and named Ahast and Ahast-2, respectively. Further, two sets of primers were designed for amplifying the missing 5' and 3' termini sequences of the genome. The complete genome of Ahast is 6,721 bp in length, with the untranslated regions (UTRs) situated in positions 1–9 and 6651–6721. The base composition of A, G, T, and C is 30.23%, 22.38%, 25.17%, and 22.21%, respectively.

The viral genome of Ahast encodes three ORFs, including ORF1a, ORF1b, and ORF2. There is a 8 nt overlap between ORF1b and ORF2. The conserve Kozak sequences of RNNAUGG were identified near the start codon of both three ORFs (GCTATGG for ORF1a, AAAATGT for ORF1b, and CTAATGG for ORF2). A translational ribosomal frameshifting signal existed in the 3' end of Ahast ORF1a Fig. 1a. The Conserved Domains analysis (https://www.ncbi.nlm.nih.gov/Structure/cdd/wrpsb.cgi) indicated that Ahast NS1a has periplasmic serine protease domain at position 459–592 aa. A conserved RdRp amino acid motif (YGDD), was situated in the N termini of NS1ab. In addition, using online analysis of the FoldIndex software program (http://bip.weizm ann.ac.il/fldbin/findex), a genome-linked viral protein (VPg) with conserved KGKSK and TEEEY was identified (data not shown), at both ends of VPg, potent restriction sites of protease QKKK were found Fig. 1b.

Sequence comparison and phylogenetic analysis. To investigate the genetic relationships of Ahast, the phylogenetic analysis was performed based on the ORF1b and ORF2 amino acid sequences of the strain in this study, 24 PAstV4 reference strians available in the GenBank database, and other four genotypes reference strains of porcine astrovirus. The result showed that five PAstV genotypes were delineated in the ORF1b phylogenetic tree, the Ahast clustered with other 24 PAstV4 reference strains formed a clade Fig. 2, while genotypes in the ORF2 phylogenetic tree did not ultimately cluster PAstVs. PAstV4 was divided into three clades, respectively, Ahast clustered with KX060809, and the other six PAstV4 strains formed a distinct clade Fig. 3. Sequence analysis using Blastp in NCBI indicated that the ORF1b of Ahast shares the highest amino acid sequence identity (98.63%) with the strain PAstV4/CHN/WG-R2/2017 (MK460231), which was identified in an anal swab of pig from Jiangxi province of China.

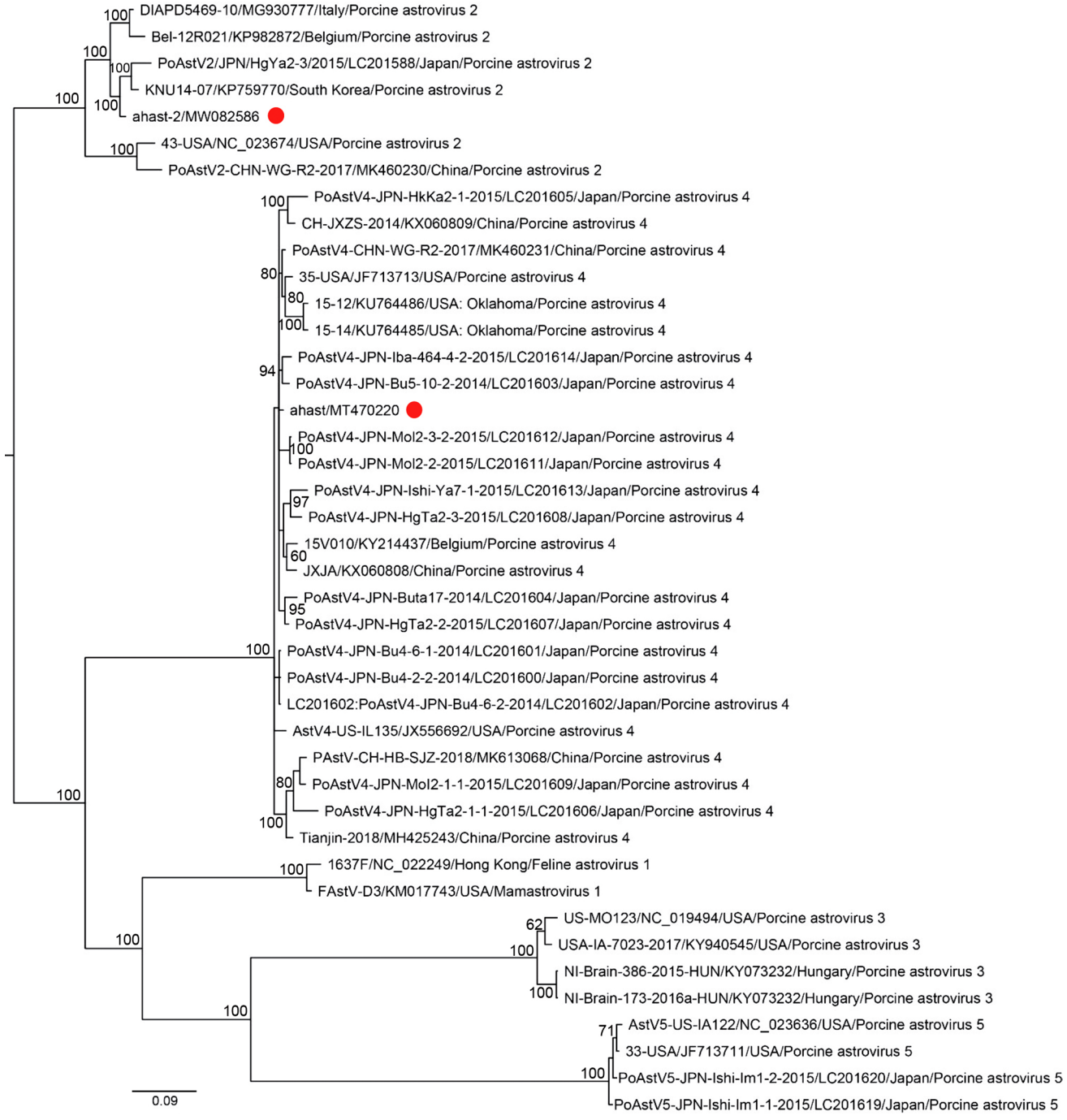

Fig. 2. Phylogenetic analysis of Ahast. Phylogenetic tree based on amino acid sequences of ORF1b of PAstVs. The tree was constructed using MrBayes 3.2.7 software and the average standard deviation of split frequencies were 0.005. The Markov chain was run for a maximum of 1 million generations, in which every 50 generations were sampled and the first 25% of Markov chain Monte Carlo (mcmc) samples were discarded as burn-in.The Ahast strain identified in this study is marked with red dot.

In contrast, the ORF2 of Ahast shares the highest amino acid sequence identity (68.81%) with the strain CH/JXZS/2014 (KX060809), which was found in the stool of sus scrofa from Hunan province of China. It implied that Ahast might be a recombinant.

Recombination analysis. To identify potential recombinant events in the Ahast genome, all 24 complete genome sequences of PAstV4, together with that of Ahast, were aligned using the MUSCLE algorithm in the MEGA-X program. Potential parental sequences and possible recombination sites were identified using RDP 5.0. The results showed that Ahast is a novel recombinant resulting from a few recombination events Fig. 4a. Among all those recombination events, two typical recombination events with a high degree of confidence (event 1 with p-value $= 3.77 \times 10^{-15}$, and event 2 with p-value $= 2.9 \times 10^{-31}$) in BootScan method were chosen to further manual bootscan analysis. In

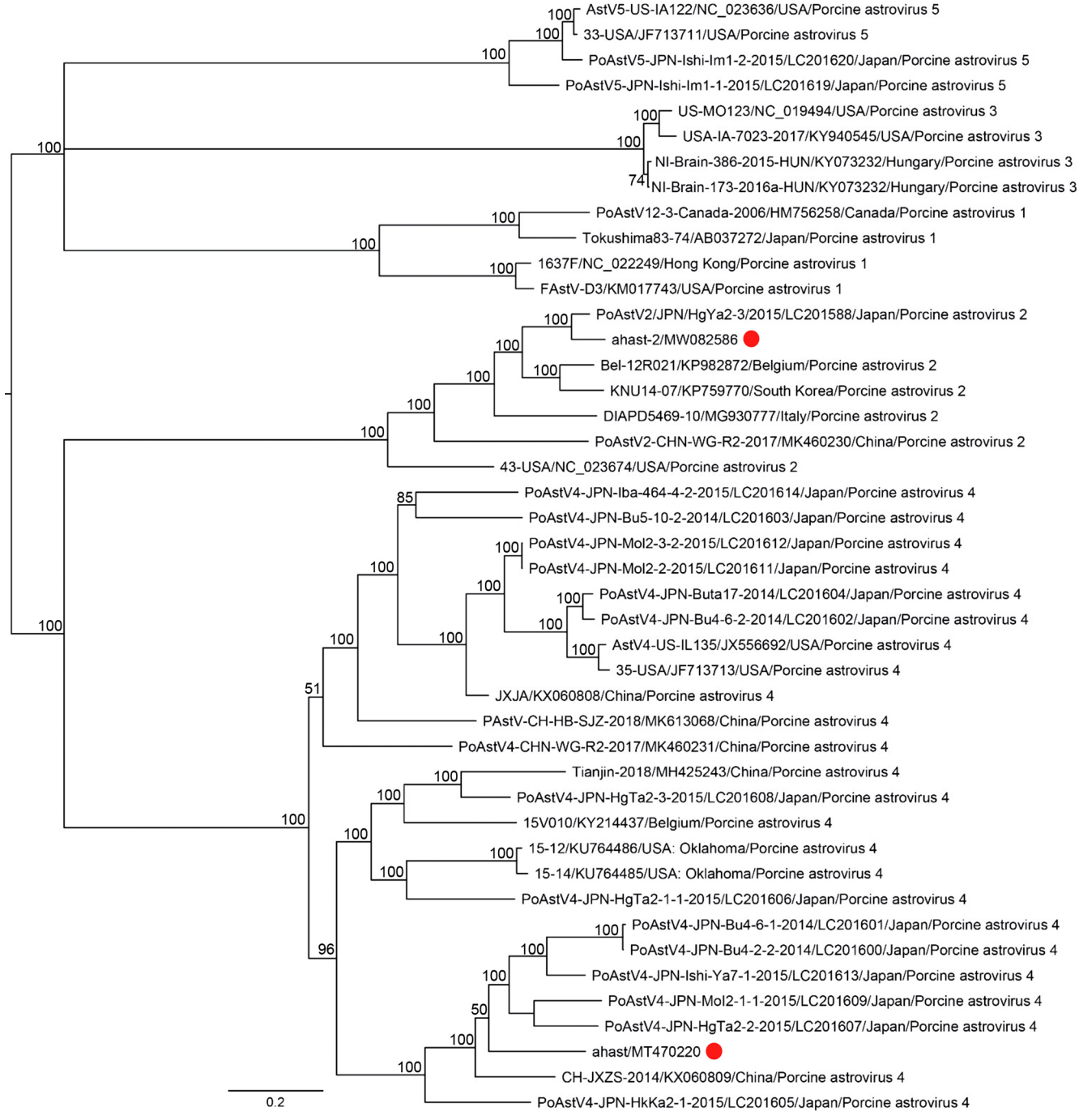

Fig. 3. Phylogenetic analysis of Ahast. Phylogenetic tree based on amino acid sequences of ORF2 of PAstVs. The tree was constructed using MrBayes 3.2.7 software and the average standard deviation of split frequencies were 0.001 respectively. The Markov chain was run for a maximum of 1 million generations, in which every 50 generations were sampled and the first 25% of Markov chain Monte Carlo (mcmc) samples were discarded as burn-in. The Ahast strain identified in this study is marked with red dot.

both of those two recombination events, The PAstV4/JPN/MoI2-1-1/2015 strain (LC201609) was a major parent, while minor parents were the PAstV4/CHN/WG-R2/2017 strain (MK460231) and the JXJA strain (KX060808), respectively Fig. 4b. Ahast showed higher sequence similarity to the JXJA strain or the PAstV4/CHN/WG-R2/2017 strain in the region of 1822–2810 nt or 3076–4540 nt separately, while in the region of 4600–6023 nt, Ahast displayed higher sequence similarity to the PAstV4/JPN/MoI2-1-1/2015 strain Fig. 4b, and 4c. To confirm this result, phylogenetic trees were constructed basing on the genome region of 1822–2810 nt, 3076–4540 nt, and 4600–6023 nt, respectively. The trees based on 1822–2810 nt or 3076–4540 nt showed that Ahast clustered with the JXJA strain or the PAstV4/CHN/WG-R2/2017 strain, while the tree based on 3076–4540 nt showed that Ahast clustered with the PAstV4/JPN/MoI2-1-1/2015 strain Fig. 4d, 4e, and 4f.

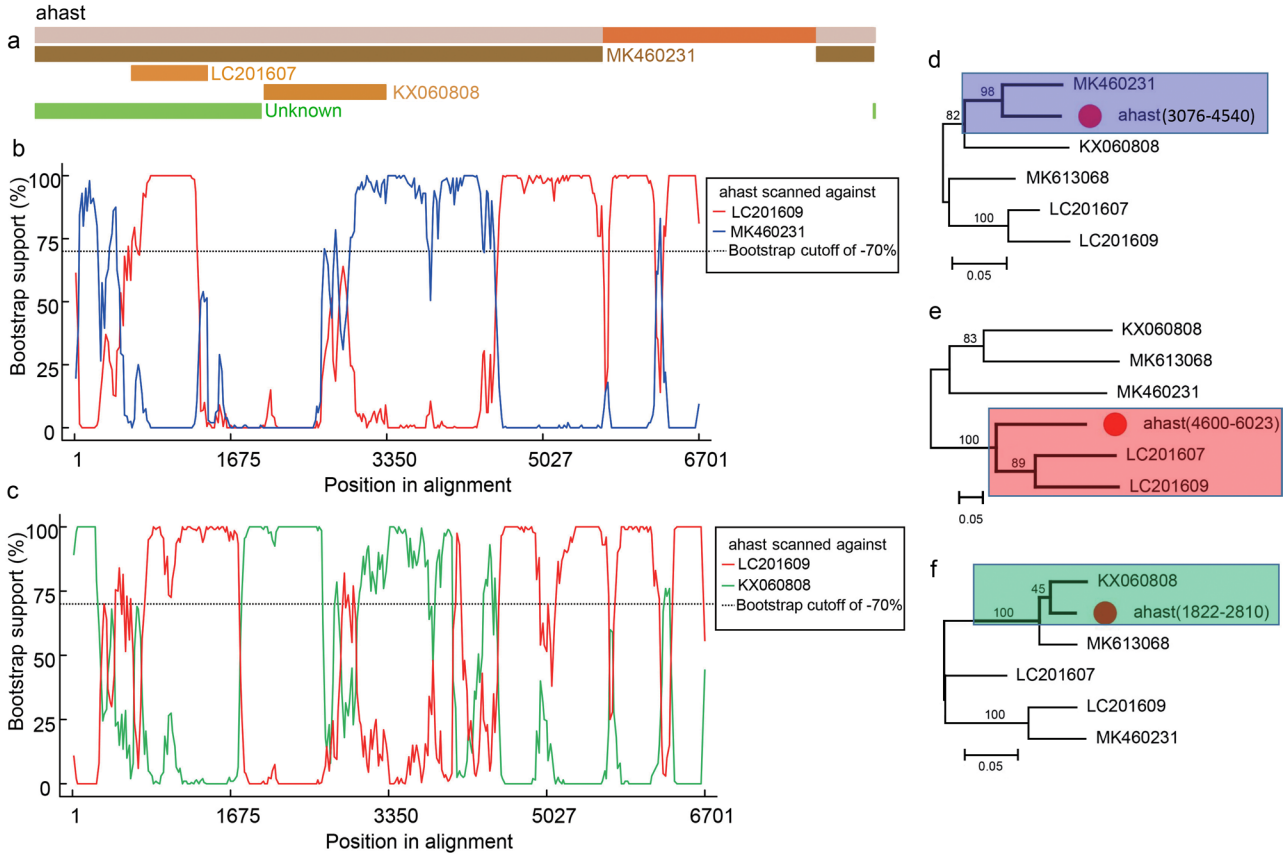

Fig. 4. Recombination analysis of Ahast. (a) Detected the potential recombination events based on complete genome of Ahast. GenBank No. of each putative recombinant is shown on upper right side of the recombinant. (b), (c) BOOTSCAN evidence for the two different recombination origins on the basis of pairwise distance, modeled with a window size 200, step size 20, and 100 Bootstrap replicates. (d), (e), and (f) Phylogenetic trees were constructed using the Maximun Likelihood in MEGA 5.0 based on the region of 3076–4540 nt, 4600–6023 nt, and 1822–2810 nt respectively. Bootstrap values (based on 500 replicates) for each node were given. The Ahast strain identified in this study is marked with red dot.

The PAstV4/JPN/MoI2-1-1/2015 strain was first reported in Japan in 2015; the PAstV4/CHN/WG-R2/2017 strain was first found in the Hunan province of China in 2019, while the JXJA strain was first detected in Jiangxi province of China in 2014. From the above data, Ahast might be a potent recombinant form one major parent and two minor parents.

To computationally verify the boundaries of different regions in the recombinant, the clean raw reads were remapped to the complete genome of Ahast, which revealed evident overlapping read coverage across the boundaries Fig. S1.

Epidemiological analysis. To investigate the prevalence of PAstV4 in this pig farm, viral RNA was extracted from all 215 feces samples. A set of nested primers were designed based on the Ahast ORF2 nucleotide sequence to perform PCR screening. Primers astWF and astWR were used for the first round of PCR, and astNF and astNR for the second round. The expected length of amplified fragment was 305 bp. The results indicated that 23 (10.7%, 23/215) samples were positive for PAstV4.

Discussion

Porcine astroviruses, as widely distributed viruses, have been isolated from many countries, including China, South Korea, Germany, Czech Republic, Canada, Croatia, Italy, Spain, Australia, Hungary, Thailand, India, and USA, which is divided into five genotypes (Indik et al. 2006; Reuter et al. 2011; Lee et al. 2013; Kattoor et al. 2019; Tassoni et al. 2019). The predominant genotypes in domestic pigs were PAstV2 and PAstV4 in China. Both PAstV2 and PAstV4 were identified in this study, which indicates that those two genotypes of porcine astrovirus circulated in the same pig farm. The prevalence of PAstV4 was 16.1% (35/218) in Hunan of China in previous studies (Xiao et al. 2017), while in the present investigation, the prevalence of PAstV4 was 10.7% (23/215), and it was slightly lower than previously reported. The difference in this prevalence may be due to differences in the type or origin of samples. The samples collected in this study were fecal from healthy pigs, but that were fecal swabs or different tissues from diarrhea pigs in previous studies.

Recombination frequently occurs among astroviruses, and it is the major mechanisms contributing to the emergence of novel strains. Our recombination analysis indicates that Ahast is a potent recombinant with multiple recombinant events. The major parent was identified in Japan, while two minor parents were found in Hunan or Jiangxi province of China. The three parental strains were isolated from different countries or districts, which might hint that the pig trade promoted viral recombination.

In conclusion, we identified a novel PAstV4 in healthy pigs and characterized its near-complete genome. Recombinant analysis indicated that it was a recombinant with multiple recombinant events. The epidemiologic study showed that the prevalence rate of Ahast was slightly lower than that of previously reported in China. More work is needed to investigate the association between virus and illness.

Acknowledgments

This work was supported by National Key Research and Development Programs of China No. 2017YFC1200201, Jiangsu Provincial Key Research and Development Projects No. BE2017693 and Independent Project of Chengdu Research Base of Giant Panda Breeding No. 2020CPB-C11.

Compliance with ethical standards

The experiments were approved and carried out under animal ethics guidelines and approved protocols of Jiangsu University.

Conflict of interest

The authors do not report any financial or personal connections with other persons or organizations, which might negatively affect the contents of this publication and/or claim authorship rights to this publication.

Literature

Altschul S, Madden TL, Schäffer AA, Zhang J, Zhang Z, Miller W, Lipman DJ. Gapped BLAST and PSI-BLAST: a new generation of protein database search programs. Nucleic Acids Res. 1997 Sep 1;25(17):3389–3402. https://doi.org/10.1093/nar/25.17.3389

Arruda B, Arruda P, Hensch M, Chen Q, Zheng Y, Yang C, Gatto IRH, Ferreyra FM, Gauger P, Schwartz K, et al. Porcine Astrovirus Type 3 in central nervous system of swine with Polioencephalomyelitis. Emerg Infect Dis. 2017 Dec;23(12):2097–2100. https://doi.org/10.3201/eid2312.170703

Bidin M, Bidin Z, Majnaric D, Tisljar M, Lojkic I. Circulation and phylogenetic relationship of chicken and turkey-origin astroviruses detected in domestic ducks (*Anas platyrhynchos domesticus*). Avian Pathol. 2012a;41(6):555–562. https://doi.org/10.1080/03079457.2012.733340

Bidin M, Lojkic I, Tisljar M, Bidin Z, Majnaric D. Astroviruses associated with stunting and pre-hatching mortality in duck and goose embryos. Avian Pathol. 2012b;41(1):91–97. https://doi.org/10.1080/03079457.2011.642796

Blomström AL, Widén F, Hammer AS, Belák S, Berg M. Detection of a novel astrovirus in brain tissue of mink suffering from shaking mink syndrome by use of viral metagenomics. J Clin Microbiol. 2010 Dec;48(12):4392–4396. https://doi.org/10.1128/JCM.01040-10

Bosch AGS, Krishna NK, Méndez E, Monroe SS, Pantin-Jackwood M, Schultz-Cherry S. Family Astroviridae. In: King AMQ, Lefkowitz E, Adams MJ, Carstens EB, edotors. Virus taxonomy: classification and nomenclature of viruses (ninth report of the International Committee on the Taxonomy of Viruses). New York (USA): Elsevier Academic Press; 2011, p. 953–959.

Bouzalas IG, Wüthrich D, Walland J, Drögemüller C, Zurbriggen A, Vandevelde M, Oevermann A, Bruggmann R, Seuberlich T. Neurotropic astrovirus in cattle with nonsuppurative encephalitis in Europe. J Clin Microbiol. 2014 Sep;52(9):3318–3324. https://doi.org/10.1128/JCM.01195-14

Bridger JC. Detection by electron microscopy of caliciviruses, astroviruses and rotavirus-like particles in the faeces of piglets with diarrhoea. Vet Rec. 1980 Dec 6;107(23):532–533.

Brnic D, Jemersic L, Keros T, Prpic J, High prevalence and genetic heterogeneity of porcine astroviruses in domestic pigs. Vet J. 2014; 202(2):390–392. https://doi.org/0.1016/j.tvjl.2014.08.015

De Benedictis P, Schultz-Cherry S, Burnham A, Cattoli G. Astrovirus infections in humans and animals – Molecular biology, genetic diversity, and interspecies transmissions. Infect Genet Evol. 2011b Oct;11(7):1529–1544. https://doi.org/10.1016/j.meegid.2011.07.024

Deng X, Naccache SN, Ng T, Federman S, Li L, Chiu CY, Delwart EL. An ensemble strategy that significantly improves de novo assembly of microbial genomes from metagenomic next-generation sequencing data. Nucleic Acids Res. 2015 Apr 20;43(7):e46. https://doi.org/10.1093/nar/gkv002

Indik S, Valíček L, Šmíd B, Dvořáková H, Rodák L. Isolation and partial characterization of a novel porcine astrovirus. Vet Microbiol. 2006 Oct;117(2–4):276–283. https://doi.org/10.1016/j.vetmic.2006.06.020

Kattoor JJ, Malik YS, Saurabh S, Sircar S, Vinodhkumar OR, Bora DP, Dhama K, Ghosh S, Banyai K, Touil N, et al. First report and genetic characterization of porcine astroviruses of lineage 4 and 2 in diarrhoeic pigs in India. Transbound Emerg Dis. 2019 Jan;66(1): 47–53. https://doi.org/10.1111/tbed.13058

Lee MH, Jeoung HY, Park HR, Lim JA, Song JY, An DJ. Phylogenetic analysis of porcine astrovirus in domestic pigs and wild boars in South Korea. Virus Genes. 2013 Feb;46(1):175–181. https://doi.org/10.1007/s11262-012-0816-8

Ling Y, Zhang X, Qi G, Yang S, Jingjiao L, Shen Q, Wang X, Cui L, Hua X, Deng X, et al. Viral metagenomics reveals significant viruses in the genital tract of apparently healthy dairy cows. Arch Virol. 2019 Apr;164(4):1059–1067. https://doi.org/10.1007/s00705-019-04158-4

Liu Q, Wang H, Ling Y, Yang SX, Wang XC, Zhou R, Xiao YQ, Chen X, Yang J, Fu WG, et al. Viral metagenomics revealed diverse CRESS-DNA virus genomes in faeces of forest musk deer. Virol J. 2020 Dec;17(1):61. https://doi.org/10.1186/s12985-020-01332-y

Lv SL, Zhang HH, Li JY, Hu WQ, Song YT, Opriessnig T, Xiao CT. High genetic diversity and recombination events of porcine astrovirus strains identified from ill and asymptomatic pigs in 2017, Hunan Province, China. Virus Genes. 2019 Oct;55(5):673–681. https://doi.org/10.1007/s11262-019-01692-w

Padmanabhan A, Hause BM. Detection and characterization of a novel genotype of porcine astrovirus 4 from nasal swabs from pigs with acute respiratory disease. Arch Virol. 2016 Sep;161(9):2575–2579. https://doi.org/10.1007/s00705-016-2937-1

Reuter G, Pankovics P, Boros Á. Identification of a novel astrovirus in a domestic pig in Hungary. Arch Virol. 2011 Jan;156(1):125–128. https://doi.org/10.1007/s00705-010-0827-5

Rivera R, Nollens HH, Venn-Watson S, Gulland FMD, Wellehan JFX Jr. Characterization of phylogenetically diverse astroviruses of marine mammals. J Gen Virol. 2010 Jan 01;91(1):166–173. https://doi.org/10.1099/vir.0.015222-0

Sajewicz-Krukowska J, Domanska-Blicharz K. Nearly full-length genome sequence of a novel astrovirus isolated from chickens with 'white chicks' condition. Arch Virol. 2016 Sep;161(9):2581–2587. https://doi.org/10.1007/s00705-016-2940-6

Tassoni L, Zamperin G, Schiavon E, Vendramin V, Cavicchio L, Mion M, Tonon FT, Monne I, Beato MS. First whole genome characterization of porcine astrovirus detected in swine faeces in Italy. Vet Ital. 2019 Sep 30;55(3):221–229. https://doi.org/10.12834/VetIt.1873.9956.1

Vu DL, Bosch A, Pintó R, Guix S. Epidemiology of classic and novel human astrovirus: gastroenteritis and beyond. Viruses. 2017 Feb 18;9(2):33. https://doi.org/10.3390/v9020033

Xiao CT, Luo Z, Lv SL, Opriessnig T, Li RC, Yu XL. Identification and characterization of multiple porcine astrovirus genotypes in Hunan province, China. Arch Virol. 2017 Apr;162(4):943–952. https://doi.org/10.1007/s00705-016-3185-0

Yi S, Niu J, Wang H, Dong G, Guo Y, Dong H, Wang K, Hu G. Molecular characterization of feline astrovirus in domestic cats from Northeast China. PLoS One. 2018 Oct 9;13(10):e0205441. https://doi.org/10.1371/journal.pone.0205441

Zhang W, Li L, Deng X, Blümel J, Nübling CM, Hunfeld A, Baylis SA, Delwart E. Viral nucleic acids in human plasma pools. Transfusion. 2016 Sep;56(9):2248–2255. https://doi.org/10.1111/trf.13692

Zhao C, Chen C, Li Y, Dong S, Tan K, Tian Y, Zhang L, Huang J, Zhang L. Genomic characterization of a novel recombinant porcine astrovirus isolated in northeastern China. Arch Virol. 2019 May;164(5):1469–1473. https://doi.org/10.1007/s00705-019-04162-8

Supplementary materials are available on the journal's website.

Polish Journal of Microbiology
2020, Vol. 69, No 4, 479–490
https://doi.org/10.33073/pjm-2020-052

ORIGINAL PAPER

Bioinformatics Analysis of Key micro-RNAs and mRNAs under the Hand, Foot, and Mouth Disease Virus Infection

SHENG LIN[1#], LIU YANG[2#], SHIBIAO WANG[1], BIN WENG[1] and MIN LIN[1*]

[1] Fujian Maternity and Child Health Hospital", Affiliated Hospital of Fujian Medical University, Fuzhou, China
[2] Unimed Scientific Inc. Wuxi, Wuxi, China

Submitted 12 October 2020, revised 9 November 2020, accepted 9 November 2020

Abstract

To clarify crucial key micro-RNAs and mRNAs associated with hand, foot, and mouth disease (HFMD) virus infection, we conducted this bioinformatics analysis from four GEO datasets. The following datasets were used for the analysis: GSE85829, GSE94551, GSE52780, and GSE45589. Differentially expressed genes (DEGs) were acquired, and the analysis of functional and pathway enrichment and the relative regulatory network were conducted. After screening common differentially expressed miRNAs (DE-miRNAs), five key miRNAs were acquired: miR-100-3p, miR-125a-3p, miR-1273g-3p, miR-5585-3p, and miR-671-5p. There were three common enriched GO terms between miRNA-derived prediction and mRNA-derived analysis: biosynthetic process, cytosol, and nucleoplasm. There was one common KEGG pathway, i.e., cell cycle shared between miRNA-based and mRNA-based enrichment. Using TarBase V8 in DIANA tools, we acquired 1,520 potential targets (mRNA) from the five key DE-miRNAs, among which the159 DE-mRNAs also included 11 DEGs. These common DEGs showed a PPI network mainly connected by SMC1A, SMARCC1, SF3B3, LIG1, and BRMS1L. Together, changes in five key miRNAs and 11 key mRNAs may play crucial roles in HFMD progression. A combination of these roles may benefit the early diagnosis and treatment of HFMD.

Key words: HFMD, micro-RNA, protein-protein interaction, microarray, regulatory network

Introduction

Hand, foot, and mouth disease (HFMD) is a common endemic childhood disease worldwide, particularly in Asia. Generally, it is triggered by two major causative agents: enterovirus 71 (EV71) and coxsackievirus A16 (CA16) (Kaminska et al. 2013; Koh et al. 2016), followed by coxsackievirus A6 (CA6) and coxsackievirus A10 (CA10) (Wang et al. 2018). This disease majorly affects children under five years old (Omana-Capeda et al. 2016). The common symptoms include fever, rashes on the volar regions of the hands and feet, herpangina, and difficulties in eating and drinking. Severe circumstances can exhibit potentially fatal complications involving the nervous system, such as brain stem encephalitis, or cardiopulmonary systems, such as pulmonary edema. Severe cases may show drastic progression and die from complicated symptoms.

There have been limited tools for effective diagnosis of HFMD. Although enterovirus infection triggers various pathological responses, the exact mechanisms underlying HFMD development remain largely unknown. For example, the regulatory roles played by EV71/CA16 infection towards endothelial cells and neural systems remain unclear. Previous studies have explored the disordered signals in different aspects, such as inflammatory profiles in cytokine expression (Teo et al. 2018; Linghua et al. 2019), long non-coding RNA (lncRNA) profiles (Meng et al. 2017), and immune cell changes (Wang et al. 2014). It is conceivable and supported that patients with HFMD may exhibit changes in expression profiles of microRNAs and mRNAs, mostly derived from blood samples (Cui et al. 2011; Hu et al. 2016; Yee et al. 2016; Zhu et al. 2016; Song et al. 2017; Hu et al. 2018; Jia et al. 2018; Li et al. 2018; Mi et al. 2018; Song et al. 2018). In addition, a comprehensive

* Corresponding authors: #Sheng Lin and Liu Yang contribute equally to this work and are co-first authors.
M. Lin, Fujian Provincial Maternity and Children's Hospital, Affiliated Hospital of Fujian Medical University, Fuzhou, China;
email: laomin158@126.com

understanding of HFMD-related expression profiles and identification key markers may provide substantial diagnostic and prognostic values. To dig the clinical significance of micro-RNA and mRNA changes under HFMD virus infection, we conducted this bioinformatics analysis to clarify crucial differentially expressed genes (DEGs), functional and pathway enrichment, and the relative regulatory network, using four published datasets. This analysis may provide deeper insight into the mechanism of HFMD pathological development and novel strategies to prevent HFMD outbreaks.

Experimental

Materials and Methods

Microarray Data. The keywords „hand-foot-and-mouth disease" or „HFMD" were used to search relevant gene expression profile data on the Gene Expression Omnibus (GEO) database (http://www.ncbi.nlm.nih.gov/geo/). The inclusion criteria were as follows: (1) the experiment was designed to analyze RNA expression (either microRNA or mRNA) in response to EV71 and CA16 infection; (2) all samples were human-derived (human cell lines or human exosomes). Four datasets were found to be informative for this analysis. All the datasets we included are as follows: (1) GSE85829: using the Platform GPL11154 Illumina HiSeq 2000 (Homo sapiens). Summary: to compare microRNA expression in 16HBE (human bronchial epithelial cells) infected with EV71 and CA16. It includes six samples according to the experimental groups: EV71-0h, EV71-6h, EV71-12h, CA16-0h, CA16-6h, and CA16-12h; (2) GSE94551: using the Platform GPL11154 Illumina HiSeq 2000 (Homo sapiens). Summary: the miRNA profiling in EV71- and CA16-infected human umbilical vein endothelial cells (HUVECs) at multiple time points. It contains six samples according to different experimental groups: EV71-0h, EV71-72h, EV71-96h, CA16-0h, CA16-72h, and CA16-96h; (3) GSE52780: using the GPL16730 Agilent-039659. Summary: it observed miRNAs of exosome in HFMD serum samples and distinguished between extremely severe HFMD and mild HFMD. It contains three samples: control, mild, and extremely severe; (4) GSE45589: using the GPL16765 Human 70-mer oligonucleotide microarray. Summary: it employed the human whole-genome microarray to analyze the transcriptome profiling in human neuroblastoma cells SH-SY5Y infected with EV71.

DEG identification. DEG analysis of the dataset was performed according to the following standards. For all the miRNA samples were the single ones in each group, DEG was regarded as a gene with a fold change (FC) ≥ 4 or ≤ 0.25 (any treatment group vs. control group). For those datasets with three-time points, DEGs were acquired at all time points. It was selected if the expression at any later time points with a fold change ≥ 4 or ≤ 0.25 vs. 0 h. For dataset GSE45589 (mRNA expression), there were two independent samples. Each sample presented the degree of FC after SH-SY5Y cells were infected with EV71 and those genes with FC ratios ≥ 2 or ≤ 0.5 and $p < 0.05$ were selected as DEGs. Heatmaps were produced to present DEGs. Those differentially expressed miRNAs (DE-miRNAs), which appeared for three times among different datasets, were defined as key miRNAs in HFMD.

Functional and pathway enrichments. The Database for Annotation, Visualization and Integrated Discovery (DAVID) (https://david.ncifcrf.gov/) and miRPath v. 3 (http://www.microrna.gr/miRPathv3/) were used for Gene Ontology (GO) functional enrichment analysis and Kyoto Encyclopedia of Genes and Genomes (KEGG) pathway enrichment analysis. The up-regulated and down-regulated DEGs were respectively conducted with GO and KEGG pathway enrichment analysis for DEGs. Any term with a p-value < 0.05 and enriched genes ≥ 2 was selected as a differential term. Enrichment was analyzed by two methods: (1) the indirect evaluation: using the DIANA Tool miRPath v. 3, the targets of the Key miRNAs were selected to perform the enrichment analysis; (2) the direct method: using the GSE45589 dataset, all up-regulated and down-regulated DEGs were analyzed.

MicroRNA-mRNA regulatory and protein-protein interaction (PPI) network. Using TarBase V8 in the DIANA tools (http://carolina.imis.athena-innovation.gr), the validated miRNA-mRNA pairs were obtained. The miRNAs and mRNAs among the screened-out DEGs were selected to construct the microRNA-mRNA regulatory network. The common mRNAs between those targeted by key miRNA and differentially expressed in the GSE45589 dataset were screened to construct the PPI network. This step was performed based on the DEG nodes using the Search Tool for the Retrieval of Interacting Genes (STRING) database (http://www.string-db.org), which provides experimental and predicted protein interaction information. The criteria of the combined score were set ≥ 0.4. The PPI network was visualized using the STRING online tools.

Results

Differentially expressed miRNAs after HFMD virus infection. We first analyzed the GSE85829 and GSE94551 datasets and found some common differentially expressed miRNAs (DE-miRNAs). In 16HBE cells based on the GSE85829 dataset, EV71 infection-induced 25 DE-miRNAs and CA16 infection-induced

13 DE-miRNAs (Fig. 1A and 1B), among which seven common DE-miRNAs were found. In the HUVEC line, according to the GSE94551 dataset, 39 DE-miRNAs were observed after EV71 infection, and 99 DE-miRNAs were found after CA16 infection (Fig. 2A and 2B), and they shared seven common DE-miRNAs (Fig. 2B). However, no intersection was found between two groups of seven common DE-miRNAs. A Venn diagram in Fig. 2C presented the common DE-miRNAs among four groups of cells. Similarly, miRNAs in serum exosomes were analyzed based on the GSE52780 dataset. A total of 258 DE-miRNAs were found (Fig. 3A), including 85 up-regulated and 173 down-regulated ones; the top ten DE-miRNAs were listed in Fig. 3B. Afterward, we screened those DE-miRNAs acquired three times in the above samples (cell lines or exosomes) in different datasets and regarded them as key miRNAs in HFMD. Ultimately, five key miRNAs were acquired: miR-100-3p (appeared four times), miR-125a-3p (appeared three times), miR-1273g-3p (appeared three times), miR-5585-3p (appeared three times), and miR-671-5p (appeared three times).

GO and KEGG enrichment. Based on the above five key miRNAs, GO functional, and KEGG pathway enrichment were performed using the miRPath v. 3 database. First, GO, and KEGG enrichment was

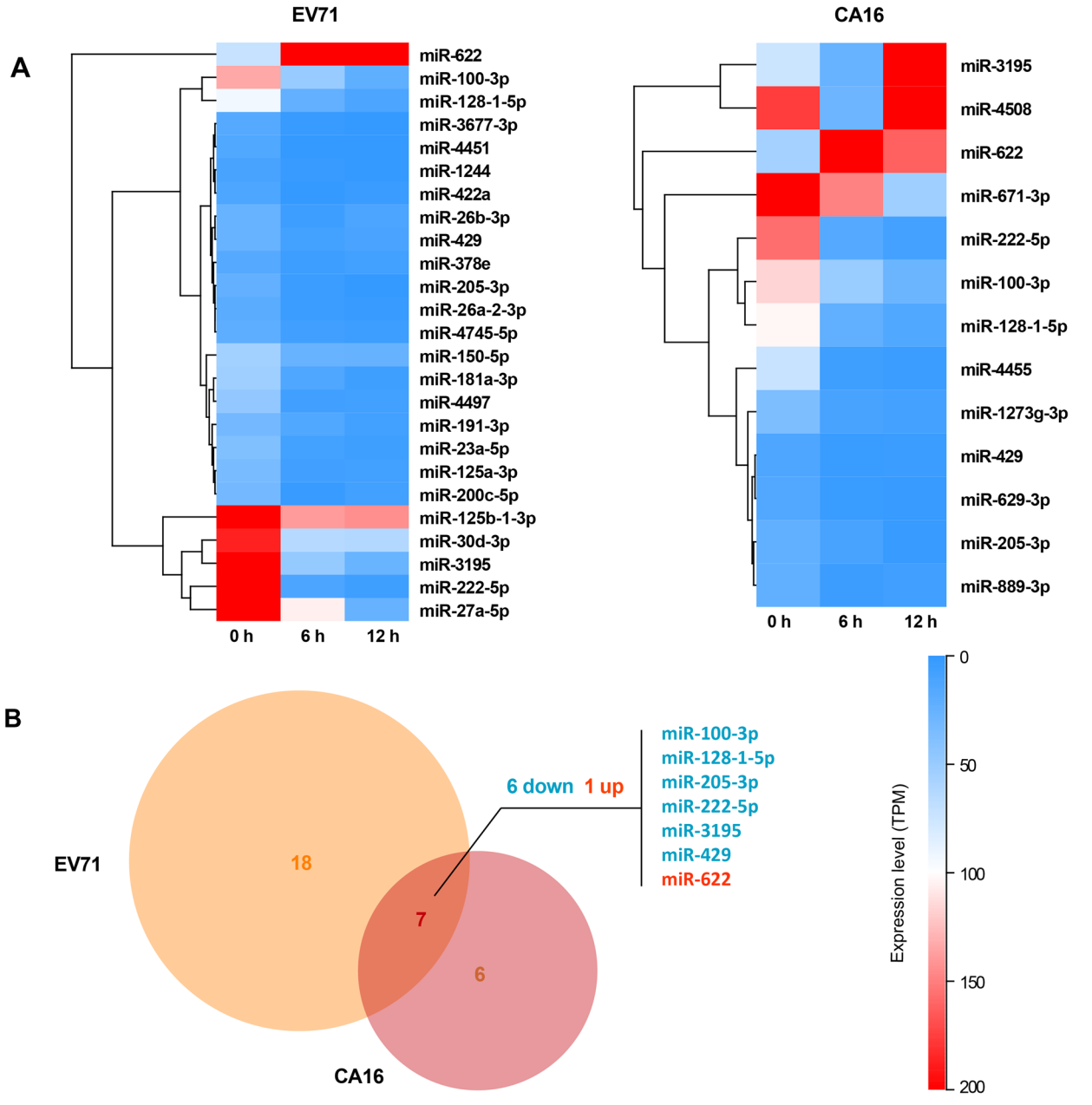

Fig. 1. Differentially expressed miRNAs after HFMD virus infection in 16HBE cells based on the GSE85829 dataset.
(A) Left: EV71 infection-induced 25 DE-miRNAs; Right: CA16 infection-induced 13 DE-miRNAs.
(B) The Venn diagram of 7 common DE-miRNAs between EV71 and CA16 infection.

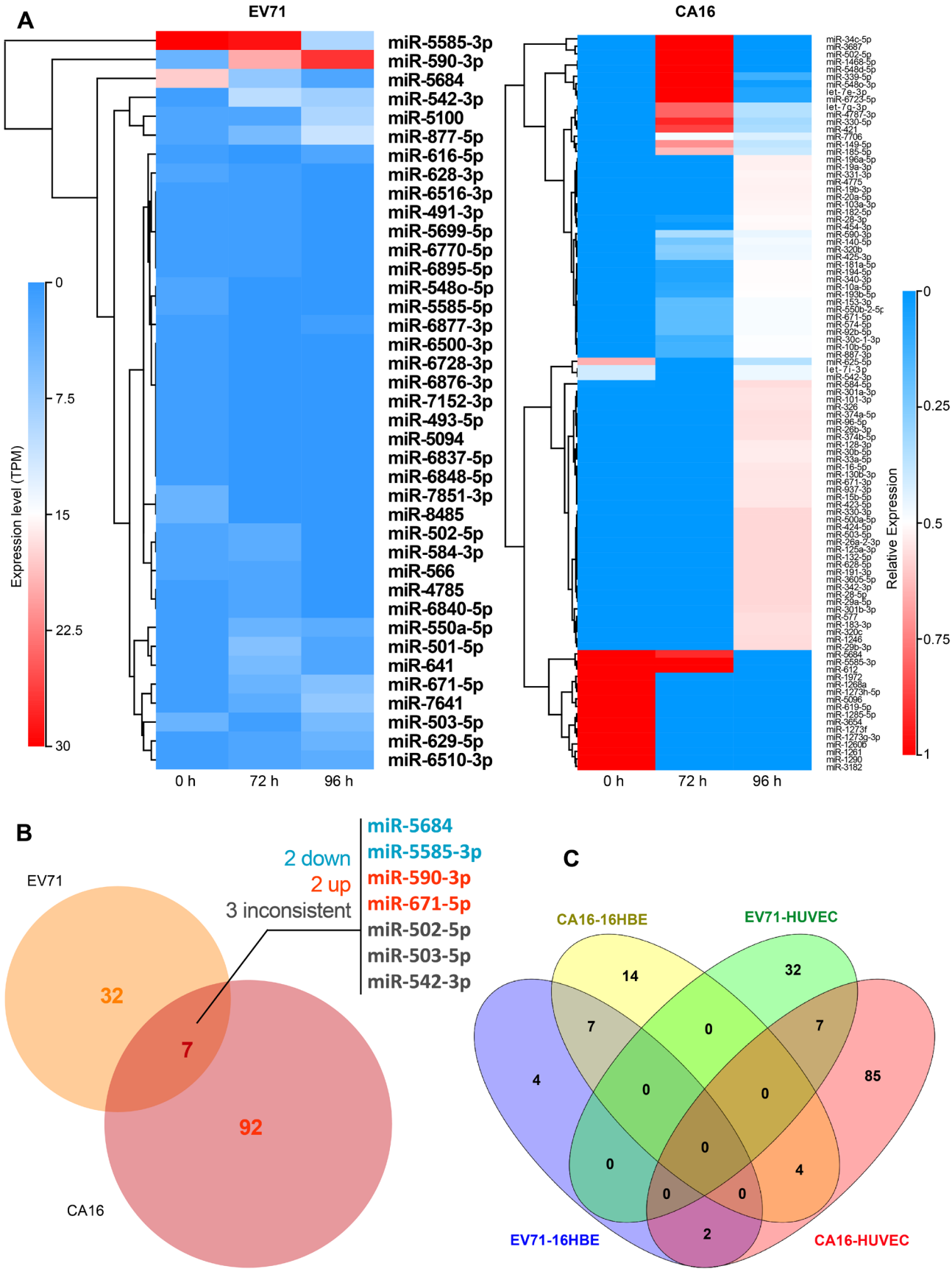

Fig. 2. Differentially expressed miRNAs after HFMD virus infection in the HUVEC cell line based on the GSE94551 dataset.

(A) Left: 39 DE-miRNAs were observed after EV71 infection; Right: 99 DE-miRNAs were found after CA16 infection.

(B) The Venn diagram of 7 common DE-miRNAs between EV71 and CA16 infection. (C) The Venn diagram of common DE-miRNAs among four groups of HFMD virus infection.

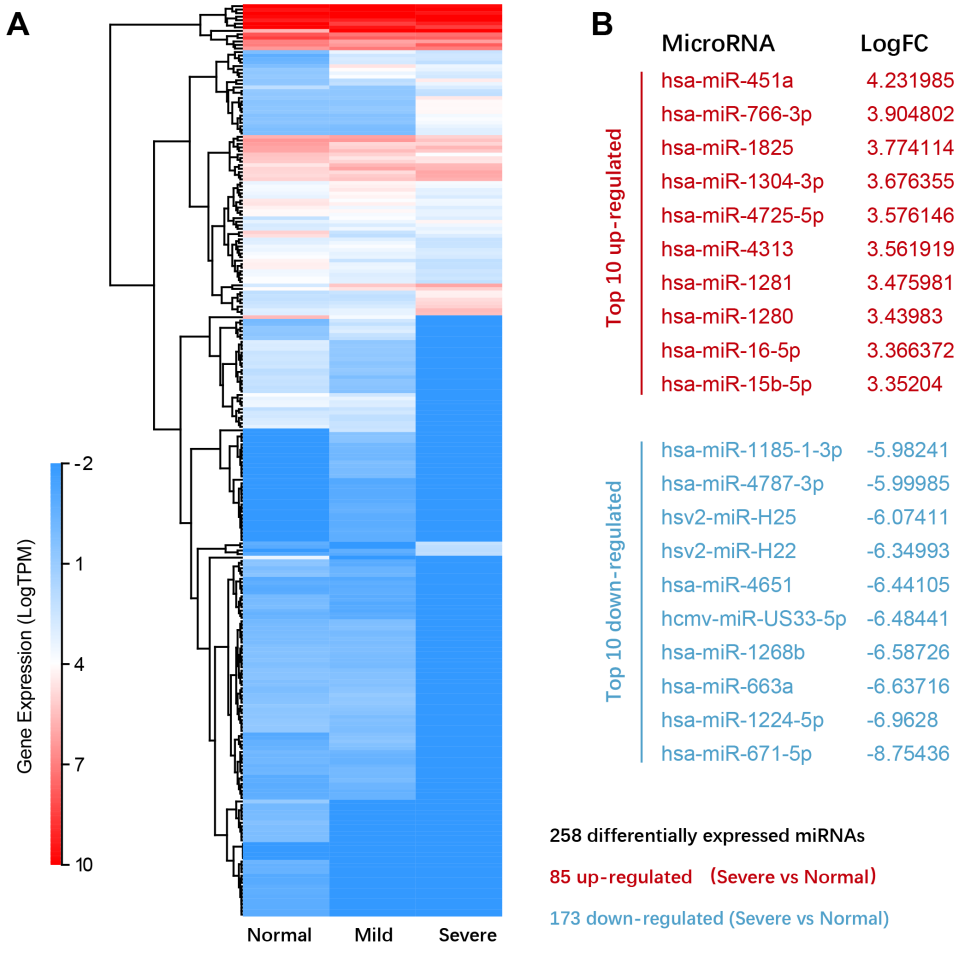

Fig. 3. MicroRNAs in serum exosomes from HFMD patients were analyzed based on the GSE52780 dataset.
(A) Heatmap of 258 DE-miRNAs was found, including 85 up-regulated and 173 down-regulated ones.
(B) The top ten up-regulated and down-regulated DE-miRNAs.

acquired by the intersection targets of the five key miRNAs (only four miRNAs were included in this database) (Fig. 4A and 4B). Further, this was verified by the union of key miRNA related GO terms or KEGG pathways; Heatmaps are shown in Fig. 4C and 4D. Overall, this result was consistent with Fig. 4 A and 4B. Parallelly, we applied the mRNA profiles in SH-SY5Y cells infected by EV71 from the GSE45589 dataset and performed the enrichment analysis. The enriched GO functions of up-regulated and down-regulated genes were listed in Fig. 4E and 4F, respectively. A total of 29 up-regulated GO functional terms were identified (meiotic nuclear division, response to radiation and regulation of the microtubule-based process, etc.), accomplished by 43 down-regulated terms (positive regulation of transcription, DNA-templated, negative regulation of the apoptotic process, and anatomical structure morphogenesis, etc.). Ten enriched KEGG pathways were shown in Fig. 4G, including two up-regulated ones (cell cycle and spliceosome) and eight down-regulated pathways (cytokine-cytokine receptor interaction, hematopoietic cell lineage, and intestinal immune network for IgA production, etc.). In comparison, there were three common enriched GO terms between miRNA-derived prediction and mRNA-derived (dataset GSE45589) analysis: biosynthetic process, cytosol, and nucleoplasm. Moreover, one common KEGG pathway, namely cell cycle, was shared between miRNA-based and mRNA-based enrichment.

Common differential mRNAs and PPI network. Using TarBase V8 in DIANA tools, we acquired 1,520 potential targets (mRNA) from the five key DE-miRNAs, among which the159 DE-mRNAs also included 11 DEGs in the GSE45589 dataset: MACF1, MARS, SF3B3, SMARCC1, BRMS1L, SMC1A, SPHK2, LIG1, CSF3, CYR61, and FGFR1OP (Fig. 5A). Theoretically, these genes were the most likely to be influenced by HFMD virus infection. GO functional analysis showed three terms might be enriched according to these DEGs: positive regulation of cell proliferation, anatomical structure morphogenesis, and ATP binding (Fig. 5B). These common DEGs showed a PPI network mainly connected by SMC1A, SMARCC1, SF3B3, LIG1, and BRMS1L (Fig. 5C), and this network locates at a core

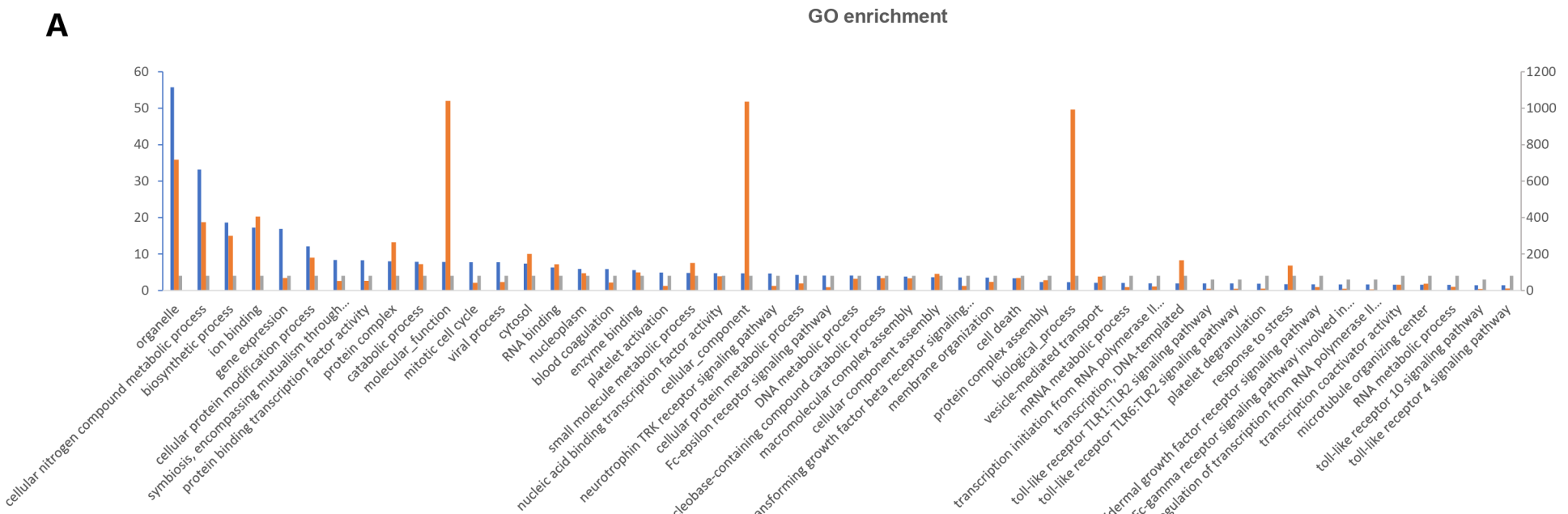

Fig. 4. GO and KEGG enrichment of key miRNAs and DE-mRNAs. Based on the above five key miRNAs, GO functional, and KEGG pathway enrichment was performed using the miRPath v.3 database.

(A) GO enrichment based on the intersection targets of the five key miRNAs (only four miRNAs were included in the miRPath database).

(B) KEGG enrichment based on the intersection targets of the four key miRNAs.

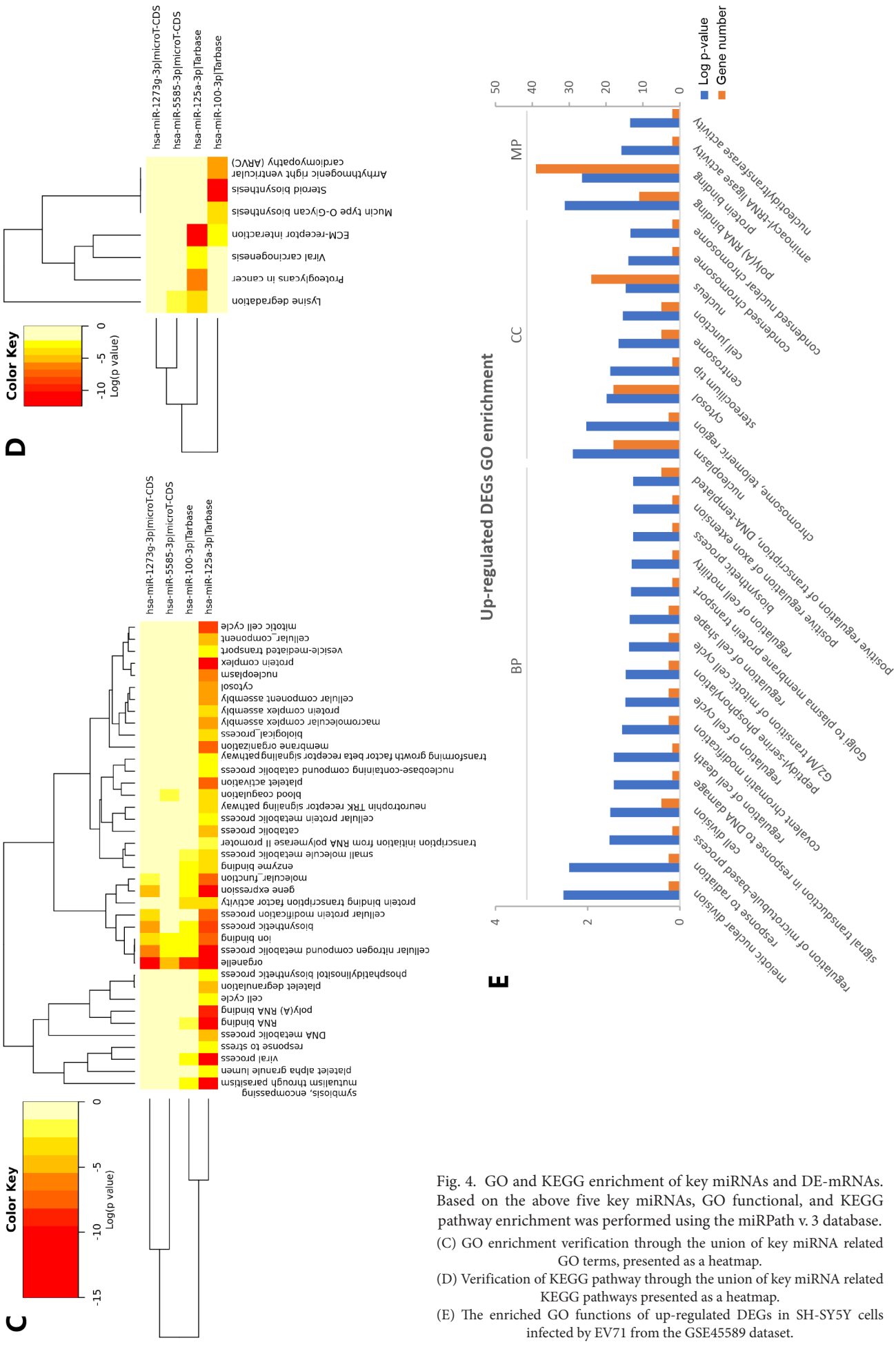

Fig. 4. GO and KEGG enrichment of key miRNAs and DE-mRNAs. Based on the above five key miRNAs, GO functional, and KEGG pathway enrichment was performed using the miRPath v. 3 database.

(C) GO enrichment verification through the union of key miRNA related GO terms, presented as a heatmap.

(D) Verification of KEGG pathway through the union of key miRNA related KEGG pathways presented as a heatmap.

(E) The enriched GO functions of up-regulated DEGs in SH-SY5Y cells infected by EV71 from the GSE45589 dataset.

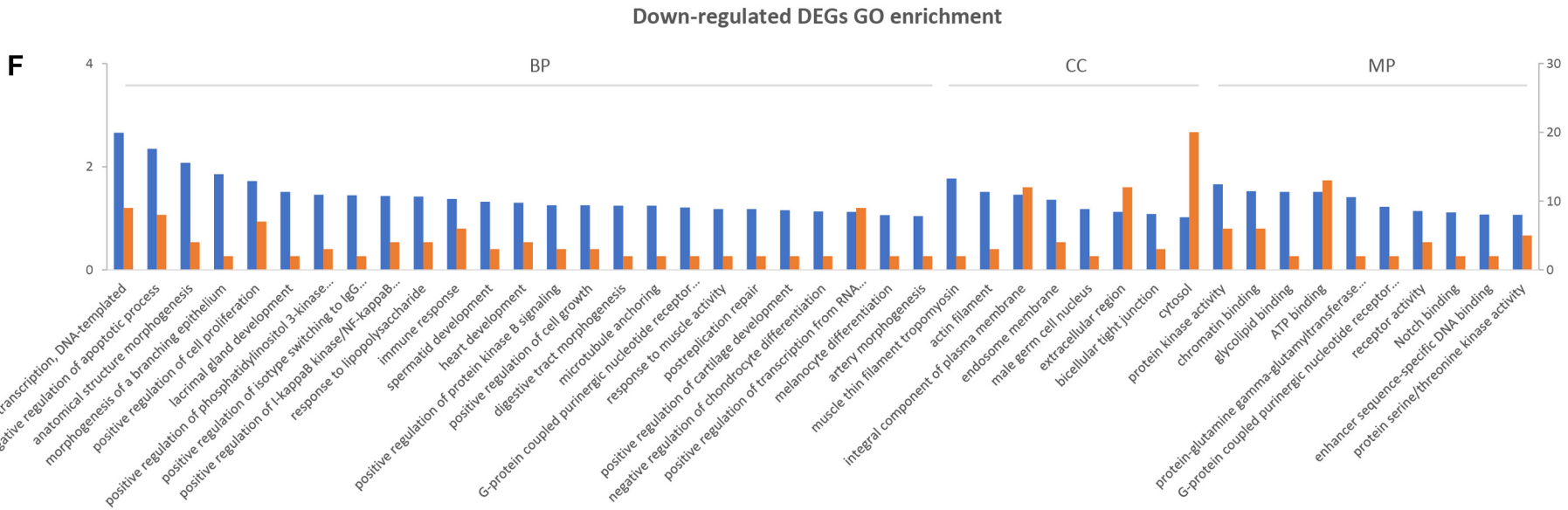

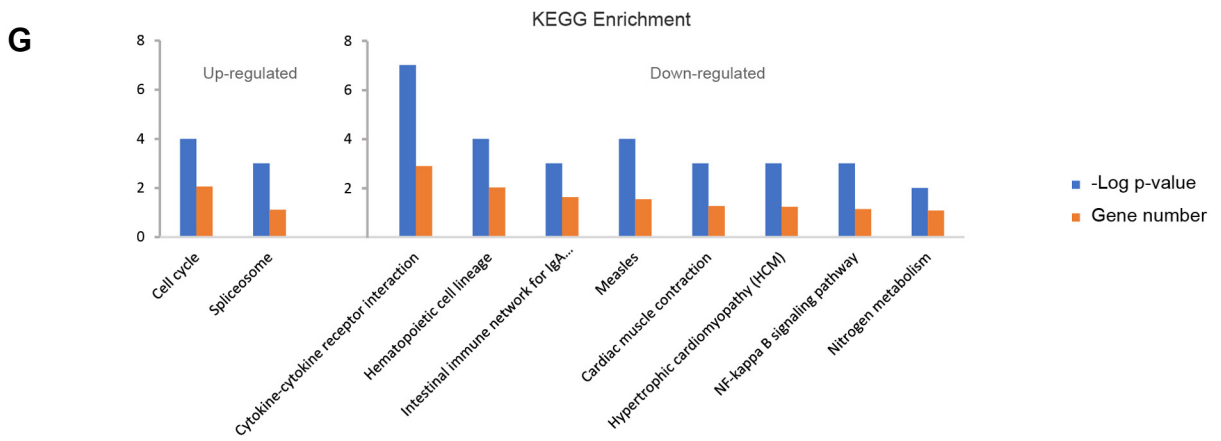

Fig. 4. GO and KEGG enrichment of key miRNAs and DE-mRNAs. Based on the above five key miRNAs, GO functional, and KEGG pathway enrichment was performed using the miRPath v.3 database.
(F) The enriched GO functions of down-regulated DEGs in SH-SY5Y cells infected by EV71 from the GSE45589 dataset.
(G) Enriched KEGG pathways in SH-SY5Y cells infected by EV71 from the GSE45589 dataset.

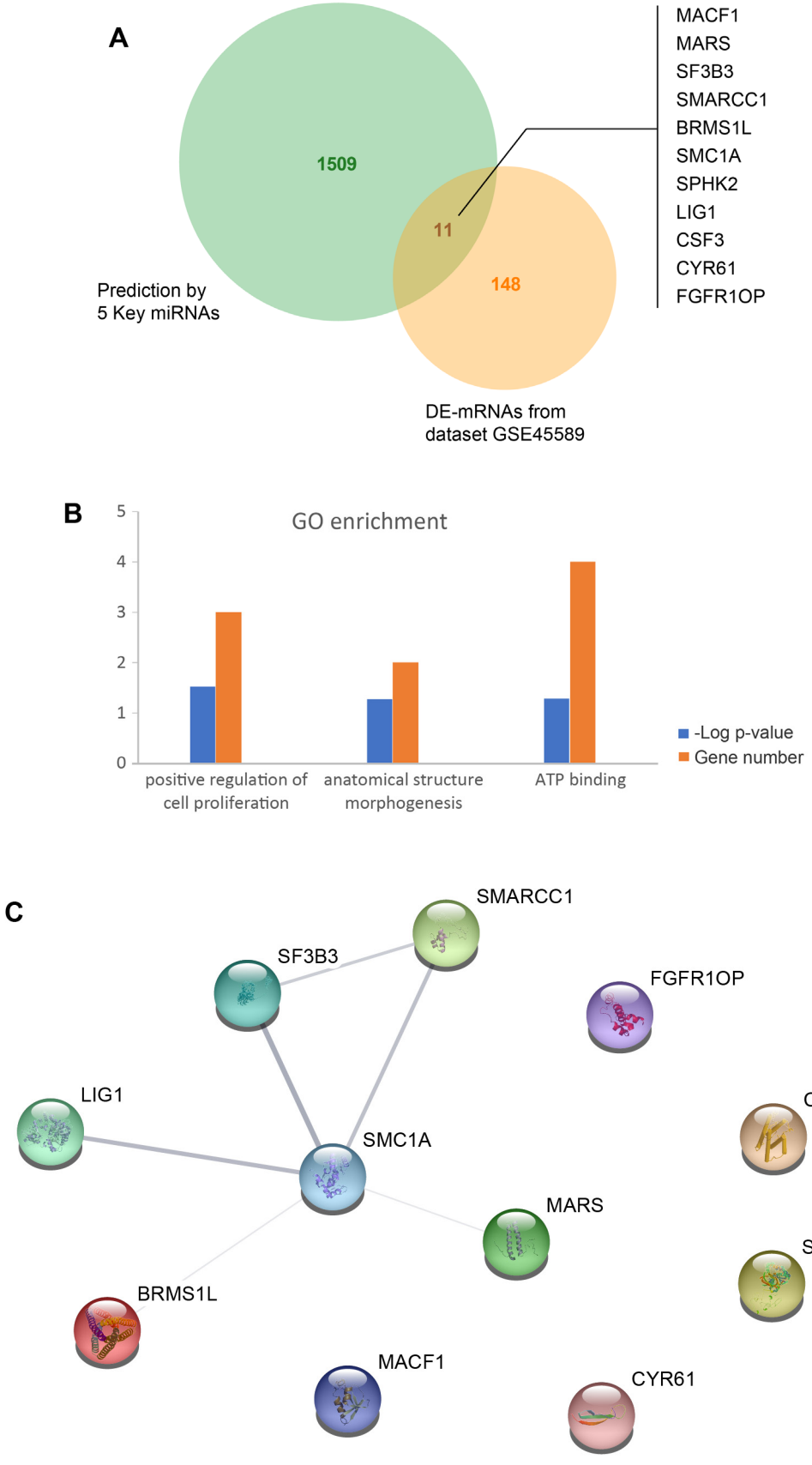

Fig. 5. Common differential mRNAs and PPI network.

(A) Using the TarBase V8 tool, we acquired 1,520 potential targets (mRNA) from the 5 key DE-miRNAs, among which 11 DEGs were also included by the 159 DE-mRNAs in the GSE45589 dataset: MACF1, MARS, SF3B3, SMARCC1, BRMS1L, SMC1A, SPHK2, LIG1, CSF3, CYR61, and FGFR1OP.
(B) GO functional analysis showed three terms might be enriched according to these DEGs.
(C) These common DEGs showed a PPI network mainly connected by SMC1A, SMARCC1, SF3B3, LIG1, and BRMS1L.

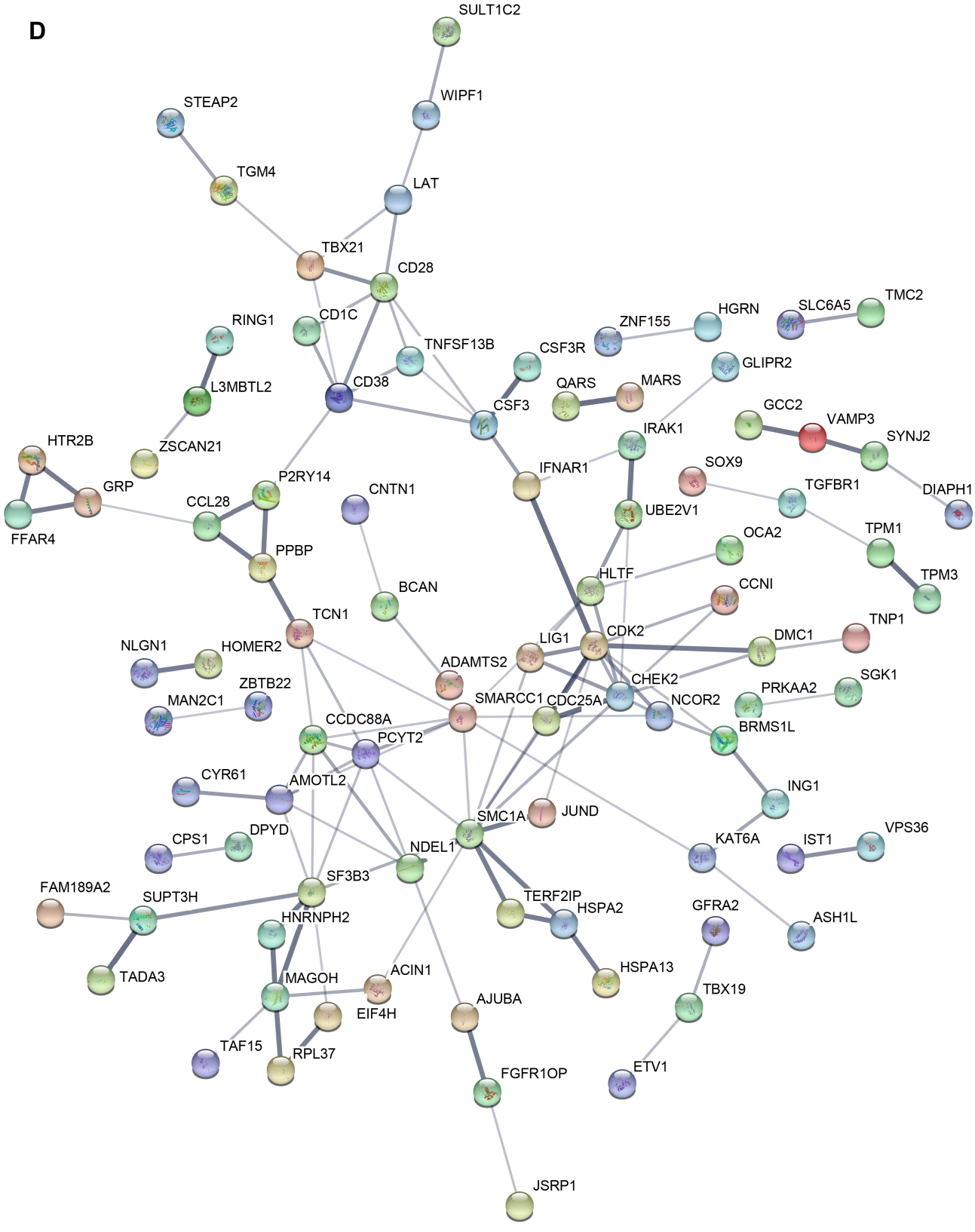

Fig. 5. Common differential mRNAs and PPI network.

(D) The PPI network constructed by the 159 DE-mRNAs in the GSE45589 dataset (the isolated nodes were removed).

place in the PPI network constructed by the 159 DE-mRNAs in the GSE45589 dataset (Fig. 5D, the isolated nodes were removed). Together, changes in five key miRNAs and 11 key mRNAs may play crucial roles in HFMD virus-induced pathological changes and can be used as diagnostic markers for the HFMD.

Discussion

In this study, we used five datasets to identify key RNA members in HFMD development. We were interested in five key miRNAs, 11 mRNAs, and several important GO and KEGG enrichment after filtering progressively. Our results might provide some theoretical perspectives about HFMD development and a potential strategy in its early warning.

At the miRNA level, several potentially useful markers have been proposed in clinical diagnosis. A survey in Singapore reported a 6-miRNA scoring model which predicts HFMD with an overall accuracy of 85.11% in the training set and 92.86% in the blinded test set, and circulating salivary miRNA hsa-miR-221 (downregulated in that work) was regarded as a highly validated marker (Mi et al. 2018). Song et al. have applied rhesus monkey peripheral blood mononuclear cells to search DE-miRNAs, and they identified 13 novel DE-miRNAs with 2501 targets (Song et al. 2018). Zhu et al. (2016) performed the microarray examination and noticed 27 DE-miRNAs (15 up-regulated and 12 downregulated) associated with CA16 and EV71 infection. There were some other important findings of specific miRNAs. MiR-1303 has been known to promote CNS lesions following CA16 infections by targeting MMP9 (Song et al. 2018). EV71 can evade the immune surveillance system to proliferate by activating miR-21 (Feng et al. 2017), antagonize the antiviral activity of host STAT3 and IL-6R through miR-124 (Chang et al. 2017), and induce autophagy by regulating miR-30a to promote viral replication (Fu et al. 2015). So far, there have been very few direct reports about the relationship between the five key miRNAs and HFMD. Only one study had surveyed the miRNA expression profile in the exosome of HFMD patients (Jia et al. 2014), and it revealed that the expression level of three miRNAs (miR-671-5p, miR-16-5p, and miR-150-3p) was significantly different between mild HFMD, extremely severe SHFMD, and the healthy controls. We also noticed that miR-671-5p was among the key miRNAs in HFMD.

The PPI network implied that five targets, SMC1A, SMARCC1, SF3B3, LIG1, and BRMS1L, might play the most crucial roles during HFMD progression. However, none of them has been paid enough attention to date, and they are worth more concerns in further researches. Taken different datasets together, we found three common enriched GO terms between miRNA-derived prediction and mRNA-derived analysis: biosynthetic process, cytosol, and nucleoplasm; and a common KEGG pathway, cell cycle, was noticed (Fig. 4). These functions and pathways suggest that HFMD viruses strongly drive the host proliferation. This fact could be also be supported by the GO functional enrichment constructed based on the 11 key mRNAs (Fig. 5B), which exhibited that positive regulation of cell proliferation was the most enriched functional term. This process may contribute to virus amplification and also be a homeostasis response to fight against virus invasion, particularly for epithelial cells. However, the definite mechanism needs more evidence to unravel.

However, this study has some limitations. First, when we probed the key roles, common DEGs were screened between EV71 and CA16 infection. However, despite belonging to the same genus, Enterovirus, these two viruses do not necessarily have similar effects. For example, Chinese scholars identified that miR-4516 presented down-regulation in EV71 infection and up-regulation in CA16 infection, and it was an important regulator of intercellular junctions by targeting PVRL1 (Hu et al. 2016). Liu et al. had analyzed miRNA profiles and acquired diverse outcomes induced by EV71 and CA16 infection (Song et al. 2017). The inconsistency was also shown in Fig. 2B. There were two common up-regulated miRNAs, two common down-regulated miRNAs, and three inconsistent ones (miR-502-5p, miR-503-5p, and miR-542-3p). Besides, the direct regulatory relationship between five key miRNAs and 11 key mRNAs had not been validated in the present study. Our further efforts would focus on the construction of diagnostic and prognostic models based on the large real-world sample using these miRNA and mRNA factors.

Conclusions

Our results shed light on the potentially crucial roles of the five miRNAs, 11 coding genes, and several functions and pathways in HFMD. A combination of these roles may benefit the early diagnosis and treatment of HFMD.

Authors' contributions

Min Lin and Liu Yang designed this work. Sheng Lin and Liu Yang analyzed all data and wrote this manuscript. Shibiao Wang and Bin Weng helped dig the data and checked the language.

Conflict of interest

The authors do not report any financial or personal connections with other persons or organizations, which might negatively affect the contents of this publication and/or claim authorship rights to this publication.

Literature

Chang Z, Wang Y, Bian L, Liu Q, Long JE. Enterovirus 71 antagonizes the antiviral activity of host STAT3 and IL-6R with partial dependence on virus-induced miR-124. J Gen Virol. 2017 Dec; 98(12):3008–3025. https://doi.org/10.1099/jgv.0.000967

Cui L, Qi Y, Li H, Ge Y, Zhao K, Qi X, Guo X, Shi Z, Zhou M, Zhu B, et al. Serum microRNA expression profile distinguishes enterovirus 71 and coxsackievirus 16 infections in patients with hand-foot-and-mouth disease. PLoS One. 2011;6(11):e27071. https://doi.org/10.1371/journal.pone.0027071

Feng N, Zhou Z, Li Y, Zhao L, Xue Z, Lu R, Jia K. Enterovirus 71-induced has-miR-21 contributes to evasion of host immune system by targeting MyD88 and IRAK1. Virus Res. 2017 Jun 2;237:27–36. https://doi.org/10.1016/j.virusres.2017.05.008

Fu Y, Xu W, Chen D, Feng C, Zhang L, Wang X, Lv X, Zheng N, Jin Y, Wu Z. Enterovirus 71 induces autophagy by regulating has-miR-30a expression to promote viral replication. Antiviral Res. 2015 Dec; 124:43–53. https://doi.org/10.1016/j.antiviral.2015.09.016

Hu Y, Song J, Liu L, Li J, Tang B, Wang J, Zhang X, Zhang Y, Wang L, Liao Y, et al. Different microRNA alterations contribute to diverse outcomes following EV71 and CA16 infections: Insights from high-throughput sequencing in rhesus monkey peripheral blood mononuclear cells. Int J Biochem Cell Biol. 2016 Dec;81 (Pt A):20–31. https://doi.org/10.1016/j.biocel.2016.10.011

Hu Y, Song J, Liu L, Zhang Y, Wang L, Li Q. MicroRNA-4516 contributes to different functions of epithelial permeability barrier by targeting poliovirus receptor related protein 1 in Enterovirus 71 and Coxsackievirus A16 infections. Front Cell Infect Microbiol. 2018 Apr 9;8:110. https://doi.org/10.3389/fcimb.2018.00110

Jia HL, He CH, Wang ZY, Xu YF, Yin GQ, Mao LJ, Liu CW, Deng L. MicroRNA expression profile in exosome discriminates extremely severe infections from mild infections for hand, foot and mouth disease. BMC Infect Dis. 2014 Sep 17;14:506. https://doi.org/10.1186/1471-2334-14-506

Kaminska K, Martinetti G, Lucchini R, Kaya G, Mainetti C. Coxsackievirus A6 and hand, foot and mouth disease: three case reports of familial child-to-immunocompetent adult transmission and a literature review. Case Rep Dermatol. 2013 Aug 7;5(2):203–9. https://doi.org/10.1159/000354533

Koh WM, Bogich T, Siegel K, Jin J, Chong EY, Tan CY, Chen MI, Horby P, Cook AR. The epidemiology of hand, foot and mouth disease in Asia: A systematic review and analysis. Pediatr Infect Dis J. 2016 Oct;35(10):e285–300. https://doi.org/10.1097/INF.0000000000001242

Li X, Huang Y, Sun M, Ji H, Dou H, Hu J, Yan Y, Wang X, Chen L. Honeysuckle-encoded microRNA2911 inhibits Enterovirus 71 replication via targeting VP1 gene. Antiviral Res. 2018 Apr;152:117–123. https://doi.org/10.1016/j.antiviral.2018.02.015

Meng J, Yao Z, He Y, Zhang R, Yang H, Yao X, Chen L, Zhang H, Cheng J. Long non-coding RNA expression profiles in different severity EV71-infected hand foot and mouth disease patients. Biochem Biophys Res Commun. 2017 Dec 2;493(4):1594–1600. https://doi.org/10.1016/j.bbrc.2017.09.141

Min N, Sakthi Vale PD, Wong AA, Tan NWH, Chong CY, Chen CJ, Wang RYL, Chu JJH. Circulating salivary miRNA hsa-miR-221 as clinically validated diagnostic marker for hand, foot, and mouth disease in pediatric patients. EBioMedicine. 2018 May;31:299–306. https://doi.org/10.1016/j.ebiom.2018.05.006

Omaña-Cepeda C, Martínez-Valverde A, del Mar Sabater-Recolons M, Jané-Salas E, Marí-Roig A, López-López J. A literature review and case report of hand, foot and mouth disease in an immunocompetent adult. BMC Res Notes. 2016 Mar 15;9:165. https://doi.org/10.1186/s13104-016-1973-y

Song J, Hu Y, Li H, Huang X, Zheng H, Hu Y, Wang J, Jiang X, Li J, Yang Z, et al. miR-1303 regulates BBB permeability and promotes CNS lesions following CA16 infections by directly targeting MMP9. Emerg Microbes Infect. 2018 Sep 19;7(1):155. https://doi.org/10.1038/s41426-018-0157-3

Song J, Hu Y, Li J, Zheng H, Wang J, Guo L, Ning R, Li H, Yang Z, Fan H, et al. Different microRNA profiles reveal the diverse outcomes induced by EV71 and CA16 infection in human umbilical vein endothelial cells using high-throughput sequencing. PLoS One. 2017 May 22;12(5):e0177657. https://doi.org/10.1371/journal.pone.0177657

Song J, Jiang X, Hu Y, Li H, Zhang X, Xu J, Li W, Zheng X, Dong S. High-throughput sequencing of putative novel microRNAs in rhesus monkey peripheral blood mononuclear cells following EV71 and CA16 infection. Intervirology. 2018;61(3):133–142. https://doi.org/10.1159/000493798

Teo FMS, Nyo M, Wong AA, Tan NWH, Koh MT, Chan YF, Chong CY, Chu JJH. Cytokine and chemokine profiling in patients with hand, foot and mouth disease in Singapore and Malaysia. Sci Rep. 2018 Mar 6;8(1):4087. https://doi.org/10.1038/s41598-018-22379-6

Wang J, Teng Z, Cui X, Li C, Pan H, Zheng Y, Mao S, Yang Y, Wu L, Guo X, et al. Epidemiological and serological surveillance of hand-foot-and-mouth disease in Shanghai, China, 2012-2016. Emerg Microbes Infect. 2018 Jan 24;7(1):8. https://doi.org/10.1038/s41426-017-0011-z

Wang SM, Chen IC, Liao YT, Liu CC. The clinical correlation of regulatory T cells and cyclic adenosine monophosphate in enterovirus 71 infection. PLoS One. 2014 Jul 10;9(7):e102025. https://doi.org/10.1371/journal.pone.0102025

Yee PT, Poh CL. Development of novel mirna-based vaccines and antivirals against Enterovirus 71. Curr Pharm Des. 2016;22(44): 6694–6700. https://doi.org/10.2174/1381612822666160720165613

Yu L, He J, Wang L, Yi H. Inflammatory profiles revealed the dysregulation of cytokines in adult patients of HFMD. Int J Infect Dis. 2019 Feb;79:12–20. https://doi.org/10.1016/j.ijid.2018.11.001

Zhu Z, Qi Y, Fan H, Cui L, Shi Z. Systematic identification and bioinformatic analysis of microRNAs in response to infections of Coxsackievirus A16 and Enterovirus 71. Biomed Res Int. 2016;2016:4302470. https://doi.org/10.1155/2016/4302470

Polish Journal of Microbiology
2020, Vol. 69, No 4, 491–501
https://doi.org/10.33073/pjm-2020-053

ORIGINAL PAPER

Multidrug-resistant Opportunistic and Pathogenic Bacteria Contaminate Algerian Banknotes Currency

LYDIA NEÏLA DJOUADI[1]*, NADJET GUEZLANE-TEBIBEL[1], KENZA MANSOURI[1], HANANE BOUMERDASSI[1], KARIM ARAB[2], MARIE-LAURE FARDEAU[3] and FARIDA NATECHE[1]

[1] Laboratory of Cellular and Molecular Biology, Faculty of Biological Sciences, Algiers, Algeria
[2] Laboratoire Valorisation et Conservation des Ressources Biologiques, Department of Agronomy, Faculty of Sciences, Université M'hamed Bougara, Boumerdes, Algeria
[3] Aix-Marseille Université, Université du Sud Toulon-Var, Marseille, France

Submitted 7 September 2020, revised 9 November 2020, accepted 11 November 2020

Abstract

Currency is one of the most exchanged items in human communities as it is used daily in exchange for goods and services. It is handled by persons with different hygiene standards and can transit in different environments. Hence, money can constitute a reservoir for different types of human pathogens. This study aimed to evaluate the potential of Algerian banknotes to shelter opportunistic pathogenic and multiresistant bacteria. To that end, 200 circulating notes of four different denominations were collected from various places and analyzed for their bacterial loads and contents. Besides, predominant strains were identified and characterized by biochemical and molecular methods, and their resistance profiles against 34 antibiotics were determined. Our results indicated that 100% of the studied banknotes were contaminated with bacteria. The total bacterial concentrations were relatively high, and different bacterial groups were grown, showing important diversity. In total, 48 predominant strains were identified as belonging to 17 genera. *Staphylococcus* and *Micrococcus* were the most prevalent genera, followed by *Bacillus*, *Pseudomonas*, and *Acinetobacter*. Antibiotic susceptibility testing showed that all the isolates harbored resistance to at least two molecules, and worrying resistance levels were observed. These findings prove that Algerian currency harbors opportunistic multiresistant bacteria and could potentially act as a vehicle for the spread of bacterial diseases and as a reservoir for antibiotic resistance genes among the community. Therefore, no cash payment systems should be developed and generalized to minimize cash handling and subsequent potential health risks.

Key words: currency, Algeria, opportunistic bacteria, antibiotic resistance, circulating resistance genes

Introduction

Microorganisms are continually present in our surroundings, and some of them are considered harmful as they possess the ability to invade and make humans ill. Therefore, their possible routes of transmission have been well studied, and it has been proven that inanimate objects or fomites can serve as a reservoir in the transmission of several human pathogens, including bacteria, viruses, and fungi (Lopez et al. 2013; Kraay et al. 2018; Stephens et al. 2019).

Currency is widely exchanged for goods and services among communities worldwide and exposed to microbial contamination. Money is handled by people with different levels of hygiene and can be stored on dirty surfaces. Indeed, unhygienic habits like improper hand washing after using the toilets, coughing, or sneezing on hands, and, then exchanging money leads to contamination of the next user. The potential of currency to act as a vehicle for communicable diseases has been investigated since the early 1970s (Abrams and Waterman, 1972) and continues to draw attention worldwide (Gabriel et al. 2013; Akoachere et al. 2014; Firoozeh et al. 2017; Abd Alfadil et al. 2018; Ejaz et al. 2018; Sunil et al. 2020).

Even though banknotes and coins both offer surface area to shelter microorganisms, it has been demonstrated that copper contained in coins acts as a limiting factor for their survival (Espírito Santo et al. 2010; Vriesekoop et al. 2010). On the contrary, banknotes are usually made of cotton, linen, or other textile fibers that can absorb humidity and provide fertile ground for microorganisms to adhere, develop, and persist. For instance, it has been reported that pathogenic bacteria like *Staphylococcus* spp., *Salmonella* spp., or *Escherichia coli* can persist on cotton-based banknotes for as long as 20 days (Vriesekoop et al. 2010), whereas the

* Corresponding author: L.N. Djouadi, Laboratory of Cellular and Molecular Biology, Faculty of Biological Sciences, Algiers, Algeria; **e-mail: lydia.djouadi@gmail.com**

influenza virus was found to survive for up to 17 days (Thomas et al. 2008).

However, some countries have replaced paper banknotes with plastic polymer banknotes, which appear to be cleaner and to contain less microbial contamination (Vriesekoop et al. 2010).

Among bacteria that can be transmitted by fomites and most significantly by currency, opportunistic bacteria represent a matter of interest as they infect weakened hosts and are related to increased mortality rates worldwide (Lynch et al. 2007). Furthermore, this type of bacteria is difficult to eradicate as they are often multiresistant to antibiotics, leading to treatment failures.

In this context, we aimed this study to assess Algerian banknotes' safety by investigating their bacterial contents and determining their possible roles in transmitting pathogenic and opportunistic bacteria in the community and the spread of antibiotic resistance genes. To date, and to the best of our knowledge, bacterial contamination of Algerian currency is studied for the first time.

Experimental

Materials and Methods

Sampling collection. A total of 200 Algerian banknotes in four denominations (50 of each 200, 500, 1000, and 2000 Algerian Dinars, DZD) were randomly collected from various places: supermarkets, gas stations, coffee shops, pizzerias, restaurants, butchers, fish shops, bus stations and banks in Algiers City during the end of the year 2018 (November-December). In addition, for each denomination five new notes, collected from the Algerian Central Bank were included in the study as negative controls.

The samples were placed into sterile polyethylene bags using gloves to avoid further contamination. The latter were transported to the laboratory, where they were directly processed.

Isolation and numeration of the bacteria. To evaluate the bacterial diversity of the studied banknotes, different culture media were used, allowing the isolation and enumeration of the total cultivable bacteria and various specific bacterial groups.

Each banknote was dropped into 10 ml of Trypticase Soy Broth (TSB, Difco) and shaken for 30 minutes with a vortex agitator to dislodge the bacteria into the broth, as described by Kalita et al. (2013). Then, 0.1 ml of the obtained suspension and of its decimal dilutions (from 10^{-1} to 10^{-5}) were inoculated into the following solid media (Difco): Nutrient agar (for the enumeration of the total bacterial number), Columbia medium (allowing the growth of the exigent bacteria), Chapman agar (for the *Staphylococci* group), Bile-Esculin agar (for the *Enterococci* group), Hektoen agar (for the *Enterobacteriaceae* family and the other non-exigent Gram-negative bacteria) and Cetrimide agar (for *Pseudomonas* spp.). The plates were then incubated for 18 to 48 hours at 37°C.

After incubation, the grown colonies were counted and the total viable cells, expressed as colony-forming units (CFU) per banknote, were determined by the count plate method.

Bacterial identification. Different, representative, and predominant colonies grown in the enumeration plates were selected for each sampling place and then purified and isolated by repeated transfers on fresh agar plates of their initial culture media.

Isolates were analyzed by microscopic observations after Gram staining, and activities of oxidase, catalase, and nitrate reductase, VP-MR test, motility, indole production, citrate utilization, and respiratory type to Bergey's manual of systematic Bacteriology (Holt et al. 1994).

Based on the results of these preliminary tests and the initial isolation media, the biochemical identification of the isolates was carried out by the corresponding API system galleries (Biomérieux) using API 20E, API 20 NE, API 50CH, API Staph, or API Strep.

Moreover, Gram and catalase-positive strains retrieved from Chapman agar were submitted to additional tests comprising tube coagulase test with rabbit plasma (Biomérieux) and Pastorex Staph-Plus™ agglutination test (Bio-Rad). Strains that responded positively to both tests were identified as *Staphylococcus aureus*.

Finally, some isolates' taxonomic status was confirmed by 16s rRNA gene sequencing as described previously (Ben Dhia Thabet et al. 2004).

Phylogenetic analysis. The phylogenetic analysis and the phylogenetic tree constructions were conducted using the Molecular Evolutionary Genetics Analysis (MEGA) software, version 10.0 (Kumar et al. 2018).

Reference 16S rRNA gene sequences were uploaded from the Genbank database (https://www.ncbi.nlm.nih.gov/). Multiple alignments of the sequences were performed by CLUSTAL W (Thompson et al. 1994). Evolutionary distances were calculated using the maximum composite likelihood method and are in the units of the number of base substitutions per site (Tamura et al. 2004). The phylogenetic trees were reconstructed with the neighbor-joining algorithm (Saitou and Nei 1987). The resultant trees' topologies were evaluated by bootstrap analysis of the neighbor-joining dataset, based on 1,000 resamplings.

Hemolysis test. The ability to digest red blood cells was tested by spot inoculation of the isolated strains on Columbia agar supplemented with 5% sheep blood. The plates were incubated at 37°C for 24 to 36 hours and the potential clear zones (for β-hemolysis)

or changes of color (for α-hemolysis) around the bacterial spots were observed.

Determination of antibiotic resistance. The bacterial strains were tested for their resistance or susceptibility towards 34 different antibiotics by the Kirby-Bauer disk diffusion method on Mueller Hinton agar plates (Difco) using the following antibiotic disks (µg or International Unit „IU"/disk): amikacin (AK) 30 µg, amoxicillin + clavulanic acid (AMC) 30 µg, ampicillin (AMP) 10 µg, aztreonam (AZT) 30 µg, cefazolin (CZ) 30 µg, cefepime (FEP) 30 µg, cefotaxim (CTX) 30 µg, cefoxitin (CEF) 30 µg, ceftazidime (CAZ) 30 µg, cefuroxime (CXM) 30 µg, cephalotin (CH) 30 µg, chloramphenicol (C) 30 µg, ciprofloxacin (CIP) 5 µg, clindamycin (CN) 2 µg, daptomycin (DAP) 30 µg, ertapenem (ERT) 10 µg, erythromycin (E) 15 µg, fosfomycin (FOS) 50 µg, fusidic acid (AF) 10 µg, gentamicin (G) 10 µg, levofloxacin (LVX) 5 µg, linezolid (LIN) 30 µg, nitrofurantoin (NIT) 100 µg, oxacillin (OX) 5 µg, penicillin (P) 10 UI, piperacillin/tazobactam (TZP) 100 + 10 µg, rifampicin (RA) 5 µg, teicoplanin (TEC) 30 µg, tetracyclin (TE) 30 µg, ticarcillin + clavulanic acid (TCC) 75 + 10 µg, tigecycline (TIG) 15 µg, tobramycin (TM) 10 µg, trimethoprim + sulfamethoxazole (SXT) 1.25 + 23.75 µg and vancomycin (VA) 30 µg (Hi-media).

The results were interpreted according to the guidelines of the Clinical and Laboratory Standards Institute. *E. coli* ATCC 25922, *Pseudomonas aeruginosa* ATCC 27853, and *Staphylococcus aureus* ATCC 25923 were used as control strains for antimicrobial susceptibility testing.

Results

A total of 220 banknotes, comprising 200, 500, 1000, and 2000 DZD denominations (200 samples consisting of 50 used banknotes for each denomination and 20 controls consisting of 5 mint banknotes for each denomination) were analyzed for their bacterial load and diversity. The predominant bacterial strains were identified, and their antibiotic resistance profiles were determined.

Bacterial enumeration. All circulating banknotes (100%) obtained from various sources were contaminated, whereas new notes from the central bank showed low or no growth (Table I).

Bacterial concentrations were related to the denominations as the most critical contamination was found among 200 DZD, 500 DZD, and 1000 DZD denominations, whereas 2000 DZD banknotes were moderately contaminated (Table I). Besides, we noted the banknotes' general bad physical state (moistness, smelliness, tearing), most significantly for 200 DZD, 500 DZD, and 1000 DZD denominations.

As expected, Columbia agar counts were the highest since the used medium is rich and allows the growth of various bacterial groups, even exigent ones. Besides, the mean for the total non-exigent flora (Nutrient agar) was relatively abundant (varying from $1{,}3 \times 10^3$ to $4{,}3 \times 10^4$ CFU/banknote).

Regarding the selective media, Chapman agar and Hektoen showed the most important rates of growth ($5{,}3 \times 10^3$ and $3{,}3 \times 10^3$, respectively), whereas Bile-Esculin and Cetrimide agar exhibited lower contamination levels.

Bacterial identification. After enumeration, the counting plates were examined, and for each sampling place the dominant colonies were selected and purified for qualitative analysis. Thereby, 48 morphologically distinct bacterial strains were obtained and characterized (Table II). Out of the total, 19 strains were isolated from 200 DZD banknotes, 16 from 500 DZD banknotes and five and eight strains from 1000 and 2000 DZD banknotes, respectively.

The morphological study showed that 28 strains were Gram-positive (58.3%) including 23 cocci and

Table I
Enumeration of different bacterial groups isolated from Algerian banknotes.

Culture Media	The banknotes studied (CFU/banknote)				New banknotes (CFU/banknote)			
	200 DZD	500 DZD	1000 DZD	2000 DZD	200 DZD	500 DZD	1000 DZD	2000 DZD
Nutrient agar (Total non-exigent flora)	$4.3 \times 10^4 \pm 9 \times 10^3$	$2.6 \times 10^4 \pm 4 \times 10^3$	$1.5 \times 10^4 \pm 6 \times 10^3$	$1.3 \times 10^3 \pm 4 \times 10^2$	200 ± 16	150 ± 27	120 ± 12	80 ± 5
Columbia agar (Exigent and non-exigent bacteria)	$5.4 \times 10^5 \pm 8 \times 10^4$	$1.8 \times 10^5 \pm 4.3 \times 10^4$	$2.1 \times 10^4 \pm 3 \times 10^3$	$2.2 \times 10^3 \pm 8 \times 10^2$	100 ± 29	50 ± 6	0	0
Chapman agar (*Staphylococcus* and other Gram-positive cocci)	$5.3 \times 10^3 \pm 4 \times 10^2$	$6.7 \times 10^3 \pm 3 \times 10^2$	$6.6 \times 10^3 \pm 9 \times 10^2$	$8{,}5 \times 10^2 \pm 7 \times 10^1$	0	0	0	0
Hektoen agar (*Enterobacteriaceae* and other non-exigent Gram-negative rods)	$3.3 \times 10^3 \pm 7 \times 10^2$	200 ± 40	100 ± 20	0	0	0	0	0
Bile-Esculin agar (*Enterococcus* spp.)	200 ± 30	500 ± 20	300 ± 13	0	0	0	0	0
Cetrimide agar (*Pseudomonas* spp.)	80 ± 2	72 ± 4	75 ± 6	20 ± 3	0	0	0	0

Values are the means of three replicates

Table II
Strains isolated from Algerian banknotes currency and their characterization.

Notes	Strains	Biochemical identification (Api System)	Molecular identification	Resistance profiles	Hemo-lysis
200 DZD	B0P1	*Staphylococcus cohnii*	*S. equorum*	P, AZT, FOS, FA	none
	B1P3	*Staphylococcus epidermidis*	*S. epidermidis*	P, OX, AMP, AMC, CZ, CH, AZT,C, CN	none
	B1N2	*Staphylococcus aureus*	ND	P, OX, AMP, AZT, GN, FA	β
	B4M1	*Staphylococcus auricularis*	ND	AZT, FA, G, T, C	none
	B3M3	*Micrococcus* sp.	ND	P, OX, E	none
	B4P8	*Micrococcus* sp.	ND	P, AK	α
	B4N6	*Micrococcus* sp.	ND	P, SXT	none
	B5M4	*Micrococcus* sp.	ND	P, T, E	none
	B0H2	*Bacillus* sp.	*B. firmus*	P, OX, CZ, CH	β
	B5P5	*Bacillus* sp.	*S. luteloa*	P, OX, AMP	none
	B7G7	*Bacillus* sp.	*B. psychrodurans*	P, OX, AMP, FA, FOS	β
	B1M0	*Rothia mucilaginosa*	ND	P, OX, FA, V, CIP, C	none
	B1C1	*Pseudomonas aeruginosa*	*Ps. aeruginosa*	P, OX, AMP, AMC, TZP, TCC, CZ, CH, CEF, CXM, ERT, FA, TEC, VA, DAP	α
	B6C1	*Brevundimonas vesicularis*	*B. vesicularis*	P, OX, AMP, CZ, CEF, FA, G, TM, FA, TEC, VA, DAP, E, CN	none
	B7M1	*Acinetobacter lwoffii*	ND	P, OX, CZ, CH, FA, TEC, VA, DAP, T, CIP, LVX	α
	B7P2	*Moraxella* sp.	ND	P, OX, AMP, AMC, FA, TEC, VA, DAP, CN	none
	B6M5	*Shewanella putrefaciens*	ND	P, OX, AMP, AZ, CH, CZ, FOS, FA, TEC, VA, DAP, SXT	β
	B6J4	*Klebsiella ozaenea*	ND	P, OX, AMP, AMC, CH, CZ, G, FA, TEC, VA, DAP, T, E, NIT	α
	B5S3	*Enterobacter sakazakii*	ND	P, OX, AMP, AMC, CZ, CH, CEF, CXM, FA, TEC, VA, DAP	α
500 DZD	C1P1	*Staphylococcus arlettae*	*S. arlettae*	P, OX, AMP, CH, CZ, CEF, AZT, TEC, VA, E, G, TM, T, E, CN	none
	C5H1	*Staphylococcus lentus*	ND	P, AMP, AMC, AZT, G, AF	α
	C5G4	*Staphylococcus saprophyticus*	*S. saprophyticus*	P, AZT, T, E, CN	none
	C1M1	*Micrococcus* sp.	ND	P, E	none
	C4J3	*Micrococcus* sp.	ND	DAP, T, E	α
	C4P3	*Micrococcus* sp.	ND	P, T	none
	C5G1	*Enterococcus faecalis*	*E. faecalis*	OX,CZ, CH, CEF, CXM, FEP,TZP, TCC, AK, G, TM, CN, E	α
	C5P3	*Enterococcus faecium*	ND	P, OX, AMP, AMC, CH, CZ, CTX, CXM, FEP, ERT, AK, G, TM, FOS, CIP, LVX, T, E, CN	α
	C2H0	*Bacillus* sp.	ND	P, OX, AMP, E	β
	C5T1	*Bacillus* sp.	ND	P, OX, AMP, CZ	β
	C5C7	*Rothia mucilaginosa*	ND	P, OX, AK, G	none
	C1N3	*Pseudomonas fluorescens*	ND	P, OX, AMP, AMC, CZ, CH, CEF, CXM, ERT, FA, TEC, VA, DAP, G, E	none
	C2C5	*Pseudomonas mendocina*	*Ps. mendocina*	P, OX, AMP, AMC, CH, CZ, CEF, CXM, CTX, CAZ, ERT, G, FOS, FA, TEC, VA, DAP, CIP, LVX	α
	C5C11	*Pseudomonas fluorescens*	*Ps. fragi*	P, OX, AMP, AMC, CH, CZ, CTX, CXM, FEP, AZT, TZP, ERT, G, TM, FA, TEC, VA, DAP, CIP, T, E, CN	α
	C3K1	*Acinetobacter lwoffii*	ND	P, OX, AMP, AMC, CZ, CH, FA, TEC, VA, DAP	none
	C4R11	*Weeksella virosa*	ND	P, OX, CIP, AK, AZT, G, TM, FA, TEC, VA, DAP	none
1000 DZD	D1C1	*Micrococcus* sp.	ND	P, FA, C	none
	D1H1	*Enterobacter cloacae*	*E. cloacae*	P, OX, AMP, AMC, AZT, CZ, CH, CEF, CXM, CTX, CAZ, FEP, ERT, FA, TEC, VA, DAP, TIG, SXT	α
	D3P5	*Klebsiella oxytoca*	ND	P, OX, AMP, CZ, G, FA, TEC, VA, DAP, C, CIP, NIT	α
	D2P1	*Alcaligenes faecalis*	*A. faecalis*	P, OX, AMP, AMC, AZT, ERT, CAZ, FEP, G, FOS, FA, TEC, VA, CIP, DAP	none
	D4C5	*Acinetobacter lwoffii*	*A. lwoffii*	P, OX, AMP, CZ, CH, G, FA, TEC, VA, DAP, E, SXT	α

Table II. Continued

Notes	Strains	Biochemical identification (Api System)	Molecular identification	Resistance profiles	Hemolysis
2000 DZD	DM4S1	*Staphylococcus aureus*	ND	P, OX, CZ, CH, AZT, G, TM	α
	DM5C1	*Staphylococcus epidermidis*	ND	P, OX, AMP, AMC, AK, G, TM, FOS, FA, TEC, VA, CIP, T, E, SXT, CN, RA, NIT	none
	DM3C3	*Micrococcus* sp.	*M. luteus*	AZT, NIT	none
	DM3C5	*Rothia dentocariosa*	ND	P, SXT, NIT	none
	DM1C2	*Klebsiella ozaeane*	*K. oxytoca*	P, OX, AMP, AMC, CH, CZ, CEF, CTX, CXM, FEP, AZT, ERT, AK, G, TM, FOS, FA, TEC, VA, DAP, C, CIP, LVX, T, TIG, E, CN	α
	DM2C3	*Serratia marscesens*	*S. rubidaea*	P, OX, AMP, AMC, CZ, CH, CEF, CTX, CAZ, ERT, FA, TEC, VA, DAP, C, CIP, LVX, SXT	none
	DM1J1	*Acinetobacter lwoffii*	ND	P, OX, CZ, CH, FA, TEC, VA, DAP, CIP, SXT	none
	DM4G6	*Chryseobacterium indologenes*	ND	P, OX, CZ, CH, CXM, CAZ, FEP, AZT, ERT, AK, G, TM, FA, TEC, VA, DAP, SXT	none

ND – not determined

five spore-forming rods whereas 20 strains were Gram-negative rods or coccobacilli (41.7%).

Biochemical identification showed that the 48 isolated strains belonged to 17 different genera. 16S rRNA gene sequencing allowed us to confirm and specify the taxonomical statutes for 18 of the isolates. The latters were submitted to phylogenetical analysis, and the resulting trees for Gram-positive and Gram-negative bacteria are shown in Fig. 1a and 1b, respectively.

The 16S rRNA sequences for the 18 strains have been registered to the NCBI Genbank database and the accession numbers attributed are as follows: B6C1: MT786742; B1C1: MT786743; C2C5: MT786744; C5C11: MT786745; D1H1: MT786746; D2P1: MT786747; D4C5: MT786748; DM1C2: MT786749; DM2C3: MT786750; B0P1: MT786751; B0H2: MT786752; B5P5: MT786753; B7G7: MT786754; C1P1: MT786755; C5G1: MT786756; C5G5: MT786757; B1P3: MT786758; DMC3: MT786759.

The isolation frequencies for each genus are presented in Table III. The most predominant groups retrieved from Algerian banknotes were catalase-positive and

Table III
Diversity of bacterial strains isolated from Algerian banknotes.

Genera	Number of strains for each denomination				Total (frequency %)
	200 DZD	500 DZD	1000 DZD	2000 DZD	
Staphylococcus	4	3	0	2	9 (18.75)
Micrococcus	4	3	1	1	9 (18.75)
Bacillus	2	2	0	0	4 (8.33)
Pseudomonas	1	3	0	0	4 (8.33)
Acinetobacter	1	1	1	1	4 (8.33)
Rothia	1	1	0	1	3 (6.25)
Klebsiella	1	0	1	1	3 (6.25)
Enterococcus	0	2	0	0	2 (4.16)
Enterobacter	1	0	1	0	2 (4.16)
Serratia	0	0	0	1	1 (2)
Brevundimonas	1	0	0	0	1 (2)
Shewanella	1	0	0	0	1 (2)
Moraxella	1	0	0	0	1 (2)
Weeksella	0	1	0	0	1 (2)
Alcaligenes	0	0	1	0	1 (2)
Chryseobacterium	0	0	0	1	1 (2)
Sporosarcina	1	0	0	1	1 (2)
Total	19	16	5	8	N = 48

catalase-negative Gram-positive cocci represented by the genera *Staphylococcus* and *Micrococcus* (18.75%, each) followed by *Bacillus*, *Pseudomonas,* and *Acinetobacter* (8.33%, each). The remaining strains were identified as belonging to the following genera: *Rothia*, *Klebsiella*, *Enterococcus*, *Serratia*, *Brevundimonas*, *Shewanella*, *Moraxella*, *Weeksella*, *Alcaligenes*, *Chryseobacterium*, and *Sporosarcina.* There were no significant differences observed in the bacteria distribution between the denominations studied.

Among *Staphylococcus* spp., two strains (B1N2 and DM4S1) showed coagulase production and responded positively to the Pastorex Staph-Plus™ agglutination test. These results confirmed the prior biochemical identification as *S. aureus* (Table II).

Hemolysis test. The results of the hemolysis test are presented in Table II. In total, 22 strains (45.8%) were able to digest blood cells and 16 (33.3%) showed α-hemolysis, whereas 6 (12.5%) were β-hemolytic.

Antibiotic susceptibility. The 48 strains were tested for their antibiotic susceptibility towards 34 antibiotics belonging to 15 different families. The antibiotypes of the 48 isolates are shown in Table II**,** and the antibiotic resistance frequencies are presented in Table IV.

All isolates presented antibiotic resistance towards 2 (strains B4P8, B4N6, C1M1, C4P3, and DM3C3, all identified as *Micrococcus* spp.) to 27 molecules (strain DM1C2 identified as *Klebsiella oxytoca*) at the same time (Tab. II).

Penicillin (P) and oxacillin (OX) showed the most important resistance frequencies. However, as Gram-negative bacteria are naturally resistant to these molecules, only Gram-positive bacteria resistance frequencies should be noted. Thus, 24/28 and 15/28 Gram-positive strains were found to be resistant to P and OX, respectively.

Generally, high resistance frequencies for aminopenicillins (54.1% and 33.3% for ampicillin (AMP) and amoxicillin + clavulanic acid (AMC), respectively) and for 1st generation cephalosporins (50 % and 43.8% for cefazolin (CZ) and cephalotin (CH), respectively) were observed whereas other β-lactams showed better efficiency than the latter.

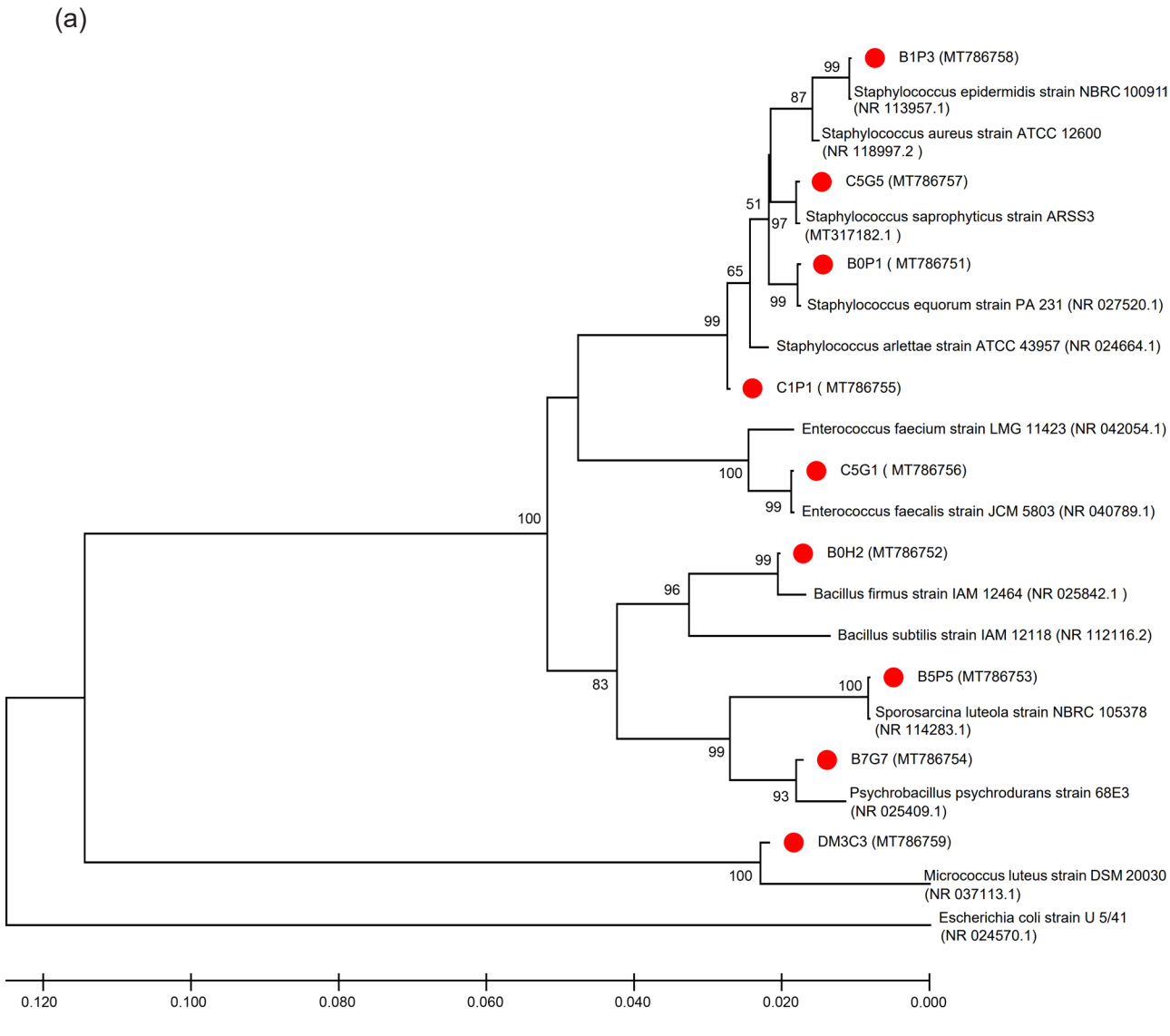

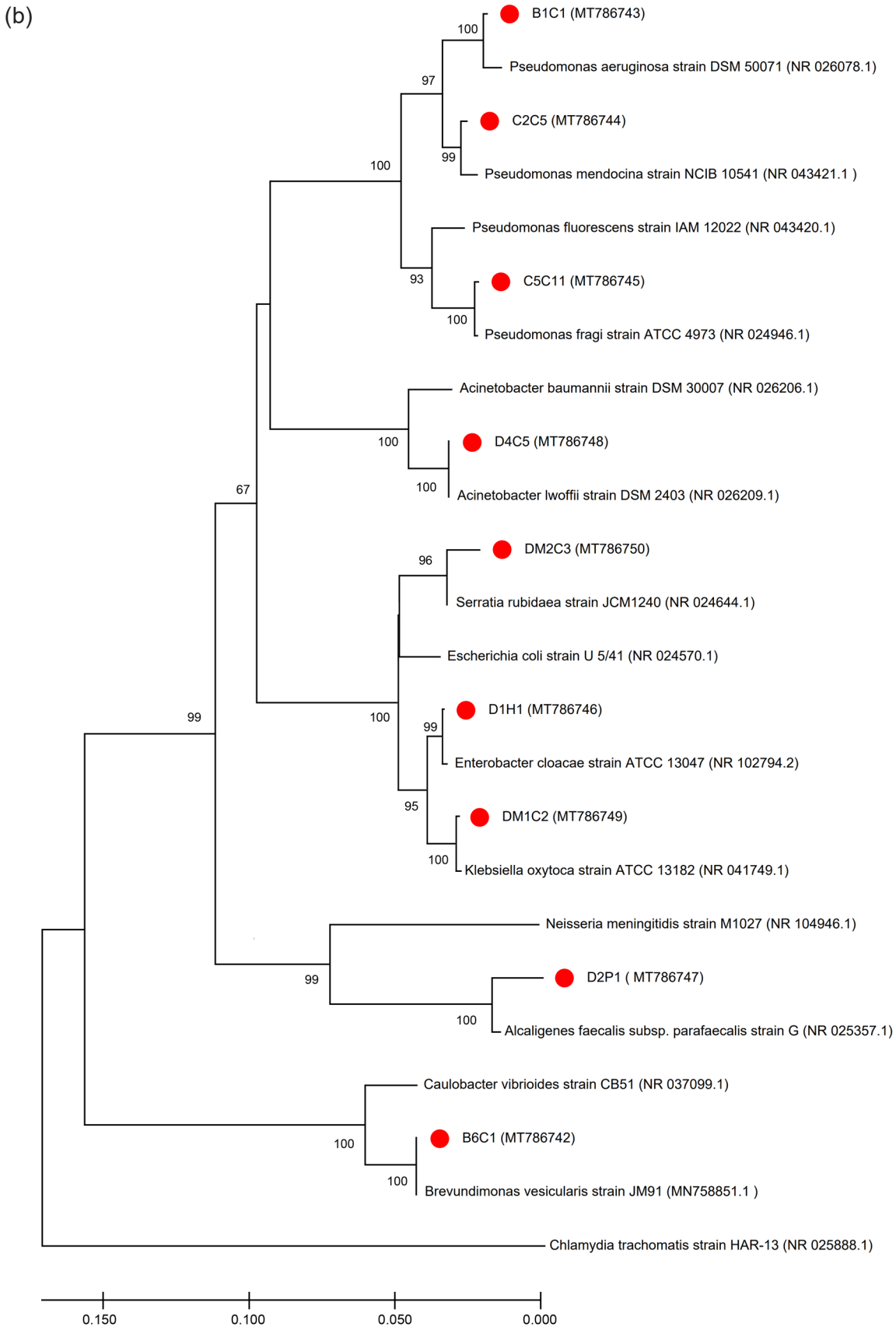

Fig. 1. Phylogenetic relationships between strains isolated from Algerian banknotes and reference bacterial strains using 16S rRNA sequences: (a) Gram-positive strains; (b): Gram-negative strains. The evolutionary distances were computed using the Tamura-Nei method and are in the units of the number of base substitutions per site. The phylogenetic trees were constructed using the Neighbor-joining algorithm. Bootstrap values (1,000 replicates) are indicated at the nodes.

Table IV
Antibiotic resistance in Algerian banknotes isolates.

Families	Antibiotics	Number of Gram-positive resistant strains (N = 28)	Number of Gram-negative resistant strains (N = 20)	Number of Total resistant strains Frequencies (%)
β-lactams	P	24	20*	44 (91.7)
	OX	15	20*	35 (72.9)
	AMP	10	16	26 (54.1)
	AMC	4	12	16 (33.3)
	CZ	7	17	24 (50)
	CH	6	15	21 (43.8)
	CEF	2	8	10 (20.8)
	CXM	2	10	12 (25)
	CTX	1	5	6 (12.5)
	CAZ	0	5	5 (10.4)
	FEP	2	5	7 (14.6)
	TZP	1	2	3 (6.2)
	TCC	1	1	2 (4.2)
	AZT	9	6	15 (31.2)
	ERT	1	9	10 (20.8)
Aminosides	AK	5	3	8 (16.7)
	G	8	10	18 (37.5)
	TM	5	5	10 (20.8)
Phosphonic acids	FOS	4	4	8 (16.7)
Fusidanines	FA	7	20*	27 (58.3)
Glycopeptides	TEC	2	20*	22 (45.8)
	VA	2	20*	22 (45.8)
Lipopeptides	DAP	1	20*	21 (43.8)
Oxazolidinones	LIN	0	0	0 (0)
Phenicols	C	4	3	7 (14.6)
Fluoroquinolones	CIP	3	9	12 (25)
	LVX	1	4	5 (10.4)
Tetracyclines	T	8	4	12 (25)
	TIG	0	2	2 (4.2)
Macrolides	E	12	7	19 (39.6)
Lincosamides	CN	6	4	10 (20.8)
Rifamycines	RA	1	2	3 (6.2)
Nitrofurantoines	NIT	3	2	5 (10.4)
Sulfamides	SXT	3	6	9 (18.8)

* – natural resistance for Gram-negative bacteria

Gentamycin (G) and erythromycin (E) showed poor efficiency (39.6% and 37.5% of resistant strains, respectively), whereas no resistance was found against linezolid (LIN).

Regarding Gram-positive bacteria, specific antibiotics (for which Gram-negative bacteria are naturally resistant), seven strains were resistant to fusidic acid (FA), two to vancomycin (VA) and teicoplanin (TEC), and one to daptomycin (DAP).

Finally, we noted that overall antibiotic resistance was more important for Gram-negative strains than for Gram-positive ones (Table IV).

Discussion

In this study, the overall bacterial contamination (100% of the banknotes) was higher than that of similar studies conducted in Iran (Firoozeh et al. 2017),

Croatia (Belić et al. 2017), Cameroon (Akaouchere et al. 2014), and Pakistan (Ejaz et al. 2018) reporting 77%, 78%, 94%, and 97% of contaminated banknotes, respectively, but comparable to the 100% rate of contaminated notes retrieved in Sudan (Abd Alfadil et al. 2018), and in India (Sunil et al. 2020). The high rates of bacterial contamination found in Algerian currency could be explained by necessary money handling as most commercial services are paid in cash. Indeed, Algeria's banking system is poorly developed, and keeping cash in houses is part of the Algerian practices. Also, it is to be noted that Algerian bills are made of a cotton-linen mix, which offers a good surface for bacterial attachment and development, especially when the latter is moist and damaged, as it has already been suggested (Vriesekoop et al. 2010). Besides, keeping money underbody surfaces and other poor hygiene practices like inproper hand washing or counting banknotes with fingers wet with saliva may play a role in the dirtiness degree.

Furthermore, it appears that the lower the denomination, the higher the bacterial load. The same observation has been made in similar studies (Akoachere et al. 2014; Girma et al. 2014; Ejaz et al. 2018) and explained that lower denominations are more often exchanged than higher ones. However, it has to be noted that 2000 DZD banknotes were issued and sent for the first time to circulation in 2011, whereas the other analyzed denominations circulate since the 1990s. The longer the banknotes remain in circulation, the greater are their chances to be soiled. Thereby, 2000 DZD notes were generally cleaner and less or not damaged when compared to 200 and 500 DZD denominations in a bad physical condition (moist and smelly). More generally, bacterial loads are a function of the banknotes' physical conditions since in the present study, bacterial counts were higher on dirty and damaged notes than on relatively clean ones, as has already been demonstrated (Kalita et al. 2013; Akoachere et al. 2014).

The total non-exigent bacterial loads were relatively significant when compared to similar studies (Kalita et al. 2013; Mändar et al. 2016), showing that Algerian currency could act as a vector for the transmission of bacterial agents in the community. Also, growth was noted on all selective media, demonstrating important bacterial diversity. Notably, Hektoen and Chapman media showed important growth rates suggesting important contamination with *Enterobacteriaceae* and *Staphylococcus* spp. These two bacterial groups are known to be implied in food-borne diseases and could certainly pose a health risk since the studies banknotes were partly collected from food vendors. Moreover, the presence of *Enterobacteriaceae* (Hektoen agar) and *Enterococcus* spp. (Bile-Esculin agar) suggests possible fecal contamination of the banknotes due to lack of hygiene like not washing hands properly after using the toilets.

Qualitative analysis, in which 48 different strains were isolated, indicated that Gram-positive bacteria were more common than Gram-negative. These results are consistent with earlier reports (Akoachere et al. 2014; Girma et al. 2014; Firoozeh et al. 2017; Ejaz et al. 2018).

The most predominant bacterial genera were *Staphylococcus* and *Micrococcus* (18.75%, each), both naturally found in the human skin and mucous membranes microbiota suggesting hand-borne contamination of the banknotes and, hence, frequent cash exchanges in the community. Coagulase-negative staphylococci and *Micrococcus* spp. are related to opportunistic infections, including community-acquired ones in immunocompromised subjects (Seng et al. 2017; Shi et al. 2017; Ianiello et al. 2019). In addition, strains B1N2 and DM4S1 were identified as *S. aureus*, a well-known pathogen responsible for a broad range of infections but particularly famous for causing food poisoning (Sergelidis and Angelidis 2017). Since *S. aureus* can survive on paper notes for more than 19 days (Gabriel et al. 2013), the presence of this bacterium poses a severe health problem.

The presence of *Bacillus* spp. and *Sporosarcina luteola*, which are spore-forming organisms, could suggest soil contamination even though *Bacillus* spp. are recognized as potential food-borne opportunistic agents (Logan 2012).

The occurrence of *Rothia* spp. confirms possible contamination of the banknotes with saliva as these microorganisms are known as colonizers of the human oral cavity causing peridontal diseases. However, the members of this genus are also implied in opportunistic infections (Ramanan et al. 2014).

More generally, all the recovered bacteria are considered opportunistic or strictly pathogens and represent a threat of infectious diseases among the population, particularly in immunocompromised subjects. These conclusions agree with similar and recent reports from other parts of the world (Firoozeh et al. 2017; Ejaz et al. 2018; Sunil et al. 2020).

To estimate one of their virulence aspects, the isolates were submitted to hemolysis test. The results indicated that 45.8% of the strains were able to produce hemolysins and could be considered potentially dangerous. Indeed, these virulence factors are responsible for cell lysis and destruction of tissues causing damages in the colonized host.

Furthermore, all 48 strains presented antibiotic resistance to at least two molecules simultaneously and showed high resistance levels.

The β-lactams family, notably penicillin and 1st generation cephalosporins, showed the highest rates of

resistance. This observation is also pointed out by analogous studies reporting low efficiency of penicillins and old cephalosporins (Akoachere et al. 2014; Firoozeh et al. 2017; Abd Alfadil et al. 2018; Ejaz et al. 2018). It can be explained by the fact that these molecules have a broad spectrum of activity and are frequently prescribed for a large panel of community-acquired infections leading to the selection of resistant bacterial strains (Melander et al. 2000). Resistance to penicillins and cephalosporins is often due to the production of extended-spectrum-β-lactamases (ESBL), which are generally plasmid-mediated and can rapidly spread among bacteria. Accordingly, a recent study conducted in Algeria describes the presence of ESBL producing Gram-negative bacteria isolated from currency and reports that the implied determinants were members of the $bla_{\text{CTX-M}}$ genes family known to be carried by highly transferrable plasmids (Bendjama et al. 2020).

Nonetheless, we noticed a high resistance frequency towards ertapenem (ERT), a carbapenem molecule, considered the last-resort antibiotic, particularly against ESBL producing Gram-negative bacteria. In this work, two highly multiresistant Gram-negative strains identified as *Klebsiella oxytoca* (DM1C2) and *Serratia rubideae* (DM2C3) were found to be ERT resistant. These findings are corroborated by Bendjama et al. (2020), who report the isolation of a carbapenem-resistant strain of *Enterobacter cloacae* from Algerian currency. It has to be noted that the reported strain carried the carbapenemase $bla_{\text{OXA-48}}$ gene, which is known to be endemic in Mediterranean countries. The existence of carbapenem-resistance genes in the community and more specifically in Gram-negative bacteria is to take very seriously since it could lead to therapeutic failures.

Likewise, glycopeptides are considered as the last-resort treatment for multiresistant Gram-positive bacteria related infections. Yet, here, we report two vancomycin (VA) and teicoplanin (TEC) resistant Gram-postitve strains identified as coagulase-negative staphylococci (C1P1 and DM5S3). Consequently, the dissemination of the implied resistance genes among other bacteria found in the community could lead to a significant health problem.

More generally, multiresistant bacteria found in currency harbor antibiotic resistance genes, often carried by transferrable elements. This idea is supported by a Pakistani study that describes various antibiotic resistance genes and integrons in bacteria isolated from paper currency (Sarwar et al. 2020).

Overall, this study demonstrates that Algerian currency is a reservoir for various antibiotic resistance genes that could spread among phylogenetically related or not related bacteria by horizontal transfers and, hence, play a role in the emergence of antibiotics multi-resistance.

Conclusions

This study shows that Algerian currency banknotes are highly contaminated with opportunistic and pathogenic antibiotic-resistant bacteria and could act as vehicles for infectious diseases in the community and play a role in disseminating antibiotic resistance genes. Given that most commercial transactions are paid in cash in Algeria, our banknotes are very frequently exchanged and handled by the population, leading to more and more bacterial contamination and greater exposure to infections. For these reasons, poor hygiene practices should be discouraged, particularly in restaurants and food shops. Furthermore, no cash transactions should be encouraged by generalizing e-payments and bank cards, and damaged or old banknotes should be frequently replaced. At the time of writing, the urge to implement these recommendations is very well illustrated by the Covid-19 pandemic. Indeed, in the battle against the new Coronavirus, it is strongly advised to avoid cash and favor electronic and bank card payments when no cash transaction systems are poorly or not available at all in Algeria.

Acknowledgments

This study was supported by the General Direction of Research and Technologies Development/Ministry of Higher Education and Scientific Research (DGRSDT/MERS, Algeria).

Conflict of interest

The authors do not report any financial or personal connections with other persons or organizations, which might negatively affect the contents of this publication and/or claim authorship rights to this publication.

Literature

Abd Alfadil NA, Suliman Mohamed M, Ali MM, El Nima EI. Characterization of pathogenic bacteria isolated from Sudanese banknotes and determination of their resistance profile. Int J Microbiol. 2018;4375164. https://doi.org/10.1155/2018/4375164

Abrams BL, Waterman NG. Dirty Money. JAMA. 1972;219(9):1202–1203. https://doi.org/10.1001/jama.1972.03190350038011

Akoachere J, Gaelle N, Dilonga HM, Nkuo-Akenji TK. Public health implications of contamination of Franc CFA (XAF) circulating in Buea (Cameroon) with drug resistant pathogens. BMC Res Notes. 2014;7(16). https://doi.org/10.1186/1756-0500-7-16

Belić D, Ilinić M, Burian S, Talapko J, Drenjančević D. Dirty croatian money: how big is the threat? Southeast Eur Med J. 2017;1(1):5–10. https://doi.org/10.26332/seemedj.v1i1.24

Ben Dhia Thabet O, Fardeau ML, Joulian C, Thomas P, Hamdi M, Garcia JL, Ollivier B. *Clostridium tunisiense* sp. nov., a new proteolytic, sulfur-reducing bacterium isolated from an olive mill wastewater contaminated by phosphogypse. Anaerobe. 2004;10(3):185–190. https://doi.org/10.1016/j.anaerobe.2004.04.002

Bendjama E, Loucif L, Chelaghma W, Attal C, Bellakh FZ, Benaldjia R, Kahlat I, Meddour A, Rolain JM. First detection of

an OXA-48-producing *Enterobacter cloacae* isolate from currency coins in Algeria. J Glob Antimicrob Resist. 2020;23:162–166. https://doi.org/10.1016/j.jgar.2020.09.003

Ejaz H, Javeed A, Zubair M. Bacterial contamination of Pakistani currency notes from hospital and community sources. Pak J Med Sci. 2018;34(5):1225–1230. https://doi.org/10.12669/pjms.345.15477

Espírito Santo C, Morais PV, Grass G. Isolation and characterization of bacteria resistant to metallic copper surfaces. Appl Environ Microbiol. 2010;75(5):1341–1348. https://doi.org/10.1128/AEM.01952-09

Firoozeh F, Dadgostar E, Akbari H, Zibaei M, Sadjjadian SS, Moshtaghi MM, Shakib A. Bacterial contamination of Iranian paper currency. Int J Enteric Pathog. 2017;5(4):106–110. https://doi.org/10.15171/ijep.2017.25

Gabriel EM, Coffey A, O'Mahony JM. Investigation into the prevalence, persistence and antibiotic resistance profiles of staphylococci isolated from euro currency. J Appl Microbiol. 2013;115(2):565–571. https://doi.org/10.1111/jam.12247

Girma G, Ketema T, Bacha K. Microbial load and safety of paper currencies from some food vendors in Jimma Town, Southwest Ethiopia. BMC Res Notes. 2014;7:843. https://doi.org/10.1186/1756-0500-7-843

Holt JG, Krieg NR, Sneath PA, Staley JT, Williams ST. Bergey's Manual of determinative bacteriology, 9th edition. Baltimore (USA): William and Wilkins; 1994.

Ianiello NM, Andrade DC, Ivancic S, Eckardt PA, Lemos Ramirez JC. Native valve infective endocarditis due to *Micrococcus luteus* in a non-Hodgkin's lymphoma patient. IDCases. 2019;18:e00657. https://doi.org/10.1016/j.idcr.2019.e00657

Kalita M, Palusińska-Szysz M, Turska-Szewczuk A, Wdowiak--Wróbel S, Urbanik-Sypniewska T. Isolation of cultivable microorganisms from Polish notes and coins. Pol J Microbiol. 2013;62(3): 281–286. https://doi.org/10.33073/pjm-2013-036

Kraay AM, Hayashi ML , Hernandez-Ceron N , Spicknall IH, Eisenberg MC, Meza R, Eisenberg JS. Fomite-mediated transmission as a sufficient pathway: a comparative analysis across three viral pathogens. BMC Infect Dis. 2018;18:540. https://doi.org/10.1186/s12879-018-3425-x

Kumar S, Stecher G, Li M, Knyaz C, Tamura K. MEGA X: Molecular Evolutionary Genetics Analysis across computing platforms. Mol Biol Evol. 2018;35(6):1547–1549. https://doi.org/10.1093/molbev/msy096

Logan NA. *Bacillus* and relatives in foodborne illness. J Appl Microbiol. 2012;112(3):417–429. https://doi.org/10.1111/j.1365-2672.2011.05204.x

Lopez GU, Gerba CP, Tamimi AH, Kitajima M, Maxwell SL, Rose JB. Transfer efficiency of bacteria and viruses from porous and nonporous fomites to fingers under different relative humidity conditions. Appl Environ Microbiol. 2013;79(18):5728–5734. https://doi.org/10.1128/AEM.01030-13

Lynch P, Pittet D, Borg MA, Mehtar S. Infection control in countries with limited resources. J Hosp Infect. 2007;65(S2):148–150. https://doi.org/10.1016/S0195-6701(07)60033-4

Mändar K, Sõber T, Kõljalg S, Rööp T, Mändar R, and Sepp E. Microbiological contamination of the euro currency in Estonia. Inf Dis. 2016;48(10):772–774. https://doi.org/10.1080/23744235.2016.1201725

Melander E, Ekdahl K, Jönsson G, Mölstad S. Frequency of penicillin-resistant pneumococci in children is correlated to community utilization of antibiotics. Pediatr Infect Dis J. 2000;19(12):1172–1177. https://doi.org/10.1097/00006454-200012000-00011

Ramanan P, Barreto JN, Osmon DR, Tosh PK. Rothia bacteremia: a 10-year experience at Mayo clinic, Rochester, Minnesota. J Clin Microbiol. 2014;52(9):3184–3189. https://doi.org/10.1128/JCM.01270-14

Saitou N, Nei M. The neighbor-joining method: a new method for reconstructing phylogenetic trees. Mol Biol Evol. 1987;4(4):406–425. https://doi.org/10.1093/oxfordjournals.molbev.a040454

Sarwar A, Ahmad I, Amin A, Saleem MA. Paper currency harbours antibiotic-resistant coliform bacteria and integron integrase. J Appl Microbiol. 2020. https://doi.org/10.1111/jam.14856

Seng R, Kitti T, Thummeepak R, Kongthai P, Leungtongkam U, Wannalerdsakun S, Sitthisak S. Biofilm formation of methicillin--resistant coagulase negative staphylococci (MR-CoNS) isolated from community and hospital environments. PLOS ONE. 2017; 12(8):e0184172. https://doi.org/10.1371/journal.pone.0184172

Sergelidis D, Angelidis AS. Methicillin-resistant *Staphylococcus aureus*: a controversial food-borne pathogen. Lett Appl Microbiol. 2017;64(6):409–418. https://doi.org/10.1111/lam.12735

Shi L, Wu D, Wei L, Liu S , Zhao P, Tu B, Xie Y, Liu Y, Wang X, Liu L, Zhang X, Xu Z, Wang F, Qin E. Nosocomial and community--acquired spontaneous bacterial peritonitis in patients with liver cirrhosis in china: comparative microbiology and therapeutic implications. Sci Rep. 2017;7:46025. https://doi.org/10.1038/srep46025

Stephens B, Azimi P, Thoemmes MS, Heidarinejad M, Allen JG, Gilbert JA. Microbial exchange via fomites and implications for human health. Curr Poll Rep. 2019;5:198–213. https://doi.org/10.1007/s40726-019-00123-6

Sunil S, Panchmal GS, Shenoy RP, Kumar V, Jodalli P, Somaraj V. Assessment of microbial contamination of Indian currency notes in circulation – An *in vitro* study. J Indian Assoc Public Health Dent. 2020;18(2):179–182. https://doi.org/10.4103/jiaphd.jiaphd_77_19

Tamura K, Nei M, Kumar S. Prospects for inferring very large phylogenies by using the neighbor-joining method. Proc Natl Acad Sci USA. 2004;101(30):11030–11035. https://doi.org/10.1073/pnas.0404206101

Thomas Y, Vogel G, Suter P, Witschi M, Koch D, Tapparel C, Kaiser L. Survival of Influenza virus on banknotes. Appl Eviron Microbiol. 2008;74(10):3002–3007. https://doi.org/10.1128/AEM.00076-08

Thompson JD, Higgins DG, Gibson TJ. CLUSTAL W: improving the sensitivity of progressive multiple sequence alignment through sequence weighting, position-specific gap penalties and weight matrix choice. Nucleic Acids Res. 1994;22(22):4673–4680. https://doi.org/10.1093/nar/22.22.4673

Vriesekoop F, Russell C, Alvarez-Mayorga B, Aidoo K, Yuan Q, Scannell A, Beumer RR, Barro N, Otokunefor K, Smith-Arnold C, et al. Dirty money: an investigation into the hygiene status of some of the world's currencies as obtained from food outlets. Foodborne Pathog Dis. 2010;7(12):1497–1502. https://doi.org/10.1089/fpd.2010.0606

Wieland K, Chhatwal P, Vonberg RP. Nosocomial outbreaks caused by *Acinetobacter baumannii* and *Pseudomonas aeruginosa*: Results of a systematic review. Am J Infect Control. 2018;46(6):643–648. https://doi.org/10.1016/j.ajic.2017.12.014

Polish Journal of Microbiology
2020, Vol. 69, No 4, 503–508
https://doi.org/10.33073/pjm-2020-043

SHORT COMMUNICATION

A Novel Improved Gram Staining Method Based on the Capillary Tube

KONG-YANG WU[1]* and TONG-XIANG YANG[2]

[1] College of Life Science, Luoyang Normal University, Luoyang, China
[2] College of Food and Bioengineering, Henan University of Science and Technology, Luoyang, China

Submitted 18 June 2020, revised 11 August 2020, accepted 2 September 2020

Abstract

In this work, an exploratory study was conducted to examine Gram staining based on the capillary tube. Each Gram staining step for all bacterial strains tested was completed in capillary tubes. The results showed that different Gram staining morphologies were clearly visible in the capillary tubes. The results presented here demonstrated that the improved method could effectively distinguish between Gram-positive and Gram-negative bacteria, and only small volumes of reagents were required in this method. Collectively, this efficient method could rapidly and accurately identify the types of bacteria. Therefore, our findings could be used as a useful reference study for other staining methods.

Key words: Gram staining, capillary tube, bacteria, and glass slide

Since Hans Christian Joachim Gram reported a staining method in 1884 (Gram 1884), such a technique has experienced more than a century of development and has become frequently used in bacteriology. From 1940 to 1960, Gram staining's clinical application reaches its peak (Kass 1987). In recent years, several automated instruments for Gram staining have also been applied for microbiological analysis (Baron et al. 2010; Li et al. 2020). With the development of modern science and technology, some new technologies are expected to replace Gram staining. For example, Sizemore et al. (1990) have developed an alternative Gram staining technique using a fluorescent lectin. Later on, several fluorescent Gram staining methods have been established, and some Gram staining techniques suitable for live bacterial suspension have been described (Mason et al. 1998; Fife et al. 2000; Forster et al. 2002; Kwon et al. 2019). Sharma et al. (2020) have found that acridine orange fluorescent staining is more sensitive than the Gram staining. Besides, Berezin et al. (2017) have established a method for detecting Gram-negative bacteria based on enhanced Raman spectroscopy. Lemozerskii et al. (2020) have also reported a method of bacterial discrimination using an acoustic resonator. However, Gram staining is still an vital detection method in practical application for many microbiologists and clinicians due to its rapidity and simplicity (Thompson et al. 2017; Jahangiri et al. 2018; Li et al. 2018a).

Over the years, Gram staining has been modified for many times, such as the Brown-Hopps method, Brown-Brenn method, and Gram-Twort method (Brown and Brenn 1931; Brown and Hopps 1973; Peck and Badrick 2017), and these approaches as mentioned earlier are widely used in anatomical pathology laboratories. Through the comparison of various improved methods, it is found that Gram's original four-step method is still used, and some researchers have adopted the three-step method, while its basic principle has not been changed. As reported by Huang and Cui (1996), the three-step Gram staining method combines the two steps of alcohol decolorization and re-staining procedure in one step. Although Gram staining is one of the most commonly used detection methods in clinical microbiology laboratories, many clinicians are skeptical of its results due to differences in operators, low control, and standardization (Samuel et al. 2016; Thomson 2016). Researchers have made efforts to improve the Gram staining's accuracy and reliability over the past few years, such as repeated training and standardization of the staining procedure (Thomson 2016; Siguenza et al. 2019). In this study, we developed a standardized Gram staining procedure for bacterial identification

* Corresponding author: K.-Y. WU, College of Life Science, Luoyang Normal University, Luoyang, China; **e-mail: kywu2007@126.com**

using a capillary tube. A modified Gram staining method based on the capillary tube has not yet been reported to the best of our knowledge. Therefore, we proposed a novel improved Gram staining method to improve the accuracy of the detection results and Gram staining efficiency.

Eight bacterial strains, *Staphylococcus aureus*, *Escherichia coli*, *Bacillus subtilis*, *Bacillus Licheniformis*, *Serratia marcescens*, *Vibrio parahaemolyticus*, *Lactobacillus delbrueckii* ssp. *bulgaricus*, and *Streptococcus thermophilus* were provided by the Laboratory of Microbial Engineering, College of Life Science, Luoyang Normal University. *L. bulgaricus* and *S. thermophilus* were inoculated into skim milk culture medium and maintained at 37°C for 12 h. *S. marcescens*, *B. Licheniformis*, *E. coli*, *B. subtilis*, *V. parahaemolyticus*, and *S. aureus* were inoculated into beef peptone agar slants and maintained at 37°C for 16 h.

Capillary tubes with an internal diameter of 0.5 mm and a length of 100 mm were purchased from the Instrument Factory of West China University of Medical Sciences. Gram staining reagent was obtained from the Anhui Chaohuhongci Medical Equipment Co., Ltd.

Procedure: (1) One or two drops of sterile water were placed in the center of a clean glass slide. An inoculating loop was hold in a flame until it was red-hot and then allowed to cool approximately 30 seconds. Subsequently, a loop of culture was transferred to the center of the slide. The sample was spread onto the slide using the inoculating loop, and a small volume of bacterial suspension was automatically transferred into the capillary tube.

(2) The capillary tube was then heated by passing over a flame for several times until the liquid was completely evaporated. The capillary tube was naturally cooled in the air for several seconds.

(3) One end of the capillary tube was hold upward, and the crystal violet solution was automatically transferred to the capillary tube, followed by standing for 1 minute. The remaining crystal violet solution of the capillary tube was then transferred to absorbent paper. The capillary tube was washed in a gentle and indirect stream of tap water for a few seconds, and samples were dried on absorbent paper.

(4) One end of the capillary tube was hold upward, and Gram's iodine solution was automatically transferred to the capillary tube, followed by standing for 1 minute. Subsequently, the capillary tube was washed using the same procedure as described above.

(5) One end of the capillary tube was hold upward, and 95% ethanol was automatically transferred to the capillary tube, followed by standing for 30 seconds. Subsequently, the capillary tube was washed using the same procedure as described above.

(6) One end of the capillary tube was hold upward, and the Safranin solution was automatically transferred to the capillary tube, followed by standing for 30 seconds to 1 minute. The subsequent procedure was the same as described above. Besides, conventional Gram staining was carried out according to the instructions from the reagent kit. According to the instructions, Gram-negative cells are in pink to red, and Gram-positive cells show a purple or blue color when observed under a microscope.

The Gram staining is always the "first-stage criteria" in the preliminary identification of bacterial species according to their cell walls (Li et al. 2018b). Eight different bacterial species were examined to investigate our approach, and the strains were selected according to the Gram staining pattern. Gram-negative bacteria *E. coli*, *V. parahaemolyticus*, and *S. marcescens* were examined. Gram-positive bacteria *S. thermophilus*, *L. bulgaricus, S. aureus, B. licheniformis* and *B. subtilis* were also assessed. Fig. 1, 2, and 3 illustrate the results of Gram staining of *E. coli*, *V. parahaemolyticus*, and *S. marcescens*, respectively. Fig. 4, 5, 6, 7, and 8 show the Gram staining results of *S. thermophilus*, *L. bulgaricus, S. aureus, B. subtilis*, and *B. licheniformis*, respectively. These results were compared with those obtained using a glass slide for Gram staining. No matter spherical or rod-shaped or not, all bacterial strains could be differentiated into two classifications: Gram-positive and

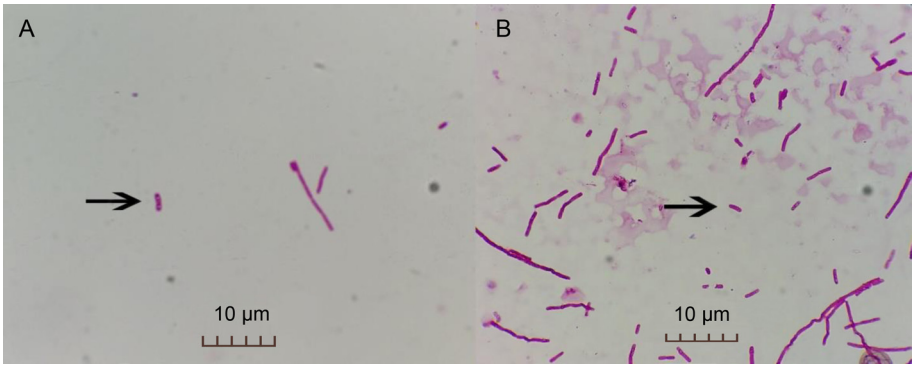

Fig. 1. The Gram staining results of *E. coli*. A – Capillary sample, B – Glass slide sample.

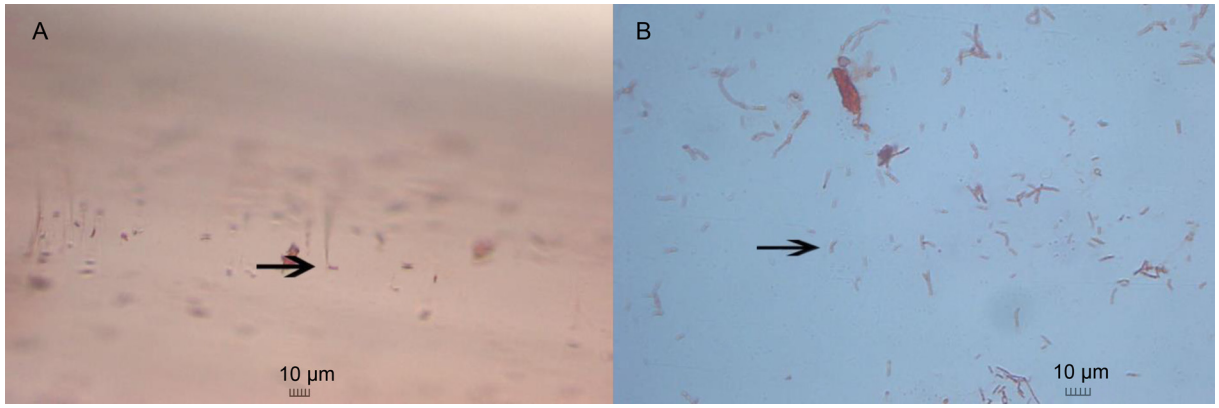

Fig. 2. The Gram staining results of *V. parahaemolyticus*. A – Capillary sample, B – Glass slide sample.

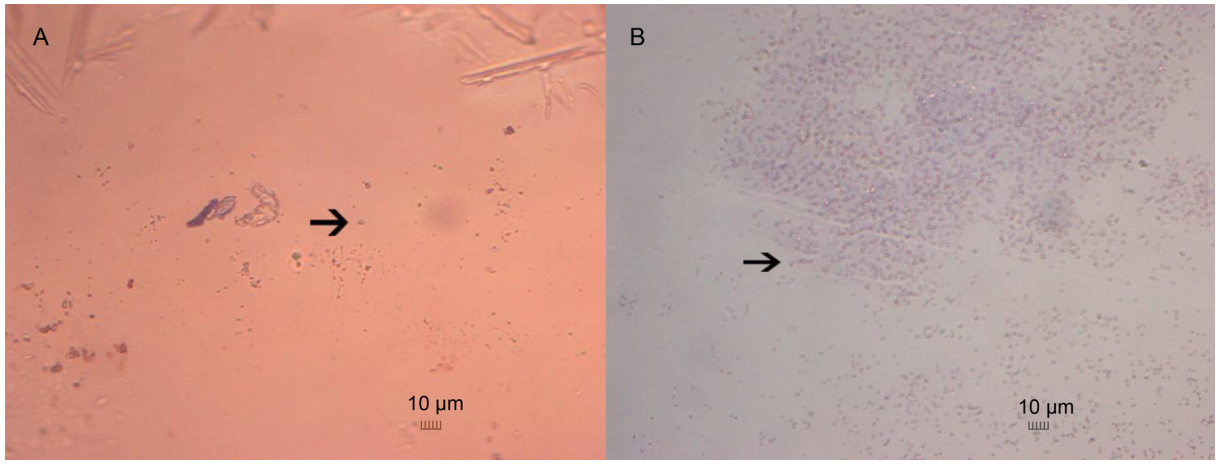

Fig. 3. The Gram staining results of *S. marcescens*. A – Capillary sample, B – Glass slide sample.

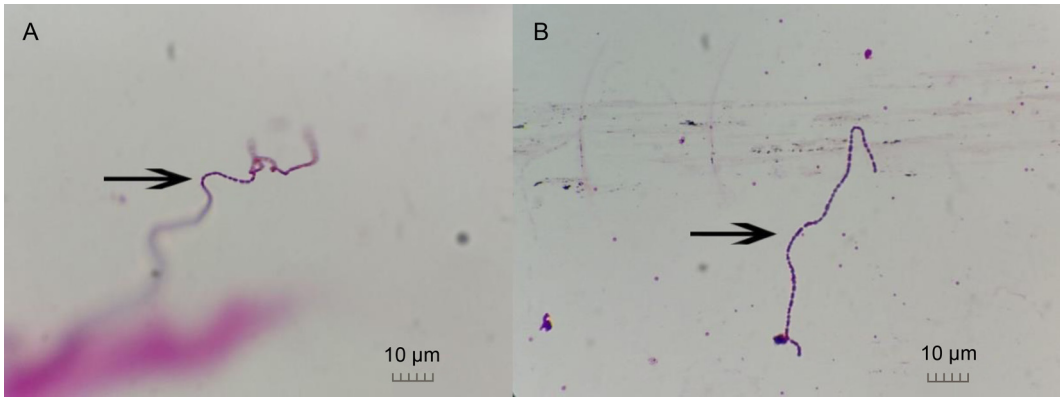

Fig. 4. The Gram staining results of *S. thermophiles*. A – Capillary sample, B – Glass slide sample.

Gram-negative. Comparing these results, we found that the results obtained by the capillary tube method were consistent with the conventional Gram staining approach. It was worth mentioning that in contrast to direct heat fixation of bacteria on glass slides, heat fixation by passing the capillary tube over a flame should be carried out quickly and carefully. If the capillary tube was overheated, it might cause the capillary tube to rupture, and it is easy to blur the field of vision, making it challenging to observe the staining result (Fig. 9). Therefore, before the experiments, it is better to conduct a preliminary experiment and achieve the desired results.

Several studies (Chimento et al. 1996; Wada et al. 2012; Li Zhu 2018b) have already pointed out that the property of the bacterial cell wall determines whether the organism will be Gram-positive or Gram-negative, and it plays a role in the choice of antibiotics when infection occurs. Since it has frequently been observed that not all bacteria react in the same manner to such staining procedure (Hale and Bisset 1956),

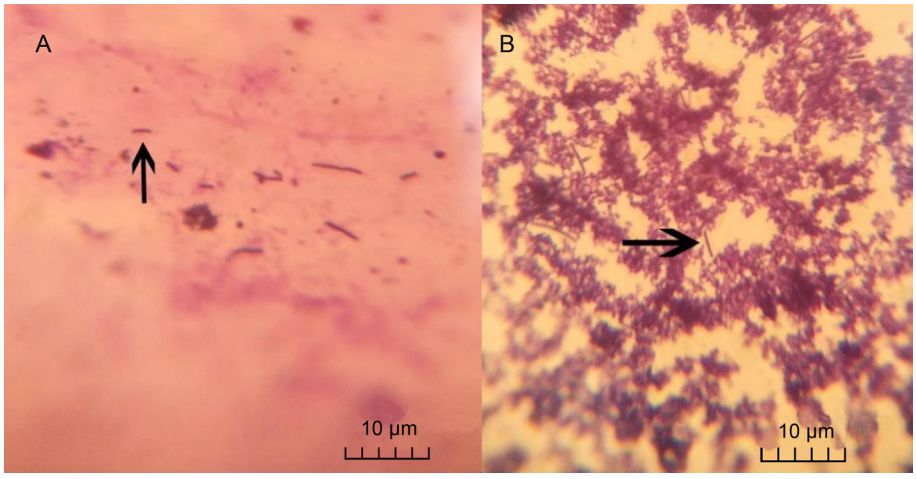

Fig. 5. The Gram staining results of *L. bulgaricus*. A – Capillary sample, B – Glass slide sample.

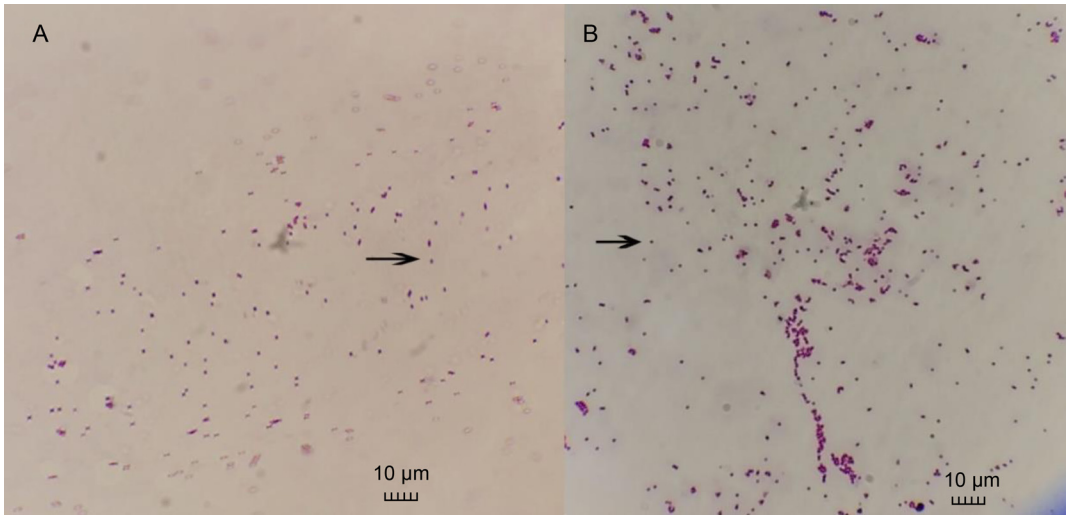

Fig. 6. The Gram staining results of *S. aureus*. A – Capillary sample, B – Glass slide sample.

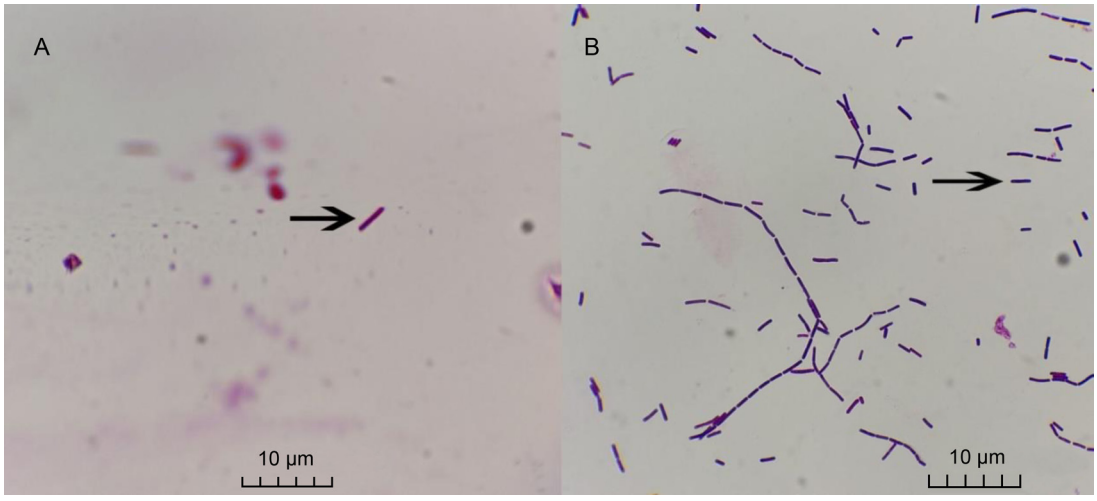

Fig. 7. The Gram staining results of *B. subtilis*. A – Capillary sample, B – Glass slide sample.

it is necessary to make more tests upon a representative selection of Gram-positive and Gram-negative bacteria in future studies.

Molecular biology techniques and high-precision measurement systems have been successfully developed, and they can distinguish bacterial types in clini-

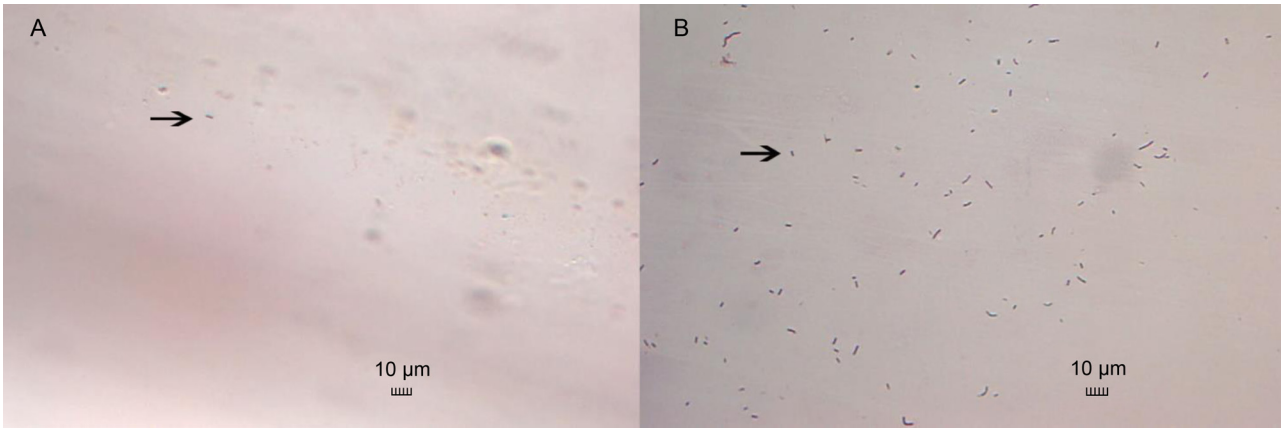

Fig. 8. The Gram staining results of *B. Licheniformis*. A – Capillary sample, B – Glass slide sample.

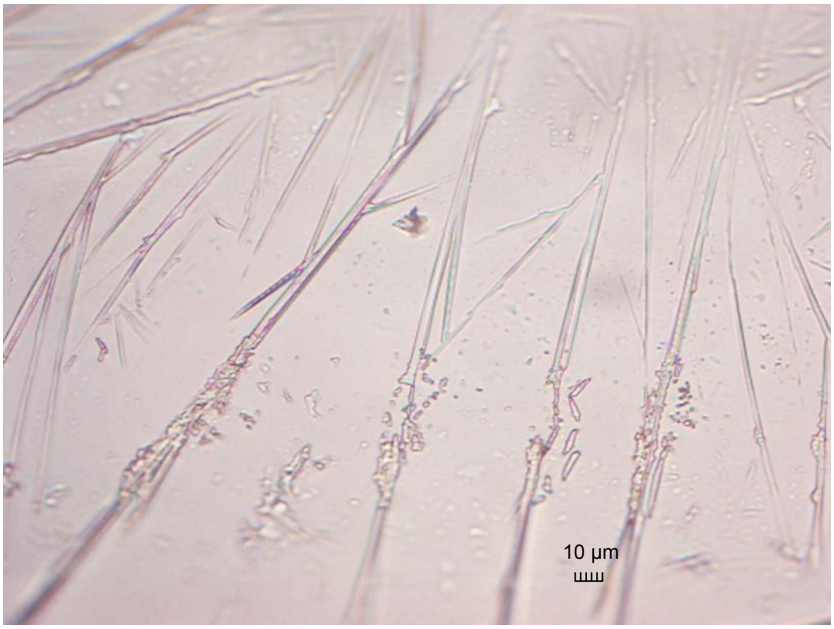

Fig. 9. The microstructure of the overheated capillary tube.

cal samples and improve microbial detection (Klaschik et al. 2002; Dolch et al. 2016; Kim et al. 2018). However, it is still urgently needed to develop a rapid and straightforward Gram staining approach to detect bacteria, especially for those who have only primary experimental conditions. Our results indicated a promising method for bacterial differentiation using the capillary tube as a carrier. Successful differentiation required only small volumes of reagents, and the results were achieved within a few minutes by applying an optical microscope. In addition, the method proposed in this paper had reference value to other staining methods requiring expensive reagents.

In the present study, the improved Gram staining method was developed based on the pure cultures, and it was only a comparison of the staining results between known Gram-negative and Gram-positive bacteria in a glass slide and capillary tube. In order to improve the accuracy and stability of the results, future study is necessary to detect more bacterial species. In addition, the modified method was not applicable for direct Gram staining of clinical samples. In the future, it may have a positive effect by developing a special method for processing clinical samples.

The experimental results demonstrated that an improved Gram staining method was suitable for differentiating the strains tested in our laboratory. The method could rapidly discriminate Gram-positive and Gram-negative bacteria. Besides, the method only required small volumes of reagents. A much more comfortable and reproducible Gram staining approach can be developed for microbiology research based on our studies.

ORCID
Kong-Yang Wu https://orcid.org/0000-0003-1086-1843

Acknowledgments

This study was supported in part by the Science and Technology Plan Projects of Henan province (No. 202102310602); the Key Scientific Research Project of Higher Education of Henan Province (Nos.18A55004 and 21A180017); the Applied Science and Technology Research Project of Luoyang Normal University (No. 2018-YYJJ-003).

Conflict of interest

The authors do not report any financial or personal connections with other persons or organizations, which might negatively affect the contents of this publication and/or claim authorship rights to this publication.

Literature

Baron EJ, Mix S, Moradi W. Clinical utility of an automated instrument for gram staining single slides. J Clin Microbiol. 2010 Jun 01; 48(6):2014–2015. https://doi.org/10.1128/JCM.02503-09

Berezin S, Aviv Y, Aviv H, Goldberg E, Tischler YR. Replacing a century old technique-modern spectroscopy can supplant gram staining. Sci Rep. 2017 Dec;7(1):3810–3816. https://doi.org/10.1038/s41598-017-02212-2

Brown JH, Brenn L. A method for the differential staining of Gram-positive and Gram-negative bacteria in tissue sections. Bull Johns Hopkins Hosp. 1931;48:69–73.

Brown RC, Hopps HC. Staining of bacteria in tissue sections: a reliable gram stain method. Am J Clin Pathol. 1973 Aug 01;60(2):234–240. https://doi.org/10.1093/ajcp/60.2.234

Chimento GF, Finger S, Barrack RL. Gram stain detection of infection during revision arthroplasty. J Bone Joint Surg Br. 1996 Sep; 78-B(5):838–839. https://doi.org/10.1302/0301-620X.78B5.0780838

Dolch ME, Janitza S, Boulesteix AL, Graßmann-Lichtenauer C, Praun S, Denzer W, Schelling G, Schubert S. Gram-negative and -positive bacteria differentiation in blood culture samples by headspace volatile compound analysis. J Biol Res (Thessalon). 2016 Dec;23(1):3. https://doi.org/10.1186/s40709-016-0040-0

Fife DJ, Bruhn DF, Miller KS, Stoner DL. Evaluation of a fluorescent lectin-based staining technique for some acidophilic mining bacteria. 2000;66:2208–2210.

Forster S, Snape JR, Lappin-Scott HM, Porter J. Simultaneous fluorescent gram staining and activity assessment of activated sludge bacteria. Appl Environ Microbiol. 2002 Oct;68(10):4772–4779. https://doi.org/10.1128/AEM.68.10.4772-4779.2002

Gram HC. Ueber die isolirte farbung der schizomyceten in schnitt und trockenpraparaten. Fortschr Med. 1884;2:185–189.

Hale CMF, Bisset KA. A comparison of the staining reactions of the cell walls of Azotobacter chroococcum and those of Gram-positive and Gram-negative bacteria. J Gen Microbiol. 1956 Dec 01;15(3):423–427. https://doi.org/10.1099/00221287-15-3-423

Huang Y, Cui J. A simlified Gram stain and its quality control. Acta Microbiol Sin. 1996;36:76–78.

Jahangiri L, Sudagar M, Ashayerizadeh O, Kolangi H, Tabarraei A. Isolation of probiotic bacteria from guppy *Poeciliareticulata* (Cyprinodontiformes: Poecilidae). Turk J Fish Aquat Sci. 2018;18(6):809–815. https://doi.org/10.4194/1303-2712-v18_6_07

Kass EH. History of the specialty of infectious diseases in the United States. Ann Intern Med. 1987 May 01;106(5):745–756. https://doi.org/10.7326/0003-4819-106-5-745

Kim SY, Park Y, Kim H, Kim J, Koo SH, Kwon GC. Rapid screening of urinary tract infection and discrimination of Gram-positive and Gram-negative bacteria by automated flow cytometric analysis using sysmex UF-5000. J Clin Microbiol. 2018 May 16;56(8):e02004-17. https://doi.org/10.1128/JCM.02004-17

Klaschik S, Lehmann LE, Raadts A, Book M, Hoeft A, Stuber F. Real-time PCR for detection and differentiation of Gram-positive and Gram-negative bacteria. J Clin Microbiol. 2002 Nov 01;40(11): 4304–4307. https://doi.org/10.1128/JCM.40.11.4304-4307.2002

Kwon HY, Liu X, Choi EG, Lee JY, Choi SY, Kim JY, Wang L, Park SJ, Kim B, Lee YA, et al. Development of a universal fluorescent probe for Gram-positive bacteria. Angew Chem Int Ed. 2019 Jun 17;58(25):8426–8431. https://doi.org/10.1002/anie.201902537

Lemozerskii VE, Gagarina AY, Bondarenko AA, Korol VV, Zimina TM. Rapid discrimination of Gram-positive and Gram-negative bacilli using an acoustic resonator. IEEE Conference of Russian Young Researchers in Electrical and Electronic Engineering (EIConRus) 2020.

Li H, Li L, Chi Y, Tian Q, Zhou T, Han C, Zhu Y, Zhou Y. Development of a standardized Gram stain procedure for bacteria and inflammatory cells using an automated staining instrument. Microbiologyopen. 2020 Sep;9(9):e1099. https://doi.org/10.1002/mbo3.1099

Li L, Ding F, Sang L, Liu J, Mao D, Liu X, Xu Q. Study on the oxygen reduction reaction catalyzed by a cold-tolerant marine strain phylogenetically related to *Erythrobacter citreus*. Bioelectrochemistry. 2018a Feb;119:51–58. https://doi.org/10.1016/j.bioelechem.2017.08.011

Li Y, Zhu J, Zhang H, Liu W, Ge J, Wu J, Wang P. High sensitivity Gram-negative bacteria biosensor based on a small-molecule modified surface plasmon resonance chip studied using a laser scanning confocal imaging-surface plasmon resonance system. Sens Actuator B Chem. 2018b Apr;259:492–497. https://doi.org/10.1016/j.snb.2017.12.042

Mason DJ, Shanmuganathan S, Mortimer FC, Gant VA. A fluorescent Gram stain for flow cytometry and epifluorescence microscopy. Appl Environ Microbiol. 1998 Jul 01;64(7):2681–2685. https://doi.org/10.1128/AEM.64.7.2681-2685.1998

Peck M, Badrick T. A review of contemporary practice and proficiency with Gram staining in anatomical pathology laboratories. J Histotechnol. 2017 Apr 03;40(2):54–61. https://doi.org/10.1080/01478885.2017.1327474

Thomson RB Jr. One small step for the gram stain, one giant leap for clinical microbiology. J Clin Microbiol. 2016 Jun;54(6):1416–1417. https://doi.org/10.1128/JCM.00303-16

Samuel LP, Balada-Llasat JM, Harrington A, Cavagnolo R. Multicenter assessment of gram stain error rates. J Clin Microbiol. 2016 Jun;54(6):1442–1447. https://doi.org/10.1128/JCM.03066-15

Sharma S, Acharya J, Banjara MR, Ghimire P, Singh A. Comparison of acridine orange fluorescent microscopy and gram stain light microscopy for the rapid detection of bacteria in cerebrospinal fluid. BMC Res Notes. 2020 Dec;13(1):29. https://doi.org/10.1186/s13104-020-4895-7

Siguenza N, Jangid A, Strong EB, Merriam J, Martinez AW, Martinez NW. Micro-staining microbes: an alternative to traditional staining of microbiological specimens using microliter volumes of reagents. J Microbiol Methods. 2019 Sep;164:105654. https://doi.org/10.1016/j.mimet.2019.105654

Sizemore RK, Caldwell JJ, Kendrick AS. Alternate gram staining technique using a fluorescent lectin. Appl Environ Microbiol. 1990;56(7):2245–2247. https://doi.org/10.1128/AEM.56.7.2245-2247.1990

Thompson AB, Wrubel D, Berkowitz FE. Gram-positive rods on a cerebrospinal fluid gram stain. Open Forum Infect Dis. 2017 Oct 01;4(4):ofx240. https://doi.org/10.1093/ofid/ofx240

Wada A, Kono M, Kawauchi S, Takagi Y, Morikawa T, Funakoshi K. Rapid discrimination of Gram-positive and Gram-negative bacteria in liquid samples by using NaOH-sodium dodecyl sulfate solution and flow cytometry. PLoS One. 2012 Oct 15;7(10):e47093. https://doi.org/10.1371/journal.pone.0047093

Polish Journal of Microbiology
2020, Vol. 69, No 4

CONTENTS

Vol. 69, 1–4, 2020

No 1

ORIGINAL PAPERS

SHORT COMMUNICATIONS

No 2

ORIGINAL PAPERS

SHORT COMMUNICATIONS

No 3

MEMORIAL TRIBUTE

ORIGINAL PAPERS

SHORT COMMUNICATION

No 4

Polish Journal of Microbiology
Vol. 69, 1–4, 2020

Author Index

Polish Journal of Microbiology
Vol. 69, 1–4, 2020

ACKNOWLEDGEMENTS

The Editors of *Polish Journal of Microbiology* wish to express their gratitude to colleagues who have reviewed the manuscripts submitted to our Journal in the past year:

A

Adamo Roberto (Italy), Africa Charlene W.J. (South Africa), Aggarwal Deepak (India), Akar Tarik (Turkey), Akinden Ömer (Germany), Ako Simon Eyongabane (Cameroon), Albores Silvana (Uruguay), Alemayehu Gezahegn (Ethiopia), Almeida Gabriel M.F. (Finland), Alpati Kavitha (India), Ambrosini Roberto (Italy), Amin Dina H. (Egypt), Amin Dina H. (Egypt), Antonelli Alberto (Italy), Ashfaq Muhammad (Germany), Athanasiou Christos (Greece), Ayala-Zavala J. Fernando (Mexico)

B

Balabanova Larissa (Russia), Barzkar Noora (Iran), Bedenic Branca (Croatia), Benckiser Gero (Germany), Bhat Sarita (India), Bhunia Arun (USA), Białas Wojciech (Poland), Blamey Jenny M. (Brazil), Bochkov Yury (USA), Boyanova Lyudmila (Bulgaria), Bruno Laura (Italy), Bugla-Płoskońska Gabriela (Poland)

C

Caimi Karina (Argentina), Caselli Elisabetta (Italy), Caswell Clayton C. (USA), Chamberland Julien (Canada), Chandra Ram (India), Chouchane Habib (Tunisia), Chrzanowski Łukasz (Poland), Crevecoeur Sophie (Canada), Cui Bo (China)

D

Dawood Mahmoud (Egypt), Della Mónica Ivana Florencia (Argentina), Demirci Mehmet (Turkey), Dénes Béla (Hungary), de Oliveira Gislane Lelis Vitela (Brazil), de Oliveira Marcelo Nagem Valeiro (Brazil), Desmet Tom (Belgium), Długosz Ewa (Poland), Dodiya Hemraj B. (USA), Donadu Matthew Gavino (Italy), Drzewiecka Dominika (Poland), Dugarjaviin Manglai (China), Duman Yucel (Turkey), Dutkiewicz Mariola (Poland)

E

Eckert Ester Maria (Italy), Efthimiou Georgios (United Kingdom), Egamberdieva Dilfuza (Uzbekistan), Eimear Brannigan (United Kingdom), Ekinci Kamil (Turkey)

F

Fancello Francesco (Italy), Feye Kristina (USA), Flores Julio Parra (Chile), Forgie Andrew (Canada), Forson Akua Obeng (Ghana)

G

Gautam Ablesh (India), Gish Robert G. (USA), Godbold Douglas (Austria), Goderska Kamila (Poland), Gottaslo Reza (Iran), Grosso Filipa (Portugal), Guler Emrah (Cyprus)

H

Haddix Pryce L. (USA), Hamat Rukman Awang (Malaysia), Han Bei (China), Han Hyon Sob (South Korea), Haq Izharul (India), Hay Roderick (United Kingdom), Helmig Rikke Bek (Denmark), Hrenovic Jasna (Croatia), Huck Olivier (France)

I

Ikeda-Ohtsubo Wakako (Japan)

J

Jaroszuk-Ściseł Jolanta (Poland), Jemli Sonia (Tunisia), Jose Polpass Arul (Israel), Junka Feliks (Poland)

K

Kandati Jithendra (India), Karpagam Krishnan Baby (India), Kayumov Airat (Russia), Kochan Piotr (Poland), Korycińska Joanna (Poland), Krzywonos Małgorzata (Poland), Kumwenda Geoffrey Peterkins (Japan)

L

Lal Mohan (India), Lambie S.M. (New Zealand), Laudy Agnieszka Ewa (Poland), Lazar Zbigniew (Poland), Li Xiang (China), Lilitanond Aroonlug (Thailand), Limtong Savitree (Thailand), Liu Huan (China), Liu Jiabin (China), Liu Mao Ke (China), Lu Binghuai (China), Lu Diannan (China)

M

Ma Ting (China), Madacki Jan (France), Majewska Małgorzata (Poland), Marshall Ian (Denmark), Martínez Daniel (Mexico), Martinez-Porchas Marcel (Mexico), Matthews Karl R. (USA), Maturano Yolanda Paola (Argentina), Miranda-Filho Kleber Campos (Brazil), Misic Dusan (Serbia), Morales Suazo Maria Cristina (Chile), Moralez-Yanez Francisco J. (Belgium), Mulder B. (Netherlands), Myszka Kamila (Poland)

N

Nasrallah Gheyath (Quatar), Ni Kuikui (China)

O

Okoh Sunday O. (South Africa), Ong Chong (Singapore), Ong Song-Quan (Malaysia), Oti Victor B. (Nigeria), Ouédraogo Samiratou (Canada)

P

Padil Vinod V.T. (Czech Republic), Paisio Cyntia E. (Argentina), Pazia-Juma Sauma (Tanzania), Perez-Hernandez Ana (Spain), Perez Alonso Vanessa P. (Brazil), Pircalabioru Gratiela (Romania), Pisani Luciana Pellegrini (Brazil), Plaza Grażyna (Poland), Popławska Monika (Poland), Prajapati Ajay Kumar (India), Prasad Rajendra (India), Pugazhendhi Arivalagan A. (Vietnam), Puglisi Ivana (Italy)

R

Race Marco (Italy), Rao D.L.N. (India), Relaño Ángela Galán (Spain), Ripolles-Avila Carolina (Spain), Rocha João (Portugal)

S

Santara Sumit Sen (USA), Savransky Vladimir (USA), Seipke Ryan (United Kingdom), Selvakumar Ramya (India), Sharma Avinash (India), Sharma Vivek Kumar (India), Shoda Makoto (Japan), Shukla Pratyoosh (India), Śliżewska Katarzyna (Poland), Smulek Wojciech (Poland), Snelling Timothy J. (United Kingdom), Solecka Jolanta (Poland), Sołowski Gaweł (Poland), Sprague Lisa (Germany), Su Diansan (China), Sun Bao Guo (China), Sun Guangyu (China), Szablewski Leszek (Poland), Szymańska-Czerwińska Monika (Poland)

T

Taner Ferdiye (Australia), Taniguchi Takeshi (Japan), Tanrikulu Yusuf (Turkey), Thies Stephan (Germany), Tian Chunjie (China), Tournier Jean-Nicolas (France), Trafny Elżbieta Anna (Poland), Traina Giovanna (Italy), Tuovinen Olli H.H. (USA), Tyagi B.K. (India)

V

Varalakshmi Perumal (India), Verma Anita (USA), Verma Pradeep (India), Vilček Štefan (Slovakia), Vivekanand Vivekanand (India)

W

Wang Guanghua (China), Wang Leyi (USA), Wang Wei (China), Wang Youchun (China), Wei Dong (China), Wińska Katarzyna (Poland), Wójkowska-Mach Jadwiga (Poland), Wu Qing (China)

X

Xu Lin (China)

Y

Yokota Shin-ichi (Japan), Yun Jin-Ho (South Korea)

Z

Zadjelovic Vinko (Unite Kingdom), Zając Zbigniew (Poland), Zasada Aleksandra Anna (Poland), Zavialov Anton V. (Finland), Zhang Haihan (China), Zhang Haihan (China), Zhang Lei (China), Zimenkov Danila V. (Russia)

Polish Journal of Microbiology
2020, Vol. 69, No 4, 519–522

INFORMACJE Z POLSKIEGO TOWARZYSTWA MIKROBIOLOGÓW

Od ostatniej informacji o działalności Zarządu Głównego Polskiego Towarzystwa Mikrobiologów, zamieszczonej w zeszytach nr 3 z 2020 r. kwartalników Advancements of Microbiology – Postępy Mikrobiologii i Polish Journal of Microbiology, ZG PTM zajmował się następującymi sprawami:

1. PTM objął Honorowym Patronatem Konferencję Mikrobiologiczną organizowaną *on-line*, w ramach Ogólnopolskich Spotkań Mikrobiologów i Epidemiologów, w dniu 30 września 2020 r. Kierownik Naukowy: Pani prof. dr hab. Ewa Augustynowicz-Kopeć. Organizator: firma MediCare; http://medicare.waw.pl/konferencje/.
2. FEMS powiększył ofertę wydawanych czasopism

   Oprócz:

https://academic.oup.com/fems-journals

Rozpoczęto wydawanie czasopism:

https://academic.oup.com/femsmicrobes

oraz

https://academic.oup.com/microlife

3. Z inicjatywy FEMS 17 września 2020 r. miało miejsce wydarzenie: International Microorganism Day. Zapraszaliśmy do uczestniczenia *on-line* w obchodach tego Międzynarodowego Mikrobiologicznego Święta. Przez cały dzień – *live streaming* – można było śledzić na bezpośredniej stronie wydarzenia, jak i na kontach Twitter, Facebook i YouTube.
4. Sekretarz i Prezes PTM zostali poproszeni o zorganizowanie wydania specjalnego zeszytu prestiżowego czasopisma: International Journal of Molecular Scieneces pt: „Multi-Drug Resistant Bacteria – A Global Problem". Zapraszamy potencjalnych autorów do zgłoszenia prac doświadczalnych lub przeglądowych – do 31 marca 2021 r. Informacja na temat zeszytu znajduje się pod adresem:

https://www.mdpi.com/journal/ijms/special_issues/multi_drug_resistant_bacteria

5. PTM udzielił poparcia Polskiemu Towarzystwu Studentów Farmacji, największej w Polsce organizacji zrzeszającej studentów farmacji, w przeprowadzeniu ogólnopolskiej akcji „Antybiotykoterapia pod Lupą Farmaceuty", która odbyła się w dniach 2.11 – 8.11.2020. Pani dr Agnieszka Sulikowska (członek OT PTM w Warszawie) przeprowadziła webinar skierowany do dorosłych odbiorców, który skupiał się na zagadnieniach związanych z antybiotykoterapią.
6. W dniu 30.10.2020 r. podjęto Uchwałę 22–2020 dotycząca przedłużenia zatrudnienia Pani sekretarki ZG PTM do 31.10.2021 r., Uchwałę 24-2020 w sprawie przedłużenia zatrudnienia Pani księgowej PTM do 31.12.2021 r. oraz uchwałę nr 23-2020 dotyczącą przyjęcia dwóch nowych członków zwyczajnych PTM.
7. W dniu 10.11.2020 r. podjęto Uchwalę 25-2020 w sprawie objęcia patronatem konferencji on-line „II Ogólnopolskie Spotkanie Mikrobiologów i Epidemiologów" organizowanej w dniu 30.11.2020 r. przez Konsultanta Wojewódzkiego w dziedzinie Mikrobiologia Lekarska Panią prof. dr hab. Ewę Augustynowicz-Kopeć. https://www.webinar-med.pl/osme/#program
8. Pani dr Agnieszka Sulikowska została przedstawicielem PTM do zespołu, który przygotuje opinię w sprawie uznania elementów programu specjalizacji i skrócenia okresu szkolenia lekarzom odbywającym specjalizację w dziedzinie mikrobiologii lekarskiej.
9. Prowadzimy rozmowy z Panem Dawidem Ceculą dyrektorem firmy Exeley Co, wydającym czasopisma PTM on-line, w sprawie przedłużenia umowy wydawniczej obejmującej Polish Journal of Microbiology, na lata 2021 i 2022.
10. Rozważana jest kwestia udziału PTM w opłacaniu składki rocznej uczestnictwa Polski (czyli uczestnictwa kraju a nie konkretnego towarzystwa naukowego w European Union of Medical Specialists, Section of Medical Microbiology (https://uems-smm.eu/uems-smm/).
11. Przypominamy o konieczności opłacenia składki członkowskiej w PTM za 2020 r.
12. Z okazji nadchodzących Świąt Bożego Narodzenia i roku 2021 dziękujemy wszystkim członkom PTM za współpracę w minionym okresie oraz życzymy dużo zdrowia, pomyślności, sukcesów oraz rychłego zakończenia pandemii COVID-19, co umożliwi nam spotkanie na XXIX Zjeździe PTM.

Warszawa, 07.12.2020 r.

SEKRETARZ
Polskiego Towarzystwa Mikrobiologów
dr hab. n. farm. Agnieszka E. Laudy

PREZES
Polskiego Towarzystwa Mikrobiologów
prof. dr hab. Stefan Tyski


XXIX OGÓLNOPOLSKI ZJAZD
POLSKIEGO TOWARZYSTWA
MIKROBIOLOGÓW
14-17 WRZEŚNIA 2021,
WARSZAWA
PTM
POLSKIE TOWARZYSTWO MIKROBIOLOGÓW
XXIX OGÓLNOPOLSKI ZJAZD
POLSKIEGO TOWARZYSTWA
MIKROBIOLOGÓW
14-17 WRZEŚNIA 2021,
WARSZAWA
Miejsce Zjazdu:
Sangate Hotel Airport
Warszawa, ul. Komitetu Obrony Robotników 32
(dawniej 17 Stycznia, róg ul. Żwirki i Wigury)
Główny Organizator Zjazdu:
Polskie Towarzystwo Mikrobiologów
ul. Stefana Banacha 1b, 02-097 Warszawa
ptm.zmf@wum.edu.pl, www.microbiology.pl

CZŁONKOWIE WSPIERAJĄCY PTM

Członek Wspierający PTM – Złoty
od 27.03.2017 r.

HCS Europe – Hygiene & Cleaning Solutions
ul. Warszawska 9a, 32-086 Węgrzce k. Krakowa
tel. (12) 414 00 60, 506 184 673, fax (12) 414 00 66
www.hcseurope.pl

Firma projektuje profesjonalne systemy utrzymania czystości i higieny dla klientów o szczególnych wymaganiach higienicznych, m.in. kompleksowe systemy mycia, dezynfekcji, osuszania rąk dla pracowników służby zdrowia, preparaty do dezynfekcji powierzchni dla służby zdrowia, systemy sterylizacji narzędzi.

Członek Wspierający PTM – Srebrny
od 12.09.2017 r.

Firma Ecolab Sp. z o.o. zapewnia: najlepszą ochronę środowiska pracy przed patogenami powodującymi zakażenia podczas leczenia pacjentów, bezpieczeństwo i wygodę personelu, funkcjonalność posiadanego sprzętu i urządzeń. Firma jest partnerem dla przemysłów farmaceutycznego, biotechnologicznego i kosmetycznego.

Członek Wspierający PTM – Zwyczajny
od 12.09.2017 r.

Merck Sp. z o.o. jest częścią międzynarodowej grupy Merck KGaA z siedzibą w Darmstadt, Niemcy i dostarcza na rynek polski od roku 1992 wysokiej jakości produkty farmaceutyczne i chemiczne, w tym podłoża mikrobiologiczne

Członek Wspierający PTM – Zwyczajny
od 06.06.2019 r.

BART Spółka z o.o. Sp. K
ul. Norwida 4, 05-250 Słupno
NIP: 1180741884, KRS: 0000573068
https://bart.pl/, email: info@bart.pl

Firma BART jest producentem i dystrybutorem surowców oraz dodatków dla przemysłu spożywczego i farmaceutycznego. Specjalizujemy się w probiotykach oraz surowcach uzyskiwanych metodami biotechnologicznymi.
Współpracujemy z renomowanymi producentami: Probiotical, Gnosis, Lesaffre